THE INTERACTION BETWEEN SULPHUR ANTIOXIDANTS AND IRON IN MINERAL OILS

BY

PETER JOHN SMITH

Thesis submitted for the degree of Ph.D. at the University of Aston in Birmingham, July 1986.

ACKNOWLEDGEMENTS

I should like to thank my personal supervisors, Professor G. Scott and Dr. S. Al-Malaika, for their help, advice and encouragement without which this work would not have been possible. My thanks also go to Dr. T. Colclough for his guidance during the time I spent with Esso at Abingdon.

In addition, I would like to thank the technical and scientific staff, both at the University of Aston and at the Esso Research Centre, for their assistance with the practical problems encountered during this research.

I kindly acknowledge the financial support by both the Science and Engineering Research Council and by Esso Chemical Ltd.

Finally, I would like to thank Miss Imelda Hawkins for her kind offer to type this thesis.

THE UNIVERSITY OF ASTON IN BIRMINGHAM

THE INTERACTION BETWEEN SULPHUR ANTIOXIDANTS AND IRON IN LUBRICATING OILS

BY PETER JOHN SMITH

Ph.D. THESIS, 1986

SUMMARY

Mechanisms of antioxidant action of zinc dialkyldithiophosphate (ZnDRP) and several structurally related compounds((basic zinc dialkyldithiophosphate (b-ZnDRP), dialkylthiophosphoryl disulphide (DRDS), dialkyldithiophosphoric acid (DRDPA), dialkylthiophosphoric acid (DRTPA)) were studied in both the presence and absence of a soluble iron catalyst (iron (III) stearate (FeST)). Oxygen absorption studies in two hydrocarbon substrates, white mineral oil and decalin, show that each of the above thiophosphoryl compounds is an effective inhibitor of oxidation at 130°C in the absence of FeST. In the presence of FeST, however, their effectiveness is severely reduced and a higher concentration of antioxidant is required to provide stabilisation against oxidation.

The initial presence of hydroperoxide is shown to have a marked effect on the antioxidant activity of each of the above thiophosphoryl compounds in both the presence and absence of FeST. All the above compounds are shown to be capable of decomposing cumene hydroperoxide (CHP) in both the presence and absence of FeST at 110°C. The long term stabilisation against hydrocarbon oxidation provided by the above thiophosphoryl compounds in the presence of added CHP may be attributed to ionic hydroperoxide decomposition, promoted by sulphur containing acids formed as a result of the oxidation of the parent additive molecule by CHP. Although reaction with FeST may lead to the removal of some of the sulphur acids, hydroperoxide decomposition is shown to still be occurring in the presence of soluble iron.

Of the above thiophosphoryl compounds, only DRDPA gives iron (III) dialkyldithiophosphate (FeDRP) on reaction with FeST. In the absence of CHP, FeDRP was shown to be an inhibitor of hydrocarbon oxidation. In the presence of CHP, however, FeDRP becomes inactive due to free radical decomposition of the hydroperoxide by the iron complex. FeDRP is shown to be an effective hydroperoxide decomposer even when present in small amounts, the mechanism of decomposition depending on the initial CHP:FeDRP ratio. The initial homolytic decomposition of hydroperoxide is caused by the FeDRP itself, but the subsequent ionic reactions are associated with the oxidation product(s) of the iron complex.

Key words: zinc dialkyldithiophosphate, iron stearate, oxidation, hydroperoxide.

LIST OF CONTENTS

LIST OF CONTENTS (continued)

LIST OF CONTENTS (continued)

LIST OF CONTENTS (continued)

LIST OF SCHEMES

LIST OF SCHEMES (continued)

LIST OF TABLES

LIST OF FIGURES

LIST OF FIGURES (continued)

LIST OF FIGURES (continued)

LIST OF FIGURES (continued)

LIST OF FIGURES (continued)

LIST OF FIGURES (continued)

CHAPTER ONE

INTRODUCTION

1.1. OXIDATION OF ORGANIC MATERIALS

The thermal oxidative degradation of organic materials has been widely studied from the later decades of the last century up to the present day. Although much of this work, especially in the earlier years, was concentrated on elucidating the mechanism by which natural rubber underwent oxidation, the conclusions drawn from it have been found to be applicable to many other technologically important organic products, such as plastics and foodstuffs, as well as lubricating oils. The latter, used to protect automobile engines against wear and corrosion during use, generally consist of complex mixtures of saturated hydrocarbons, and are particularly susceptible to oxidative degradation as in use they may be exposed to temperatures as high as 160°C.

The accepted mechanism of oxidation of organic compounds[1] is shown in Scheme 1.1.

INITIATION	Production of $R^{\cdot}$ or $RO_2^{\cdot}$	(1)
PROPAGATION	$R^{\cdot} + O_2 \longrightarrow RO_2^{\cdot}$	(2)
	$RO_2^{\cdot} + RH \longrightarrow RO_2H + R^{\cdot}$	(3)
TERMINATION	$R^{\cdot} + R^{\cdot}$	(4)
	$R^{\cdot} + RO_2^{\cdot}$ → non-radical products	(5)
	$RO_2^{\cdot} + RO_2^{\cdot}$	(6)

Scheme 1.1. Mechanism of oxidation of organic compounds

In the absence of an added initiator, the initiation step, whereby free radicals are introduced into the system, is due to the thermal decomposition of hydroperoxides. (reaction 7).

$$2\ RO_2H \longrightarrow RO_2^{\cdot} + RO^{\cdot} + H_2O \qquad (7)$$

Each free radical formed during the initiation step is capable of forming many molecules of hydroperoxide via the propagation steps (2) and (3). These can then initiate further oxidation chains leading to the formation of yet more hydroperoxide. A chain reaction is therefore rapidly set up. If this continued unhindered, very rapid oxidation would occur, leading ultimately to an explosion. The reason that this does not occur is due to the removal of free radicals by the termination reactions (4), (5) and (6). Under conditions of plentiful oxygen supply, reaction (6) predominates because the reaction of alkyl radicals and oxygen, (2), is very fast. Reaction (4) is only important at low oxygen pressures.

1.2. CATALYSIS BY METAL IONS

The presence of certain transition metal ions having two oxidation states of comparable stability, e.g. $Co^{2+/3+}$, $Fe^{2+/3+}$, can lead to the decomposition of hydroperoxide by reactions (8) and (9)[2].

$$Fe^{2+} + RO_2H \longrightarrow Fe^{3+} + OH^- + RO\cdot \quad (8)$$

$$Fe^{3+} + RO_2H \longrightarrow Fe^{2+} + H^+ + RO_2\cdot \quad (9)$$

$$\text{Overall, } 2\ RO_2H \xrightarrow{Fe^{2+}/Fe^{3+}} RO\cdot + RO_2\cdot + H_2O \quad (10)$$

Although the end products of reaction (10) are identical to those of reaction (7), the activation energy of the former is much lower. Catalysis of oxidation is therefore observed in the presence of trace amounts of ions of iron or certain other transition metals. The presence of as little as 5 ppm iron ions (soluble iron) has been found to result in catalysis of lubricating oil oxidation[3], this small initial concentration being capable of such an effect due to the regeneration of the catalyst via reactions (8) and (9).

Lubricating oils are particularly susceptible to soluble iron catalysed oxidation as the total iron content of used oils has been found to be as high as 800ppm[3]. Although most of this consists of particulate iron metal or iron oxides, produced as a result of wear processes, some soluble iron is also formed. "Soluble iron", i.e. complexes and salts of iron which are soluble in oil, is thought to be formed by direct chemical attack on the engine metal by oxidation products of the oil such as carboxylic acids, alcohols, aldehydes and ketones[4]. The need for the iron to be in a soluble form for catalysis to occur is emphasised by the inability of iron metal or iron oxides to promote the oxidation of lubricating oils[3].

1.3. THE PREVENTION OF OXIDATION

An examination of Scheme 1.1. (Section 1.1.) reveals several ways in which the oxidative chain reaction may be interrupted. The most obvious method is by the removal of oxygen from the system. Although this can be achieved, for example, during the processing of plastics such as polypropylene, it is clearly not possible to exclude oxygen from an automobile engine. Antioxidants are therefore required to protect lubricating oils against thermal oxidation in the engine. These operate by removing the species capable of initiating, propagating or catalysing oxidation. The antioxidant mechanisms of relevance to the inhibition of lubricating oil oxidation are described in Sections 1.3.1.-1.3.3.

1.3.1. HYDROPEROXIDE DECOMPOSITION (PD)

Decomposition of the hydroperoxide formed in step (3) (Scheme 1.1.) to non-radical products will mean that no further initiation can occur. Two types of hydroperoxide decomposition are known. Stoichiometric hydroperoxide decomposition, (PD-S), whereby one hydroperoxide molecule is decomposed by each antioxidant molecule is typified by the use of trialkyl phosphites as polymer stabilisers[5] (reaction 11).

$$(RO)_3P + R^1O_2H \longrightarrow (RO)_3P{=}O + R^1OH \qquad (11)$$

Of much greater use are catalytic hydroperoxide decomposers. (PD-C). One molecule of these compounds, of which zinc dialkyldithiophosphates (ZnDRP, I) are an example, can lead to the decomposition of many molecules of hydroperoxide to inert products, i.e. species not capable of initiating or propagating oxidation.

$$\{(RO)_2PSS\}_2Zn$$

(I) ZnDRP

The mechanism of hydroperoxide decomposition by ZnDRP is discussed in detail in Section 1.4.1.

1.3.2. CHAIN BREAKING ANTIOXIDANT MECHANISMS (CB)

A further way in which the oxidation chain may be stopped is by reaction of the free radicals produced in the propagation steps (2) and (3) to give products that are incapable of initiating further chains, i.e. radical scavenging. Deactivation of alkyperoxyl radicals occurs via donation of an electron by an antioxidant. (CB-D mechanism). Hindered phenols and aromatic amines are commonly used as CB-D antioxidants. (reactions (12) and (13)).

$$RO_2^{\cdot} + ArOH \longrightarrow ArO^{\cdot} + RO_2H \qquad (12)$$

$$RO_2^{\cdot} + Ar_2NH \longrightarrow Ar_2N^{\cdot} + RO_2H \qquad (13)$$

In addition to their hydroperoxide decomposing activity, ZnDRPs are also capable of acting as radical traps and their mechanism of action is discussed further in Section 1.4.3.

Deactivation of alkyl radicals may occur via acceptance of an electron by an antioxidant such as nitroxyl radical. (CB-A mechanism, reaction 14). This mechanism is however only important under conditions where a significant concentration of alkyl radicals is present, i.e. when there is a deficiency of oxygen or when the rate of initiation (reaction 1) is very high.[6]

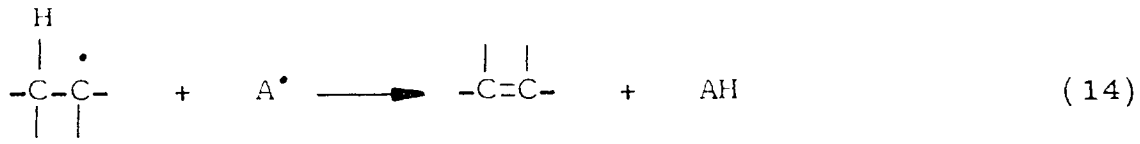

(14)

1.3.3. METAL ION DEACTIVATION

In the case of metal-ion catalysed oxidation it is clear that removal of the metal ions will lead to a reduction in the extent of oxidation. Metal-ion deactivators are usually chelating agents and can work in several ways. If the metal ion can be complexed to its maximum co-ordination number or if one valency state can be stabilised at the expense of others, then inhibition of metal-ion catalysed oxidation may be achieved. In addition, any reaction between metal ion and complexing agent leading to the formation of an insoluble metal complex may also lead to inhibition. If, however, the metal-ion deactivator is not itself an antioxidant, oxidation may still be able to proceed at the uncatalysed rate.

1.4. MECHANISMS OF ANTIOXIDANT ACTION OF ZINC DIALKYL DITHIOPHOSPHATES

ZnDRPs have been used as lubricating oil additives for the past 40-50 years. In addition to being anti-wear agents, they are also extremely efficient antioxidants under the conditions experienced in a typical internal combustion engine. The mechanisms by which ZnDRPs act as antioxidants have been established over the past 30 years and are reviewed in Sections 1.4.1. - 1.4.4.

1.4.1. ZnDRPs AS HYDROPEROXIDE DECOMPOSERS

The ability of a ZnDRP to decompose cumene hydroperoxide (CHP, II) was first demonstrated in 1956 by Kennerly and Patterson.[7]

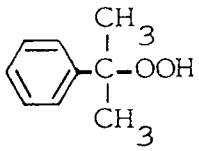

(II) CHP

Of a variety of organic, sulphur containing compounds tested, ZnDRP was found to be the most effective decomposer of CHP in white oil at 150°C. The high yield of phenol formed, up to 75%, was indicative of an ionic decomposition mechanism of the type proposed by Hock and Lang,[8] (Scheme 1.2.), where E represents an electrophilic species.

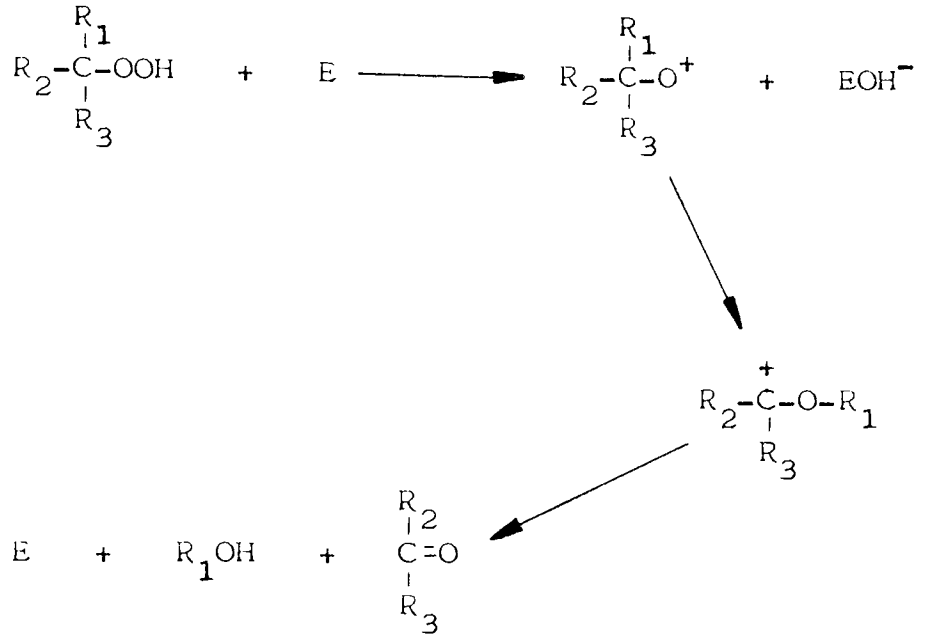

Scheme 1.2. Ionic decomposition of hydroperoxides.[8]

Kennerly and Patterson[7] considered that the species responsible for hydroperoxide decomposition was not the original zinc complex but rather the product(s) of the ZnDRP/CHP interaction. No suggestion was made regarding its identity. In addition to the ionic CHP decomposition, the existence of free radical processes was also evident from the pro-oxidant effects observed when CHP was decomposed by ZnDRP in the presence of air. The occurrence of an initial pro-oxidant effect on addition of ZnDRP to an oxidising hydrocarbon containing CHP has been observed by some authors[7,9,10] but not by others.[11,12] These apparently conflicting results probably arise from the wide range of experimental conditions employed in these studies.

Similarities between the behaviour of ZnDRP and the structurally related zinc dialkyldithiocarbamate(ZnDMC) as inhibitors of the tetralin hydroperoxide initiated oxidation of tetralin at 50°C led Holdsworth and co-workers[12] to suggest that a common hydroperoxide decomposing species was derived from each zinc complex. Sulphur dioxide was suggested as the catalyst responsible for the ionic decomposition of hydroperoxides as it was observed to be formed on reacting ZnDMC with CHP. In addition, the gas was found to rapidly decompose CHP to phenol and acetone. No evidence was, however, presented to show that sulphur dioxide was formed by the reaction of ZnDRP and CHP, and subsequent work[13,14] has also failed to detect the gas.

Husbands and Scott[15] later showed that sulphur dioxide only undergoes a stoichiometric reaction with hydroperoxides during which some free radical generation occurs. The product of the reaction, sulphur trioxide, was however found to be a powerful catalyst for the decomposition of CHP to phenol and acetone. (Scheme 1.3.)

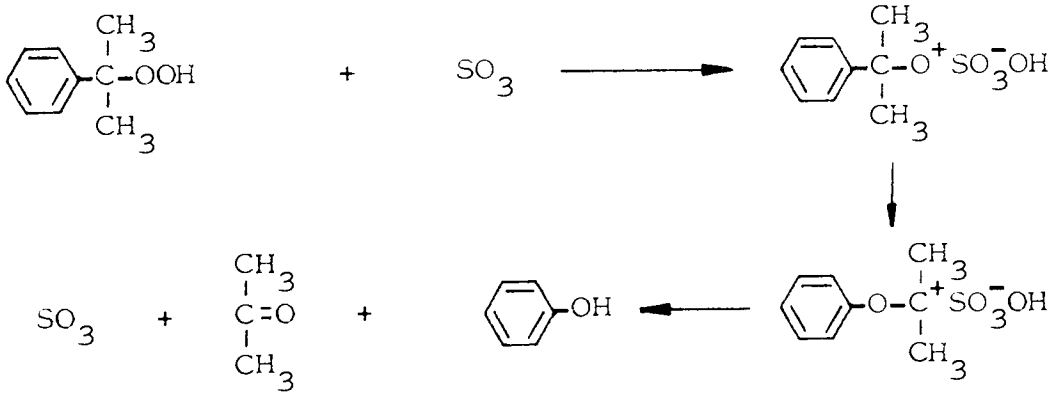

Scheme 1.3. Ionic decomposition of CHP by sulphur trioxide[15]

The reaction of ZnDRP with CHP in non-oxidisable systems has been studied by several groups of workers. Burn and co-workers,[13] in 1971, demonstrated the existence of three distinct stages occurring during the decomposition of CHP by ZnDRP at 70°C in chlorobenzene. An initial rapid stage was followed by a period of slow reaction, ("induction period"), after which a further fast reaction took place to destroy all the remaining CHP. The importance of each stage was determined by the initial CHP:ZnDRP ratio used. The use of a catalytic amount of ZnDRP (CHP:ZnDRP = 100:1) led to the decomposition of CHP predominantly by the third stage reaction, which was shown to occur via an ionic mechanism to form phenol and acetone. Alternatively, a stoichiometric amount of ZnDRP (CHP:ZnDRP = 2:1) was found to decompose CHP mainly by the first stage reaction, which was shown to be a homolytic process as evidenced by the formation of α-cumyl alcohol. This initial decomposition of hydroperoxide, which was responsible for the pro-oxidant effect observed during the oxidation of hydrocarbons in the presence of ZnDRP and CHP,[7,9,10] has been shown[16] to occur via the intermediate formation of a ZnDRP/CHP complex. (reaction 15)

$$\{(RO)_2PSS\}_2Zn + RO_2H \rightleftharpoons [\{(RO)_2PSS\}_2Zn.....RO_2H] \downarrow \text{free radicals} \qquad (15)$$

The existence of the induction period, which was longest in the presence of a high ZnDRP concentration, was attributed to the formation of a zinc containing precipitate during the rapid first stage of hydroperoxide decomposition. A similar precipitate has, however, been proposed by Rabl and Mostecky[17] as being responsible for the ionic decomposition of CHP.

Most of the initial ZnDRP present was consumed during the first stage reaction,[13] thereby illustrating that the catalyst for the third stage ionic decomposition was a product derived from the ZnDRP/CHP interaction. The catalytic species could not be identified by Burn and co-workers[13] but it was considered to be formed via free radical reactions because addition of a radical trap delayed the onset of the ionic CHP decomposition stage. Although the dialkylthiophosphoryl disulphide (DRDS,III) was isolated as a major product of the first stage reaction, this was not considered to be the catalyst, as it was found to be inactive as a hydroperoxide decomposer at low concentrations. DRDS has, however, been claimed by Shkhiyants and co-workers[18] to be the species responsible for ionic hydroperoxide decomposition.

$$\{(RO)_2PSS\}_2$$

(III) DRDS

A three stage reaction between ZnDRP and CHP at 70°C was also observed by Ohkatsu and co-workers[19], who claimed that the catalyst for ionic hydroperoxide decomposition was sulphuric acid. To account for the increase in the length of the induction period with increasing ZnDRP concentration, it was proposed that any unreacted ZnDRP present after the end of the first stage could trap any sulphuric acid formed, thus giving zinc sulphate. This seems unlikely, however, in view of the findings of Burn and co-workers,[13] that most of the ZnDRP used was destroyed in the first stage of its reaction with CHP.

A variety of sulphur containing products formed by the oxidation of ZnDRP by CHP have been identified by different groups of workers.[10,13,20] Sanin and co-workers[20] found that the initial oxidation products derived from ZnDRP (CHP:ZnDRP = 2:1) were basic zinc dialkyldithiophosphate (b-ZnDRP, IV) and DRDS,(Scheme 1.4.), the latter also having been isolated by Burn and co-workers[13] as a product of the rapid first stage decomposition of CHP by ZnDRP. Further oxidation of the disulphide[20] led to the formation of dialkylphosphoryl disulphide (DRODS,V), which on hydrolysis gave dialkyl-thiophosphoric acid (VI) and dialkylphosphoric acid (DRPA,VII),(Scheme 1.4.). Dialkylthiophosphoryl trisulphide (VIII) was also identified as a product of the prolonged oxidation of ZnDRP by CHP. Of these products, (III), (IV), (V) and (VIII) were found to be active inhibitors of hydrocarbon oxidation.[20]

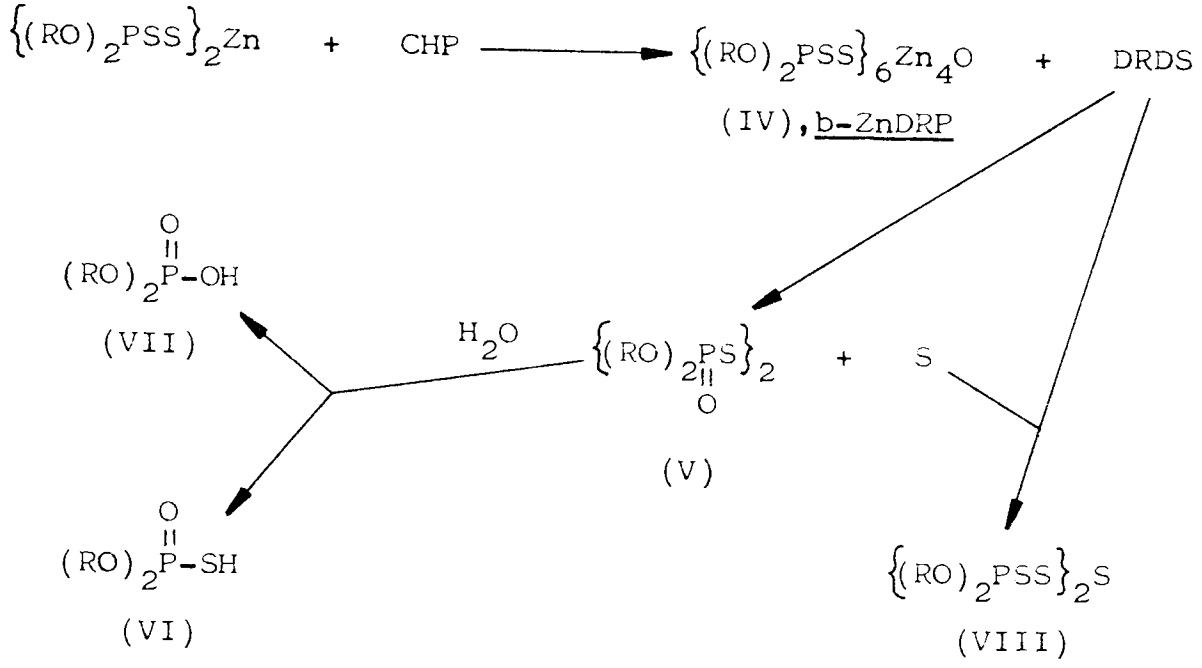

Scheme 1.4. Oxidation of ZnDRP by CHP

Rossi and Imperato[10] also identified DRODS as a product of the reaction of ZnDRP and CHP (CHP:ZnDRP = 4:1), but considered it to be formed by the oxidation of b-ZnDRP formed in the initial reaction.(Scheme 1.5.). Three stages of CHP decomposition were observed, similar to the results of Burn and co-workers[13] and Ohkatsu and co-workers.[19]

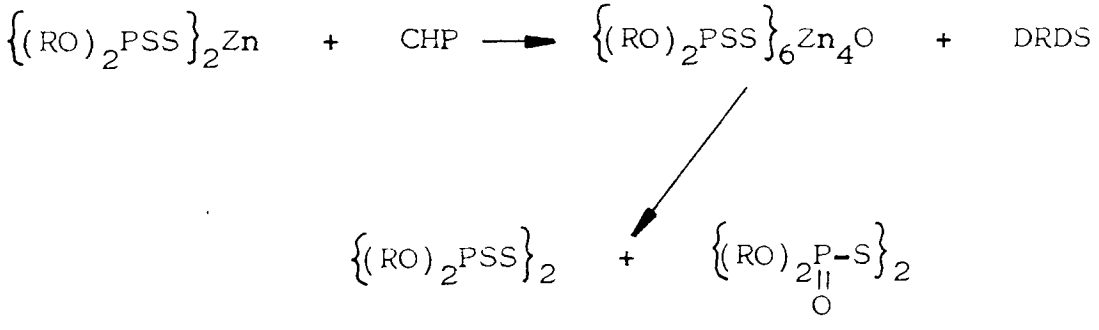

Scheme 1.5 Oxidation of ZnDRP by CHP[10]

The oxidation of DRDS, identified by each of the above authors[10,13,20] as an initial product during the oxidation of ZnDRP by CHP, has been studied in detail by Grishina and co-workers.[21] The reaction, (CHP:DRDS = 20:1), was found to proceed slowly at 80°C and led mainly to the formation of esters of dialkylthiophosphoric acid, (IX),(X), along with a small amount of DRPA. In addition, it was considered that the oxidation of elemental sulphur, liberated during the reactions summarised in Scheme 1.6., could lead to the formation of sulphuric and alkylsulphonic acids, these being derived from sulphur dioxide and alkylpolysulphides respectively.

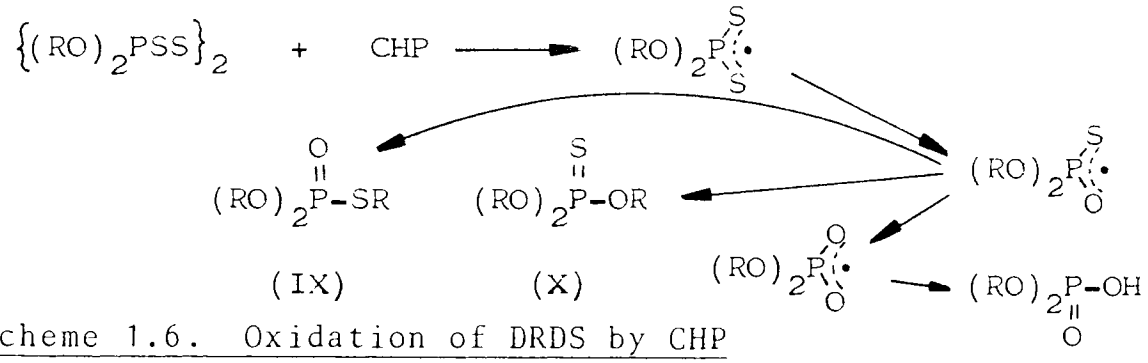

Scheme 1.6. Oxidation of DRDS by CHP

The products arising from the oxidation of DRDS by CHP have also been studied by Al-Malaika and Scott,[22] who showed that sulphur trioxide, formed from the oxidation of sulphur dioxide by CHP, was responsible for the ionic decomposition of CHP. The sulphur dioxide was considered to be formed by elimination from unstable intermediate compounds (Scheme 1.7.) in a reaction which also yielded dialkylthiophosphoric acid.(DRTPA, XI).

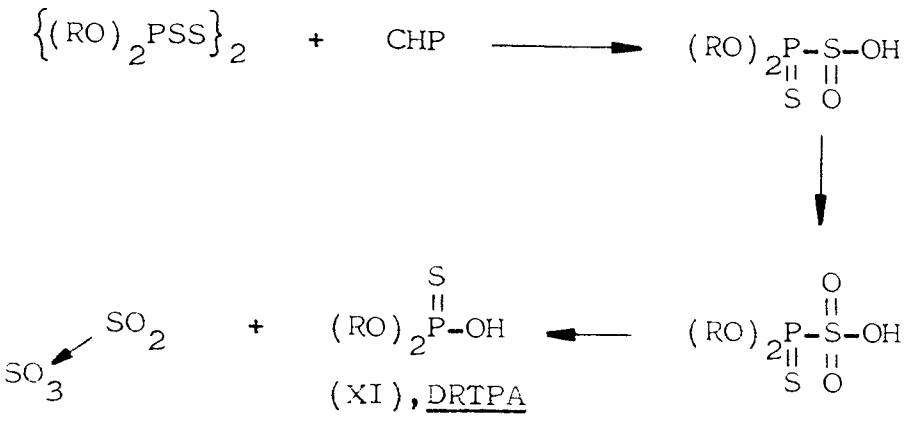

Scheme 1.7. Oxidation of DRDS by CHP[22]

In addition to the phosphorus containing species already mentioned as products identified as being formed from the reaction of ZnDRP or DRDS with CHP, several others have also been observed, such as esters of dialkyldithiophosphoric acid, (XII);[23] esters of dialkylphosphoric acid, (XIII);[23] and zinc dialkylthiophosphate (ZnDRT, XIV).[24]

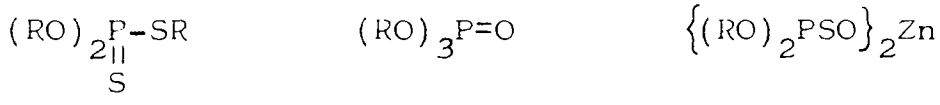

(XII) (XIII) ZnDRT(XIV)

Although dialkyldithiophosphoric acid (DRDPA, XV), has not been observed as a product of the reaction of ZnDRP and CHP, it has been proposed as the catalyst responsible for the ionic decomposition of CHP.[25,26]

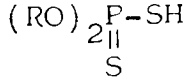

(XV) DRDPA

Bridgewater and co-workers[25] proposed that the same species, DRDPA, was formed from ZnDRP, b-ZnDRP and DRDS although the hydroperoxide decomposing ability of each was found to be different. DRDPA was considered to be formed from ZnDRP via hydrolysis by any traces of moisture present. Several observations have been made, however, which are not consistent with DRDPA being the catalyst. Firstly the activity of DRDPA as a hydroperoxide decomposer was found to be less than that of ZnDRP.[25] In addition, the reaction of DRDPA with CHP has been shown by Johnson and co-workers[27] and by Grishina and co-workers[26] to lead to the formation of DRDS and α-cumyl alcohol, i.e. a homolytic hydroperoxide decomposition. Cherkasova and co-workers[28] have, however, shown that a molecule of DRDPA can react with up to 20,000 CHP molecules, with both radical and ionic decomposition processes occurring.

1.4.2. HYDROPEROXIDE DECOMPOSITION BY OTHER METAL DITHIOPHOSPHATES (MDRPs)

Although a three step decomposition of CHP has been reported to be caused in the presence of other metal dialkyldithiophosphates, such as CuDRP[29] and NiDRP,[30] it is, for several reasons, wrong to assume that all MRDPs act as hydroperoxide decomposers by exactly the same mechanism. Firstly, for no metal other than zinc has the existence of a basic dithiophosphate been proved,

this would be expected to affect the early stages of CHP decomposition as b-ZnDRP has shown to be a major product of the initial reaction of ZnDRP and CHP.[10,20,24] The formation of acetophenone in the presence of NiDRP,[30] rather than α-cumyl alcohol which is formed from the use of ZnDRP,[10,13,15,20] may be a reflection of such differences in the initial mechanism of CHP decomposition. In addition, the length of the secondary induction period was found to decrease with increasing NiDRP concentration,[30] whereas for ZnDRP the induction period increased in duration as the metal complex concentration was increased.[13,19].

The dependence of the first and third stages on the initial NiDRP concentration has, however, been found[30] to be similar to that reported for the zinc complex.[13,19] Thus the first stage homolytic decomposition was favoured when a high NiDRP concentration was present[30] and corresponds to the process described by Howard and co-workers[31] as being responsible for the pro-oxidant effect of NiDRP in the presence of hydroperoxides. The third stage ionic decomposition of CHP was most important when a low NiDRP concentration was employed.[30] Ionic decomposiiton of CHP by catalytic amounts of NiDRP and FeDRP has also been reported by Holdsworth and co-workers.[12]

The differences between the hydroperoxide decomposing behaviour shown by ZnDRP and NiDRP have been explained[14] in terms of the relative resistance to hydrolysis of the two metal complexes. The easily hydrolysed zinc complex is very sensitive to traces of moisture present, the DRDPA formed being the catalyst for ionic hydroperoxide

decomposition. Other, more resistant MDRPs, including NiDRP, also act via the formation of DRDPA, but here the acid is formed by the interaction of MDRP and hydroperoxide.

1.4.3. ZnDRPs AS ALKYLPEROXYL RADICAL TRAPS

The ability of ZnDRPs to trap alkylperoxyl radicals, $RO_2^{\cdot}$, was first demonstrated in 1964 by Colclough and Cuneen[32] who found that the zinc complex was capable of inhibiting the AZBN (azo-bisbutyronitrile) catalysed oxidation of squalene at 60°C. It was considered that deactivation of the alkylperoxyl radicals took place via an electron transfer mechanism,(reaction 16), although no evidence was produced to support this.

$$RO_2^{\cdot} + \{(RO)_2PSS_2\}Zn \longrightarrow RO_2^{-} + (RO)_2PSS\overset{+\cdot}{Z}nSSP(OR)_2 \quad (16)$$

In addition to ZnDRP, other sulphur containing metal complexes such as zinc dialkyldithiocarbamate and zinc dialkyl xanthate were also found to be able to scavenge alklyperoxyl radicals.[32] A more detailed study of the reaction of various MDRPs with alkylperoxyl radicals was carried out by Burn.[33,34] In addition to ZnDRP, the dithiophosphates of potassium, lead, iron (III), nickel, cadmium and copper (I) were also found to act as radical traps. The thiophosphoryl disulphide (DRDS) was, however, found to be unable to deactivate alkylperoxyl radicals.[33]

and several groups of workers have since confirmed this finding.[11,27,35,36] Similarly, zinc dilaurylphosphate was found to be unreactive towards alkylperoxyl radicals.[33] From this evidence Burn considered that the presence of both sulphur and a metal atom was necessary for the deactivation of an alkylperoxyl radical to occur. Scheme 1.8. was proposed to account for the observed behaviour.

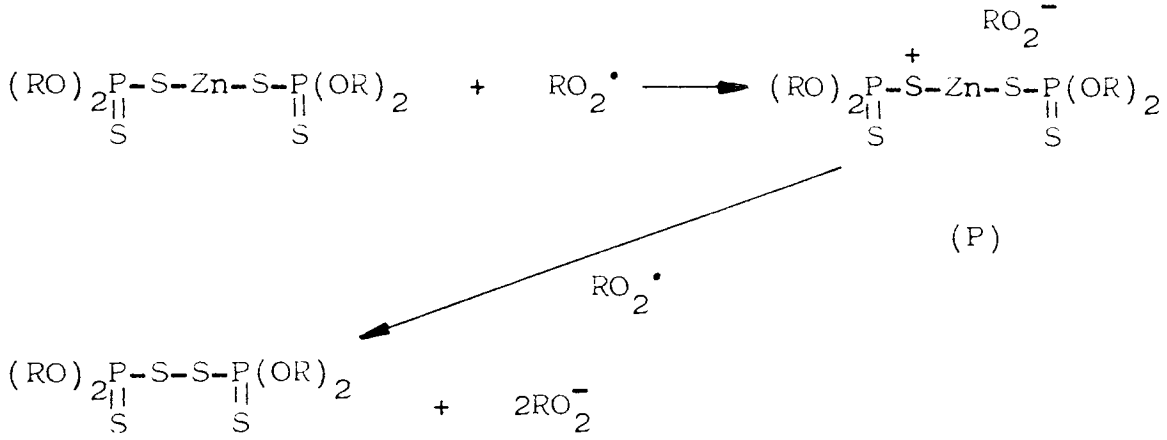

Scheme 1.8. Deactivation of alkylperoxyl radicals by ZnDRP.[33]

The initial electron transfer reaction from sulphur atom to peroxyl radical was considered by Sanin and co-workers[20] to occur at the thiolic, rather than thionic sulphur atom present in the ZnDRP molecule. The function of the metal atom was to provide an easy route for heterolysis of the peroxyl radical stabilised intermediate (P) in Scheme 1.8.[33]

Although Burn[33] could only isolate a 10% yield of DRDS from the reaction of ZnDRP with alkylperoxyl radicals, Willermet and Kandah[36] showed that up to 60% DRDS was in fact formed during the reaction. Several

other minor products were also found, including an unidentified phosphorus containing but sulphur free compound. A white precipitate of hydrated zinc sulphate accounted for all the zinc present in the original ZnDRP.

The possibility of the reaction of alkylperoxyl radicals with MDRPs occuring at the metal atom was favoured by Howard and co-workers[11,37] on account of the observed lack of reaction between alkylperoxyl radicals and either DRDS or triesters of dialkyldithiophosphoric acid, e.g. (XII). Two mechanisms were considered to be possible. (reactions 17 and 18).

$$RO_2^{\cdot} + \{(RO)_2PSS\}_2Zn \rightarrow RO_2^{-} + \overset{+}{Z}nSSP(OR)_2 + (RO)_2PSS^{\cdot} \quad (17)$$

$$RO_2^{\cdot} + \{(RO)_2PSS\}_2Zn \longrightarrow ROO\text{–}ZnSSP(OR)_2 + (RO)_2PSS^{\cdot} \quad (18)$$

The free dithiophosphate radical formed in both reactions (17) and (18) could then undergo further reaction with a second alkylperoxyl radical to give inert products. (reaction 19).

$$(RO)_2PSS^{\cdot} + RO_2^{\cdot} \longrightarrow \text{inert products} \quad (19)$$

The effect of hydroperoxides on the radical scavenging efficiency of ZnDRP has been studied by Korcek and co-workers[35] and by Johnson and co-workers.[27] Although, in agreement with earlier work,[33] ZnDRP was itself found to be an effective radical scavenger, the interaction of ZnDRP with hydroperoxides was found to lead to the formation of a very powerful radical trap of unknown composition.[27,35] Such ZnDRP/hydroperoxide interactions

were considered [35] to be responsible for the variation in the reported value of 'n',[11,34] the number of alkylperoxyl radicals trapped by one ZnDRP molecule, between 1 and 4. Of the known products of the ZnDRP/hydroperoxide interaction, DRDS[27,35] and b-ZnDRP[35] were found to be inactive as radical traps. Although DRDPA is know to be an effective radical trap,[11,20,36] it too formed a more powerful species on reaction with hydroperoxides.[27,35]

1.4.4. ZnDRPs AS METAL-ION DEACTIVATORS

It has been shown by workers at Esso[3] that the addition of a ZnDRP to a base oil containing traces of soluble iron completely overcomes the catalysis of oxidation promoted by the iron (III) ions in its absence. A similar effect has also been observed[3] for a range of MRDPs (M = Na, Ca, Mg) when present in a fully formulated lubricant used in a standard engine test. These findings led Colclough and Gibson[3] to propose that, in addition to hydroperoxide decomposition and alkylperoxyl radical trapping, MDRPs possess a third antioxidant mechanism, i.e. iron deactivation. A reaction scheme, whereby iron dialkyldithiophosphate (FeDRP, XVI) is formed as an unstable intermediate decomposing to an inactive iron compound was proposed (Scheme 1.9.), although no evidence for the formation of the iron complex (FeDRP) was given. The apparent instability in air of FeDRP has been observed by several authors.[38,39,40].

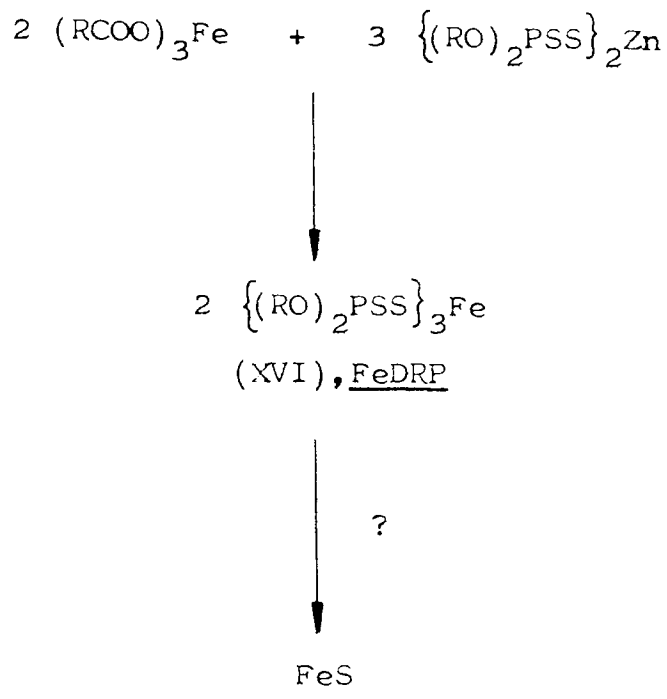

Scheme 1.9 Possible mechanism of soluble iron deactivation by ZnDRP[3]

Although several groups of workers[41,42,43] have shown that the reaction of iron metal and a ZnDRP leads to metal exchange, resulting in the formation of FeDRP (reaction 20),[43] no work has been carried out on the reaction of iron salts with ZnDRPs and related compounds. In addition, no work has been reported on the effect of ZnDRPs on hydrocarbon oxidation catalysed by soluble iron.

$$3\ \{(RO)_2PSS\}_2\ Zn + 2\ Fe^{3+} \longrightarrow 2\ \{(RO)_2PSS\}_3Fe + 3Zn^{2+} \qquad (20)$$

1.5 RELEVANCE OF LABORATORY STUDIES TO "IN-VITRO" SYSTEMS

Although the work summarised in Sections 1.4.1.-1.4.4. has led to a better understanding of the way in which ZnDRPs function as antioxidants, it is dangerous to assume that exactly the same processes are necessarily occurring in fully formulated lubricants in use in automobile engines. Whereas the mechanistic studies have largely been carried out in clean systems and have generally concentrated on one particular interaction (e.g. ZnDRP/hydroperoxide), the environment present in an engine is much more complex. In addition to interactions with primary oxidation products, i.e. $RO_2^{\cdot}$ and RO_2H, ZnDRPs may also undergo reaction with secondary oxidation products such as carboxylic acids. Hydrolytic and thermal decomposition is also a possibility, along with reaction with soluble iron and with products of the combustion process, such as nitrogen oxides and lead compounds.

Furthermore, the presence, in a fully formulated lubricating oil, of other additives, particularly dispersants and detergents, can lead to interactions with both ZnDRP and its degradation products, thus modifying the degree of inhibition achieved. Attempts to clarify the mechanisms of ZnDRP action during the everyday use of lubricating oils in automotive engines are summarised in Section 1.6.

1.6 MECHANISMS OF ZnDRP DEPLETION DURING USE IN LUBRICANTS

According to Johnson and co-workers,[27] the oxidation of a lubricant in an engine is initiated by free radicals formed during the combustion process. Hydroperoxides build up and are thermally decomposed (engine temperatures are as high as 160°C) to generate further free radicals, which can then continue the oxidative chain reaction. Although, in a new oil, the depletion of ZnDRP has been found to occur primarily via reactions with combustion derived free radicals,[35] the addition of a fresh oil, containing ZnDRP, to an old, oxidised oil leads to a rapid drop in the radical trapping ability of the antioxidant.[35] This has been attributed to the interaction of ZnDRP with hydroperoxides. In addition to the expected products of such an interaction, i.e. DRDS and b-ZnDRP, the formation of an unidentified, but very effective, radical trapping species has also been demonstrated. Carboxylic acids, which are known to be secondary products of the oxidation of hydrocarbons, are also capable of converting ZnDRP to this strong antioxidant. The formation of this species from either interaction, i.e. ZnDRP/hydroperoxide or ZnDRP/carboxylic acid, required the additional presence of alkylperoxyl radicals. The existence of a reaction between ZnDRP and carboxylic acids has also been demonstrated by Willmermet and co-workers.[44] Although, in practice, fresh oil is not added to a highly oxidised oil, bad drainage of the latter may lead to the presence of appreciable amounts of contaminants, enabling the above reactions to take place.

Although, as mentioned above, the depletion of ZnDRP in a new oil is thought to occur initially by reaction with alkylperoxyl radicals, oxidative decomposition promoted by hydroperoxides has also been found to take place, both in fully formulated oils[30,44-48] and in mineral oil alone.[48] A wide variation in the nature of the products formed has, however, been reported. Marshall,[45] Barber and Yamaguchi,[46] and Sanin and co-workers[20] have demonstrated the formation of highly oxygenated phosphorus species during the use of a fully formulated lubricant containing ZnDRP. Products of this type are typical of the interaction of ZnDRP and a hydroperoxide such as CHP.[10,20,23,24] Alternatively, Coy and Jones[48] have demonstrated the formation of "soluble phosphate compounds", via ZnDRT (XIV) as an intermediate, also during the use of a fully formulated oil. Despite the differences observed in the type of products formed, it is clear that oxidative degradation is the major pathway of ZnDRP depletion in fully formulated lubricants in automobile engines. No evidence has been found to suggest that thermal decomposition is an important pathway of ZnDRP degradation under such conditions. Esters of trithio- and tetrathiophosphoric acids, e.g. (XVII) and (XVIII), which have been shown to be the major products of the thermal (hydrolytic) decomposition of ZnDRPs,[23,49,50] have not been observed during the use of zinc complexes as antioxidants in engine lubricants.

$(RS)_3P=O$ (XVII)

$(RS)_3P=S$ (XVIII)

Of the other additives present in a fully formulated commercial lubricating oil,[31] the presence of dispersants and detergents has been found to most seriously affect the antioxidant performance of ZnDRPS.[3] Dispersants, which are present to prevent the formation of, or which can keep in suspension, substances that would give rise to sludge, are usually amine functional compounds,[31] and have been found to react with ZnDRPs to give either ionic or non-ionic complexes.[52] In addition to reacting with the parent zinc complex, dispersants have also been shown to be able to react with sulphur containing acids.[53] The latter interaction leads to a retardation of the third stage ionic decomposition of hydroperoxides (Section 1.4.1.), thus lowering the activity of ZnDRPs in a fully formulated lubricant relative to that in a base oil alone.

In contrast, the presence of a detergent, such as calcium sulphonate, which is necessary to deal with deposits formed during engine running at high temperatures,[31] has been shown to have little effect on the ionic decomposition of hydroperoxides by ZnDRP.[53] Although no reaction has been observed between the zinc complex and calcium sulphonate,[53] the interaction of sodium or magnesium sulphonate with ZnDRP has been shown to lead to the formation of the corresponding

metal dithiophosphate.[52] Detergents or dispersants do not, however, significantly affect the oxidation of unstabilised base oils.[3]

1.7. AIMS OF PRESENT WORK

(a) A series of thio- and dithiophosphate compounds (ZnDRP, b-ZnDRP, DRDS, DRDPA, DRTPA) will be prepared.

(b) The antioxidant activity of each of the above compounds will be evaluated, initially using the technique of oxygen absorption. The effect of each additive as an inhibitor of hydrocarbon oxidation will be studied under identical experimental conditions throughout so that comparisons between each antioxidant may readily be made. In addition to the effects of the above additives as inhibitors of the oxidation of pure hydrocarbon substrates, their activity in the presence of added hydroperoxide (CHP) will also be studied, again under the same experimental conditions.

(c) On the basis of the results obtained from the oxygen absorption studies in the presence of CHP, further work will be carried out on the hydroperoxide decomposing activity of each of the above compounds. The disappearance of CHP in an inert medium will be monitored by an iodometric technique. By maintaining identical experimental conditions for each of the reactions, a comparison of each of the additives as hydroperoxide decomposers may be made. The formation of phosphorus containing products from the oxidation of each of the above additives by CHP will be studied by phosphorus-31 nuclear magnetic resonance spectroscopy (^{31}P NMR) in order to try to identify the compound(s) ultimately responsible for the antioxidant activity of the dithiophosphates.

Although a substantial amount of work has already been reported on some of the above additives as antioxidants in both the presence and absence of added hydroperoxides, a wide variety of experimental conditions have been employed. The work in sections (b) and (c) is therefore necessary to establish the properties of the dithiophosphates as inhibitors under standardised conditions. The information thereby obtained may then be used as the control data for the results achieved in the presence of iron stearate.(FeST).

(d) Using the same experimental conditions as employed for the work described in section (b), the activity of the dithiophosphates as antioxidants in the presence of FeST will be evaluated by the oxygen absorption technique. Studies will be made in both the absence and presence of added CHP. Comparison of the results obtained here with those from the work in section (b) will indicate the extent to which the various antioxidants can overcome the catalytic effect of the FeST.

(e) The effectiveness of the dithiophosphates as hydroperoxide decomposers in the presence of FeST will be studied in an inert medium under the same conditions as in section (c). In addition, the decomposition products derived from the CHP will be identified by gas-liquid chromatography (GLC) in order to determine the type of hydroperoxide decomposition occurring. Comparison of the results obtained here with those from the work in section (c) will indicate if, and how, the presence of FeST modifies the way in which the dithiophosphates decompose hydroperoxides.

From the results obtained in sections (d) and (e), an understanding of the way in which FeST affects the antioxidant mechanism of the dithiophosphates will hopefully be achieved. In particular, it is desirable to know whether the iron catalyst may be deactivated via complex formation by reaction with either the original antioxidant compound or derived oxidation products,or whether it is merely the mechanisms of antioxidant action known to occur in the absence of FeST, i.e. radical scavenging and hydroperoxide decomposition, that are still operating and are sufficient to counteract the effect of the FeST.

(f) The preparation of FeDRP will be attempted and, if successful, the iron complex will be evaluated in the same way as the other dithiophosphates.(Sections (b) and(c)) In addition, the conditions under which FeDRP may be formed "in-situ" from the reaction of the dithiophosphates with various iron containing compounds, including FeST, will be investigated. Ultra-violet/visible spectroscopy (UV-VIS) will be used to follow the build-up or decay of FeDRP in the above experiments.

CHAPTER TWO

EXPERIMENTAL

2.1. MATERIALS EMPLOYED

2.1.1. MATERIALS SYNTHESISED

Schemes 2.1 and 2.2 outline the preparation of the phosphorus containing additives evaluated as potential antioxidants in Chapters 3-6.

With the exception of iron (III) di-isopropyl-dithiophosphate (FeDiPP, prepared at Reading University) and di-isopropylthiophosphoryl disulphide (DiPDS, prepared at Esso Research Centre, Abingdon), all the additives used were prepared by the methods described in Sections 2.1.1.1. - 2.1.1.17.

2.1.1.1. PREPARATION OF DI-ISOBUTYLDITHIOPHOSPHORIC ACID (DiBDPA)

$$4\ ROH + P_2S_5 \longrightarrow 2(RO)_2PSSH + H_2S \qquad (21a)$$

810.3g (3.65 moles) phosphorus pentasulphide was added in portions to 1183.1g (15.99 moles) isobutanol over a period of 5 hours at 80°C under an atmosphere of nitrogen. Heating was continued for a further 30 minutes after which the solution was cooled to 60°C and stripped of hydrogen sulphide by bubbling nitrogen through it for 1 hour. (The hydrogen sulphide was trapped by subsequently passing the nitrogen

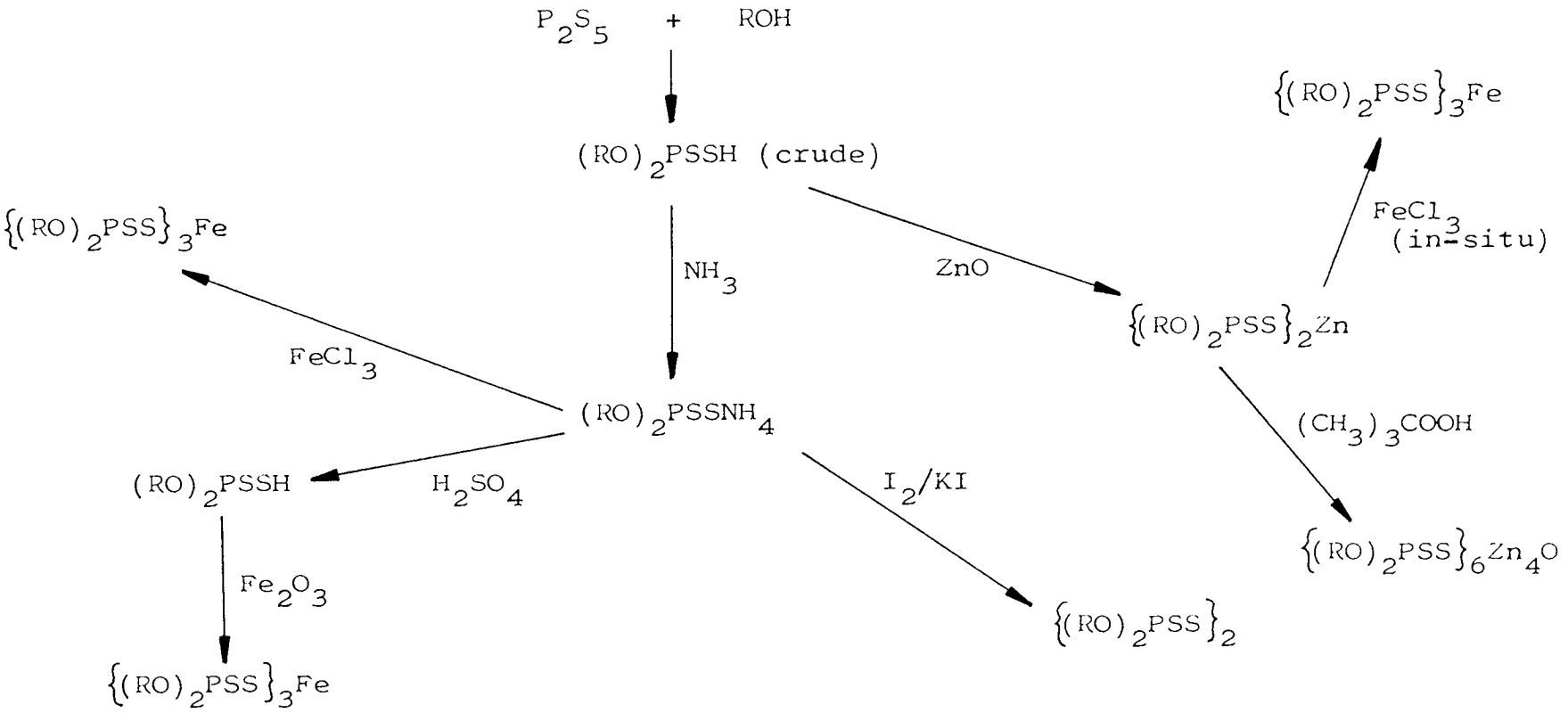

Scheme 2.1. Preparation of dithiophosphates

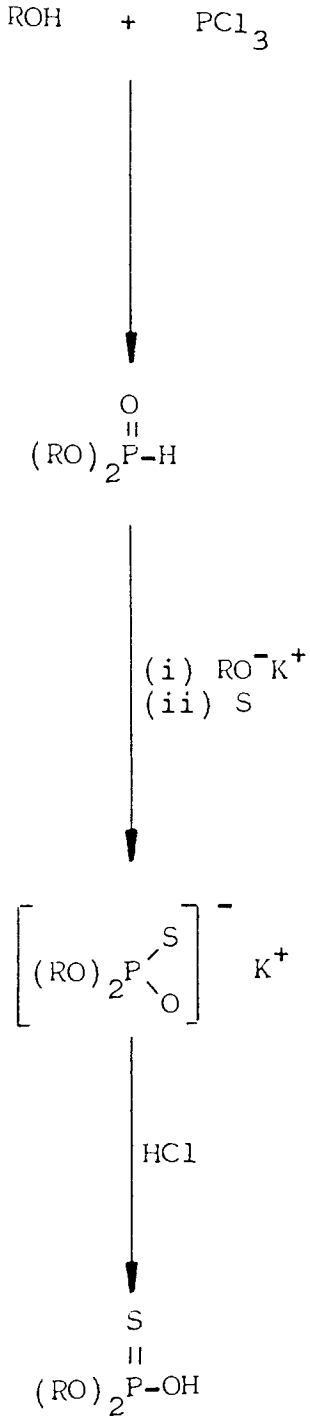

Scheme 2.2. Preparation of dialkylthiophosphoric acid (DRTPA)

flow through an aqueous solution of sodium hydroxide). The solution was then filtered to remove unreacted phosphorus pentasulphide giving 1852.3g of a green liquid.

Analysis

(a) Acid value (A.V., weight in mg of potassium hydroxide needed to neutralise 1g of the product).

A.V. (theoretical)	231.8
A.V. (found)	207.1

As the product was in fact a solution of the required acid in isobutanol, the above result allowed an estimate of the percentage acid present to be made.

$$\% \text{ acid present} = \frac{201.7}{231.8} \times 100$$

$$= \underline{89\%}$$

(b) Phosphorus content

% P (theoretical)	12.01%
% P (found)	12.18%

(c) ^{31}P NMR spectrum (neat liquid, Figure A.1., Appendix)

The major peak at 85.6 ppm was due to the acid. Slight impurity peaks at 70.2, 67.8 and 64.4 ppm were also observed.

2.1.1.2. PREPARATION OF DI-s-BUTYLDITHIOPHOSPHORIC ACID (DsBDPA)

$$4ROH + P_2S_5 \longrightarrow 2(RO)_2PSSH + H_2S \qquad (21b)$$

Procedure as for 2.1.1.1., 809.8g (3.65 moles) phosphorus pentasulphide and 1184.0g (16.00 moles) butan-2-ol yielded 1853.3g green liquid.

Analysis

(a) Acid value (A.V.)

A.V. (theoretical)	231.8
A.V. (found)	207.6

% acid present = 90%

(b) Phosphorus content

% P (theoretical)	12.81%
% P (found)	12.12%

(c) ^{31}P NMR spectrum (neat liquid, Figure A.2., Appendix)

The major peak at 82.4 ppm was due to the acid. Slight impurity peaks at 66.6 and 62.6 ppm were also observed.

2.1.1.3. PREPARATION OF DI-n-HEXYLDITHIOPHOSPHORIC ACID (DnHDPA)

$$4\ ROH + P_2S_5 \longrightarrow 2(RO)_2PSSH + H_2S \qquad (21c)$$

Procedure as for 2.1.1.1., 60.6g (0.59 moles) n-hexanol and 30g (0.14 moles) phosphorus pentasulphide yielded 81.1g of a brownish-green liquid. No analysis of the product was carried out.

2.1.1.4. PREPARATION OF PURIFIED DI-s-BUTYLDITHIOPHOSPHORIC ACID (DsBDPA)

$$(RO)_2PSSH + NH_3 \longrightarrow (RO)_2PSSNH_4 \qquad (22a)$$

$$2(RO)_2PSSNH_4 + H_2SO_4 \longrightarrow 2(RO)_2PSSH + (NH_4)_2SO_4 \qquad (23a)$$

387.2g crude acid (as prepared in section 2.1.1.2.) was dissolved in hexane and treated with ammonia gas introduced under the surface of the stirred solution. The solid which formed was filtered off and washed with hexane giving 262.6g (71% yield) white powder. 40.2g of the product was recrystallised from benzene to give 29.8g white platelets, m.pt. 135-136°C.

18.1g (0.07 moles) recrystallised ammonium salt was dissolved in 30cm³ distilled water, and 10g ice was added. A mixture of 5.6g (0.06 moles) 98% sulphuric acid and 15g ice was then added. After vigorous shaking, the lower layer which separated out was washed twice with water, dried over magnesium sulphate and filtered, to give 6.5g (48% yield) of a pale green liquid.

Analysis

(a) Elemental composition

% C	= 39.7,	% H	= 7.9	(theoretical)
% C	= 40.0,	% H	= 7.9	(found)

(b) IR spectrum (liquid film, Figure A.3., Appendix)

$965cm^{-1}$	-POC
$650cm^{-1}$	-P=S
$2500cm^{-1}$	-P-SH

2.1.1.5. PREPARATION OF PURIFIED DI-n-HEXYLDITHIOPHOSPHORIC ACID (DnHDPA)

$$(RO)_2PSSH + NH_3 \longrightarrow (RO)_2PSSNH_4 \quad (22b)$$

$$2(RO)_2PSSNH_4 + H_2SO_4 \longrightarrow 2(RO)_2PSSH + (NH_4)_2SO_4 \quad (23b)$$

Procedure as for 2.1.1.4., using crude acid prepared in Section 2.1.1.3. The ammonium salt formed was not recrystallised but was instead washed several times with boiling hexane.

The product was a pale green liquid.

Analysis

(a) Elemental composition

An attempt to determine the elemental composition of the product was unsuccessful.

(b) IR spectrum (liquid film, Figure A.4., Appendix)

990 cm^{-1}	-POC
655 cm^{-1}	-P=S
2500 cm^{-1}	-P-SH

(c) ^{31}P NMR spectrum (solution in chloroform, Figure A.5., Appendix)

Only one peak, having a chemical shift of 85.6 ppm, was observed.

2.1.1.6. PREPARATION OF DI-s-BUTYLTHIOPHOSPHORYL DISULPHIDE (DsBDS)

$$2(RO)_2PSSNH_4 + I_2 \longrightarrow \{(RO)_2PSS\}_2 + 2NH_4I \qquad (24a)$$

The disulphide was prepared by the method described by Mikeska.[54] 23.6g (0.09 moles) ammonium di-s-butyldithiophosphate (as prepared and recrystallised in Section 2.1.1.4) was dissolved in 250cm³ distilled water. The resulting solution was boiled with charcoal and filtered, in order to remove a small amount of a black, oily contaminant which was present. A solution of 60g iodine in 500cm³ 12% aqueous potassium iodide was added dropwise, under an atmosphere of nitrogen, until the colour of the iodine persisted. The organic layer was extracted with chloroform and the extracts were washed with sodium thiosulphate solution to destroy excess iodine. The solution was then dried over magnesium sulphate, filtered and stripped under vacuum to leave 19.2g (81% yield) of a yellow viscous liquid.

Analysis

(a) IR spectrum (liquid film, Figure A.6., Appendix)

970cm^{-1} -POC

645cm^{-1} -P=S

No -SH band at 2500 cm^{-1}

(b) ^{31}P NMR spectrum (solution in chloroform, Figure A.7., Appendix)

A triplet peak 83.1/82.5/81.8 ppm was due to the disulphide. An additional peak, due to a slight impurity, was observed at 66.6 ppm.

2.1.1.7. PREPARATION OF DI-ISOBUTYLTHIOPHOSPHORYL DISULPHIDE (DiBDS)

$$(RO)_2PSSH + NH_3 \longrightarrow (RO)_2PSSNH_4 \qquad (22c)$$

$$2(RO)_2PSSNH_4 + I_2 \longrightarrow \{(RO)_2PSS\}_2 + 2NH_4I \qquad (24b)$$

387.2g crude acid (as prepared in Section 2.1.1.1.) was treated with ammonia, by the procedure described in Section 2.1.1.4., to give 270.5g (73% yield) of a white powder. 44.2g was recrystallised from benzene to give 22.1g white platelets, m.pt. 145-146°C. 20.4g (0.08 moles) of the ammonium salt was used to prepare 17.2g (84% yield) disulphide by the procedure described in Section 2.1.1.6.[54]

Analysis

(a) Elemental composition

% C = 39.8,	% H = 7.5	(theoretical)
% C = 39.0,	% H = 7.4	(found)

(b) IR spectrum (liquid film, Figure A.8., Appendix)

$1000cm^{-1}$ -POC

$660cm^{-1}$ -P=S

No -SH band at $2500\ cm^{-1}$

(c) ^{31}P NMR spectrum (solution in chloroform, Figure A.9., Appendix)

The major peak, at 85.6 ppm, was due to the disulphide. Additional peaks at 84.9, 79.2, 70.2 and 67.9 ppm were due to slight impurities.

2.1.1.8. PREPARATION OF ZINC DI-ISOBUTYLDITHIOPHOSPHATE (ZnDiBP)

$$2(RO)_2PSSH + ZnO \longrightarrow \{(RO)_2PSS\}_2Zn + H_2O \qquad (25a)$$

1000.2g (3.69 moles) acid (as prepared in Section 2.1.1.1.) was added dropwise, with stirring, to a slurry of 159.2g (1.97 moles) zinc oxide in $135cm^3$ heptane. The addition was carried out at a temperature of 70°C under an atmosphere of nitrogen, and took 3 hours. When addition was complete, the solution was heated for a further one hour, then cooled and filtered using a filteraid. The solution was stripped under vacuum giving a green solid, which was recrystallised from heptane to give 839g (83%

yield) white crystals, m.pt. 106-108°C. (literature 107°C;[55] 110-111°C[56]).

Analysis

(a) Elemental composition

%C = 35.1, %H = 6.6, %P = 11.3, %S = 23.4, %Zn = 11.9

(theoretical)

%C = 35.3, %H = 6.9, %P = 11.4, %S = 22.6, %Zn = 11.9

(found)

(b) IR spectrum (KBr disc, Figure A.10., Appendix)

$995cm^{-1}$	-POC
$660cm^{-1}$	-P=S

(c) ^{31}P NMR spectrum (solution in chloroform, Figure A.11., Appendix).

The major peak at 98.9 ppm was due to the zinc complex. Slight impurities having chemical shifts of 103.0 (basic ZnDiBP), 79.2, 68.0 and 46.2 ppm were also present.

2.1.1.9. PREPARATION OF ZINC DI-s-BUTYLDITHIOPHOSPHATE (ZnDsBP)

$$2(RO)_2PSSH + ZnO \longrightarrow \{(RO)_2PSS\}_2 Zn + H_2O \qquad (25b)$$

Procedure as described in Section 2.1.1.8., 100.2g (3.70 moles) crude acid (as prepared in Section 2.1.1.2.) and 158.4g (1.96 moles) zinc oxide yielded 658.5 g (65% yield) white crystals, m.pt. 56-57°C. (literature[55] 50°C).

Analysis

(a) Elemental composition

%P = 11.3, %S = 23.4, %Zn = 11.9 (theoretical)

%P = 11.3, %S = 23.1, %Zn = 11.9 (found)

(b) IR spectrum (KBr disc, Figure A.12., Appendix)

$995cm^{-1}$ -POC

$660cm^{-1}$ -P=S

(c) ^{31}P NMR spectrum (solution in chloroform, Figure A. 13., Appendix)

The major peak at 94.1 ppm was due to the zinc complex. A slight impurity having a chemical shift of 43.1 ppm was also present.

2.1.1.10. PREPARATION OF BASIC ZINC DI-ISOBUTYLDITHIO-PHOSPHATE (b-ZnDiBP)

$$4\left\{(RO)_2PSS\right\}_2 Zn + (CH_3)_3COOH \rightarrow \left\{(RO)_2PSS\right\}_6 Zn_4O + \left\{(RO)_2PSS\right\}_2 + (CH_3)_3COH \quad (26a)$$

317.3g (0.58 moles) zinc di-isobutyldithiophosphate (as prepared and recrystallised in Section 2.1.1.8.) was dissolved in 600 cm^3 heptane. 18.7g (0.15 moles) of a 70% solution of t-butyl hydroperoxide in water was added over a period of 45 minutes and the solution was allowed to stand at room temperature for a further 2 hours. After filtration using "Superaid", the solution was stripped under vacuum to leave a yellow solid, which was recrystallised from heptane to give 192.3g (77% yield) white crystals, m.pt. 145°C. (literature[57] 138-140°C).

Analysis

(a) Elemental composition

%C = 33.4, %H = 6.3, %P = 10.8, %S = 22.3, %Zn = 15.1 (theoretical)

%C = 33.6, %H = 6.5, %P = 10.8, %S = 21.9, %Zn = 15.3 (found)

(b) IR spectrum (KBr disc, Figure A.14., Appendix)

$995cm^{-1}$	-POC
$660cm^{-1}$	-P=S
$480cm^{-1}$	ZnO

(c) ^{31}P NMR spectrum (solution in chloroform)

Chemical shift (ppm)	(i)	(ii)
103.0 (b-ZnDiBP)	90%	90%
98.0 (ZnDiBP)	4%	6%
85.7 (DiBDS)	3%	0%
48.4	2%	3%

(i) after one recrystallisation (Figure A.15., Appendix)

(ii) after two recrystallisations (Figure A.16., Appendix)

It is clear from the above that the basic zinc complex could only be obtained 90% pure, and that a small amount of the normal zinc complex was always present.

2.1.1.11. PREPARATION OF BASIC ZINC DI-s-BUTYLDITHIOPHOSPHATE (b-ZnDsBP)

$$4\ \{(RO)_2PSS\}_2\ Zn + (CH_3)_3COOH \longrightarrow \{(RO)_2PSS\}_6\ Zn_4O + \{(RO)_2PSS\}_2 + (CH_3)_3COH \qquad (26b)$$

Procedure as described in Section 2.1.1.10., 307.9 g (0.56 moles) zinc di-s-butyldithiophosphate (as prepared and recrystallised in Section 2.1.1.9.) and 18.2g (0.14 moles) 70% t-butyl hydroperoxide gave 150.7g (62% yield) white crystals, m.pt. 129-130°C.

Analysis

(a) Elemental composition

%P = 10.8, %S = 22.3, %Zn = 15.1 (theoretical)

%P = 10.8, %S = 21.8, %Zn = 14.8 (found)

(b) IR spectrum (KBr disc, Figure A.17., Appendix)

$870cm^{-1}$	-POC
$660cm^{-1}$	-P=S
$480cm^{-1}$	ZnO

(c) ^{31}P NMR spectrum (solution in chloroform)

Chemical shift (ppm)		(i)	(ii)
99.4	(b-ZnDsBP)	80%	83%
93.6	(ZnDsBP)	10%	15%
82.6	(DsBDS)	7%	1%
46.0		1%	1%

(i) after one recrystallisation (Figure A.18., Appendix)

(ii) after two recrystallisations (Figure A.19., Appendix)

2.1.1.12. PREPARATION OF DI-ISOBUTYL HYDROGEN PHOSPHITE

$$3\ ROH + PCl_3 \longrightarrow (RO)_2PHO + RCl + 2HCl \qquad (27)$$

The hydrogen phosphite was prepared by the method described by Foss.[58] To 66.6g (0.9 moles) isobutanol in 75cm³ carbon tetrachloride, was added slowly 41.3g (0.3 moles) phosphorus trichloride in 50cm³ carbon tetrachloride. The addition took place over 75 minutes. The mixture was refluxed (90°C) for 30 minutes and then nitrogen was passed through for 60 minutes as the solution was cooling. The solvent was stripped off under vacuum. Vacuum distillation of the residue gave a colourless liquid, b.pt. 105-106°C (12 mm Hg).

Analysis

(a) IR spectrum (liquid film, Figure A.20., Appendix)

$2420cm^{-1}$	-PH
$1260cm^{-1}$	-P=O
$980cm^{-1}$	-POC

(b) ^{1}H NMR spectrum (solution in d-chloroform, Figure A.21., Appendix).

Chemical shift (ppm)	Assignment
0.9 - 4.0	alkyl group protons
12.6	$(RO)_2P\underline{H}O$

2.1.1.13. PREPARATION OF DI-ISOBUTYLTHIOPHOSPHORIC ACID (DiBTPA)

$$(RO)_2PHO + ROK \longrightarrow (RO)_2POK + ROH \quad (28)$$

$$(RO)_2POK + S \longrightarrow (RO)_2PSOK \quad (29)$$

$$(RO)_2PSOK + HCl \longrightarrow (RO)_2P(S)OH + KCl \quad (30)$$

The acid was prepared by the method described by Foss.[58] 7.6g (0.20 moles) potassium was added to 100cm³ isobutanol. The resultant solution was added to 39g (0.201 moles) of the hydrogen phosphite prepared in Section 2.1.1.12., and 100cm³ diethyl ether was added. 7g (0.22 moles) sulphur was added in portions. The solution was allowed to cool and was then filtered. The filtrate was stripped under reduced pressure until almost dry. The resulting wet solid was washed with 40/60 petroleum ether and allowed to dry. The white powder obtained was dissolved in water, and dilute hydrochloric acid was added. The oily layer which separated out on shaking was washed several times with water, dried over magnesium sulphate and filtered.

Analysis

(a) IR spectrum (liquid film, Figure A.22., Appendix)

$1015cm^{-1}$	-POC	
$640cm^{-1}$	-P=S	
$3250cm^{-1}$	-P-OH	
$2350cm^{-1}$	-P-SH	(v. weak)

No -P=O band at $1260\ cm^{-1}$

(b) ^{31}P NMR spectrum (solution in chloroform, Figure A.23., Appendix).

Only one peak, having a chemical shift of 63.0 ppm, was observed.

(c) ^{1}H NMR spectrum (solution in d-chloroform, Figure A.24., Appendix)

Chemical shift (ppm)	Assignment
0.9 - 4.0	alkyl group protons
7.4	$(RO)_2P(S)O\underline{H}$

No peaks having a chemical shift greater than 10 ppm were observed.

2.1.1.14. ATTEMPTED PREPARATION OF IRON (III) DI-s-BUTYL DITHIOPHOSPATE (FeDsBP)

$$3\ (RO)_2PSSNH_4 + FeCl_3 \longrightarrow \{(RO)_2PSS\}_3Fe + 3NH_4Cl \quad (31)$$

25.9g (0.1 moles) ammonium di-s-butyldithiophosphate (as prepared and recrystallised in Section 2.1.1.4.) was dissolved in 150cm³ distilled water. The resulting solution was boiled with charcoal and filtered, in order to remove a small amount of a black, oily contaminant which was present. 5.4g (0.033 moles) iron (III) chloride was dissolved in 100cm³ distilled water, and the solution was added, with stirring, to the solution of the ammonium salt at room temperature. The resultant black precipitate was filtered off and washed twice with distilled water. The black solid was dissolved in acetone, and the solution was dried over magnesium sulphate and filtered. Evaporation of the acetone left an inhomogeneous solid, consisting of both black and reddish-brown constituents. An attempt to wash the solid with dilute aqueous sodium hydroxide solution led to an increase in the amount of the brown material present.

Analysis

(a) Elemental composition (before sodium hydroxide wash)

% C	= 37.0,	% H	= 6.9	(theoretical)
% C	= 34.2,	% H	= 6.6	(found)

2.1.1.15. PREPARATION OF IRON (III) DI-ISOBUTYLDITHIOPHOSPHATE (FeDiBP) "in-situ"

Example:- Preparation of a 4 x 10^{-3} $moldm^{-3}$ solution of FeDiBP in decalin, for use in oxygen absorption experiments (Section 6.2.1.).

$$3\ \{(RO)_2PSS\}_2Zn + 2\ FeCl_3 \longrightarrow \{(RO)_2PSS\}_3Fe + 3\ ZnCl_2 \qquad (32)$$

A 6 x 10^{-3} $moldm^{-3}$ solution of zinc di-isobutyldithiophosphate (ZnDiBP) in decalin was prepared. To this was added a solution of iron (III) chloride in distilled water so that the molar ratio of ZnDiBP:$FeCl_3$ was 1:1.33. The black organic layer which separated out on vigorous shaking was washed repeatedly with distilled water to remove any unreacted iron (III) chloride, then dried over magnesium sulphate and filtered. The resultant black solution was used immediately.

Analysis

The ultra-violet/visible spectrum of the solution was run and the absorbance of the 596 nm band measured. Comparison of this value with that obtained when an authentic sample of iron (III) di-isopropyldithiophosphate obtained from Reading University was dissolved in n-dodecane, indicated that a "yield" of 97.5% had been achieved.

Different concentrations of FeDiBP were prepared by varying the initial concentration of ZnDiBP used. A similar procedure to that described above for decalin was used to prepare FeDiBP solutions in chlorobenzene for use in hydroperoxide decomposition experiments. (Section 6.2.2.).

2.1.1.16 PREPARATION OF IRON (III) DI-ISOPROPYLDITHIOPHOSPHATE (FeDiPP)

$$6\ (RO)_2PSSH + Fe_2O_3 \longrightarrow 2\ \{(RO)_2PSS\}_3Fe + 3H_2O \quad (33)$$

Purified di-isopropyldithiophosphoric acid was prepared via crude acid (prepared as in Section 2.1.1.1.) and ammonium salt (prepared as in Section 2.1.1.4.). 17.9g (0.08 moles) pure acid was dissolved in $50cm^3$ freshly distilled heptane and the solution was added dropwise, with stirring, to a slurry of 2.5g (0.015 moles) iron (III) oxide in refluxing heptane (freshly distilled). When addition was complete (30 minutes) heating was continued for a further 30 minutes after which the reaction mixture was filtered, whilst hot, to remove unreacted iron (III) oxide. The black needles which crystallised out on cooling were filtered off and rapidly washed with cold, freshly distilled heptane. 9.6g (50% yield) black crystals, m.pt. 112°C, were obtained.

Analysis

(a) IR spectrum (Nujol mull, Figure A.25., Appendix)

$960cm^{-1}$ -POC

$635cm^{-1}$ -P=S

The iron complex used to obtain the results presented in Chapter 6 was prepared at Reading University: m.pt. 110-111°C, IR spectrum; $970cm^{-1}$ (-POC), $640cm^{-1}$ (-P=S).

2.1.1.17. PREPARATION OF IRON (III) STEARATE (FeST)

$$C_{17}H_{35}CO_2H + NaOH \longrightarrow C_{17}H_{35}CO_2Na + H_2O \qquad (34)$$

$$3\ C_{17}H_{35}CO_2Na + FeCl_3 \longrightarrow (C_{17}H_{35}CO_2)_3Fe + 3NaCl \qquad (35)$$

Iron (III) stearate was prepared by the method of Vold and Hattiangdi.[60] 60g (0.21 moles) stearic acid was dissolved in $150cm^3$ absolute ethanol at 60°C, and neutralised to phenolphthalein with a 2 $moldm^{-3}$ solution of sodium hydroxide in water. The resulting gel was liquefied by warming, and the solution added slowly with vigorous stirring to a hot solution of 40.6g (0.25 moles) iron (III) chloride in aqueous 50% ethanol. The precipitated soap was washed free of soluble impurities with distilled water, and then of any adherent unreacted stearic acid or sodium stearate with ethanol and acetone. After pressing out solvent, the soap was oven dried at 50°C for 24 hours before being ground to leave a salmon-pink powder, m.pt. 88-89°C. (literature 90°C,[60] 91°C[61]).

Analysis

(a) Elemental composition

% C	= 71.6,	% H	= 11.6	(theoretical)
% C	= 70.9,	% H	= 11.7	(found)

(b) IR spectrum (Nujol mull, Figure A.26., Appendix)

$1590cm^{-1}$
$1380cm^{-1}$ } 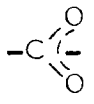

2.1.2. PURIFICATION OF COMMERCIAL MATERIALS

2.1.2.1. DECALIN

Decalin was purified by the method described by Plant.[62] Technical grade material was distilled under vacuum in a nitrogen purged flask, and a 90% centre cut fraction was taken, b.pt. 35°C (Imm Hg). The decalin was shaken with several portions of 10% sulphuric acid until no darkening occurred in either the aqueous or organic phase. The hydrocarbon was then washed several times with water, 10% sodium hydroxide solution and water again, and was then dried over calcium sulphate. The decalin was redistilled under vacuum in apparatus which again had been purged with nitrogen; a slow nitrogen purge was continued during distillation. A 90% centre cut, b.pt. 35°C (1mm Hg) was again taken.

It was necessary that this one batch of purified material was used for all the oxygen absorption experiments, as the different oxidisability of the cis and trans forms of decalin meant that any change in the cis : trans ratio would lead to a variation in the susceptibility of the substrate to oxidation. Once purified, the hydrocarbon was stored under nitrogen, in the dark at 0°C, and the flask was always repurged with nitrogen after a decalin sample had been withdrawn. Immediately prior to use, the hydrocarbon was passed through a column of activated silica to remove any traces of hydroperoxide.

2.1.2.2. CUMENE HYDROPEROXIDE (CHP)

CHP was purified by the method described by Kharasch and co-workers.[63] Commercially available cumene hydroperoxide (supplied as a 75% solution in cumene, water and sodium bicarbonate) was dissolved in freshly distilled diethyl ether, and the solution was cooled to 0°C. A cooled 25% aqueous solution of sodium hydroxide was added, and the white solid that separated out was filtered off and washed thoroughly with 25% aqueous sodium hydroxide and then with a large volume of diethyl ether. When thoroughly dry, the sodium salt was suspended in diethyl ether, and the hydroperoxide was liberated by treatment with a less than equivalent amount of acetic acid. The ether layer was exhaustively washed with dilute sodium bicarbonate solution, followed by further washings with water. After drying over magnesium sulphate, the solution was filtered and stripped of solvent under reduced pressure. The residual liquid was distilled under vacuum, and the fraction boiling at 55°C ($\sim$ 0.1mm Hg) was collected.

Iodometric analysis showed this to be at least 97% pure cumene hydroperoxide. The purified hydroperoxide was stored at 0°C in the dark.

2.1.2.3. t-BUTYL HYDROPEROXIDE (TBH)

Commercial t-butyl hydroperoxide was in the form of a 70% solution in water. The procedure used to purify it was the same as that used for the purification of CHP described in Section 2.1.2.2.[63] The fraction boiling at 55°C (10mm Hg) was found by iodometric analysis to be at least 98% pure t-butyl hydroperoxide. The purified material was stored at 0°C in the dark.

2.1.2.4. CHLOROBENZENE

Chlorobenzene (technical grade) was dried over phosphorus pentoxide, filtered and distilled. The fraction boiling at 132°C (760 mm Hg) was collected and stored in the dark prior to use.

2.1.2.5. PROPAN-2-OL

Propan-2-ol (technical grade) was dried over magnesium sulphate, filtered and distilled. The fraction boiling at 82°C (760mm Hg) was collected and stored in the dark prior to use.

2.1.2.6. ACETIC ACID

Acetic acid (technical grade) was dried over magnesium sulphate, filtered and distilled. The fraction boiling at 116-117°C (760mm Hg) was collected and stored in the dark prior to use.

2.1.3. OTHER MATERIALS

2.1.3.1. TECHNICAL WHITE OIL

The technical white mineral oil used as a substrate for oxygen absorption experiments (Section 2.2.1.) was Marcol 172, supplied by Esso Chemical Limited. Although the exact composition of Marcol 172 is not specified, it is predominantly paraffinic in origin,[64] and is a highly refined product. Once received, it was stored in the dark at 0°C under a blanket of nitrogen.

2.1.3.2. CYCLOHEXANE

'Spectrosol' grade cyclohexane (ex BDH) was used for all ultra-violet/visible spectroscopy (UV-VIS) carried out at 25°C. (Section 2.2.4.)

2.1.3.3. n-DODECANE

'Puriss' grade n-dodecane (ex Koch-Light) was used for all UV-VIS work carried out at 50°C (Section 2.2.4.).

2.1.3.4. MISCELLANEOUS

'Analar' grade sodium iodide and 'Analar' grade sodium thiosulphate pentahydrate was used in the hydroperoxide determination experiments. (Section 2.2.2.). General purpose grade α-cumyl alcohol, α-methyl styrene, phenol, acetophenone, iodobenzene and triphenyl phosphine were used in gas-liquid chromatography. (Section 2.2.3.).

2.2. EXPERIMENTAL TECHNIQUES

2.2.1. OXYGEN ABSORPTION

The determination of the resistance of hydrocarbon substrates to thermal oxidation at 130°C was carried out using the oxygen absorption technique. The apparatus used is shown in Figure 2.1. Each "cell", capable of measuring one oxidation reaction, consisted of two identical 3-necked 50cm^3 round bottom flasks (a sample flask and a dummy flask), each fitted with a glass tap and a stopper. Both flasks were connected, via side arms, to a Pye-Ether pressure transducer (range 5psi), which in turn was wired to a Leeds Northrup Speedomax chart recorder. The sample flask contained a small glass-sheathed bar magnet. All glass joints were thoroughly greased with silicon grease.

The cell was placed in position in a thermostatted bath of silicon oil (130 ± 0.5°C), so that the greased joints were just above the level of the oil. The sample flask was so placed as to be in close proximity to an external horseshoe magnet attached to an overhead stirrer.

Before oxygen absorption measurements could be taken, it was first necessary to calibrate the cell. Firstly, air was removed by syringe from the sample flask, through a needle glued into the top of the tap, until the reading obtained on the recorder was in the centre of the chart, i.e. 50 divisions. Then, a fixed amount (2cm^3) air was removed from the sample flask and the deflection in divisions that resulted was noted. In order to measure oxidation

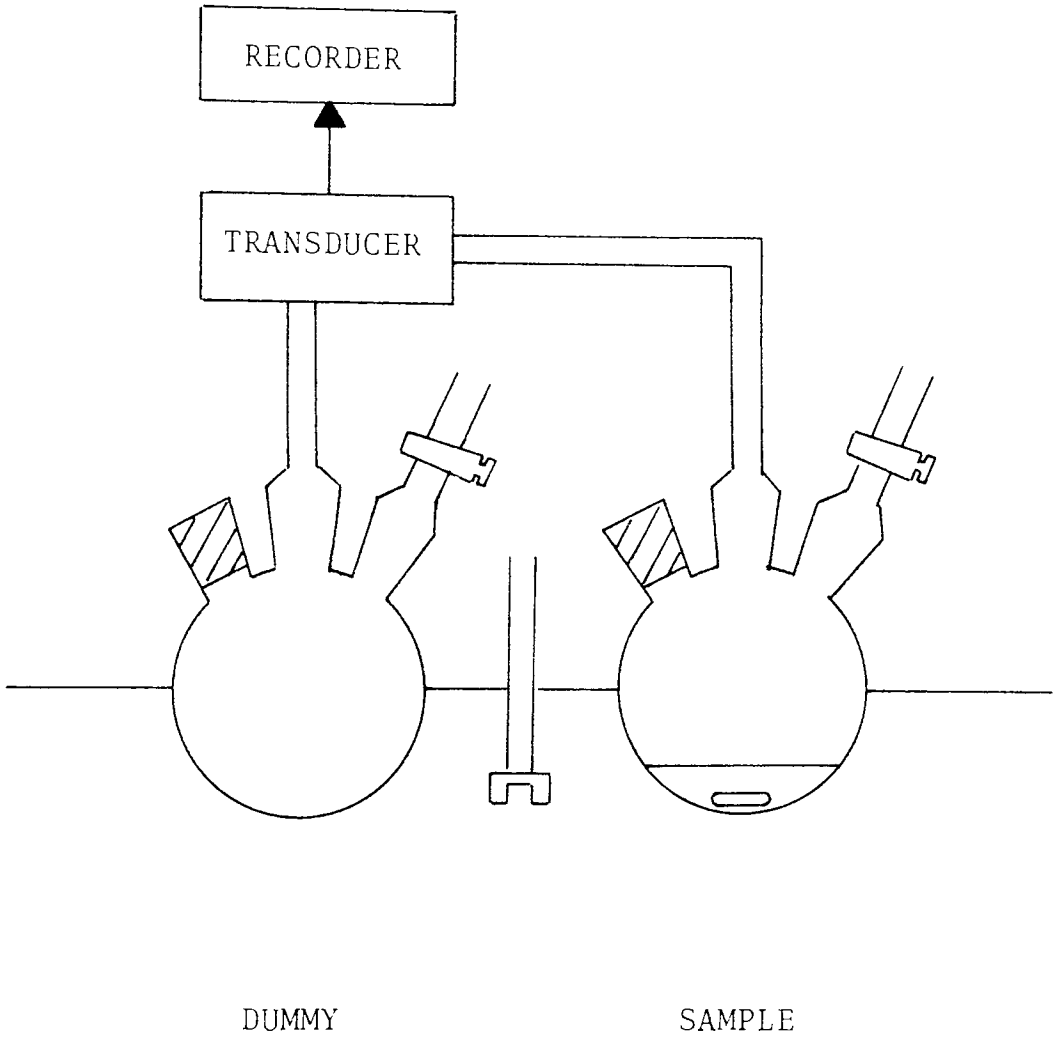

Figure 2.1. Oxygen absorption apparatus

up to a 1% (weight/weight) uptake of oxygen, it was necessary for the recorder to be able to measure the absorption of 40cm³ oxygen. This required that the removal of 2cm³ oxygen should give a deflection on the chart of 5 divisions. Accordingly the sensitivity of the recorder was adjusted until the removal of 2cm³ oxygen led to such a deflection. Once initially calibrated, the apparatus should not have needed further adjustment, as the experimental conditions were not changed in any way. In practice, however, a fresh calibration was performed once a month.

Solutions of the additives under study, i.e. antioxidant, initiator (CHP) and catalyst (FeST), were made up prior to use, and in many cases required vigorous and prolonged stirring in order to attain complete solubility. Two oxidisable substrates were studied, white oil and decalin. Although white mineral oil is not used as the basis of commercial lubricants, it was considered desirable to use it for oxygen absorption studies on account of its highly refined nature. The base oils commonly used in commercial formulations contain natural antioxidants, including sulphur compounds, which may have complicated the evaluation of the dithiophosphates as inhibitors. Although the white mineral oil used (Marcol 172) is a highly refined product,[64] its exact chemical composition is unknown. It was therefore necessary to repeat the oxygen absorption studies in an oxidisable substrate of known composition. Decalin was chosen as a model compound as initial studies using this substrate

gave results comparable to those obtained with white mineral oil.

The method of sample addition was different for each substrate. When white oil was used, solutions of the components under study were individually and directly introduced into the sample flask via a pipette. When decalin was used however, solutions of the individual components were mixed externally, and sample introduction took place via a single pipetting action. This was done to reduce the amount of irritating decalin vapour escaping into the atmosphere above the oil bath. In each case, the total volume of oxidisable substrate used was 5.0cm^3. By varying the concentration of the additive solutions or the relative volume of each solution used, and sometimes diluting with pure substrate, the required concentrations of antioxidant (1×10^{-4} - 5×10^{-3} moldm^{-3}), CHP (1×10^{-2} moldm^{-3}) and FeST (2×10^{-4} moldm^{-3}) were obtained.

Once the sample had been introduced, a stream of pure oxygen was passed into the flask for a period of 20 seconds, after which the sample flask was stoppered and the overhead stirrer activated. The rate of oxidation of unstabilised white oil was found to be independent of stirring rate within experimental error. In practice, a consistent stirring rate was impossible to achieve anyway, on account of variations in the motor speed of the overhead stirrer. For all oxygen absorption experiments, a moderate rate of stirring was aimed for, which eliminated the possibility of bubbling or splashing but at the same time ensured a thorough agitation of the substrate.

In order to check that the system was not leaking, a small volume of oxygen was removed from the sample flask with a syringe, so that the recorder reading was in the range 10 - 20 divisions. As the oxygen in the sample flask warmed up, so the pressure increased slightly, leading to a decrease in the chart reading. Within five minutes, however, the pressure had become constant and the chart reading at this time was taken as the "initial deflection".

In general, samples were left either until the chart pen had reached the extreme right hand side of the chart, i.e. c.35cm^3 oxygen absorbed, or for 72 hours, whichever occurred earlier. In certain cases however, the sample was allowed to oxidise for times as long as 200 hours. For each sample, the result was obtained as a continuous trace of chart deflection (in divisions) versus oxidation time. The chart deflection was corrected by subtraction of the "initial deflection", and this corrected deflection (in divisions) was converted to cm^3 oxygen absorbed by multiplying by a factor of 0.4 (remembering that a deflection of 5 divisions = 2.0cm^3). A curve of oxygen absorbed versus oxidation time could then be plotted.

In general each system was evaluated at least three times, which resulted in three slightly different oxidation curves. For relatively simple curves, such as those obtained for unstabilised white oil (Figure 3.1), or decalin (Figure 3.2.), an average curve, based on the average volume of oxygen absorbed at various oxidation times, could easily be constructed and errors obtained were within ± 15%. Similarly, an average induction period length could be calculated and used to represent the data obtained from systems such as the stabilisation of white oil by ZnDRP

(Figure 3.3.). Again, errors were no more than ± 15%. When the oxidation behaviour was more complex, such as in Figure 4.3., the construction of an average curve was more difficult. As a result of the combination of varying induction period lengths, varying rate of rapid oxidation, varying length of duration of rapid oxidation and varying rate of retarded (3rd stage) oxidation, the average curve constructed for this type of system (e.g. Figure 4.3.) was an overall description of the behaviour observed, rather than a true mathematical average. For the above reasons, errors were difficult to calculate in this type of system, although the pattern of behaviour was reproducible.

2.2.2. HYDROPEROXIDE DETERMINATION

The build-up or decay of hydroperoxides, in both inert and oxidisable systems, was measured by the hydroperoxide determination technique.

2.2.2.1. HYDROPEROXIDE DECOMPOSITION IN INERT SYSTEMS

In order to provide an inert, non-oxidising medium in which to study the decomposition of cumene hydroperoxide (CHP) by ZnDRP and related compounds, chlorobenzene was used as solvent at a temperature of 110°C. In addition, nitrogen gas was passed through the reactant mixture during the course of each experiment, thereby eliminating any effects that atmospheric oxygen might have on the reactions occurring.

All hydroperoxide decomposition experiments were carried out in a special reaction vessel shown in Figure 2.2. Prior to each experiment, the empty vessel was placed in position in a thermostatted oil bath (110 ± 0.5°C) for at least 10 minutes, so that thermal equilibrium could be established. A suitable volume of pure chlorobenzene was then introduced into the reaction vessel and left to equilibrate for 5 minutes, after which $5cm^3$ of an 8×10^{-2} $moldm^{-3}$ solution of CHP in chlorobenzene was added. After a further 5 minutes, a 4×10^{-3} $moldm^{-3}$ solution in chlorobenzene of the hydroperoxide decomposer to be studied was added to the reaction vessel, so that the total volume of the solution amounted to $40cm^3$ in each experiment. Control of the final additive concentration was achieved by varying the volumes of pure chlorobenzene and additive solution used. When necessary, the presence of 2×10^{-4} $moldm^{-3}$ iron stearate was provided by the substitution of $10cm^3$ of the pure chlorobenzene with $10cm^3$ of an 8×10^{-4} $moldm^{-3}$ solution of iron stearate in chlorobenzene.

The time at which the additive solution was introduced into the reaction vessel was taken as the beginning of the experiment. As well as providing an inert atmosphere, the introduction of nitrogen through the gas inlet tube ensured agitation of the reaction mixture. The rate of flow of gas was standardised at the beginning of each experiment with the help of a crude manometer. The "initial flow rate" was adjusted to the same value for each experiment and no further change was made, even though in most cases it decreased as the reaction proceeded.

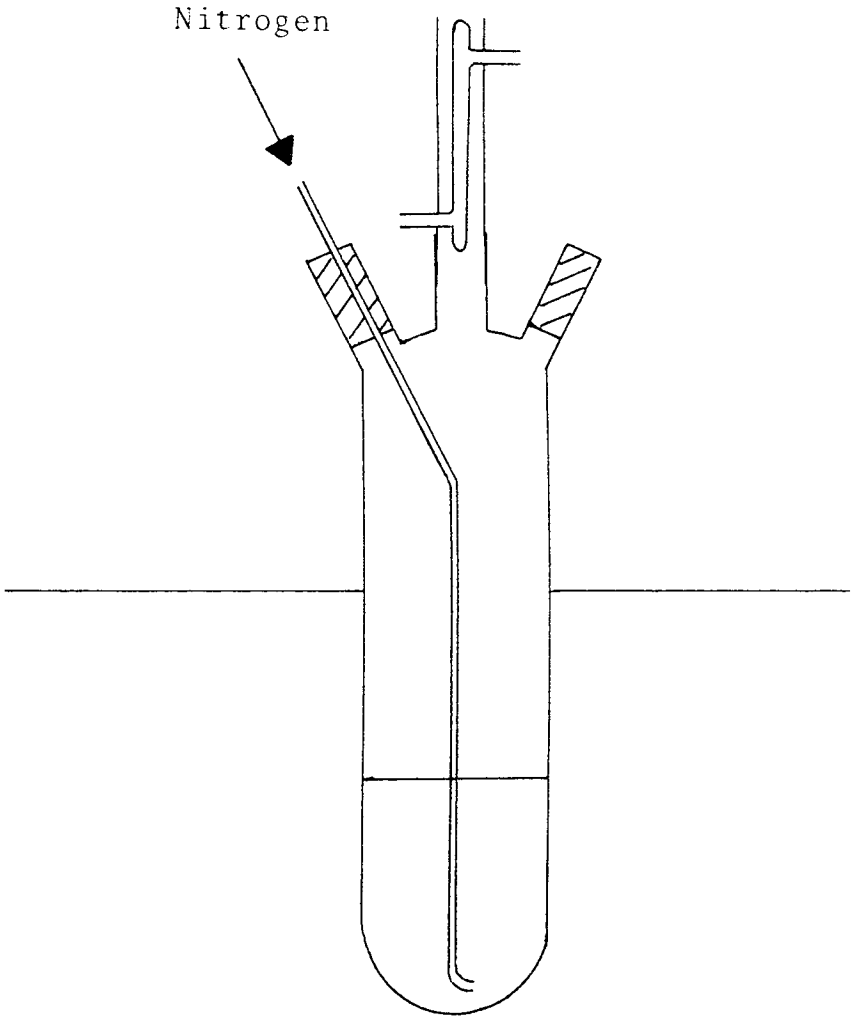

Figure 2.2. Hydroperoxide decomposition apparatus

At suitable time intervals, a 1cm³ portion of the reaction mixture was withdrawn with a pipette and added to a 50 cm³ flat-bottomed flask equipment with a ground glass neck. Eash flask contained 10cm³ of each of the following solutions, added prior to the beginning of the hydroperoxide decomposition experiment:-

(a) 2.5% w/v sodium iodide in propan-2-ol

(b) 10% v/v acedic acid in propan-2-ol

These flasks were wrapped with aluminium foil to prevent photolysis of the sodium iodide.

Once the 1cm³ portion of the raction mixture had been added, the flask was fitted with a condenser and the contents were heated to reflux, with vigorous stirring, on a hot plate for 6 minutes. After this time, the flask was allowed to cool for 2½ minutes, and 5cm³ distilled water was added. The aluminium foil was then removed and the contents of the flask were titrated, with stirring, with a 2×10^{-3} moldm^{-3} solution of sodium thiosulphate in distilled water. The end point was taken as the transformation from yellow to colourless.

During the early stages of the reactions, samples were withdrawn for analysis every 6 minutes, but at reaction times greater than 30 minutes the intervals were gradually increased until samples were being taken once an hour.

The iodometric technique described above depends on the oxidation, in acidic solution, of iodide to iodine by any remaining CHP present. (reaction 36)

$$RO_2H + 2\ I^- + 2H^+ \longrightarrow ROH + I_2 + H_2O \qquad (36)$$

The solutions of sodium iodide and acetic acid were sufficiently concentrated to provide a large excess of iodide and hydrogen ions, thus ensuring that all the CHP reacted. Titration of the yellow solution of iodine produced by reaction (36) with sodium thiosulphate solution, proceeded via reaction (37).

$$2\ S_2O_3^{=} + I_2 \longrightarrow S_4O_6^{=} + 2\ I^- \qquad (37)$$

yellow — colourless

By using the exact procedure described above, a 10 cm^3 titre was equivalent to 100% CHP remaining, i.e. no decomposition. The percentage of CHP remaining at any given time could therefore be instantly determined by multiplying the titre volume by 10. The results presented in Chapters 5 and 6 are shown in terms of percentage CHP remaining as a function of reaction time.

Determination of the CHP content of samples for NMR analysis (Section 2.2.5.) was carried out in a similar way to that described above, except that the higher initial concentration of CHP present (0.2 - 2 $moldm^{-3}$) necessitated the use of a higher concentration of sodium thiosulphate solution.

2.2.2.2. HYDROPEROXIDE BUILD-UP IN OXIDISABLE SUBSTRATES

The same procedure and apparatus used to follow the decomposition of CHP in inert media (Section 2.2.2.1., Figure 2.2.) was used to monitor the build-up of hydroperoxides in white oil and decalin, except that oxygen, rather than nitrogen, was passed through the solution under study.

2.2.3. GAS LIQUID CHROMATOGRAPHY

Gas liquid chromatography (GLC) was used to identify the products arising from the decomposition of CHP by the dithiophosphates. The nature of the products formed from CHP was dependent on the mode of decomposition (see Section 5.3.1.1.), and therefore important evidence regarding the mechanism of CHP decomposition could readily be gained by using GLC.

All work was carried out using a Pye-Unicam GCD Chromatograph fitted with a flame ionisation detector. Dual glass columns packed with polyethylene glycol adipate on Chromosorb W were used. In order to obtain a good separation, a temperature programme was used. The temperature of the column was held at 85°C for 5 minutes, after which it was increased, at a rate of 10°C per minute, until a temperature of 150°C was reached. Thereafter, the temperature was kept constant until all the decomposition products had been eluted. A nitrogen flow rate of 30cm^3 per minute was used.

Before any samples could be analysed, a calibration curve was constructed for each of the possible decomposition products of CHP (Scheme 5.2), with the exception of acetone which, due to its low boiling point, would not be expected to remain in solution at the reaction of 110°C used for the hydroperoxide determination experiments. Several solutions, of varying concentration in chlorobenzene, were prepared for each compound. A fixed amount of 1μdm^3 (the standard injection volume used in all the GLC work performed) iodobenzene

was injected into $1cm^3$ of each sample, and $1\mu dm^3$ of this material was then analysed.

For each concentration used, the areas of the sample peak and the iodobenzene peak in the resulting chromatogram were calculated by multiplying the peak height by the peak width at half height. A graph of (sample:iodobenzene) peak area ratio versus (sample:iodobenzene) molar ratio was then constructed. For each of the potential CHP decomposition products used a straight line was given.

The build-up or decay of the various decomposition products of CHP (Scheme 5.1) was followed as a function of reaction time. At suitable reaction times, $1cm^3$ samples were withdrawn from CHP decomposition experiments (see Section 2.2.2.) and rapidly frozen in dry ice/acetone to quench any further reaction. Prior to freezing, excess triphenylphosphine was added to the sample, in order to convert any undecomposed CHP to α-cumyl alcohol. Burn and co-workers[13] have shown that CHP may, on a GLC column, decompose to more than one product.

Samples were stored frozen until just before analysis took place. Two chromatograms were obtained for each sample and the areas of each of the product peaks observed were calculated. During each day that samples were being analysed, a solution of $1 \times 10^{-2} moldm^{-3}$ CHP in chlorobenzene, having first been treated with excess triphenylphosphine, was run in order to find the peak area corresponding to a 100% yield of α-cumyl alcohol. Once this was known, the areas corresponding to a 100% yield

of the other decomposition products, i.e. acetophenone α-methyl styrene and phenol, could also be determined from the calibration curves initially set up. Actual product yields were then calculated from the formula:-

$$\text{Actual product yield} = \frac{\text{peak area obtained}}{\text{100\% peak area}} \times 100\%$$

The total yield of α-cumyl alcohol obtained needed to be corrected in order to allow for the contribution of that arising from the reaction of undecomposed CHP and triphenylphosphine. The amount of undecomposed CHP present at any time was determined from the hydroperoxide decomposition curves (Chapters 5 and 6), and subtracted from the total yield to give the true yield of cumyl alcohol. In a few cases this resulted in a small negative value for the yield of α -cumyl alcohol obtained, and these values were taken as being zero. A further consequence of the above correction procedure was that large errors in the α -cumyl alcohol yields quoted in Chapters 5 and 6 were possible when only small amounts (i.e. < 5% were formed. Caution is therefore needed before stating that no α-cumyl alcohol was found in a particular system. (See Section 6.2.2.2.). The retention volumes of the peaks due to chlorobenzene and α-methyl styrene were very similar, with the result that small yields of the latter (< 10%) were not detectable under the conditions used.

2.2.4. ULTRA-VIOLET/VISIBLE SPECTROSCOPY

Ultra-violet/visible (UV-VIS) spectroscopy was mainly used to monitor the disappearance of FeDRP in the presence of TBH. All spectra were measured using a Beckman DU-7 Ultra-Violet/Visible Computing Spetrophotometer. The UV-VIS spectrum of a $2.5x10^{-4}moldm^{-3}$ solution of FeDRP in cyclohexane is shown in Figure 2.3. The absorption maxima at 359,499 and 596 nm were all found to obey the Beer-Lambert law for concentrations in the range of $0-2.5x10^{-4}moldm^{-3}$. All studies of the disappearance of FeDRP in the presence of TBH were therefore carried out using a fixed initial FeDRP concentration of $2.5x10^{-4}moldm^{-3}$, with the concentration of TBH being varied from $1x10^{-4}$ - $5x10^{-3}moldm^{-3}$. The UV-VIS spectrum of a $5x10^{-3}moldm^{-3}$ solution of TBH in cyclohexane is shown in Figure 2.4. The use of TBH was preferred to CHP as the latter shows strong ultra-violet absorption due to its aromatic character.

Two solvents were used, depending on the reaction temperature required. At 25°C, spectroscopic grade cyclohexane was used, but when a reaction temperature of 50°C was necessary this could not be used due to its high volatility, and puriss grade n-dodecane was used instead.

Reactions of FeDRP with TBH were followed in two ways by UV-VIS spectroscopy. Firstly, by using the REPSCAN facility, the entire spectrum from 200-700nm could be scanned at suitable time intervals and successive scans superimposed upon each other. Alternatively, the TIME DRIVE facility allowed the change in absorbance

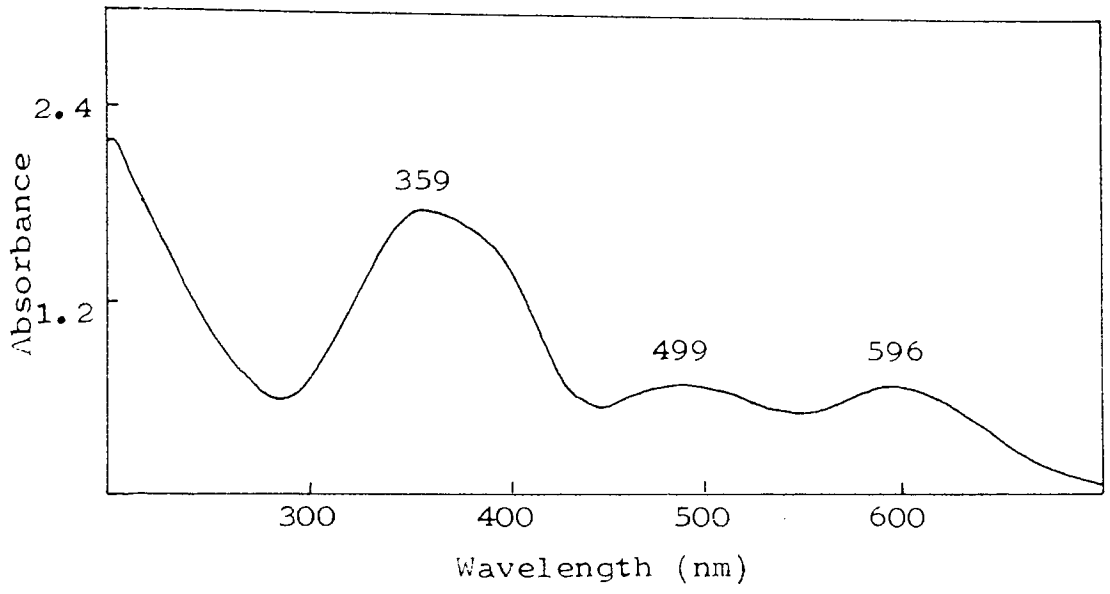

Figure 2.3. UV-VIS spectrum of 2.5×10^{-4} moldm^{-3} FeDiPP in cyclohexane. (Numbers are λmax of absorption bands)

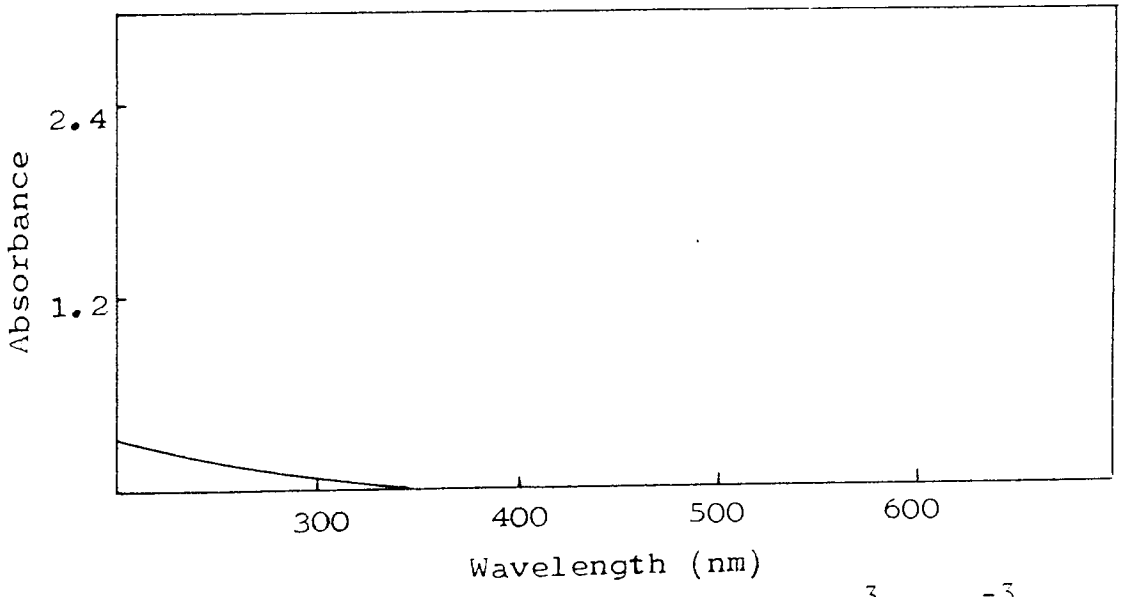

Figure 2.4. UV-VIS spectrum of 5×10^{-3} moldm^{-3} TBH in cyclohexane.

of a particular absorption maximum to be measured as a function of time. The latter method enabled the direct and continuous measurement of the concentrations of FeDRP and decomposition products present in the systems under study. The FeDRP absorption maximum at 596nm was used to follow the disappearance of the iron complex, as this was least likely to be affected by bands due to decomposition products. A shoulder at 260nm was chosen to follow the corresponding build-up of products arising from the decomposition of FeDRP.

Concentrated stock solutions of FeDRP ($5x10^{-4}moldm^{-3}$) and TBH (various concentrations), in the hydrocarbon solvent of choice, were stored at 0°C in the dark under nitrogen. Once at room temperature, $1.5cm^3$ of FeDRP solution was pipetted into a quartz cell, which was then placed in the thermostatted chamber of the instrument for one minute to attain the required temperature (±0.1°C). Then, $1.5cm^3$ of the chosen stock TBH solution was added, and the cell was stoppered and inverted once before being placed back in the instrument, which was then activated. Zero time was taken as the moment at which the instrument was activated, so it was important to carry out the addition and mixing as quickly as possible, especially when a high initial concentration of TBH was used, as the reactions were initially very fast. The above procedure was identical for both REPSCAN and TIME DRIVE facilities.

2.2.5. NUCLEAR MAGNETIC RESONANCE SPECTROSCOPY

^{31}P nuclear magnetic resonance spectroscopy (^{31}P NMR) was used to identify the phosphorus containing products arising from the reaction of the dithiophosphates with CHP. All spectra were measured on a Jeol FX-90Q Fourier Transform Nuclear Magnetic Resonance Spectrometer. The accumulation time needed to obtain a spectrum was dependent on the phosphorus content of the sample. In order to accomodate the number of samples to be measured, an accumulation time of 30 minutes or less was considered desirable. This necessitated the phosphorus concentration of the samples to be at least 0.2 $moldm^{-3}$ and, in practice, the additive concentrations used were in the range of 0.1-0.2 $moldm^{-3}$.

Variation of the initial CHP concentration allowed the study of a range of different CHP:ZnDRP ratios from 1:1 to 10:1. Under these conditions the minimum concentration of a phosphorus containing species that could be detected was around $1x10^{-3}moldm^{-3}$, thus emphasising the limitation of the technique. Oxidation products of the dithiphosphates are shown in Chapter 5 to be effective antioxidants at concentrations far below this level. Overnight accumulation enabled the use of a ZnDRP concentration of $2x10^{-2}moldm^{-3}$, which allowed the study of a CHP:ZnDRP ratio of 50:1 to be made, but was only available on one occasion.

The reactions of the dithiophosphates with CHP at 110°C (Section 5.2.3.) were carried out in the reaction vessel shown in Figure 2.2., and samples were removed for analysis at suitable reaction times, frozen in dry ice/acetone and stored at -20°C until their spectra were recorded. This was necessary because any remaining CHP present in the samples count not be decomposed by triphenylphosphine (Section 2.2.3.), as this could also react with some of the possible decomposition products of ZnDRP, e.g. reaction (38).

$$(RO)_2PSSH + Ph_3P \longrightarrow (RO)_2P(S)H + Ph_3PS \quad (38)$$

Products formed were identified by their ^{31}P chemical shift values (δ) which were compared either with those obtained from authentic samples or with literature data. All chemical shifts were referenced to an external standard of aqueous 85% phosphoric acid. This was not added directly to the sample, in order to prevent the possibility of any reaction with the phosphorus containing products present. Instead, the position of the single peak observed in the spectrum of the acid was noted and set at Oppm. By measuring all subsequent samples under the same conditions, this position could readily be located on each spectrum and chemical shifts relative to phosphoric acid calculated.

The figures quoted in Section 5.2.3. are percentage phosphorus yields rather than percentage product yields. The latter could only be calculated if the identity of all the products formed was definitely known, which was not the case here. Decomposition products containing only one phosphorus atom per molecule were therefore actually present in rather higher levels than those reported in Tables 5.3.-5.12. as being the detected "concentrations".

The interaction of the dithiophosphates with CHP in the presence of FeST could not be studied by ^{31}P NMR because of the effect of the highly paramagnetic Fe^{3+} ion which led to very noisy spectra being obtained.

CHAPTER THREE

THE INHIBITION OF HYDROCARBON AUTOXIDATION BY ZINC DIAKYLDITHIOPHOSPHATES AND RELATED COMPOUNDS

3.1. OBJECT

Although the literature contains very many studies of the inhibition of hydrocarbon oxidation by zinc dialkyldithiophosphates (ZnDRP), the conditions used have varied widely. These variations in the temperatures and substrates used have consequently led to the observation of a wide range of effects caused by ZnDRP.[e.g.10,11] In this chapter the effect of ZnDRPs as inhibitors of the oxidation of hydrocarbon substrates are determined under a similar set of experimental conditions. In addition to ZnDRP, several structurally related compounds (basic zinc dialkyldithiophosphate (b-ZnDRP), dialkylthiophosphoryl disulphide (DRDS), dialkyldithiophosphoric acid (DRDPA) and dialkylthiophosphoric acid (DRTPA)) are also examined under the same conditions.

The method used to determine the effectiveness of these compounds as antioxidants is the oxygen absorption technique described in Section 2.2.1. Two hydrocarbon substrates are used, decalin is used as a pure model compound and studies in this substrate supplement those in a white mineral oil (Marcol 172). For each substrate the effects of the above compounds are determined in the presence and absence of 1×10^{-2} moldm^{-3} cumene

hydroperoxide (CHP). The use of a range of additive concentrations (typically $1x10^{-4}$ - $2x10^{-3}$ $moldm^{-3}$) enables the activity of the dithiophosphates (DRP) to be examined at varying CHP:DRP ratios. All oxygen absorption results presented in this chapter are obtained at a temperature of 130°C. The build-up of hydroperoxides during the oxidation of the unstabilised substrates at 130°C is measured by the hydroperoxide determination technique described in Section 2.2.2.

Scheme 3.1 summarises the work carried out in the present chapter.

3.2. RESULTS

3.2.1. OXIDATION OF HYDROCARBONS IN THE ABSENCE OF ADDED HYDROPEROXIDES

The oxidation of pure white oil alone at 130°C is shown in Figure 3.1. After a very short induction period of less than 15 minutes, the rate of oxygen absorption was rapid and auto-accelerating. After only 4 hours 1% oxygen absorption had occurred and the oxidation rate showed no sign of decreasing. The oxidation of decalin alone at 130°C is shown in Figure 3.2. The observed behaviour was very similar to that which occurred with the white oil under the same conditions (Figure 3.1.) except that the oxidation of decalin was about one-third faster.

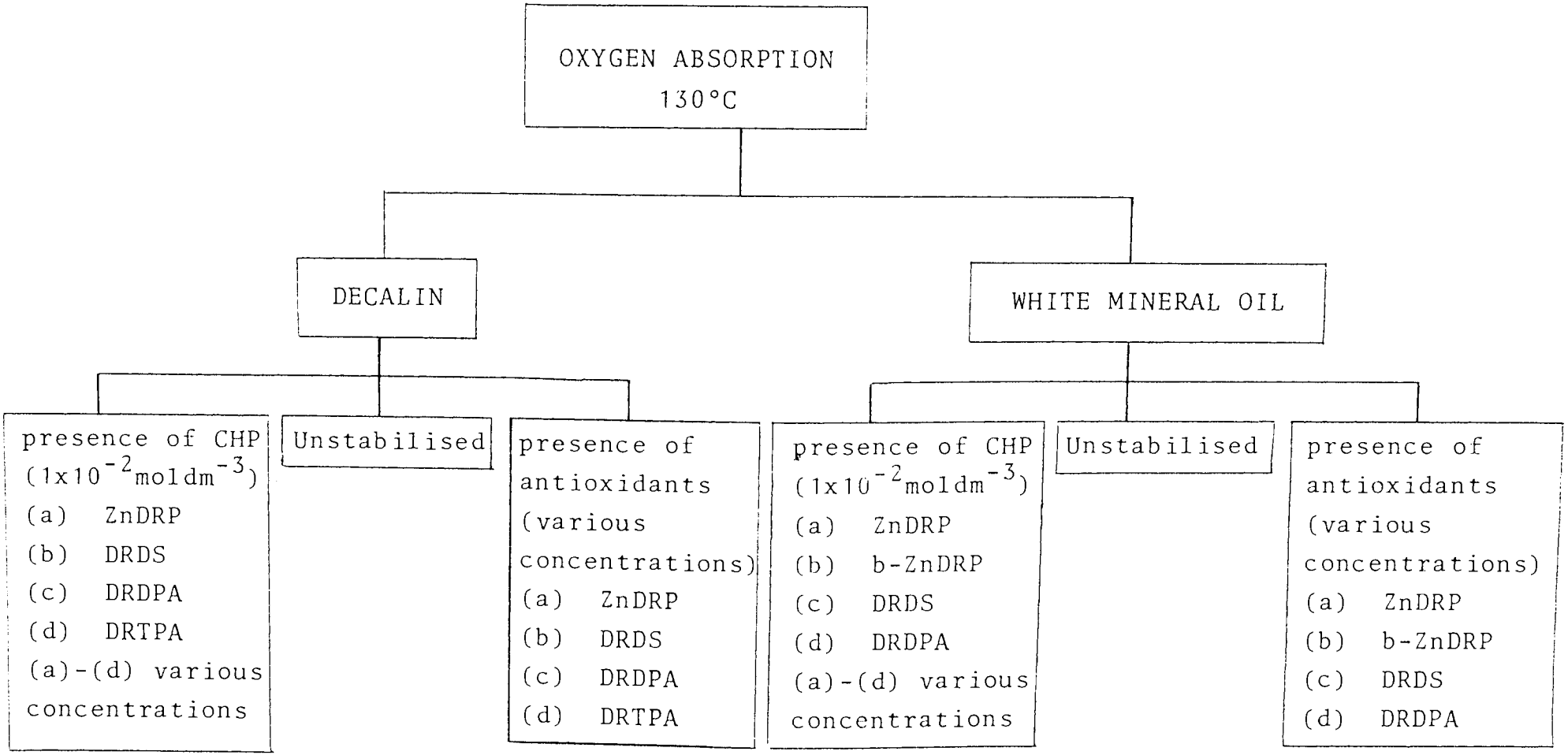

Scheme 3.1. Experiments described in Chapter 3

The build-up of hydroperoxides during the oxidation of the two substrates is shown in the insets of both Figures 3.1. and 3.2. It is clear that the hydroperoxide build-up and oxygen absorption curves follow very similar patterns for both hydrocarbons.

3.2.1.1. EFFECT OF ZnDRP AND b-ZnDRP

The effect of isobutyl and s-butyl normal and basic zinc complexes (ZnDiBP, ZnDsBP, b-ZnDiBP and b-ZnDsBP) on uncatalysed white oil oxidation is shown in Figure 3.3. Comparison of the four was carried out on the basis of equal phosphorus content of $3.1 \times 10^{-2} gdm^{-3}$. All of the zinc complexes show similar behaviour; a long induction period where no oxygen was absorbed followed by a period of rapid auto-accelerating oxidation. The lengths of the induction periods observed under these conditions fall within the range 64-88 hours (Figure 3.3.). In the presence of each of the additives 1% oxygen had been absorbed within 4 hours of the end of the induction period.

The effect of ZnDiBP as an inhibitor of the oxidation of decalin under similar conditions is shown in Figure 3.4. At a ZnDiBP concentration of $5 \times 10^{-4} moldm^{-3}$ the behaviour observed was similar to that which occurred in white oil at the same concentration (Figure 3.3), except that the length of the induction period was severely reduced from 64 hours to 10 hours. The use of a higher

concentration of ZnDiBP ($2x10^{-3}moldm^{-3}$) led to an increase in the length of the induction period observed (Figure 3.4), which was followed by a gradual auto-retarding uptake of oxygen. This contrasts the rapid auto-accelerating oxidation observed at lower ZnDiBP concentrations ($5x10^{-4}moldm^{-3}$).

The effects of ZnDsBP, b-ZnDiBP and b-ZnDsBP as oxidation inhibitors were not studied in decalin.

3.2.1.2. EFFECT OF DRDS

All the disulphides studied (DRDS; R = i-Bu, s-Bu, i-Pr) were good antioxidants for white oil at 130°C (Figure 3.5.). An induction period was followed by a slow uptake of oxygen which was auto-retarding. In the case of DiBDS, increasing the concentration of the disulphide led to a decrease in the rate of oxidation, although the length of the induction period did not appear to be significantly affected. The order of effectiveness as determined by the lengths of the induction period shown in Figure 3.5. was found to be:-

DsBDS >> DiBDS > DiPDS

The effect of DiBDS on the oxidation of decalin under similar conditions is shown in Figure 3.6. It is clear that DiBDS is less effective as an antioxidant in decalin than in white oil. A DiBDS concentration of $5x10^{-4}moldm^{-3}$, which was very effective in white

oil (Figure 3.5.), had virtually no effect on the oxidation of decalin (Figure 3.6). A concentration of $1x10^{-3}moldm^{-3}$ or greater was needed before a slow auto-retarding oxygen absorption, similar to that occurring in white oil (Figure 3.5.) was observed in decalin (Figure 3.6.). The induction periods preceding the oxidation were much shorter in decalin than those observed for DiBDS in white oil.

The effects of DsBDS and DiPDS as oxidation inhibitors were not studied in decalin.

3.2.1.3. EFFECT OF DRDPA

At concentrations of $5x10^{-4}moldm^{-3}$ and $1x10^{-3}moldm^{-3}$, the s-butyl substituted dithiophosphoric acid (DsBDPA) was not a particularly good antioxidant for white oil at 130°C (Figure 3.7.). A short induction period of 8-15 hours was followed by a rapid and auto-accelerating uptake of oxygen.

In decalin the effect of the n-hexyl substituted acid (DnHDPA) was studied (Figure 3.8.). At the lowest concentration used, $5x10^{-4}moldm^{-3}$, no inhibition was observed, but at concentrations above $2x10^{-3}moldm^{-3}$ DnHDPA was an effective antioxidant for decalin. An induction period of 10 - 30 hours was followed by an auto-retarding uptake of oxygen. The use of a DnHDPA concentration of $4x10^{-3}moldm^{-3}$ provided extremely good protection against the thermal oxidation of decalin (Figure 3.8.). Concentrations of DRDPA in the range of $2x10^{-3}$ - $4x10^{-3}moldm^{-3}$ were not tested in white oil.

3.2.1.4. EFFECT OF DRTPA

The effect of the isobutyl substituted thiophosphoric acid (DiBTPA) on the uncatalysed oxidation of decalin at 130°C is shown in Figure 3.9. Although no inhibition was achieved by the lowest concentration used ($5x10^{-4}moldm^{-3}$), the use of DiBTPA concentrations above $2x10^{-3}moldm^{-3}$ did lead to effective stabilisation. A short induction period of around 3 hours was followed by a slow auto-accelerating oxygen uptake.

The effect of DiBTPA was not studied in white oil.

3.2.2. OXIDATION OF HYDROCARBONS IN THE PRESENCE OF CHP

The oxidation of white oil containing $1x10^{-2}moldm^{-3}$ CHP at 130°C is shown in Figure 3.1. The short induction period observed in the uninitiated oxidation was not apparent in the presence of CHP; instead a very rapid oxygen uptake occurred immediately.

The oxidation of decalin under identical conditions proceeded in a very similar fashion (Figure 3.2.).

3.2.2.1. EFFECT OF ZnDRP AND b-ZnDRP

The effect of ZnDiBP on the CHP ($1x10^{-2}moldm^{-3}$) initiated oxidation of white oil at 130°C is shown in Figure 3.10. At a ZnDiBP concentration of $5x10^{-4}moldm^{-3}$ the induction period of 64 hours that occurred in the absence of hydroperoxide (Figure 3.3.) was reduced

to 7 hours in the presence of CHP (CHP:ZnDiBP = 20:1, Figure 3.10.). The subsequent uptake of oxygen was however much slower in the presence of CHP (Figure 3.10.) than in its absence (Figure 3.3.), so that the long term activity of ZnDiBP was improved by the addition of the hydroperoxide.

The effect of ZnDiBP on the CHP initiated oxidation of decalin is shown in Figure 3.11. As occurred in white oil, the lengths of the induction periods observed in decalin in the absence of hydroperoxide (Figure 3.4.) were greatly decreased by the addition of the CHP (Figure 3.11.). The induction periods were followed by a short period of rapid oxidation lasting no more than 3 hours which led into a slow auto-retarding oxygen uptake similar to that observed with white oil. Although the long term activity of ZnDiBP at a concentration of $5x10^{-4}moldm^{-3}$ was improved by the addition of CHP (CHP:ZnDiBP = 20:1), the hydroperoxide had much less effect in enhancing the activity of a higher concentration ($2x10^{-3}moldm^{-3}$) of the zinc complex. (CHP:ZnDiBP = 5:1). At all concentrations studied the overall effectiveness of ZnDiBP as an inhibitor of CHP initiated oxidation was less in decalin than in white oil.

The effect of b-ZnDiBP on the oxidation of white oil in the presence of $1x10^{-2}moldm^{-3}$ CHP is shown in Figure 3.12., and it is clear that it is not as effective as ZnDiBP at equivalent phosphorus concentrations (Figure 3.11).

At a b-ZnDiBP concentration of $3.33x10^{-4}moldm^{-3}$ (equivalent to a ZnDiBP concentration of $1x10^{-3}moldm^{-3}$), a slow uptake of oxygen occurred immediately without induction period (Figure 3.12.). A concentration of $1.67x10^{-4}moldm^{-3}$ (equivalent ZnDiBP concentration = $5x10^{-4}moldm^{-3}$) was totally ineffective.

The effect of b-ZnDiBP on the oxidation of decalin initiated by CHP was not studied.

3.2.2.2. EFFECT OF DRDS

The effect of DRDS on the oxidation of white oil containing $1x10^{-2}moldm^{-3}$ CHP is shown in Figure 3.13. An immediate rapid uptake of oxygen occurred which led into a second, much slower stage. The degree of oxidation that occurred during the first stage decreased as the DiBDS concentration increased.

Similar effects were observed in decalin (Figure 3.14.), except that the first stage was more pronounced than in white oil. At a DiBDS concentration of $5x10^{-4}moldm^{-3}$ the slow oxidation stage was not achieved before 1% oxygen absorption had occurred.

3.2.2.3. EFFECT OF DRDPA

The effect of DsBDPA on the oxidation of white oil containing $1x10^{-2}moldm^{-3}$ CHP is shown in Figure 3.15. Excellent stabilisation was achieved in the

presence of hydroperoxide despite the very low concentration, $5x10^{-4}moldm^{-3}$, of DsBDPA used. The induction period of 8 hours that occurred in the absence of CHP (Figure 3.7.) was increased to 18 hours in the presence of CHP (Figure 2.15). The subsequent rate of oxidation was very slow, so that the effectiveness of DiBDPA was improved by the presence of the hydroperoxide.

The behaviour of DnHDPA in decalin containing $1x10^{-2}moldm^{-3}$ CHP was similar to that of DsBDPA in white oil (Figure 3.15.), except that no induction periods were observed (Figure 3.16). Under comparable conditions, oxidation took place more readily in decalin than in white oil, as was the case for all the inhibitors studied in Sections 3.2.1. and 3.2.2.

3.2.2.4. EFFECT OF DRTPA

The effect of DiBTPA on the oxidation of decalin containing $1x10^{-2}moldm^{-3}$ CHP is shown in Figure 3.17. At a concentration of $2x10^{-3}moldm^{-3}$ DiBTPA, a slow oxygen uptake was observed, similar to that which occurred in the absence of CHP (Figure 3.9.). At a lower concentration of $5x10^{-4}moldm^{-3}$ there was also a slow absorption of oxygen for a long period of 60 hours, but this ended sharply and a rapid auto-accelerating oxygen uptake followed (Figure 3.17.).

The effect of DiBTPA in the presence of CHP was not studied in white oil.

3.3. DISCUSSION

3.3.1. OXIDATION OF HYDROCARBONS IN THE ABSENCE OF ADDED HYDROPEROXIDES

The auto-accelerating nature of the uninhibited oxidation of both white oil (Figure 3.1.) and decalin (Figure 3.2.) would be expected on consideration of the general autoxidation scheme outlined in Section 1.1. (Scheme 1.1). During the initial stages of oxidation, the concentration of hydroperoxide present is low (insets on Figures 3.1. and 3.2.) and therefore chain initiation by hydroperoxide decomposition is restricted, but because the oxidation proceeds via a chain reaction the hydroperoxide concentration, and consequently the oxidation rate, increase rapidly thereafter.

The greater oxidisability of decalin (Figure 3.2.) compared to white oil (Figure 3.1.) must be due to the presence of two tertiary hydrogen atoms. The exact composition of the white oil is unknown, although it is known[64] to be predominantly paraffinic in nature (Section 2.1.3.1.) and therefore unlikely to contain as many tertiary hydrogens as decalin. The observation for both substrates that the oxidation rate showed no tendency to retard, even when as much as 1% oxygen had been absorbed, shows that under the experimental conditions used there is no possibility of a lack of oxygen being responsible for any inhibition observed in the presence of additives.

3.3.1.1. EFFECT OF ZnDRP AND b-ZnDRP

The similar effects shown by ZnDRP and b-ZnDRP for all alkyl groups at equivalent phosphorus concentrations (Figure 3.3.) strongly suggests that all the zinc complexes studied share a common inhibition mechanism towards hydrocarbon oxidation under the conditions used. Furthermore, the existence of an induction period before oxidation (Figures 3.3. and 3.4.) suggests that the additives themselves must be responsible, at least initially, for the inhibition observed. ZnDRPs have been shown to act both as alkylperoxyl radical traps[32] and as hydroperoxide decomposers.[7] Basic ZnDRPs are not however capable of trapping alkylperoxyl radicals.[35] The shorter induction periods observed in decalin (Figure 3.4.) are due to its greater oxidisability (see Section 3.3.1.).

The observation that, in the presence of $5x10^{-4}moldm^{-3}$ ZnDRP (or $1.67x10^{-4}moldm^{-3}$ b-ZnDRP), the rates of oxidation after the end of the induction period (Figures 3.3. and 3.4.) are very close to those of the uninhibited substrates (Figures 3.1. and 3.2. respectively), shows that the antioxidant species responsible for the inhibition that occurs must be completely consumed by the end of the induction period, and that the product(s) derived from them are ineffective as antioxidants at the concentration(s) at which they are formed. On this basis, increasing the ZnDRP concentration used to $2x10^{-3}moldm^{-3}$ might be expected to merely increase the length of the induction period observed without affecting the subsequent rate of oxidation.

The auto-retarding oxidation actually observed in decalin when a ZnDRP concentration of $2x10^{-3}moldm^{-3}$ is used (Figure 3.4.) shows that the product(s) derived from the original zinc complex are in fact active but need to be present at a level above a certain critical concentration for inhibition to occur after the end of the induction period. Under the conditions of the oxygen absorption experiments, there are three possible routes for the decomposition of ZnDRP:-

(a) thermal decomposition

(b) reaction with alkylperoxyl radicals, $RO_2^{\cdot}$

(c) reaction with hydroperoxides, RO_2H

The thermal decomposition temperature of a primary alkyl ZnDRP is reported as 189-214°C,[65] so that the first route would not appear to be important at 130°C. In addition, the large differences in induction period given by the same concentration of ZnDRP in the two substrates ($5x10^{-4}moldm^{-3}$, Figures 3.3. and 3.4.) cannot be adequately explained by such a mechanism. It is most probable therefore that it is the reaction of ZnDRP with the products of the oxidation process, i.e. $RO_2^{\cdot}$ and/or RO_2H, that is responsible for the disappearance of the zinc complex. The reaction of ZnDRP with hydroperoxide is known[10] (see also Section 5.3.3.1.) to give DRDS and b-ZnDRP as the major products, especially at RO_2H:ZnDRP molar ratios of less than 1:1. This condition is easily satisfied during the

induction period when the concentration of hydroperoxide is never able to reach a measurable value due to the presence of the ZnDRP. The reaction of b-ZnDRP with hydroperoxide also gives DRDS[10] (see also Section 5.3.3.3.). The activity of the zinc complexes in the presence of excess hydroperoxide is dealt with in Section 3.3.2.1., with a more detailed study of the reactions of the dithiophosphates with CHP presented in Chapter 5.

The reaction of ZnDRP with $RO_2^{\cdot}$, studied by Willermet and Kandah,[36] was also found to give DRDS as the main product. Small amounts of other compounds were also formed but these assumed less importance as the concentration of $RO_2^{\cdot}$ decreased. As the concentration of alkylperoxyl radicals present during the induction period must be very low, DRDS is likely to be the only significant product formed by the scavenging of alkylperoxyl radicals by ZnDRP.

The disulphide, therefore, must be the only major product that can be formed during the induction period. DRDS is reported[11] to be unable to scavenge alkylperoxyl radicals, thus once all the original zinc complex has been destroyed, the ability of the substrate to resist oxidation may be sufficiently reduced to end the induction period. The further oxidation of DRDS to the species responsible for the auto-retardation observed after this time is discussed in Section 3.3.1.2.

3.3.1.2. EFFECT OF DRDS

The induction periods observed in white oil (Figure 3.5.) show that DRDS can itself inhibit oxidation to some extent. The reduction in length of the induction period caused in decalin (Figure 3.6.) is due to the greater oxidisability of the substrate (see Section 3.3.1.); this is also responsible for the ineffectiveness of a low concentration ($5x10^{-4}moldm^{-3}$) of DRDS (Figure 3.6.). The similar behaviour observed for both the purified crystalline DiPDS and the liquid DiBDS eliminated the possibility that the induction period caused by the latter was due to the presence of some impurities.

From Figures 3.5. and 3.6. it is clear that DRDS, formed from ZnDRP (Section 3.3.1.1.), cannot be directly responsible for the induction periods that arise from the use of the zinc complexes (Figures 3.3. and 3.4.). This is not to say that as DRDS is formed from ZnDRP during the induction period it is not acting as an inhibitor - it surely is - but that the existence of the induction period is primarily associated with the presence of the zinc complex itself. Furthermore, the yield of DRDS formed from ZnDRP must be significantly lower than 100% to account for the lack of inhibition after the induction period caused by a concentration of $5x10^{-4}moldm^{-3}$ ZnDRP (Figure 3.3.), as an equivalent concentration of DRDS is sufficient to achieve inhibition (Figure 3.5.).

The auto-retarding oxidation observed in both substrates (Figures 3.5. and 3.6.) indicates that DRDS must undergo further reaction to form more and more powerful antioxidants. The inability of DRDS to react with alkylperoxyl radicals[11] means that the formation of these products can only occur via oxidative decomposition promoted by hydroperoxides (RO_2H). The pro-oxidant effect caused by DRDS in the presence of RO_2H (CHP) is favoured when an excess of RO_2H is present, i.e. CHP:DRDS > 10:1, (Figures 3.13. and 3.14.). During the induction period (Figures 3.5. and 3.6.), however, the RO_2H concentration is very low and a pro-oxidant effect does not occur from the reaction of DRDS with any hydroperoxide formed in the substrate. The reaction of DRDS with CHP has been shown[10] to occur rapidly and without an induction period at CHP:DRDS ratios of less than 5:1 (see Section 5.3.3.4.).

The reaction of DRDS with CHP has been shown[22] to give sulphur acids via several intermediate compounds (Scheme 1.7., Section 1.4.1.) which are capable of reacting with hydroperoxides. The auto-retarding nature of hydrocarbon oxidation in the presence of DRDS (Figures 3.5. and 3.6.), and also in the later stages when a high concentration of ZnDRP is used (Figure 3.4.) is consistent with such a mechanism.[22]

3.3.1.3. EFFECT OF DRDPA

The induction periods caused by DRDPA (Figures 3.7. and 3.8.) show that the original acids are capable of acting as inhibitors, but the lack of any subsequent inhibition when a low concentration of DRDPA ($\leqslant 1x10^{-3}moldm^{-3}$) is used in white oil (Figure 3.7.) shows that they are completely consumed rather quickly. The slow auto-retarding oxidation observed when higher concentrations ($\geqslant 2x10^{-3}moldm^{-3}$) of DRDPA were used in decalin (Figure 3.8.) suggests that the products formed during the induction period may only be active when present at a level above a certain critical concentration. The slow oxidation (Figure 3.8.) is similar to that caused by the build-up of sulphur acids from ZnDRP and DRDS (Section 3.3.1.2.), and it is likely that these acids are responsible for the auto-retardation here also.

DRDPAs are known to react with alkylperoxyl radicals to give a strong antioxidant species,[35] and in addition they have been found to be very good hydroperoxide decomposers.[28] The oxidation of DRDPA by hydroperoxide has been shown by Grishina and co-workers[26] and by Johnson and co-workers[27] to lead to the formation of DRDS (reaction 39).

$$2(RO)_2PSSH + RO_2H \longrightarrow \{(RO)_2PSS\}_2 + ROH + H_2O \quad (39)$$

The generation of the sulphur acids responsible for the observed auto-retardation (Figure 3.8.) may therefore be via the oxidation of DRDS (Section 3.3.1.2.). Alternatively, these acids may be formed as by-products of reaction (39). (see Sections 3.3.2.3. and 5.3.3.5.).

3.3.1.4. EFFECT OF DRTPA

The absence of an induction period during the oxidation of decalin in the presence of DRTPA (Figure 3.9.) shows that the original acid is ineffective as an inhibitor. Despite this initial inactivity, the slow auto-retarding oxidation which occurs at high concentrations ($\geq 2x10^{-3}moldm^{-3}$) of acid shows that a strong inhibitor is readily formed by the oxidation of DRTPA. This slow oxidation is similar to that given by the dithiophosphates (Sections 3.3.1.1. - 3.3.1.3.), and therefore it is probable that the products responsible are very similar to the sulphur acids formed in Scheme 1.7.

No work has been reported on the reaction of DRTPA with alkylperoxyl radicals, but the reaction of DRTPA with CHP has been shown in this work (Section 5.2.3.6.) to occur readily to give the phosphoryl disulphide (DRODS) as an initial product. Further oxidation of DRODS by hydroperoxide via a mechanism analogous to that proposed by Al-Malaika and Scott[22] (Scheme 1.7.) could lead to the formation of sulphur acids (Scheme 3.2.).

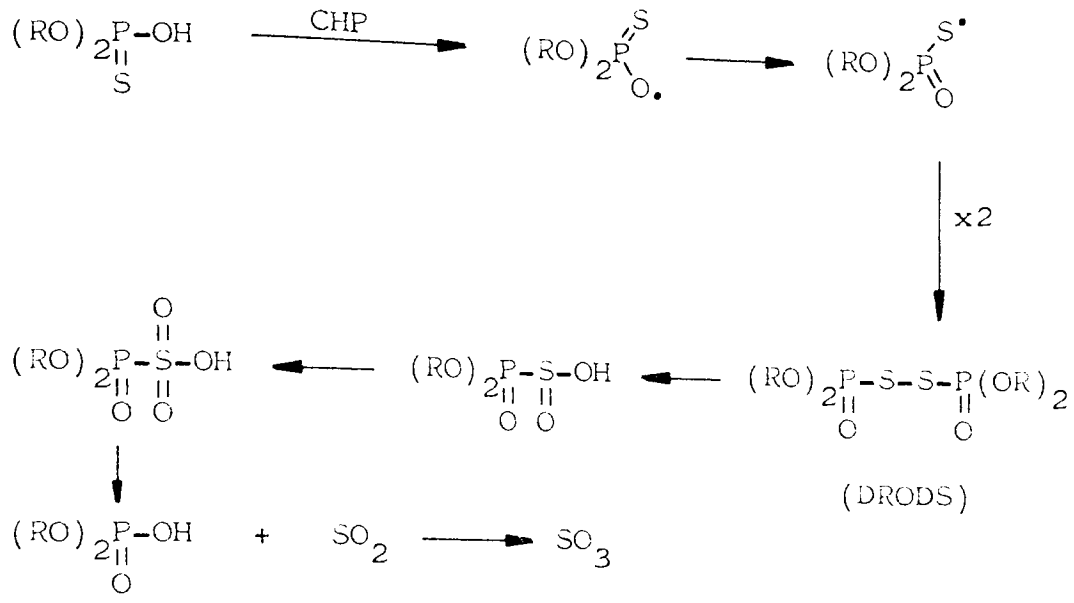

Scheme 3.2. Possible antioxidant mechanism of DRTPA

3.3.2. OXIDATION OF HYDROCARBONS IN THE PRESENCE OF CHP

The presence of 1 x 10^{-2}moldm^{-3} CHP added to the substrates at room temperature means that when heat is applied, the initiation of free radical oxidation chains by hydroperoxide decomposition (reaction (7), Section 1.1.) can immediately occur. Therefore, the induction periods during the uninitiated oxidations (controls, Figures 3.1. and 3.2.), when chain initiation is restricted by the low concentration of hydroperoxide present, does not exist in the presence of added CHP, and oxidation occurs rapidly from the start of the experiments (Figures 3.1. and 3.2.). The differing rates of oxidation of the two substrates are a reflection of their relative oxidisability (see Section 3.3.1.).

3.3.2.1. EFFECT OF ZnDRP AND b-ZnDRP

The very short induction periods given by ZnDRP in the presence of CHP (Figures 3.10. and 3.11.) show that the original zinc complex must be used up very quickly by reaction with the hydroperoxide. This is indeed shown to be the case in Section 5.3.3.2. The subsequent slow auto-retarding oxidation which occurs at ZnDRP concentrations of greater than $5x10^{-4}moldm^{-3}$ is an indication that the products of the reaction of ZnDRP and excess CHP are very strong antioxidants, i.e. the sulphur containing acids discussed in Section 3.3.1.2. The presence of excess CHP (CHP:ZnDRP = 5-10:1) will lead to the rapid oxidation of all the ZnDRP (Section 5.3.3.2.) to give a high concentration of these acidic products, whereas the oxidation of ZnDRP via DRDS in the presence of very low concentrations of hydroperoxide (Section 3.3.1.1.) is relatively slow, and a substantial part of the ZnDRP may be used up in competing side reactions.

As a result, the concentration of sulphur acids formed from ZnDRP in the initial absence of hydroperoxide will probably be much lower than that arising from ZnDRP in the presence of added CHP. This would explain why the use of a concentration of $5x10^{-4}moldm^{-3}$ ZnDRP shows such different behaviour in the initial presence (Figures 3.10. and 3.11.) and absence (Figures 3.3. and 3.4.) of CHP. At a higher concentration of ZnDRP ($2x10^{-3}moldm^{-3}$), a sufficiently high concentration

of sulphur acids can be formed from the zinc complex for inhibition to occur, whether or not hydroperoxides are present initially, and an auto-retarding behaviour is observed in both situations (compare Figures 3.4. and 3.11.).

The existence of a rapid stage before the auto-retardation observed during the oxidation of decalin containing $5x10^{-4}moldm^{-3}$ ZnDRP (Figure 3.11.), shows that free radical processes must be occurring during the oxidation of ZnDRP to sulphur acids. These must be limited however, as the use of the less easily oxidised white oil does not show the same rapid oxidation stage at the same ZnDRP concentration (Figure 3.10). The existence of a pro-oxidant step during the oxidation of hydrocarbons containing ZnDRP and CHP has been reported[10] in some cases but not in others,[11] thus illustrating the dependence of the observed behaviour on the experimental conditions (Section 3.1.).

The relative ineffectiveness of b-ZnDRP (Figure 3.12.) compared to ZnDRP at an equal phosphorus concentration shows that the oxidation of b-ZnDRP to sulphur acids by CHP is not as readily achieved as the corresponding oxidation of ZnDRP. The auto-retardation observed when a high concentration ($3.33x10^{-4}moldm^{-3}$) of b-ZnDRP is used does however show that it is still occurring.

The reaction of ZnDRP and b-ZnDRP with hydroperoxides is studied in detail in Sections 5.3.3.1.-5.3.3.3. and 5.3.1.1.-5.3.1.2.

3.3.2.2. EFFECT OF DRDS

It is clear from Figures 3.13. and 3.14. that DRDS is unable to inhibit hydrocarbon oxidation in the presence of excess CHP, i.e. when CHP:DRDS > 10:1, until it has undergone reaction to further products, i.e. sulphur acids. At a higher DRDS concentration ($2x10^{-3}moldm^{-3}$, CHP:DRDS = 5:1), these acids will be formed in high concentrations and can introduce the slow auto-retarding oxidation earlier (Figure 3.14.) than observed when a low initial DRDS concentration, such as $1x10^{-3}moldm^{-3}$, is used. A pro-oxidant step is however still observed, which shows that the formation of such acids is arising via a homolytic DRDS/CHP interaction (see Sections 5.3.2.3. and 5.3.3.4.).

Further reduction of the CHP:DRDS ratio (towards 0:1) would be expected to result in only the auto-retarding stage, which indeed is observed when DRDS is used in the absence of any added hydroperoxide (Figure 3.6.). The reaction of DRDS with hydroperoxides is studied in detail in Sections 5.3.3.4. and 5.3.1.2.

3.3.2.3. EFFECT OF DRDPA

The ability of DRDPA to inhibit CHP initiated oxidation of both white oil (Figure 3.15.) and decalin

(Figure 3.16.) without the severe oxidation of the substrate associated with the use of DRDS under the same conditions (Figures 3.13. and 3.14.), indicates that, in addition to the formation of DRDS (reaction (39), Section 3.3.1.3.), the interaction of DRDPA with CHP must also lead to the generation of other very powerful antioxidant species, i.e. sulphur acids. (reaction (40), see also Section 5.3.3.5.).

$$(RO)_2PSSH + RO_2H \longrightarrow \{(RO)_2PSS\}_2 + \text{sulphur acids} \quad (40)$$

DRDPA has been proposed as the ultimate antioxidant species responsible for the ionic stage during the decomposition of CHP by metal dialkyldithiophosphates (MDRP : M = Zn,[25] Cu(I),[14] Ni,[14] Co(II)[14]). Although the acid may indeed be formed during the interaction of ZnDRP with CHP, its existence in any system where hydroperoxides are present can only be transitory, which does not satisfy the requirement of it being a catalytic species. The dramatic increase in the degree of inhibition caused by the acid when CHP is present is further evidence that DRDPA is not the most powerful hydroperoxide decomposing species that can be formed from the dithiophosphates.

The reaction of DRDPA with hydroperoxides is studied in detail in Sections 5.3.1.3. and 5.3.3.5.

3.3.2.4. EFFECT OF DRTPA

The increase in activity of a low concentration of DRTPA ($5x10^{-4}moldm^{-3}$) when CHP is present (Figure 3.17.), is similar to that observed with DRDPA, and it is therefore likely that the interactions of each type of acid with CHP occur via closely related mechanisms. The conversion of DRTPA to DRODS (Scheme 3.2.), along with small amounts of other powerful antioxidant species, would therefore seem likely. Further oxidation of the DRODS by CHP would lead to the formation of additional antioxidant species via Scheme 3.2.

The fact that DRTPA is a less effective inhibitor of CHP initiated oxidation than DRDPA under the same conditions is probably due to the formation from DRTPA of fully oxygenated products (Scheme 3.2.), which cannot be further oxidised, whereas the corresponding products from the oxidation of DRDPA by CHP (i.e. DRTPA in Scheme 1.7.) can be oxidised (by Scheme 3.2.) to further antioxidant species. The reaction of DRTPA with hydroperoxides is studied in detail in Sections 5.3.1.4. and 5.3.3.6.

3.4. SUMMARY OF CHAPTER THREE

The oxidation of white oil (Figure 3.1.) and decalin (Figure 3.2.) at 130°C proceeds rapidly and in an auto-accelerating fashion. Decalin is the more susceptible to oxidation, on account of it having two

tertiary hydrogen atoms at the junction of the cyclohexane rings. The addition of $1x10^{-2}moldm^{-3}$ CHP to the substrate leads in each case to an increase in oxidation, especially in the very early stages (Figures 3.1. and 3.2.).

In the initial absence of CHP, ZnDRP and b-ZnDRP can themselves act as very effective antioxidants, resulting in a long induction period during which no oxidation occurs at all. The lack of any inhibition at the end of the induction period when a low concentration of zinc complex is used (Figures 3.3. and 3.4.), indicates that the concentration of active antioxidant species formed, i.e. sulphur containing acids, is very low under these conditions. In contrast, the initial presence of hydroperoxide leads to the formation of a relatively high concentration of sulphur containing acids. The ZnDRP/CHP interaction which leads to the formation of such species results in the immediate destruction of the original zinc complex, and the induction period is very short. The pro-oxidant effect observed (Figures 3.10. and 3.11.) is due to the homolytic decomposition of CHP resulting in the production of free radicals. The major initial product of the ZnDRP/CHP interaction, i.e. DRDS, is then further oxidised by hydroperoxide to the sulphur acids responsible for the slow auto-retarding oxidation observed in the later stages of hydrocarbon oxidation in the presence of CHP and ZnDRP (Figures 3.10. and 3.11.). The generation of sulphur acids from the oxidation of ZnDRP by CHP cannot be wholly via the intermediate

formation of DRDS, as the disulphide is less effective than ZnDRP as an inhibitor of CHP initiated oxidation.

The inability of DRDS itself to inhibit oxidation in the presence of excess hydroperoxide (Figures 3.13. and 3.14.) is clearly shown by the large amounts of oxygen absorbed by the substrates before any retardation commences. This is especially true at very high CHP : DRDS molar ratios. Under conditions where hydroperoxides are present at a very low level however, DRDS is able to very effectively inhibit hydrocarbon oxidation. (Figures 3.5. and 3.6.). Under such conditions, it may be that very slow oxidation of the DRDS is leading to the continual formation of small amounts of very powerful antioxidants such as sulphur containing acids.

The dithiophosphoric acid (DRDPA) and the thiophosphoric acid (DRTPA) show many similarities and it is therefore likely that parallel antioxidant mechanisms exist for both types of acid. Although it is known that oxidation of the acids by CHP to their respective disulphides occurs very readily (Sections 5.3.3.5. and 5.3.3.6.), the better inhibition given by DRDPA in the presence of CHP (Figures 3.15. and 3.16.), compared to DRDS under the same conditions (Figures 3.13. and 3.14.), suggests that additional antioxidant species must rapidly be formed from the DRDPA/CHP (DRTPA/CHP) interaction, (reaction 40).

Further oxidation of the respective disulphides formed (DRDS and DRODS) can lead to the formation of more sulphur acids. The lesser degree of inhibition given by DRDPA or DRTPA in the initial absence of CHP (Figures 3.7. - 3.9.) indicates the concentration of oxidation products formed is greatly reduced under less severe conditions. Consequently, a greater initial concentration of either DRDPA or DRTPA is needed in the absence of CHP to achieve the level of sulphur containing acids necessary for effective long-term inhibition.

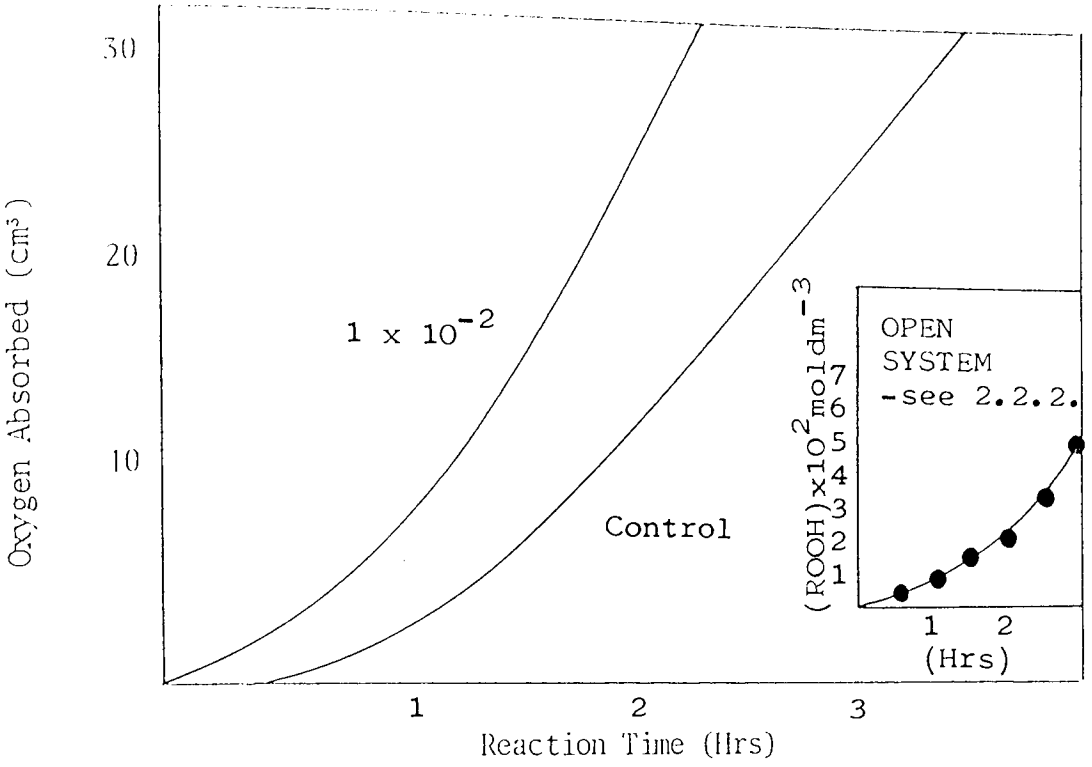

Figure 3.1. Thermal Oxidation of White Oil at 130°C in the Absence and Presence of CHP. Number on Curve is Concentration of CHP in moldm^{-3}. (Inset Shows Hydroperoxide Build-up During Oxidation of White Oil)

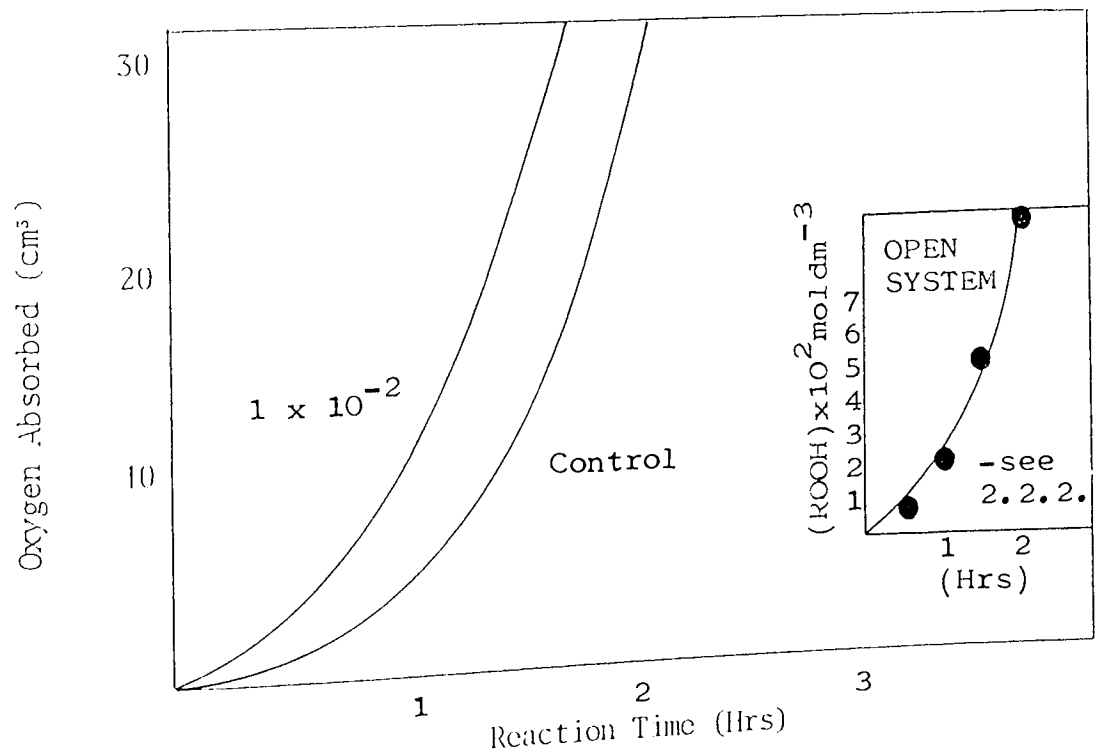

Figure 3.2. Thermal Oxidation of Decalin at 130°C in the Absence and Presence of CHP. Number on Curve is Concentration of CHP in moldm^{-3}. (Inset Shows Hydroperoxide Build-up During Oxidation of Decalin)

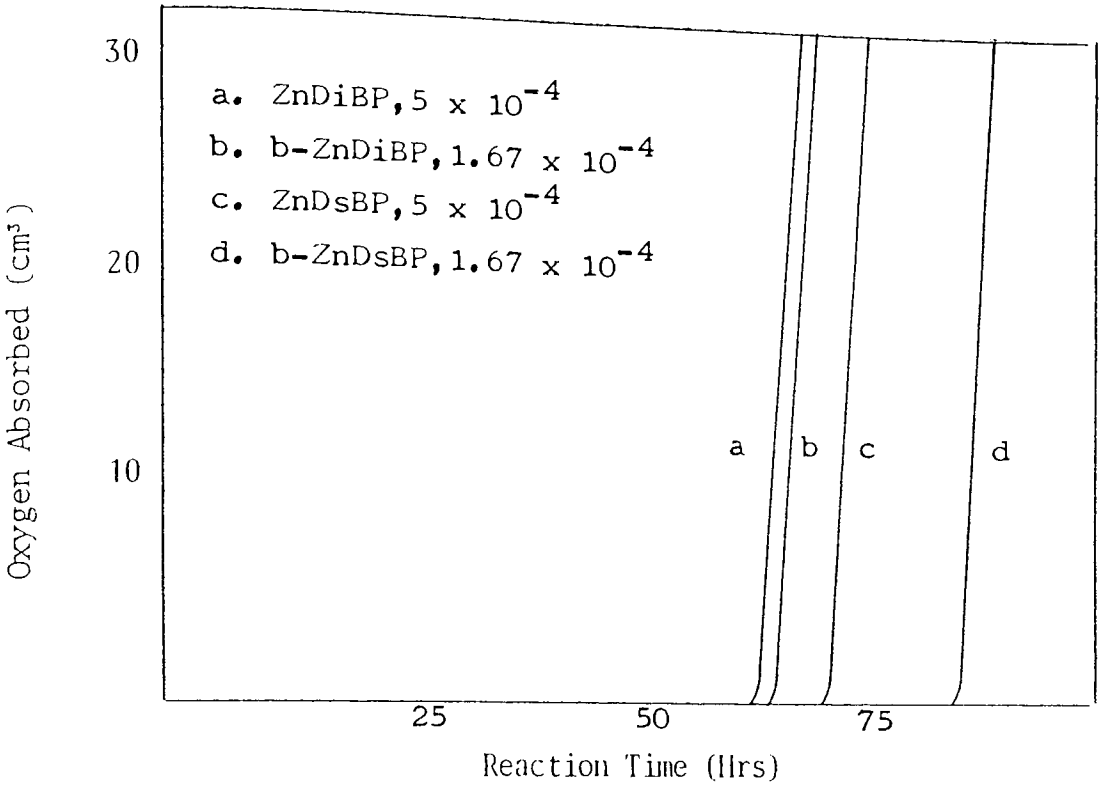

Figure 3.3. Effect of ZnDRP and b-ZnDRP on the Oxidation of White Oil at 130°C. Numbers on Curves are Concentrations in moldm^{-3}.

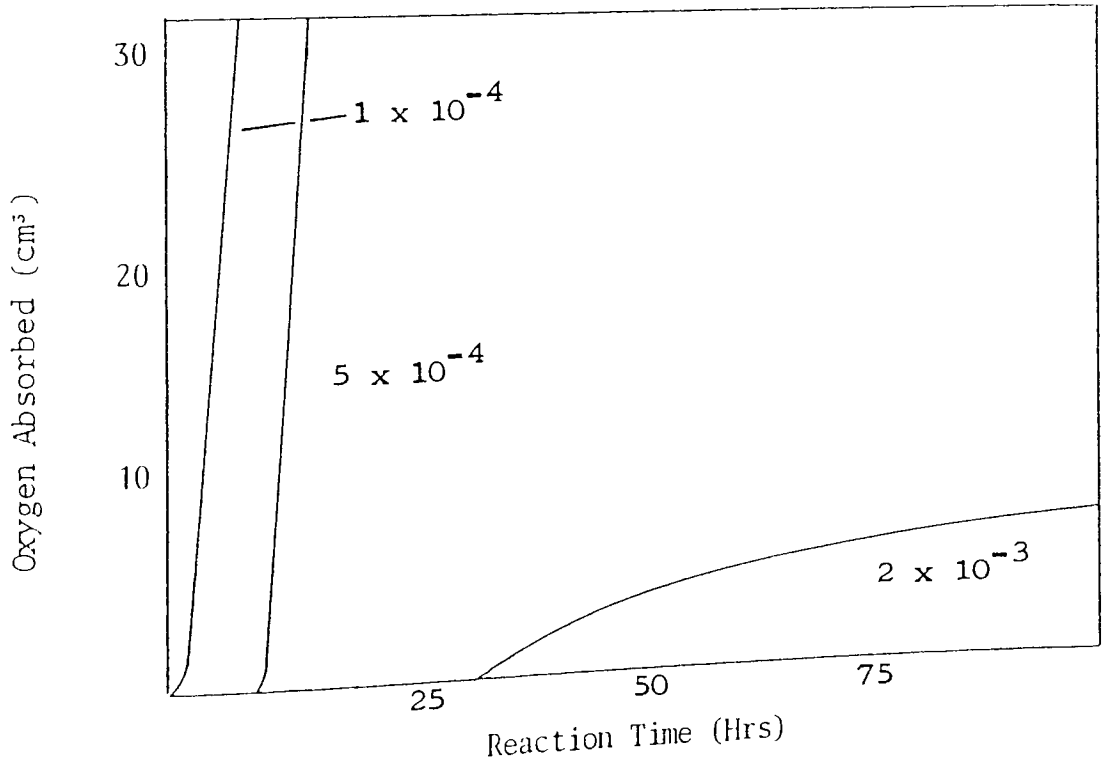

Figure 3.4. Effect of ZnDiBP on the Oxidation of Decalin at 130°C. Numbers on Curves are Concentrations of ZnDiBP in moldm^{-3}.

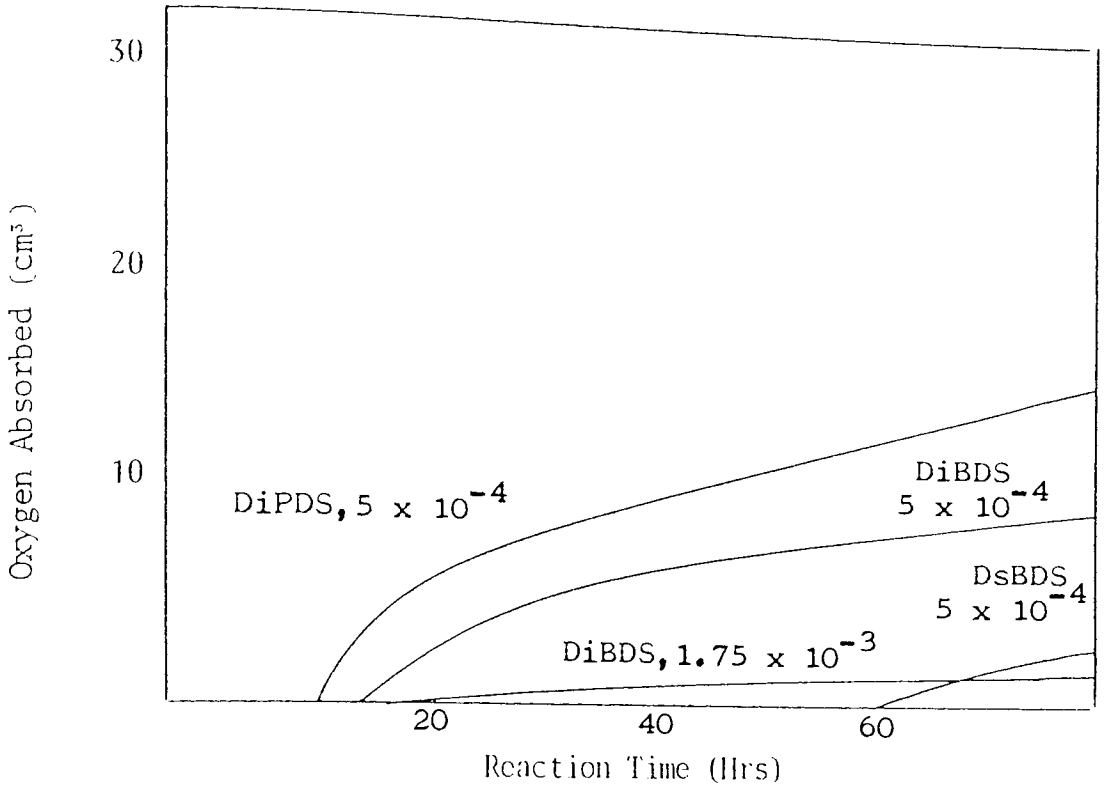

Figure 3.5. Effect of DRDS on the Oxidation of White Oil at 130°C. Numbers on Curves are Concentrations of DRDS in moldm^{-3}.

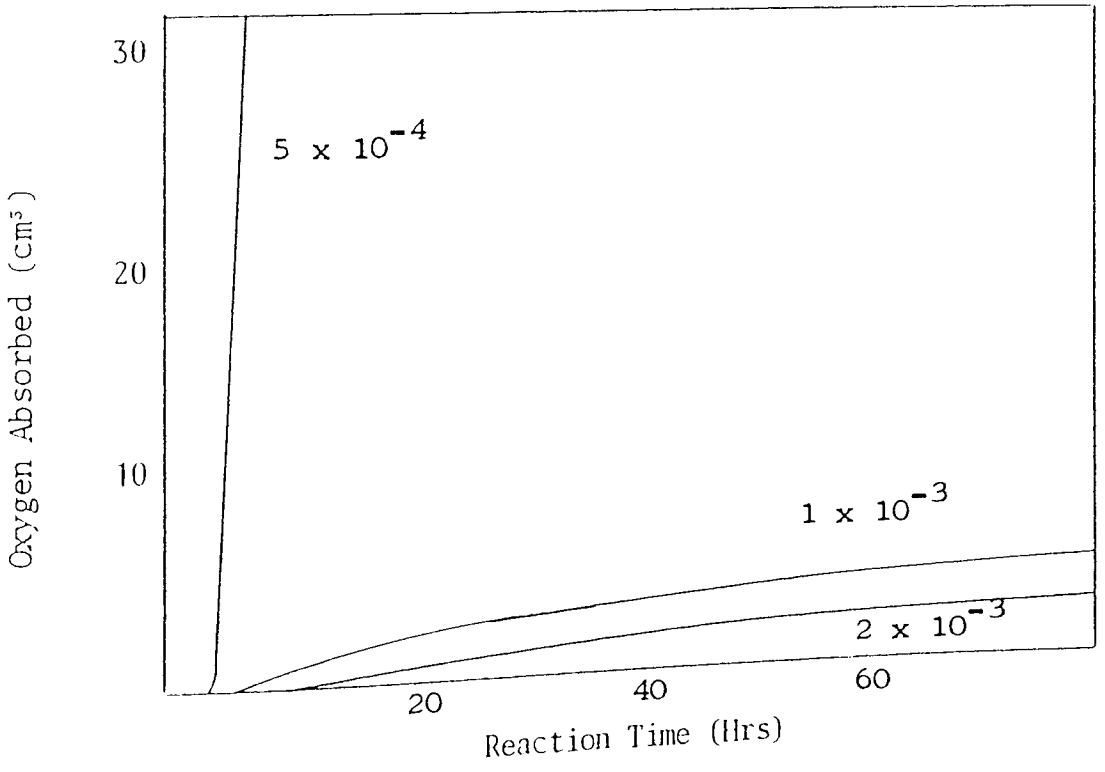

Figure 3.6. Effect of DiBDS on Oxidation of Decalin at 130°C. Numbers on Curves are Concentrations of DiBDS in moldm^{-3}.

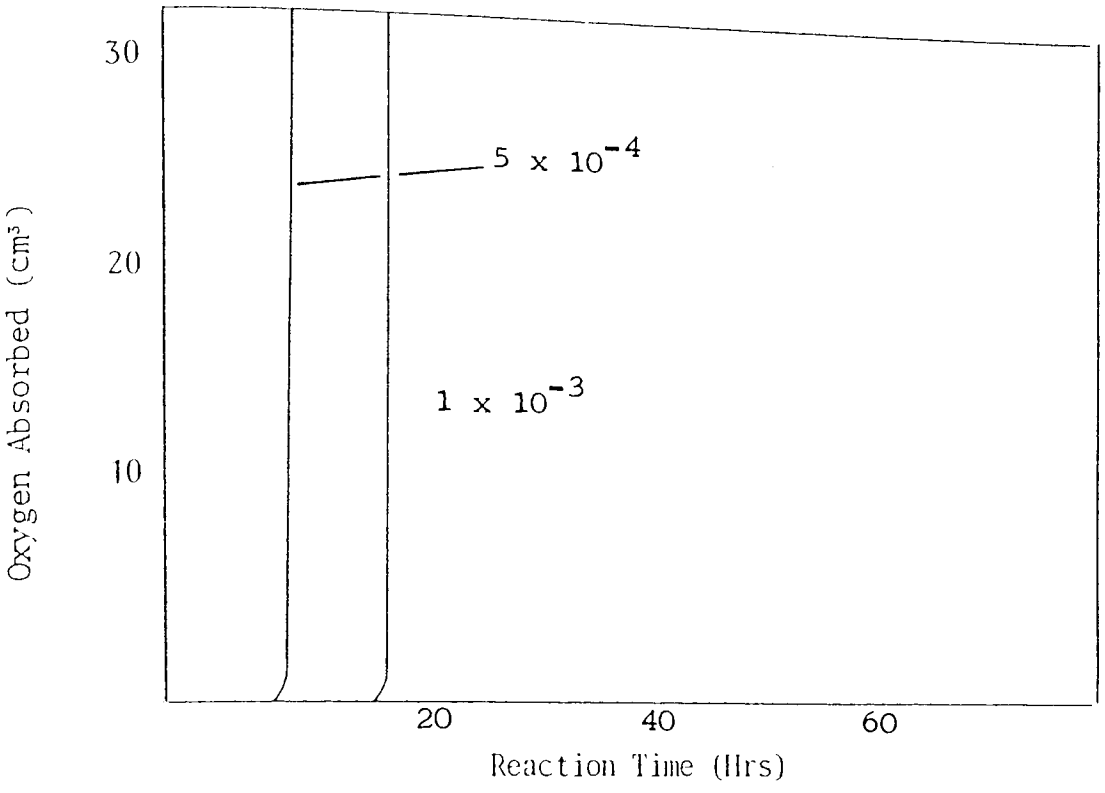

Figure 3.7. Effect of DsBDPA on the Oxidation of White Oil at 130°C. Numbers on Curves are Concentrations of DsBDPA in moldm^{-3}.

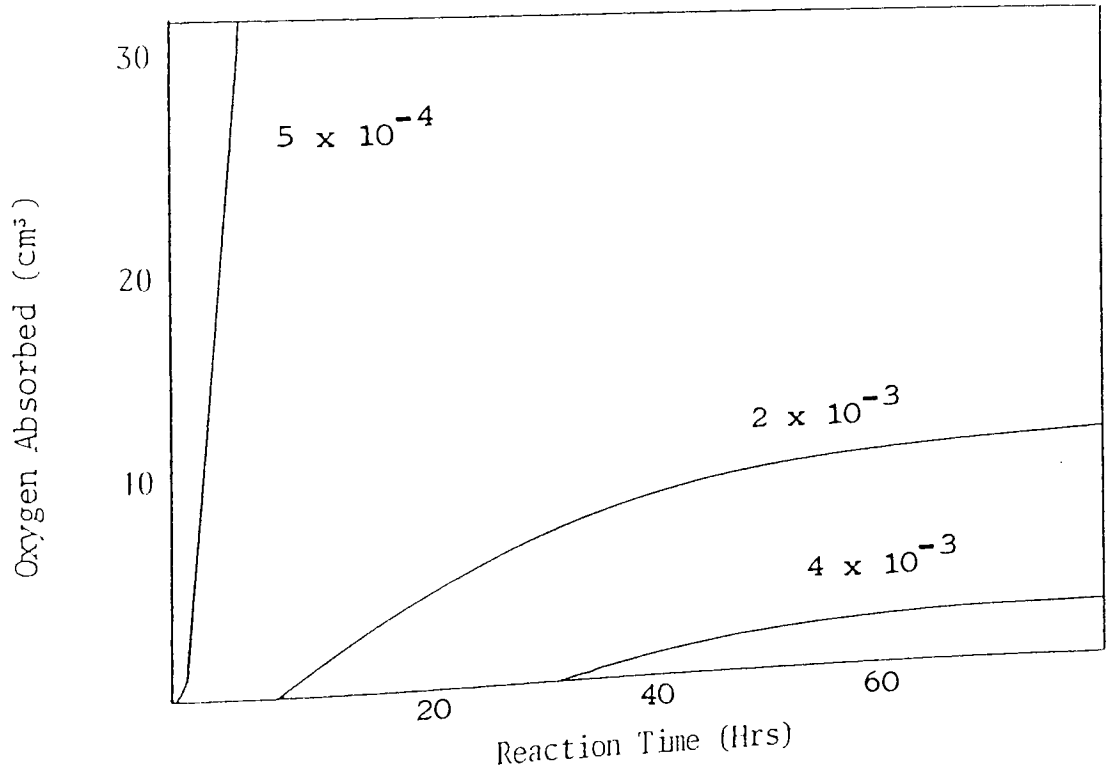

Figure 3.8. Effect of DnHDPA on the Oxidation of Decalin at 130°C. Numbers on Curves are Concentrations of DnHDPA in moldm^{-3}.

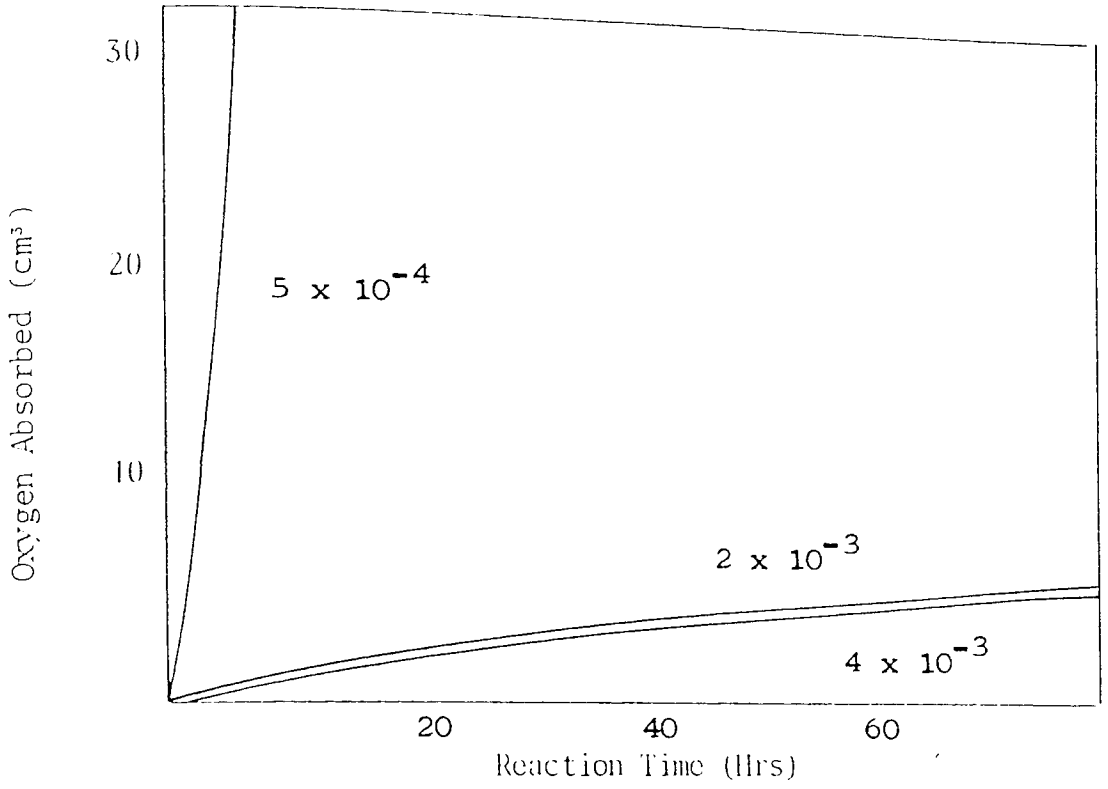

Figure 3.9. Effect of DiBTPA on the Oxidation of Decalin at 130°C. Numbers on Curves are Concentrations of DiBTPA in moldm^{-3}.

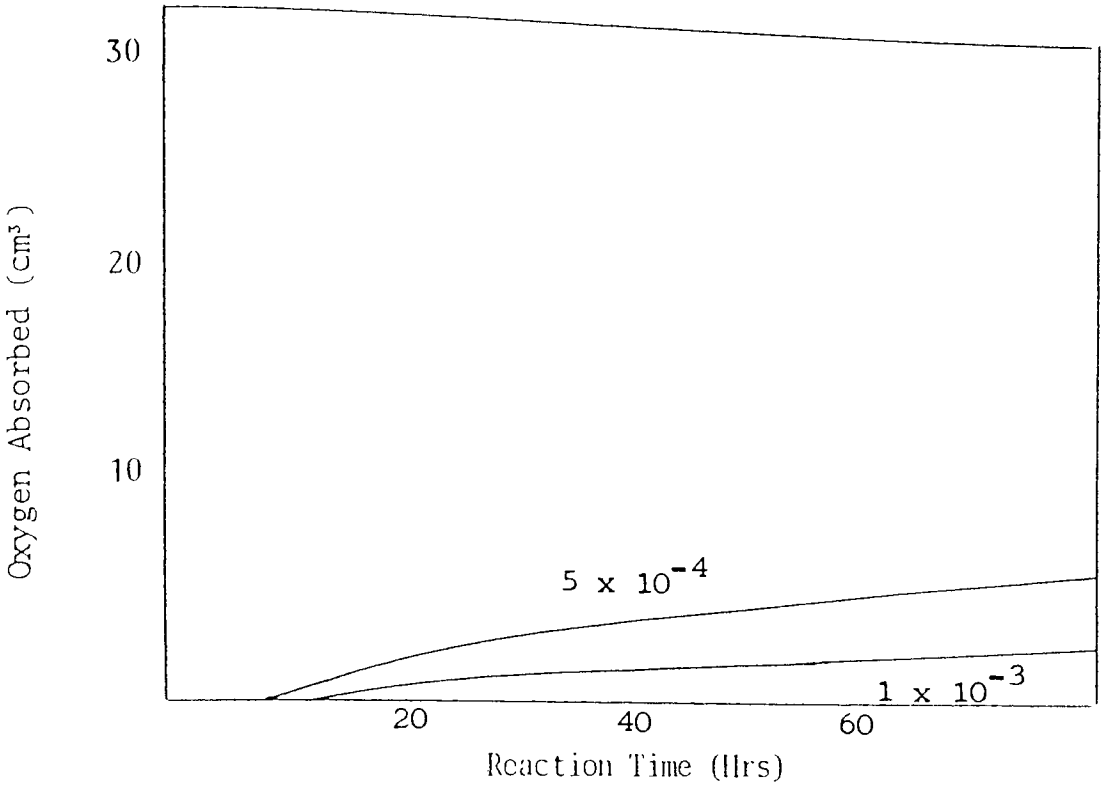

Figure 3.10. Effect of ZnDiBP on the Oxidation of White Oil at 130°C in the Presence of 1 x 10^{-2}moldm^{-3} CHP. Numbers on Curves are Concentrations of ZnDiBP in moldm^{-3}.

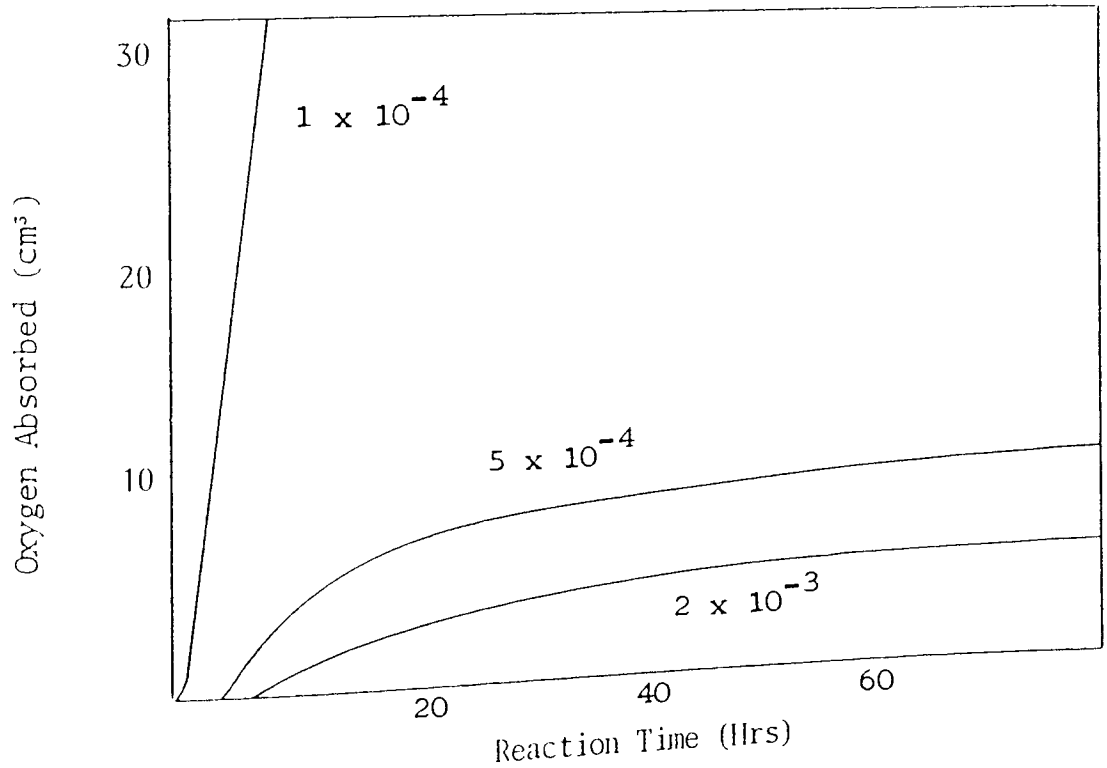

Figure 3.11. Effect of ZnDiBP on the Oxidation of Decalin at 130°C in the Presence of 1 x 10^{-2}moldm^{-3} CHP. Numbers on Curves are Concentrations of ZnDiBP in moldm^{-3}.

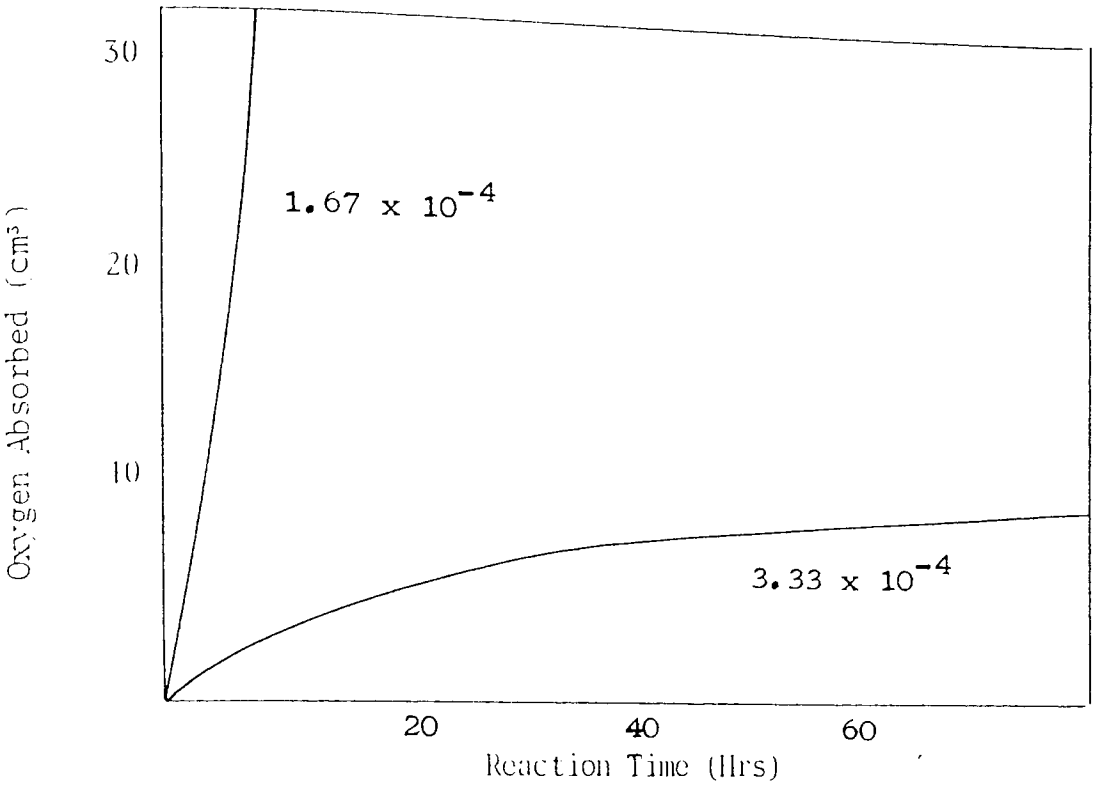

Figure 3.12. Effect of b-ZnDiBP on the Oxidation of White Oil at 130°C in the Presence of 1 x 10^{-2}moldm^{-3} CHP. Numbers on Curves are Concentrations of b-ZnDiBP in moldm^{-3}.

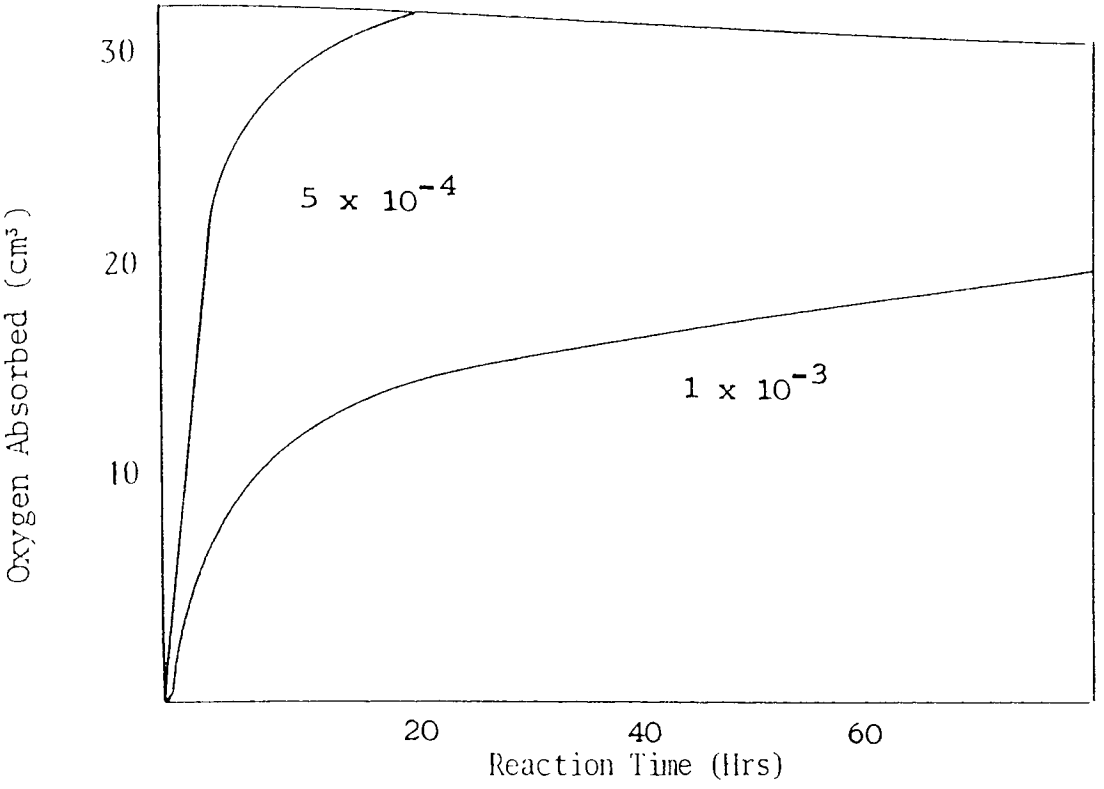

Figure 3.13. Effect of DiBDS on the Oxidation of White Oil at 130°C in the Presence of 1 x 10^{-2}moldm^{-3} CHP. Numbers on Curves are Concentrations of DiBDS in moldm^{-3}.

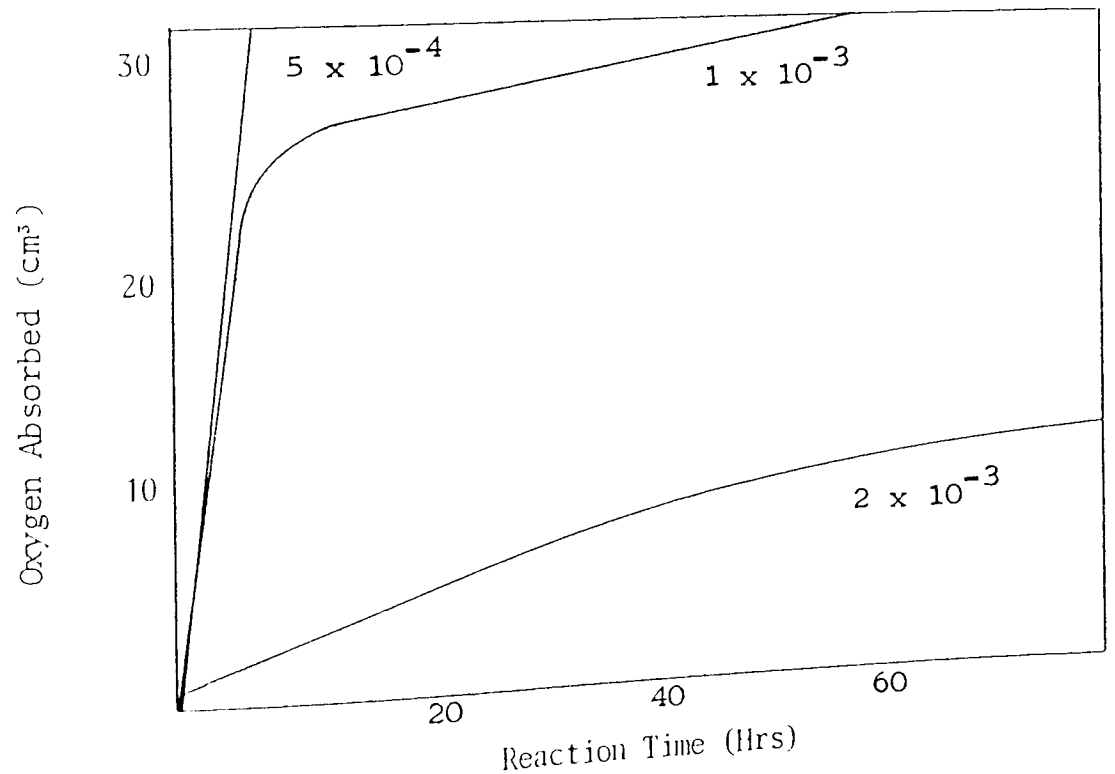

Figure 3.14. Effect of DiBDS on the Oxidation of Decalin at 130°C in the Presence of 1 x 10^{-2}moldm^{-3} CHP. Numbers on Curves are Concentrations of DiBDS in moldm^{-3}.

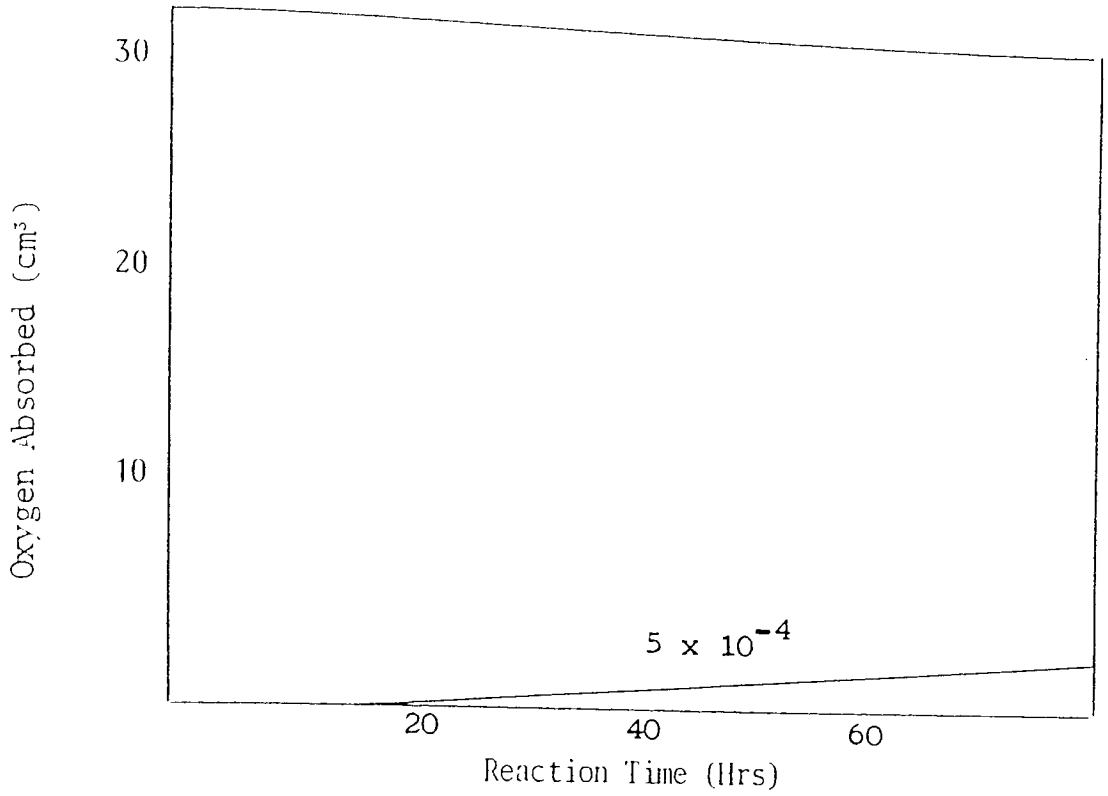

Figure 3.15. Effect of DsBDPA on the Oxidation of White Oil at 130°C in the Presence of 1 x 10^{-2}moldm^{-3} CHP. Number on Curve is Concentration of DsBDPA in moldm^{-3}.

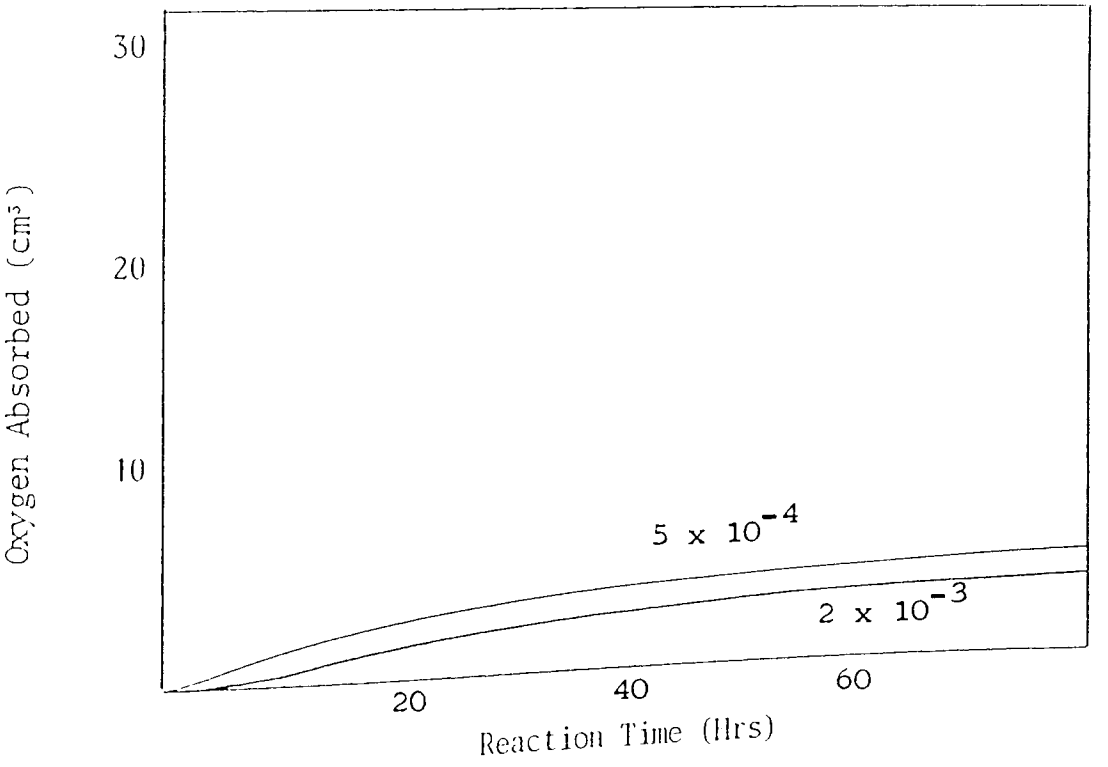

Figure 3.16. Effect of DnHDPA on the Oxidation of Decalin at 130°C in the Presence of 1 x 10^{-2}moldm^{-3} CHP. Numbers on Curves are Concentrations of DnHDPA in moldm^{-3}.

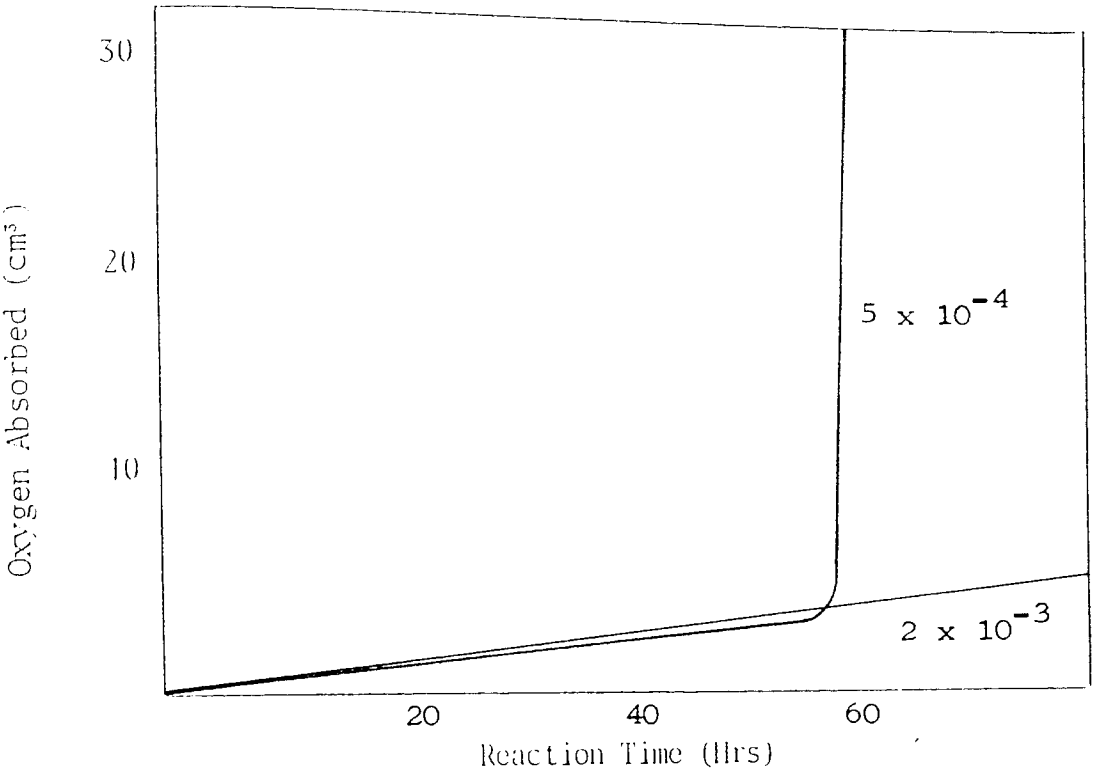

Figure 3.17. Effect of DiBTPA on the Oxidation of Decalin at 130°C in the Presence of 1 x 10^{-2}moldm^{-3} CHP. Numbers on Curves are Concentrations of DiBTPA in moldm^{-3}.

PAGES 110

AND 111

MISSING.

CHAPTER FOUR

THE INHIBITION OF IRON CATALYSED HYDROCARBON AUTOXIDATION BY ZINC DIALKYLDITHIOPHOSPHATES AND RELATED COMPOUNDS

4.1. OBJECT

The effects of zinc dialkyldithiophosphate (ZnDRP) and several structurally related compounds (dialkylthiophosphoryl disulphide (DRDS), basic zinc dialkyldithiophosphate (b-ZnDRP), dialkyldithiophosphoric acid (DRDPA) and dialkylthiosphoric acid (DRTPA)) on the thermal oxidation of hydrocarbon substrates have been studied in Chapter 3. In this chapter the effects of the above additives on iron (Fe^{3+}) catalysed thermal oxidation are studied using the same conditions.

The oxygen absorption technique (Section 2.2.1.) used to study the uncatalysed oxidations needs no modification to obtain information about the corresponding Fe^{3+} catalysed oxidations. The hydrocarbon substrates used, at a temperature of 130°C, are again white mineral oil and decalin so that the oxidations in the presence of iron are carried out under identical conditions to the uncatalysed oxidations studied in Chapter 3.

Iron (III) stearate (FeST), at a concentration of $2x10^{-4}moldm^{-3}$, is used as the soluble iron catalyst. The effect of the dithiophosphates on FeST catalysed oxidations, carried out both in the absence and presence of $1x10^{-2}moldm^{-3}$ cumene hydroperoxide (CHP), are studied to show whether the formation of strong antioxidants from the oxidation of dithiophosphates by hydroperoxides (Section 3.3.2.) is still occurring in the presence of soluble iron. The additive concentrations used are similar to those used in the absence of FeST (Section 3.1.) although the reduced stability of the iron containing systems enables the additional study of some higher concentrations to be made. Antioxidant concentrations used are therefore in the range $5x10^{-4}$ - $5x10^{-3}moldm^{-3}$. Scheme 4.1. summarises the work carried out in the present chapter.

4.2. RESULTS

4.2.1. IRON CATALYSED OXIDATION OF HYDROCARBONS IN THE ABSENCE OF ADDED HYDROPEROXIDES

The oxidation of white oil in the presence of FeST at 130°C is shown in Figure 4.1. No induction period was observed even at the lowest concentration of FeST used, $2x10^{-4}moldm^{-3}$. Higher concentrations of FeST slightly increased the rate of oxidation. At the highest concentrations shown in Figure 4.1.,

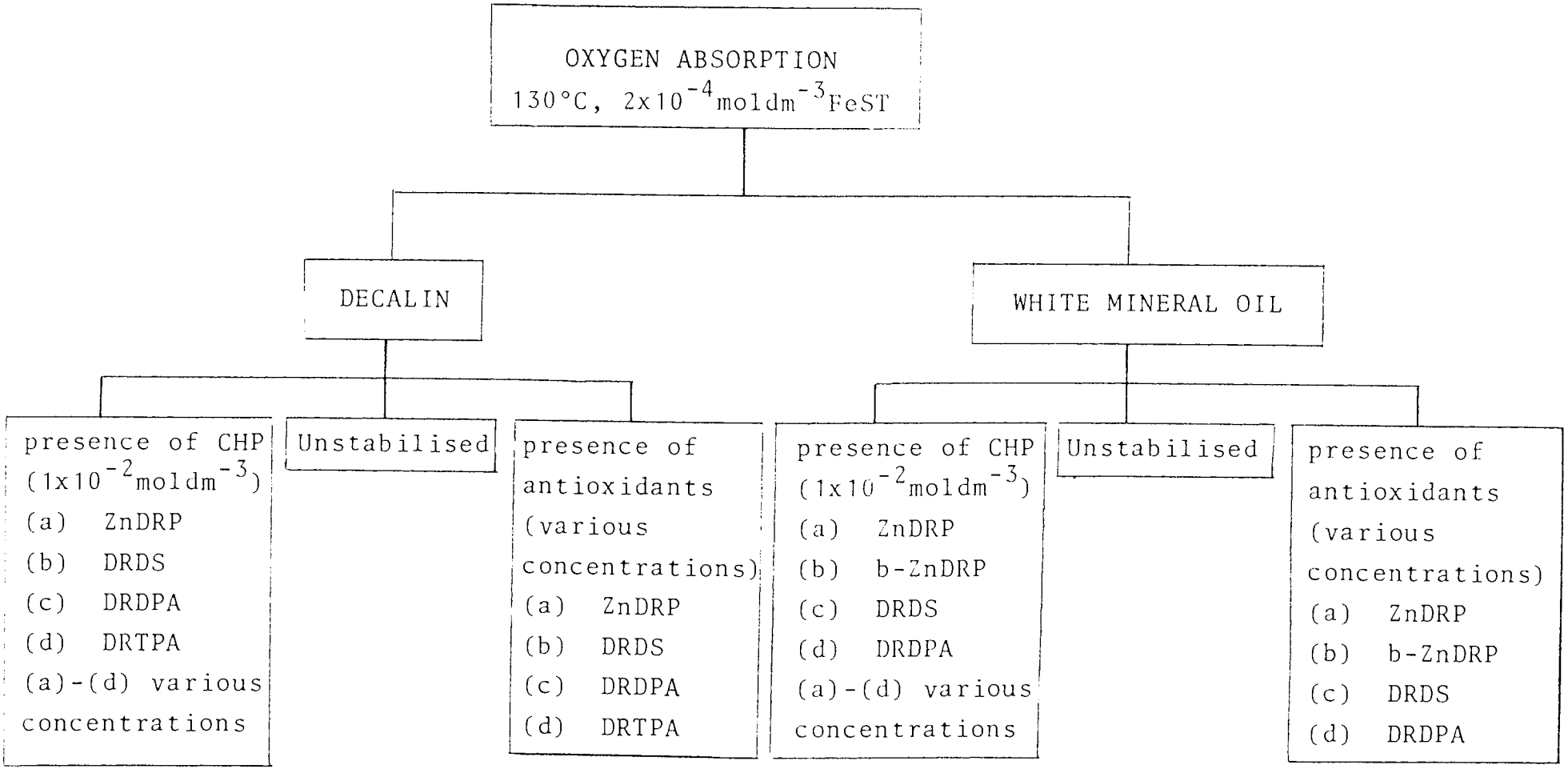

Scheme 4.1. Experiments described in Chapter 4

i.e. $6x10^{-4}$ - $8x10^{-4}moldm^{-3}$, the oxidation rate had reached a maximum, and was not increased (or decreased) even when a much higher concentration, $1.6x10^{-3}moldm^{-3}$, was used. (not shown in Figure 4.1.).

The presence of $2x10^{-4}moldm^{-3}$ FeST had a similar effect on the oxidation of decalin as shown in Figure 4.2. As for the uncatalysed substrates, the oxidation occurred more readily in decalin (Figure 4.2.) than in white oil. (Figure 4.3.).

4.2.1.1. EFFECT OF ZnDRP AND b-ZnDRP

The effects of the zinc complexes on the FeST ($2x10^{-4}moldm^{-3}$) catalysed oxidation of white oil are shown in Figures 4.3. (ZnDiBP) and 4.5. (b-ZnDiBP). For both ZnDiBP dnd b-ZnDiBP the oxidation took place in three clear stages. A short induction period, the length of which increased with increasing zinc complex concentration, was followed by a rapid uptake of oxygen which in turn led into a slower third stage. The extent of the second fast stage was less for ZnDiBP compared to b-ZnDiBP (at an equivalent phosphorus concentration), and decreased with increasing concentration of both types of zinc complex. The rate of the third stage seemed to be independent of the concentration or type of zinc complex used. This slow stage was not achieved by concentrations of ZnDRP less than $5x10^{-4}moldm^{-3}$.

The FeST catalysed oxidation of decalin in the presence of ZnDiBP is shown in Figure 4.4. Although the oxidation occurred faster in decalin than in white oil (Figure 4.3.), three stages were again observed. (Figure 4.4.). For ZnDiBP concentrations up to $5x10^{-3}moldm^{-3}$ the slow third stage was not achieved until a considerable amount of oxidation (0.6% oxygen absorbed) had occurred.

The effect of b-ZnDiBP on the FeST catalysed oxidation of decalin was not studied.

4.2.1.2. EFFECT OF DRDS

DiBDS was not an effective inhibitor of FeST catalysed oxidation of white oil at 130°C. (Figure 4.6.). Even in the presence of a high concentration of $1.75x10^{-3}moldm^{-3}$ DiBDS, severe oxidation of the white oil occurred before any inhibition was apparent. The subsequent slow oxidation which occurred was similar in appearance to the FeST catalysed oxidation in the presence of ZnDiBP and b-ZnDiBP (Figures 4.3. and 4.5.).

The inability of DiBDS to inhibit the FeST catalysed oxidation of decalin is clear from Figure 4.7. No retardation of the oxidation was observed at concentrations up to $5x10^{-3}moldm^{-3}$.

4.2.1.3. EFFECT OF DRDPA

The effect of the s-butyl substituted acid (DsBDPA) on the FeST catalysed oxidation of white oil is shown in Figure 4.8. Little inhibition was observed at DsBDPA concentrations up to $1x10^{-3}moldm^{-3}$. At a concentration of $1.75x10^{-3}moldm^{-3}$ DsBDPA, rapid oxidation occurred initially but led into a slower absorption of oxygen again similar to that observed in the third stage of oxidations inhibited by ZnDiBP (Section 4.2.1.1.).

The effect of the n-hexyl substituted acid (DnHDPA) on the FeST catalysed oxidation of decalin is shown in Figure 4.9. No inhibition occurred at concentrations up to $4x10^{-3}moldm^{-3}$ DnHDPA. On mixing of the solutions of DnHDPA in decalin and FeST in decalin, prior to the addition of the sample to the reaction flask (see Section 2.2.1.), the characteristic green colour of iron (III) dialkyldithiophosphate (FeDRP, see Chapter 6) was apparent. The formation of FeDRP was not able to be observed during the corresponding experiments using white oil, because of the different method of addition used, whereby mixing of the additives took place in the sample flask (Section 2.2.1.).

4.2.1.4. EFFECT OF DRTPA

The iso-butyl substituted acid (DiBTPA) was similar to DnHDPA (Section 4.2.4.), in that it was totally ineffective as an inhibitor of the FeST catalysed oxidation of decalin at 130°C. (Figure 4.10). The

mixing of solutions of DiBTPA in decalin and FeST in decalin resulted in an orange-red colouration, characteristic of iron (III) dialkylthiophosphate. (FeDRT)[66]

The effect of DiBTPA was not studied in white oil.

4.2.2. IRON CATALYSED OXIDATION OF HYDROCARBONS IN THE PRESENCE OF CHP

4.2.2.1. EFFECT OF ZnDRP and b-ZnDRP

The effects of the zinc complexes on white oil oxidation catalysed by both FeST and $1x10^{-2}moldm^{-3}$ CHP are shown in Figures 4.11. (ZnDiBP) and 4.13. (b-ZnDiBP). Although the lowest ZnDiBP concentration used, $5x10^{-4}moldm^{-3}$, was ineffective, the use of higher concentrations gave a reasonable degree of inhibition. No induction periods were observed, instead an initial slight pro-oxidant step was followed by a slow oxygen uptake. (Figure 4.11.) At an equivalent phosphorus concentration b-ZnDiBP gave similar effects (Figure 4.13.), although it was slightly less effective than ZnDiBP

The effect of ZnDiBP on the FeST/CHP catalysed oxidation of decalin, shown in Figure 4.12., was very similar to that observed in white oil, except that the extent of the initial pro-oxidant step was much greater. The effect of b-ZnDiBP was not studied in decalin.

4.2.2.2. EFFECT OF DRDS

The effect of DiBDS on white oil oxidation catalysed by both FeST and CHP is shown in Figure 4.14. At a concentration of $5x10^{-4}moldm^{-3}$, DiBDS gave no inhibition, but at concentrations above $1x10^{-3}moldm^{-3}$ a period of rapid oxidation was followed by a slower uptake of oxygen.

The effect of DiBDS on the FeST/CHP catalysed oxidation of decalin is shown in Figure 4.15. Little inhibition occurred at a DiBDS concentration of $2x10^{-3}moldm^{-3}$, but at a much higher concentration ($5x10^{-3}moldm^{-3}$) similar behaviour to that observed with white oil was seen. In both substrates a considerable degree of oxidation occurred during the initial stages before the second, slower stage was established.

4.2.2.3. EFFECT OF DRDPA

For both white oil and decalin the activity of DRDPA as an inhibitor of FeST catalysed oxidation was improved by the addition of CHP. In white oil (Figure 4.16.), a low concentration of DsBDPA, $5x10^{-4}moldm^{-3}$, gave a short induction period of under 10 hours before rapid oxidation occurred. Very good stabilisation was achieved however at a higher concentration of $1x10^{-3}moldm^{-3}$. An induction period of 15 hours was followed by a very slow uptake of oxygen.

The effect of DnHDPA on the FeST/CHP catalysed oxidation of decalin is shown in Figure 4.17. At a concentration of $5x10^{-4}moldm^{-3}$ a period of rapid oxidation was followed by a slower uptake of oxygen. The use of a higher concentration of $2x10^{-3}moldm^{-3}$ DnHDPA resulted in the slow oxidation of the decalin from the beginning of the experiment, without any observable rapid stage. As in the absence of CHP (Section 4.2.1.3.), the green colouration of FeDRP was observed to form, although this disappeared on standing for about 10 minutes.

4.2.2.4. EFFECT OF DRTPA

The activity of DRTPA as an inhibitor of FeST catalysed oxidation was improved by the initial presence of CHP. Although a low concentration of $5x10^{-4}moldm^{-3}$ DiBTPA gave no inhibition (Figure 4.18.), the use of $2x10^{-3}moldm^{-3}$ led to an oxygen uptake which, despite being quite fast, was considerably slower than that observed in the absence of CHP. (Figure 4.10). The red colouration of $FeDRT^{66}$ (see Section 4.2.1.4.) built up and then decayed on mixing of the solutions of FeST, CHP and DiBTPA. The effect of DiBTPA was not studied in white oil.

4.3. DISCUSSION

4.3.1. IRON CATALYSED OXIDATION OF HYDROCARBONS IN THE ABSENCE OF ADDED HYDROPEROXIDES

The catalytic pro-oxidant effect of soluble iron (Fe^{3+}) is clearly demonstrated by the increase in hydrocarbon oxidation that occurs in the presence of FeST. (Figures 4.1. and 4.2.). The absence of an induction period is indicative that the concentration of hydroperoxides present must build up very rapidly from the very start of the oxidation. This in turn is a consequence of the rapid decomposition of hydroperoxides to free radicals by the Fe^{2+}/Fe^{3+} redox system.[2] (reactions 8,9 and 10, see Section 1.2.)

$$Fe^{2+} + RO_2H \longrightarrow Fe^{3+} + RO^{\cdot} + OH^{-} \qquad (8)$$

$$Fe^{3+} + RO_2H \longrightarrow Fe^{2+} + RO_2^{\cdot} + H^{+} \qquad (9)$$

$$2RO_2H \xrightarrow{Fe^{2+}/Fe^{3+}} RO^{\cdot} + RO_2^{\cdot} + H_2O \qquad (10)$$

The recycling of the catalytic species by reactions (8) and (9) that only a very low concentration of FeST needs to be initially present for a substantial pro-oxidant effect to occur. The effect of "catalyst-inhibitor conversion",[67] whereby certain metal ions, e.g. Cu^{+}, Mn^{2+}, can act as pro-oxidants at low concentrations but as antioxidants at high concentrations, has not been observed in the presence of iron salts. The lack of any inhibition in the presence of high concentrations of FeST (Figure 4.1.), confirms this to be the case for concentrations up to $1.6 \times 10^{-3} mol dm^{-3}$.

4.3.1.1. EFFECT OF ZnDRP AND b-ZnDRP

It is clear from Figures 4.3., 4.4. and 4.5. that the effectiveness of the zinc complexes as antioxidants is severely reduced by the presence of FeST. An extension of the mechanism proposed for the action of ZnDRP and b-ZnDRP as inhibitors of uncatalysed oxidation, (Sections 3.3.1.1. and 3.3.1.2.), may still however by used to account for their action in the presence of FeST. The short induction periods observed in white oil, Figures 4.3. and 4.5.), are associated with the presence of the ZnDRP and b-ZnDRP, and their abrupt end must be due to the total consumption of the zinc complex. The subsequent period of rapid oxidation shows that the products derived from the zinc complex are themselves inactive as inhibitors of FeST catalysed oxidation. It is only on further oxidation of these products (probably mainly DRDS) that effective inhibitors are formed, which are responsible for the third, slow oxidation stage. These inhibitors, strong sulphur containing acids, are formed much more readily from a high initial concentration of zinc complex, which accounts for the less pronounced second stage of rapid oxidation observed at the higher ZnDRP (or b-ZnDRP) concentrations used. (Figures 4.2. and 4.5.). The mechanism(s) by which the sulphur acids operate in the presence of FeST are discussed in Section 4.4.

Due to the higher oxidisability of the substrate, the induction periods given by ZnDRP in decalin are very short and the rapid oxidation stage is more pronounced (Figure 4.4.) As a result the third, slower stage does not occur until severe oxidation has taken place even when a very high concentration of ZnDRP is present.

4.3.1.2. EFFECT OF DRDS

The initial rapid absorption of oxygen that occurs during the oxidation of either white oil (Figure 4.6., DRDS:FeST = 5:1 - 9:1), or decalin (Figure 4.6., DRDS:FeST = 15:1 - 25:1) in the presence of DRDS shows that the disulphide is unable itself to act as an inhibitor in the presence of FeST. Thus although DRDS is an effective inhibitor under relatively mild oxidation conditions (Section 3.3.1.2.), it is very poor when oxidation catalysts (CHP and/or FeST) are present.

The retardation observed in white oil (Figure 4.6.) when a high concentration of DRDS ($1.75 \times 10^{-3} mol dm^{-3}$, DRDS:FeST = 9:1) is used must be due to strong sulphur acids formed as a result of the oxidation of DRDS by hydroperoxides (Section 3.3.1.2.), which build up during the rapid initial stage. The formation of these acids is more readily achieved from a high initial DRDS concentration.

The intermediate formation of DRDS from ZnDRP and b-ZnDRP (Sections 3.3.1.1., 3.3.1.2. and 4.3.1.1.), and subsequent oxidation to sulphur containing acids can therefore explain the occurrence of the second and third stages of the FeST catalysed oxidation of hydrocarbons in the presence of the zinc complexes. The mechanism(s) by which these sulphur acids inhibit the iron catalysed oxidation are discussed in Section 4.4.

4.3.1.3. EFFECT OF DRDPA

The bulk reaction of DRDPA and FeST (reaction 41) has been shown to give FeDRP (Section 6.2.3.2.), and is clearly occurring "in-situ" on mixing of the solutions prior to the oxygen absorption experiments.

$$3(RO)_2PSSH + (R'COO)_3Fe \longrightarrow \{(RO)_2PSS\}_3Fe + 3R'COOH \quad (41)$$

FeDRP is a reasonably good inhibitor of the thermal oxidation of decalin (Section 6.2.1.), and although the maximum concentration at which it may be formed here is only $2x10^{-4}moldm^{-3}$ it would not be expected to act as a pro-oxidant when formed "in-situ". In addition, at the DRDPA concentrations used in Figures 4.8. 4.9., there is always an excess of DRDPA over FeST

(DRDPA:FeST = 10:1 - 20:1). Thus completion of reaction (41) should use up all of the FeST and leave much of the DRDPA unreacted. In view of the antioxidant activity of the individual species, FeDRP (Figure 6.1.) and DRDPA (Figures 3.7. and 3.8.), the observed lack of inhibition (Figures 4.8. and 4.9.) is therefore surprising. The presence of stearic acid (R'COOH, R' = $C_{17}H_{35}$) as a product of reaction (41) must therefore have a severe effect on the ability of FeDRP and/or DRDPA to inhibit the thermal oxidation of hydrocarbons.

The retardation that occurs when a high concentration of acid is used in white oil (Figure 4.8.), shows that oxidation of DRDPA to sulphur containing acids is needed before effective inhibition can take place. Comparison of Figures 4.6. and 4.8. shows that, when FeST is present, the formation of these sulphur acids is achieved more readily from DRDPA than from DRDS.

4.3.1.4. EFFECT OF DRTPA

The inactivity of DRTPA in the presence of FeST (DRDPA:FeST = 10:1 - 20:1, Figure 4.10.), along with the formation of the red colour of FeDRT, shows that behaviour analogous to that discussed in Section 4.3.1.3. for DRDPA is occurring for DRTPA. FeDRT is formed "in-situ" by reaction (42).

$$3\ (RO)_2PSOH + (RCOO)_3Fe \longrightarrow \{(RO)_2PSO\}_3\ Fe + 3\ RCOOH \quad (42)$$

4.3.2. IRON CATALYSED OXIDATION OF HYDROCARBONS IN THE PRESENCE OF CHP

4.3.2.1. EFFECT OF ZnDRP and b-ZnDRP

It is clear from the rapid initial oxidation observed in Figures 4.11., 4.12. and 4.13. that both types of zinc complex are themselves unable to inhibit FeST catalysed oxidation when CHP is initially present. In the long term, however, their stabilising effect is far better than when hydroperoxides are initially absent. (Figures 4.3., 4.4. and 4.5.). This was also the case with corresponding oxidations carried out in the absence of FeST. (Chapter 3).

It would therefore appear that the presence of FeST has little effect on the direct oxidation of high concentrations of ZnDRP (or b-ZnDRP), by CHP to give sulphur containing acids which is known to occur in its absence (Sections 3.3.2.1. and 5.3.3.2.). The slow uptake of oxygen observed at ZnDRP concentrations above $1x10^{-3}moldm^{-3}$ (ZnDRP:FeST > 5:1, Figures 4.11. and 4 12.) is characteristic of the formation of such products. The rate of the slow oxidation is however rather faster in the presence of FeST (compare Figure 3.10. and 4.11.), which suggests that the FeST is having an effect on the hydroperoxide decomposing activity of the sulphur acids. The inactivity of a concentration of $5x10^{-4}moldm^{-3}$ ZnDRP (ZnDRP:FeST = 2.5 :1, Figures 4.11. and 4.12.), shows that the

concentration of sulphur acids needed to provide effective stabilisation against FeST catalysed oxidation must be greater than that required to inhibit the corresponding uncatalysed oxidation (Figures 3.10. and 3.11.).

In Section 5.3.2.2. the presence of FeST is shown to have little effect on the decomposition of CHP by relatively high concentrations of ZnDRP, i.e. CHP:ZnDRP < 5:1.

4.3.2.2. EFFECT OF DRDS

It is clear from Figures 4.14. and 4.15. that the ability of DRDS to inhibit the FeST catalysed oxidation of hydrocarbons is improved by the initial presence of $1x10^{-2}moldm^{-3}$ CHP. The slow uptake of oxygen, characteristic of the formation of sulphur containing acids, achieved at high concentrations of DRDS in the presence of CHP (Figure 4.15.) is not apparent in its absence. (Figure 4.7.).

Comparison of Figures 3.13. and 3.14. with 4.14. and 4.15. respectively, shows that the presence of FeST increases the extent of the rapid initial oxidation stage, but does not significantly affect the formation of the sulphur acids. Thus, as for the zinc complexes (Section 4.3.2.1.), it may be concluded that FeST has little effect on the reaction between DRDS and CHP. The fact that the rate of the slow oxidation in the presence of FeST (Figure 4.15.) is somewhat

faster than that in the absence of FeST (Figure 3.14.), does however suggest that the FeST is having some effect on the sulphur acids once they have been formed. A similar conclusion was reached in Section 4.3.2.1. Section 5.3.2.3. deals in more detail with the effect of FeST on the decomposition of CHP by DRDS.

The addition of excess CHP to a hydrocarbon containing DRDS will therefore only lead to an improvement in overall stability of the substrate when it is very susceptible to oxidation in its (CHP) absence (compare Figures 4.14. and 4.15.). Although the same CHP/DRDS interactions must be occurring in the absence of FeST, the effect of CHP on the very efficient stabilisation given by DRDS alone (Figures 3.5 and 3.6.) leads to an increase in the extent of oxidation observed. (Figures 3.13. and 3.14.).

4.3.2.3. EFFECT OF DRDPA

The ability of DRDPA to inhibit the FeST catalysed oxidation of hydrocarbons is vastly improved by the initial presence of $1x10^{-2}moldm^{-3}$ CHP (Figures 4.16 and 4.17.) which shows that the reaction between CHP and DRDPA to give sulphur acids (reaction 40, Section 3.3.2.3.) must still be occurring despite the presence of FeST. The appearance of the dark green colour of FeDRP shows there is competition between CHP and FeST for the DRDPA, which is responsible

for the reduction in inhibition observed when FeST is added to a system containing CHP and DRDPA. (compare Figures 3.15. and 3.16 with 4.16. and 4.17. respectively).

In view of its instability towards CHP (Section 6.2.2.), the formation of FeDRP in a system containing CHP is rather surprising. FeDRP is known to give a pro-oxidant effect in the presence of CHP. (Figure 6.2.). To account for the inhibition observed (Figures 4.16. and 4.17), the sulphur acids formed by the oxidation of DRDPA by CHP (reaction 40) must be able to completely overcome this pro-oxidant effect thereby demonstrating their extreme power as hydroperoxide decomposers. The formation of further sulphur acids from the reaction of FeDRP with CHP (Section 6.2.2.4.) may also contribute to the long-term inhibition observed. (Figures 4.16. and 4.17.). The above reactions are summarised in Scheme 4.2.

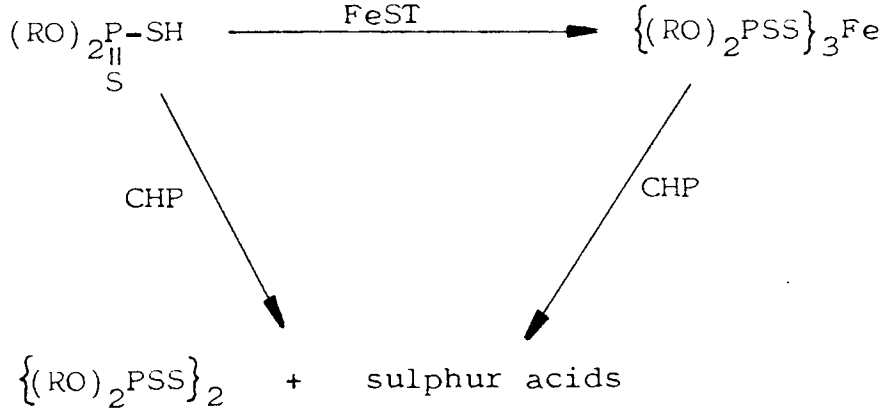

Scheme 4.2. Reactions of DRDPA in the presence of FeST and CHP

4.3.2.4. EFFECT OF DRTPA

The effectiveness of DRTPA as an inhibitor of decalin oxidation initiated by both FeST and CHP (Figure 4.18.), is less than that of DRDPA under the same conditions. (Figure 4.17.). Despite this, the type of effect given by DRTPA is similar to that of DRDPA, and therefore a mechanism analogous to that shown in Scheme 4.2. may be used to explain its action.

4.4. SUMMARY OF CHAPTER FOUR

The oxidation of both white oil (Figure 4.1.) and decalin (Figure 4.2.) is catalysed by as little as 10ppm ($2x10^{-4}moldm^{-3}$) FeST, the observed catalysis being due to the decompositon of hydroperoxides by the Fe^{2+}/Fe^{3+} redox system. Due to the presence of two tertiary hydrogen atoms, decalin is the more susceptible to iron catalysed oxidation in both the presence and absence of inhibitors. (see Section 3.4.).

In the absence of added hydroperoxide the effectiveness of ZnDRP and b-ZnDRP as antioxidants is severely reduced in the presence of $2x10^{-4}moldm^{-3}$ FeST. (Figures 4.3. - 4.5.). The induction periods observed are relatively short, which shows that the original zinc complexes are consumed more rapidly in the presence of FeST. The products initially formed from ZnDRP

or b-ZnDRP are inactive under these conditions, and a period of rapid oxidation follows the end of the induction period. The formation of sulphur acids from the further oxidation of the initial decomposition products of ZnDRP results in a period of slow oxidation, (Figures 4.3. - 4.5.), similar to that observed in the absence of FeST. (Chapter 3, Figure 3.4.).

DRDS is shown to be initially ineffective as an inhibitor of iron catalysed oxidation. (Figures 4.6. and 4.7.). The slow uptake of oxygen observed in the later stages (Figure 4.6.) is similar to that of the third stage seen in the presence of ZnDRP. (Figure 4.3.). The intermediate formation of some DRDS during the inhibition of hydrocarbon oxidation by ZnDRP is therefore likely, despite the presence of FeST.

In the presence of added CHP, ZnDRP is rapidly oxidised, and no induction period is observed. (Figures 4.11. - 4.12.). The slow auto-retarding oxidation observed is evidence that, in the presence of FeST, hydroperoxide decomposition promoted by sulphur acids, formed from the interaction of ZnDRP and CHP, is still occurring. The effectiveness of these acids is however somewhat reduced when compared to their activity under similar conditions in the absence of FeST. This indicates that partial consumption

of the sulphur acids by reaction with the FeST is probably taking place. The possibility that the acids may overcome the effect of the FeST as a catalyst for hydroperoxide decomposition by reducing the hydroperoxide content of the system to zero is unlikely, as the continuing uptake of oxygen during the slow stage implies that a finite, if very low, concentration of hydroperoxides must remain present. The generation of sulphur acids from the oxidation of ZnDRP by CHP, cannot be wholly via the intermediate formation of DRDS as the disulphide is less effective than ZnDRP as an inhibitor of hydrocarbon oxidation catalysed by both CHP and FeST.

The reaction of DRDPA with FeST leads to the formation of FeDRP. This contrasts with the lack of reaction given by ZnDRP or DRDS with FeST. The lack of inhibition given by DRDPA in the presence of FeST (Figures 4.8. and 4.9.) must be due to the stearic acid formed as a by-product of the reaction which produces FeDRP. In the presence of added CHP, however, the formation of very powerful sulphur acids from the DRDPA/CHP interaction is able to overcome the effect of any stearic acid formed in the competing DRDPA/FeST reaction, and effective inhibition results. (Fugres 4.16 and 4.17). Any FeDRP produced "in-situ" by the latter reaction is rapidly oxidised by the CHP. Under corresponding conditions DRTPA appears

to act via mechanisms analogous to those described above for DRDPA. The lesser degree of inhibition achieved for DRTPA (Figure 4.18.), is probably due to its lower sulphur content which limits the amount of sulphur acids formed.

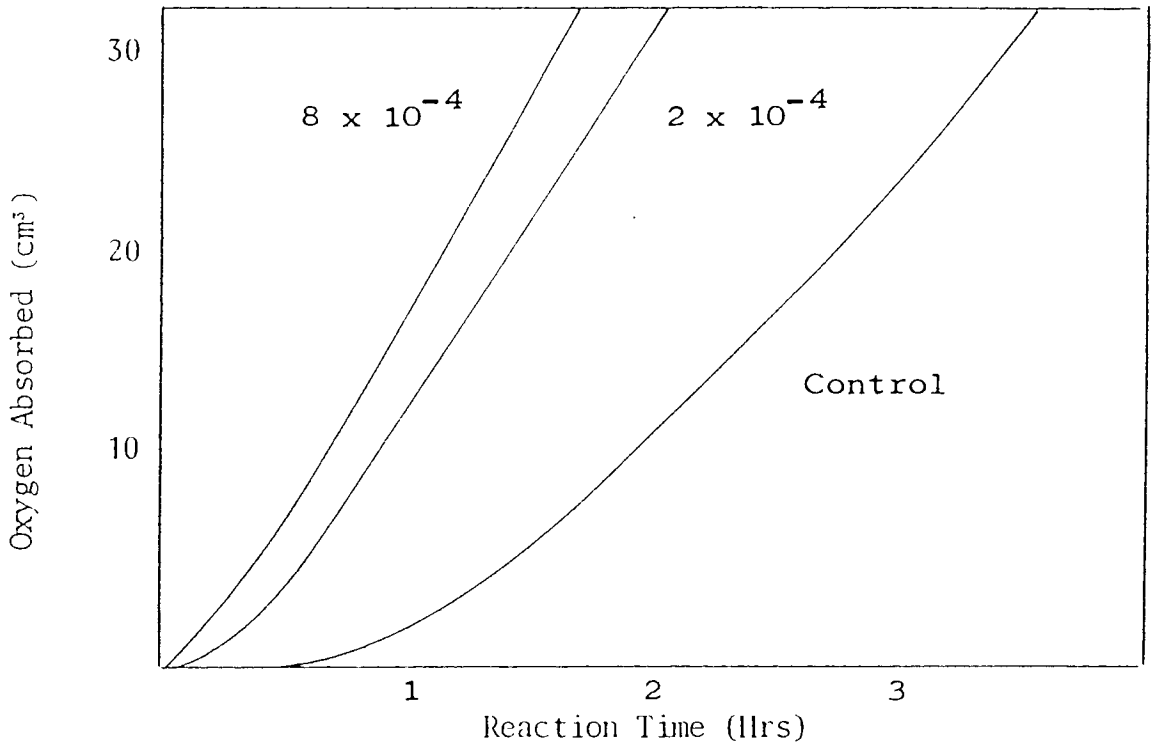

Figure 4.1. Oxidation of White Oil at 130°C in the Presence of FeST. Numbers on Curves are Concentrations of FeST in moldm^{-3}.

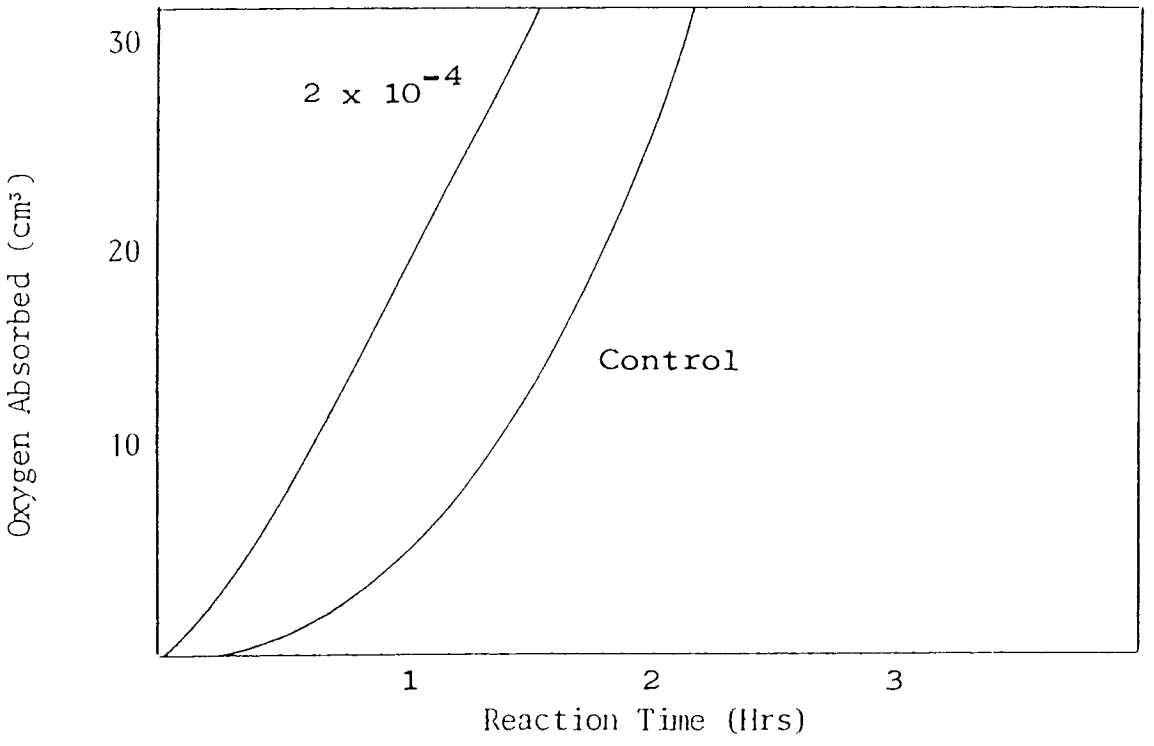

Figure 4.2. Oxidation of Decalin at 130°C in the Presence of FeST. Number on Curve is Concentration of FeST in moldm^{-3}.

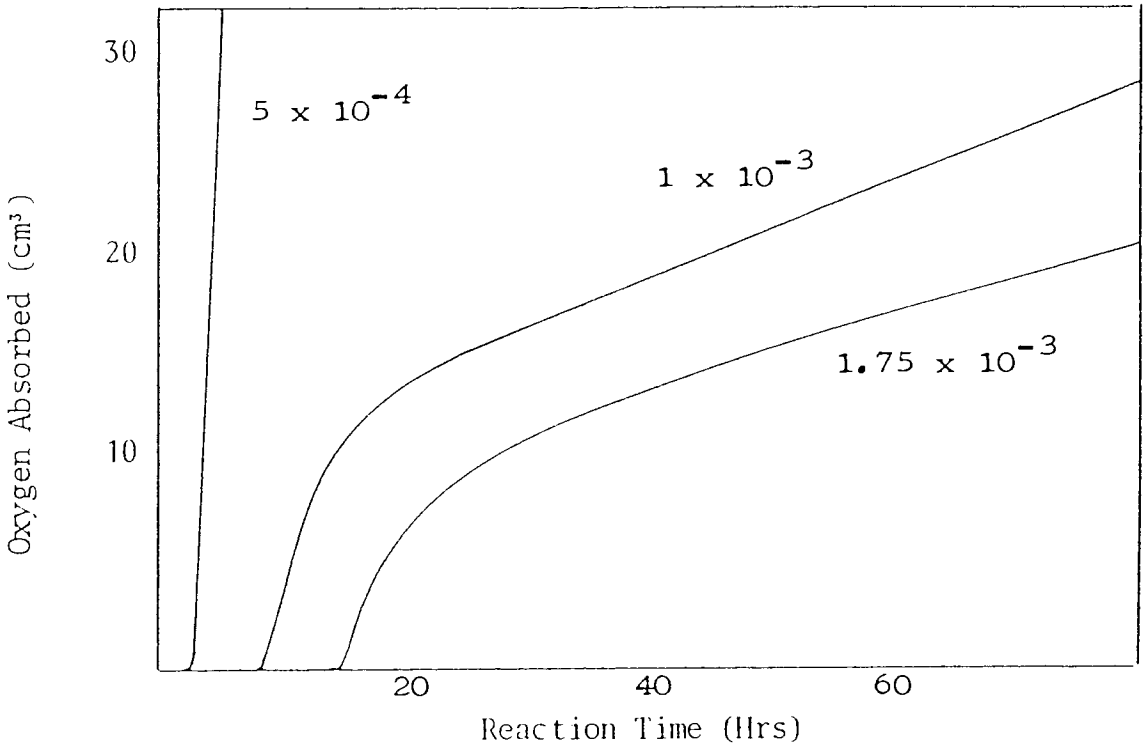

Figure 4.3. Effect of ZnDiBP on the Oxidation of White Oil at 130°C in the Presence of 2 x 10^{-4}moldm^{-3} FeST. Numbers on Curves are Concentrations of ZnDiBP in moldm^{-3}.

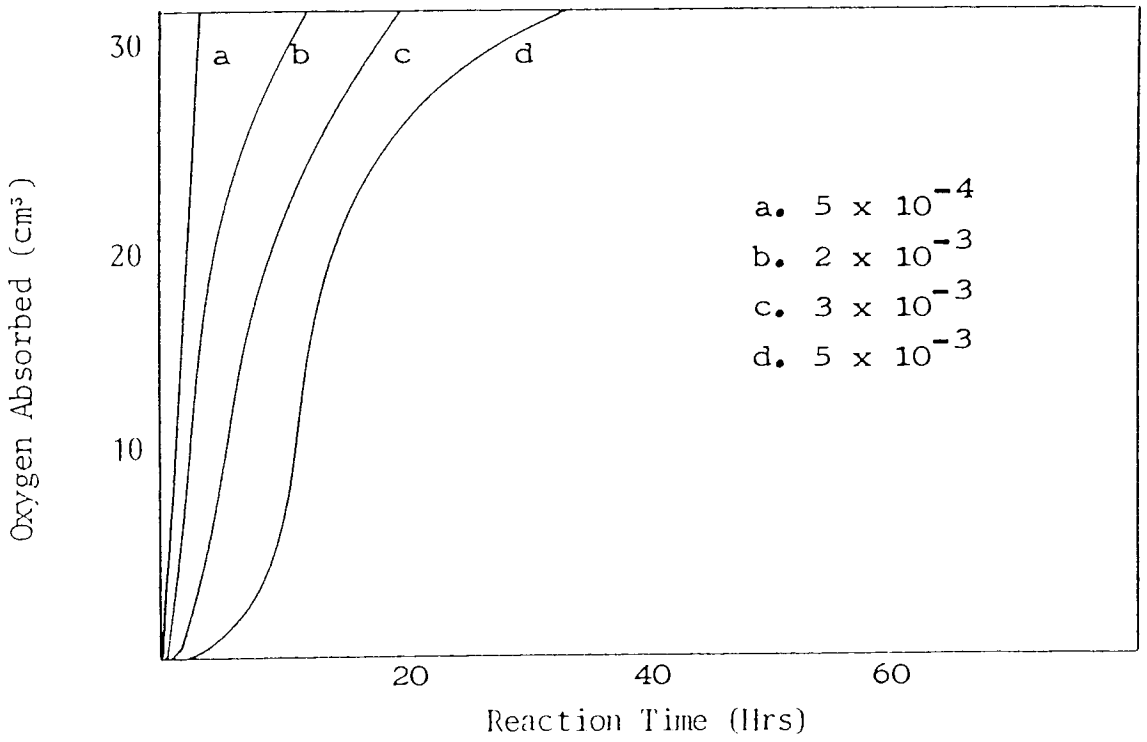

Figure 4.4. Effect of ZnDiBP on the Oxidation of Decalin at 130°C in the Presence of 2 x 10^{-4}moldm^{-3} FeST. Numbers on Curves are Concentrations of ZnDiBP in moldm^{-3}.

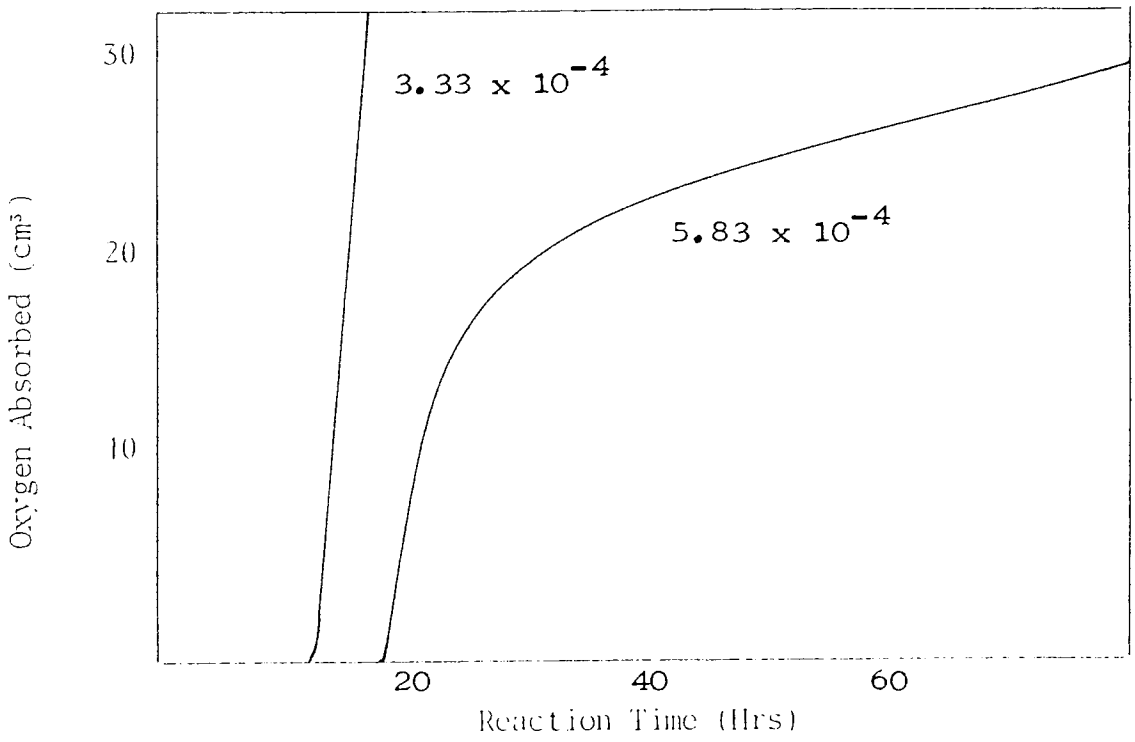

Figure 4.5. Effect of b-ZnDiBP on the Oxidation of White Oil at 130°C in the Presence of 2 x 10^{-4}moldm^{-3} FeST. Numbers on Curves are Concentrations of b-ZnDiBP in moldm^{-3}.

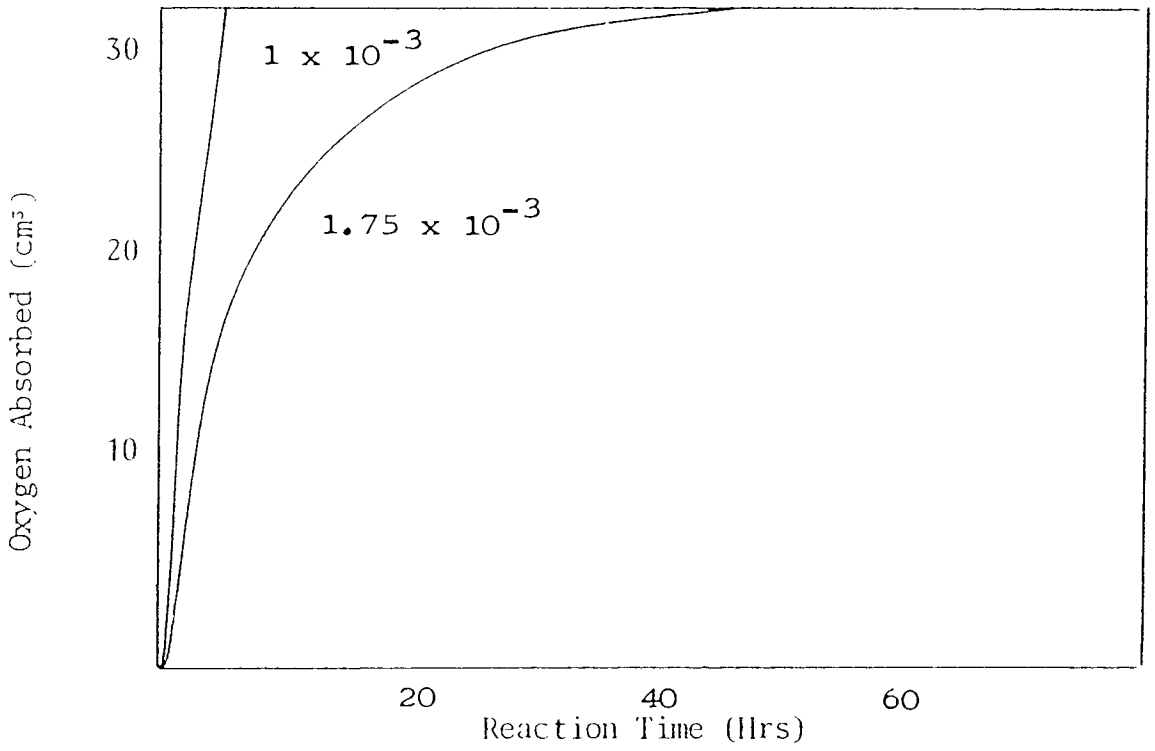

Figure 4.6. Effect of DiBDS on the Oxidation of White Oil in the Presence of 2×10^{-4} moldm^{-3} FeST. Numbers on Curves are Concentrations of DiBDS in moldm^{-3}.

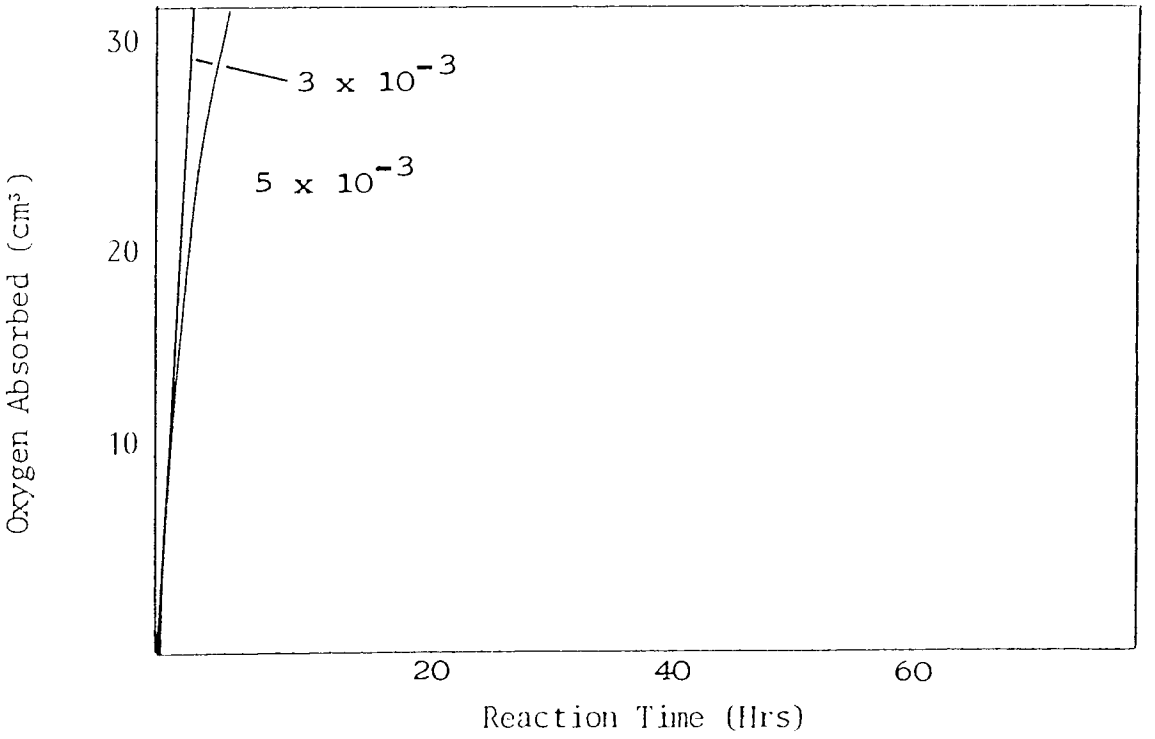

Figure 4.7. Effect of DiBDS on the Oxidation of Decalin at 130°C in the Presence of 2×10^{-4} moldm^{-3} FeST. Numbers on Curves are Concentrations of DiBDS in moldm^{-3}.

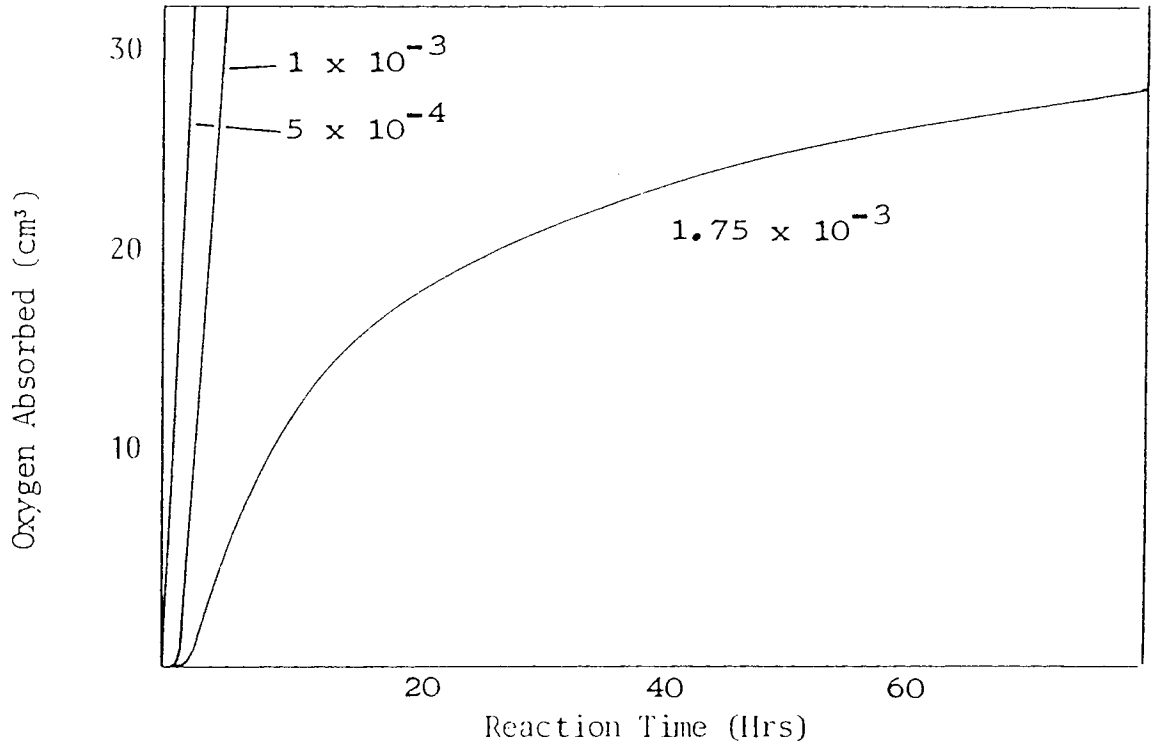

Figure 4.8. Effect of DsBDPA on the Oxidation of White Oil at 130°C in the Presence of 2×10^{-4} moldm^{-3} FeST. Numbers on Curves are Concentrations of DsBDPA in moldm^{-3}.

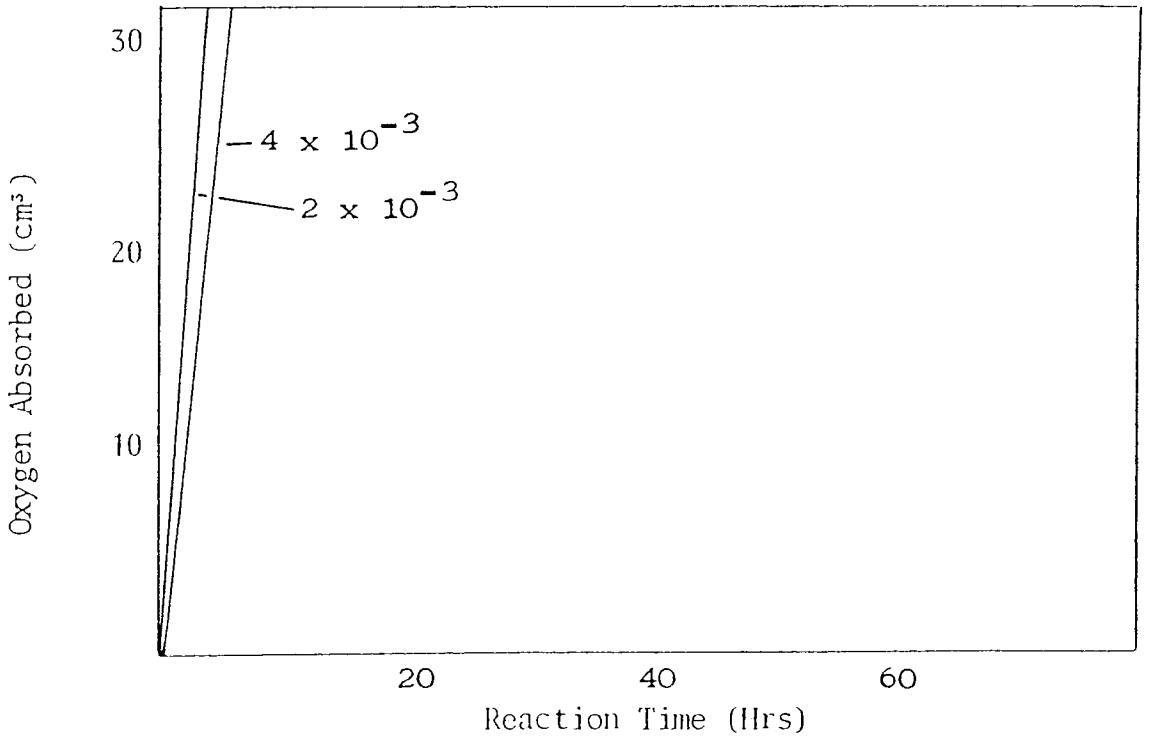

Figure 4.9. Effect of DnHDPA on the Oxidation of Decalin in the Presence of 2×10^{-4} moldm^{-3} FeST. Numbers on Curves are Concentrations of DnHDPA in moldm^{-3}.

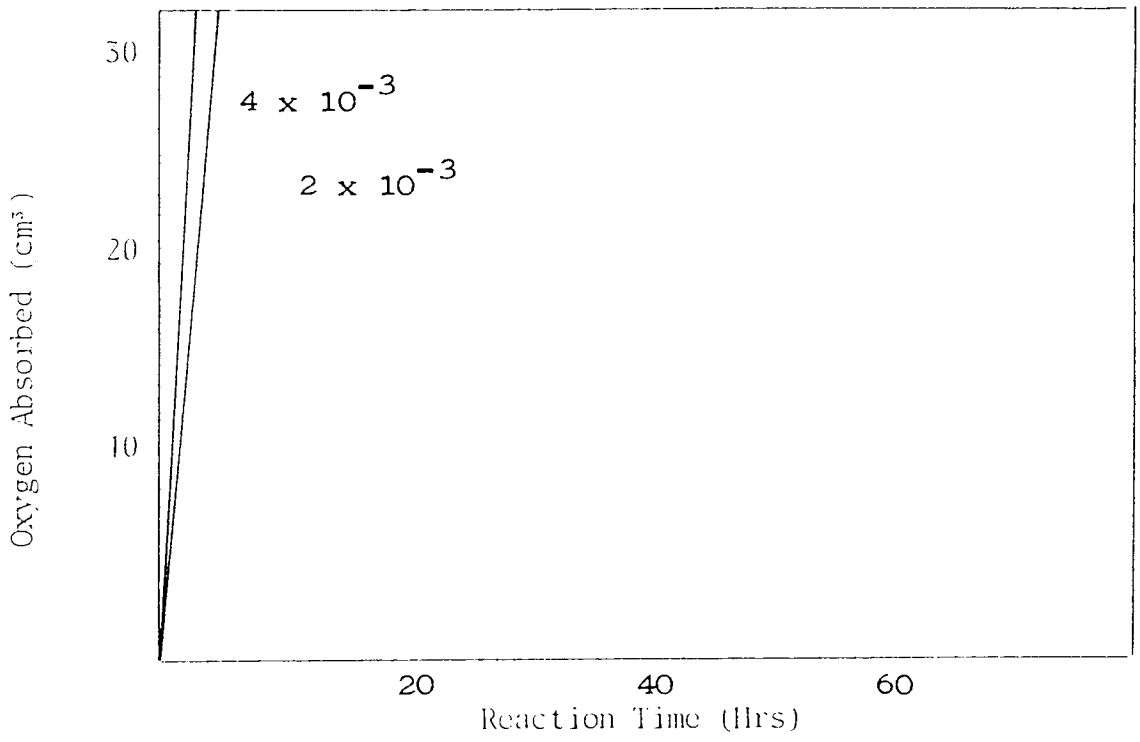

Figure 4.10. Effect of DiBTPA on the Oxidation of Decalin at 130°C in the Presence of 2×10^{-4} moldm^{-3} FeST. Numbers on Curves are Concentrations of DiBTPA in moldm^{-3}.

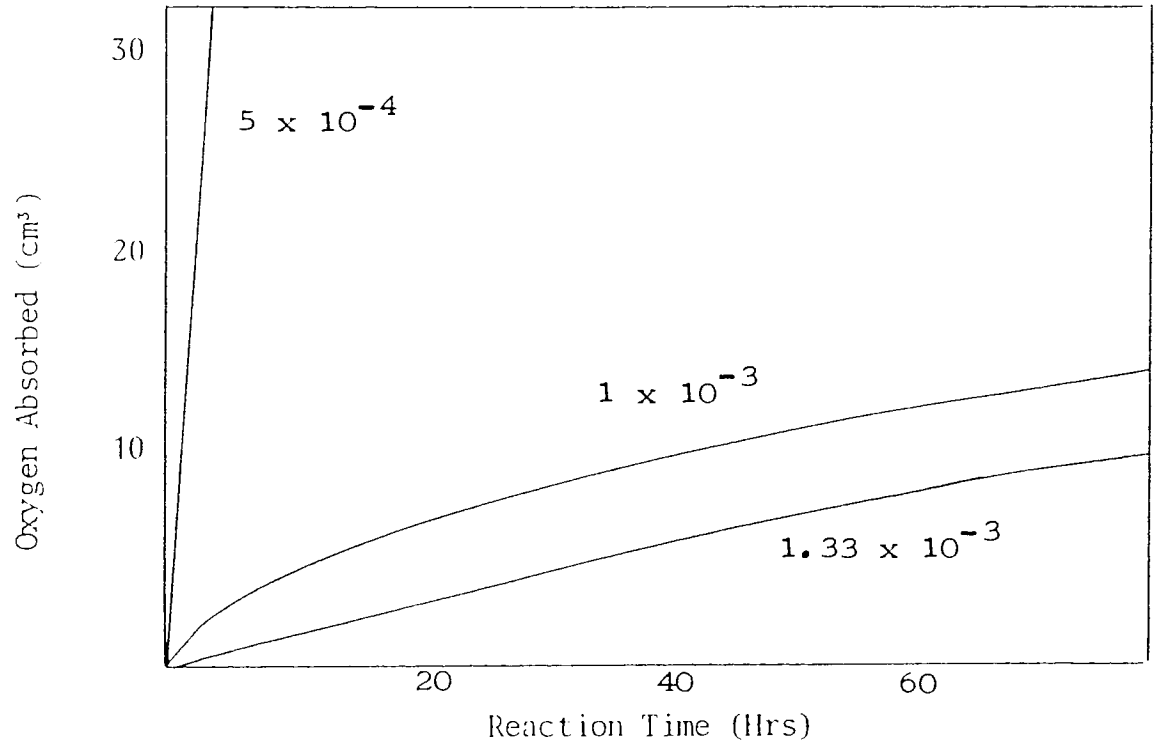

Figure 4.11. Effect of ZnDiBP on the Oxidation of White Oil at 130°C in the Presence of 1 x 10^{-2}moldm^{-3} CHP and 2 x 10^{-4}moldm^{-3} FeST. Numbers on Curves are Concentrations of ZnDiBP in moldm^{-3}.

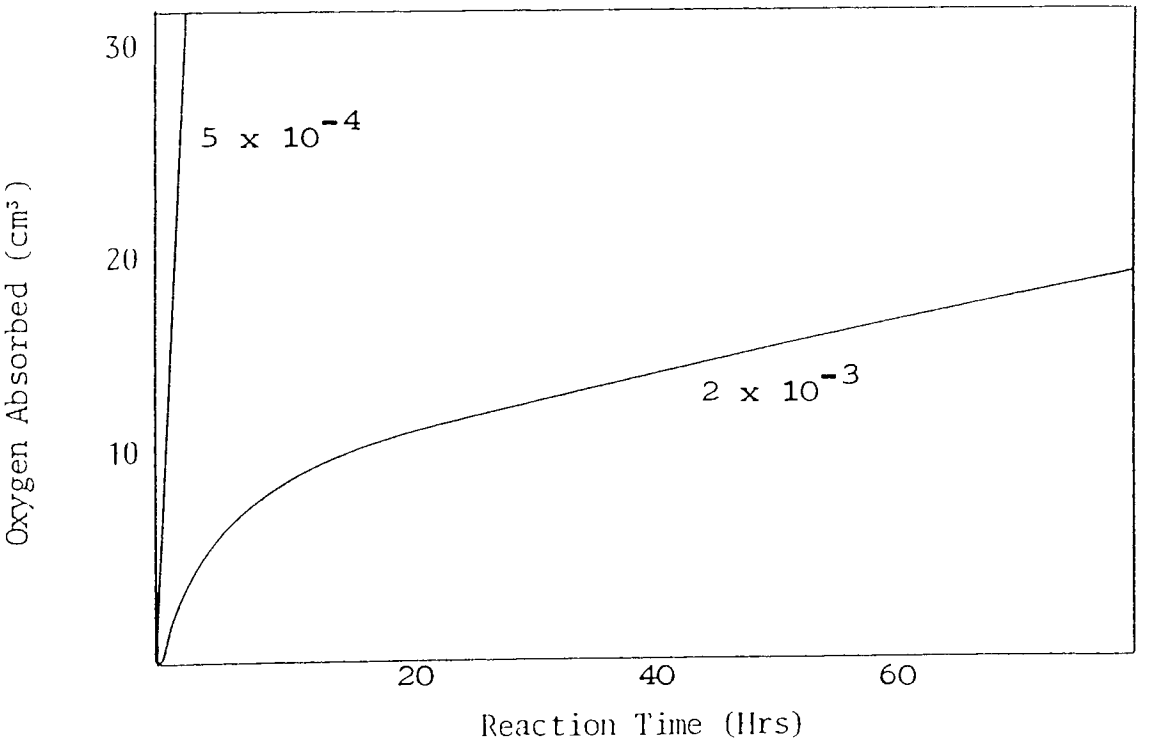

Figure 4.12. Effect of ZnDiBP on the Oxidation of Decalin at 130°C in the Presence of 1 x 10^{-2}moldm^{-3} CHP and 2 x 10^{-4}moldm^{-3} FeST. Numbers on Curves are Concentrations of ZnDiBP in moldm-3

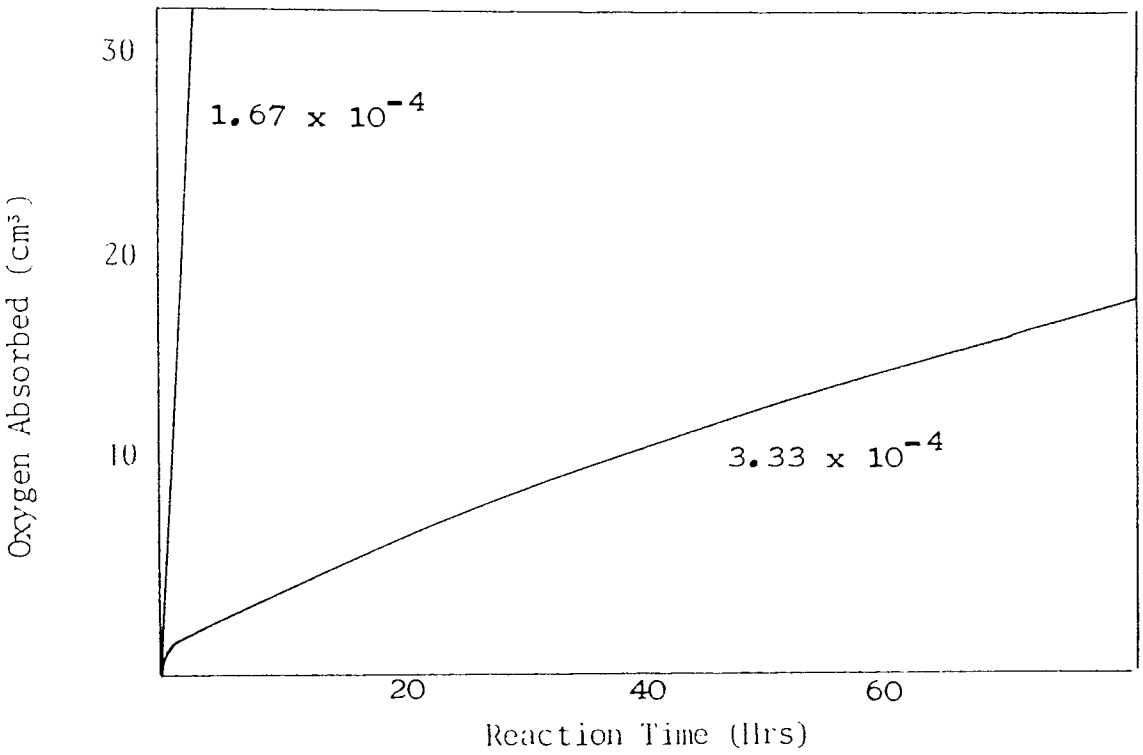

Figure 4.13. Effect of b-ZnDiBP on the Oxidation of White Oil at 130°C in the Presence of 1 x 10^{-2}moldm^{-3} CHP and 2 x 10^{-4}moldm^{-3} FeST. Numbers on Curves are Concentrations of b-ZnDiBP in moldm^{-3}.

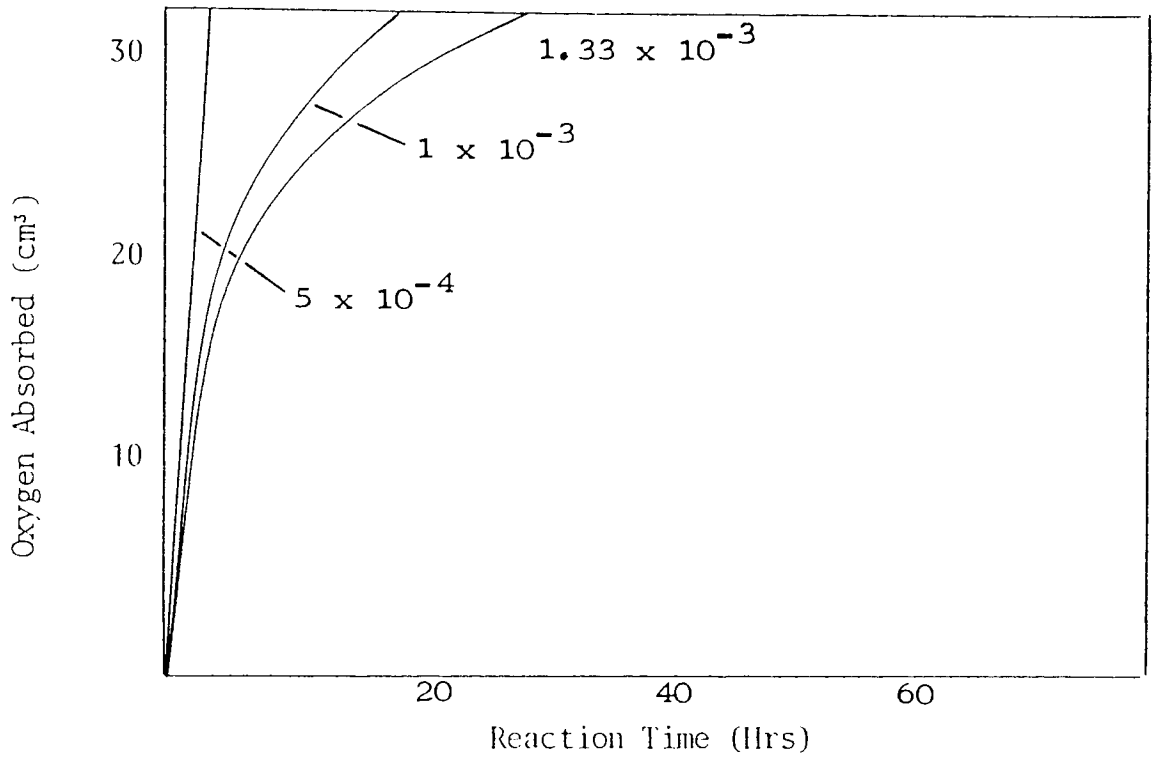

Figure 4.14. Effect of DiBDS on the Oxidation of White Oil at 130°C in the Presence of 1 x 10^{-2}moldm^{-3} CHP and 2 x 10^{-4}moldm^{-3} FeST. Numbers on Curves are Concentrations of DiBDS in moldm^{-3}.

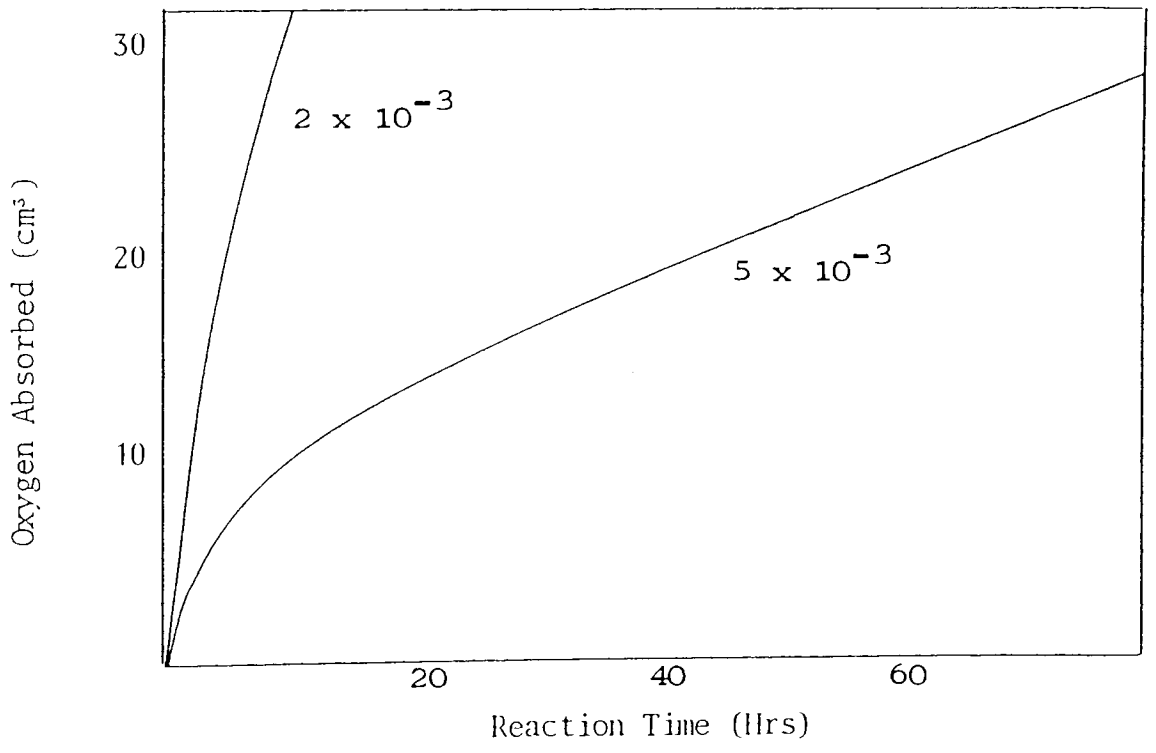

Figure 4.15. Effect of DiBDS on the Oxidation of Decalin at 130°C in the Presence of 1 x 10^{-2}moldm^{-3} CHP and 2 x 10^{-4}moldm^{-3} FeST. Numbers on Curves are Concentrations of DiBDS in moldm^{-3}

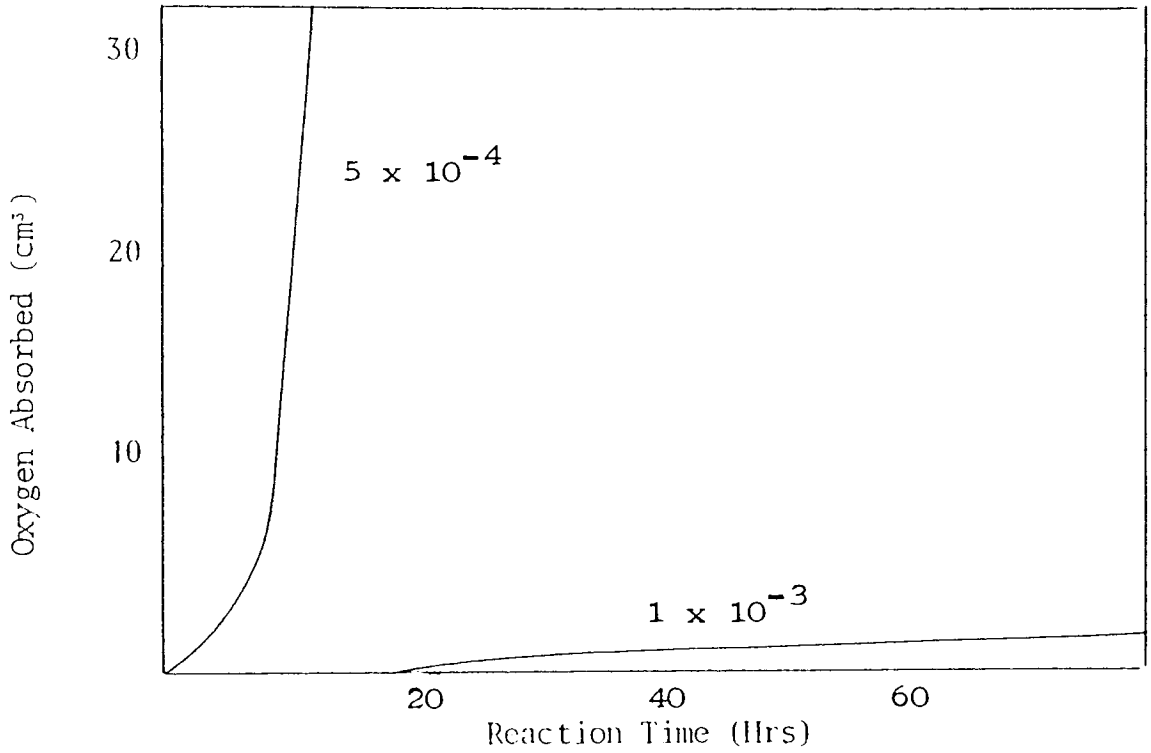

Figure 4.16. Effect of DsBDPA on the Oxidation of White Oil at 130°C in the Presence of 1 x 10^{-2}moldm^{-3} CHP and 2 x 10^{-4}moldm^{-3} FeST. Numbers on Curves are Concentrations of DsBDPA in moldm^{-3}.

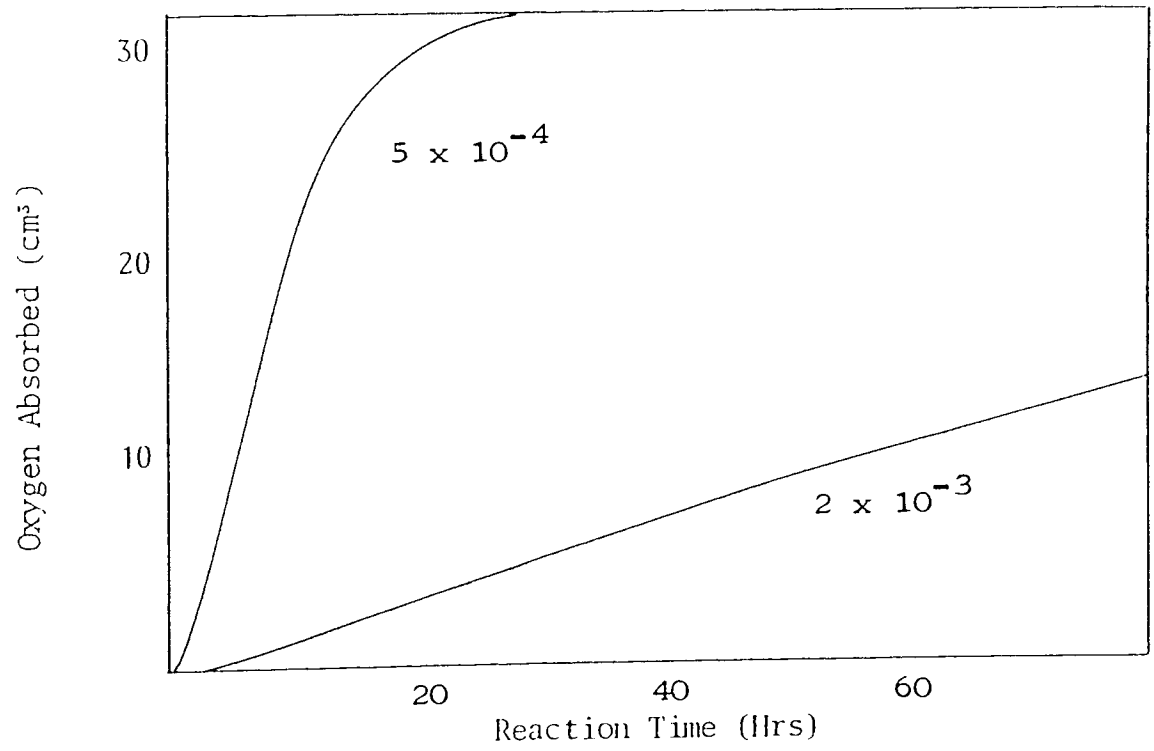

Figure 4.17. Effect of DnHDPA on the Oxidation of Decalin at 130°C in the Presence of 1 x 10^{-2}moldm^{-3} CHP and 2 x 10^{-4}moldm^{-3} FeST. Numbers on Curves are Concentrations of DnHDPA in moldm^{-3}.

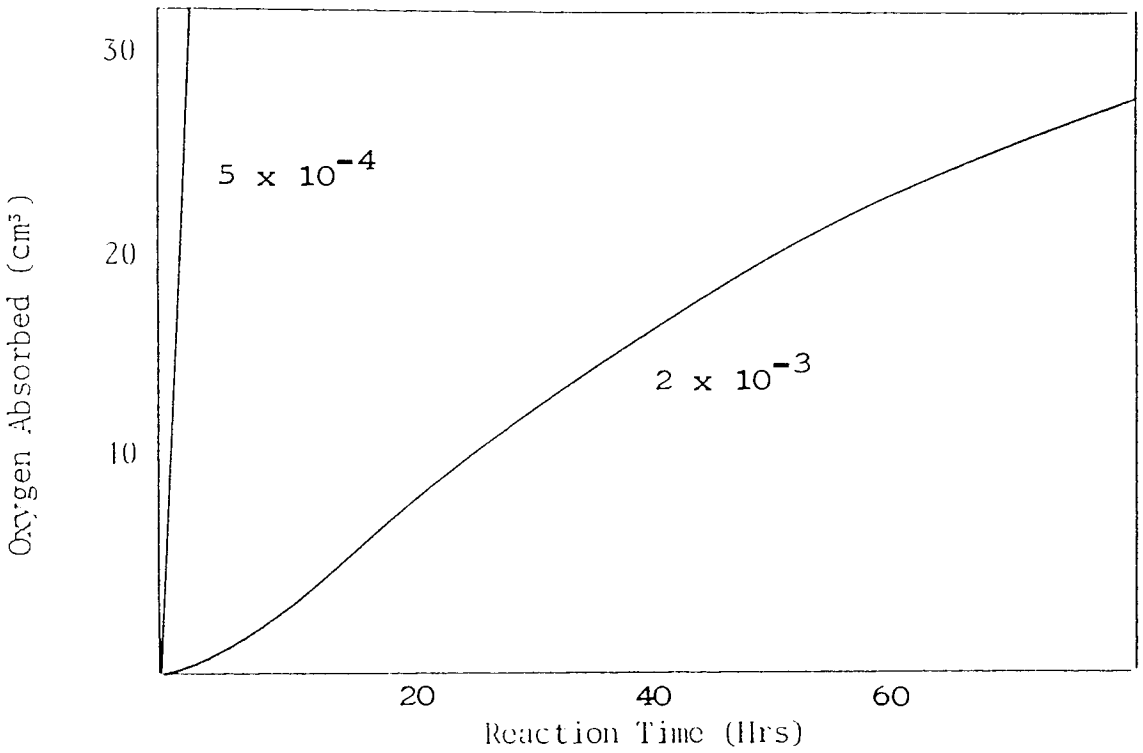

Figure 4.18. Effect of DiBTPA on the Oxidation of Decalin at 130°C in the Presence of 1 x 10^{-2}moldm^{-3} CHP and 2 x 10^{-4}moldm^{-3} FeST. Numbers on Curves are Concentrations of DiBTPA in moldm^{-3}.

CHAPTER FIVE

THE REACTIONS OF ZINC DIALKYLDITHIOPHOSPHATES AND RELATED COMPOUNDS WITH HYDROPEROXIDES

5.1. OBJECT

The effectiveness of the dialkyl dithiophosphates, (zinc dialkyldithiophosphates (ZnDRP), basic zinc dialkyldithiophosphates (b-ZnDRP), dialkylthiophosphoryl disulphides (DRDS), and dialkyldithiophosphoric acids (DRDPA)), along with the dialkylthiophosphoric acids (DRTPA), as inhibitors of cumene hydroperoxide (CHP) initiated oxidation of hydrocarbons, both in the presence and absence of iron (III) stearate (FeST), has been demonstrated in Chapters 3 and 4. The observed behaviour is consistent with the idea that it is the products of the dithiophosphate - hydroperoxide reaction that are the true antioxidant species.[7] In this chapter the reactions between the dithiophosphates and CHP are studied, both in the presence and absence of FeST.

The disappearance of CHP in the presence of the dithiophosphates in chlorobenzene at 110°C is measured as a function of time by the hydroperoxide determination method. (Section 2.2.2.). Analysis of the decomposition products derived from CHP is carried out by gas-liquid chromatography (GLC), (Section 2.2.3.) so that the mechanism of CHP

decomposition by each of the dithiophosphates may be determined. In the hydroperoxide decomposition experiments the initial concentration of CHP is fixed at $1x10^{-2}moldm^{-3}$ and the dithiophosphate concentrations are varied between $1x10^{-4}$ - $2x10^{-3}moldm^{-3}$ so that the CHP:dithiophosphate ratios are similar to those used in the oxygen absorption experiments. (Chapters 3 and 4). A fixed FeST concentration of $2x10^{-4}moldm^{-3}$ is used when appropriate.

The phosphorus containing products of the reactions of the dithiophosphates with CHP are identified by ^{31}P nuclear magnetic resonance spectroscopy. (^{31}P NMR) (Section 2.2.5.). Unfortunately the sensitivity of the technique, combined with restrictions on instrument time available, means that the concentrations of both dithiophosphate ($1x10^{-1}$ - $2x10^{-1}moldm^{-3}$) and CHP ($2x10^{-1}$ - $5x10^{-1}moldm^{-3}$) used in most of the ^{31}P NMR experiments are much higher than those used in the hydroperoxide decomposition studies. In addition ^{31}P NMR cannot be carried out in the presence of paramagnetic iron (III) compounds and therefore no reactions involving FeST are studied by this technique.

Scheme 5.1. summarises the work carried out in the present chapter.

5.2. RESULTS

5.2.1. DECOMPOSITION OF CHP BY DITHIOPHOSPHATES IN THE ABSENCE OF FeST

5.2.1.1. DECOMPOSITION OF CHP BY ZnDRP AND b-ZnDRP

The decomposition of $1x10^{-2}moldm^{-3}$ CHP by various concentrations of the isobutyl substituted zinc complexes (ZnDiBP and b-ZnDiBP) in chlorobenzene at 110°C is shown in Figures 5.1. and 5.2. An initial fast decomposition step was followed by a slower second stage for all concentrations of zinc complex used. At equivalent phosphorus concentrations, e.g. $1x10^{-4}moldm^{-3}$ ZnDiBP and $3.33x10^{-5}moldm^{-3}$ b-ZnDiBP, the extent of decomposition achieved by the two types of zinc complex was very similar. The first stage lasted about 10 minutes and was most apparent at high ZnDiBP or b-ZnDiBP concentrations. The rate of the second stage seemed to be independent of the initial concentration of zinc complex and continued until the end of the experiment (c. 7 hours) at all concentrations studied. Very little decomposition of CHP was achieved by ZnDiBP concentrations of less than $2.5x10^{-4}moldm^{-3}$ or by b-ZnDiBP concentrations of less than $5x10^{-5}moldm^{-3}$.

The build up of products arising from the decomposition of CHP by ZnDiBP (CHP:ZnDiBP = 5:1) is shown in Figure 5.3. The initially formed products are acetophenone and α-cumyl alcohol. Although the concentration of acetophenone continues to rise throughout,

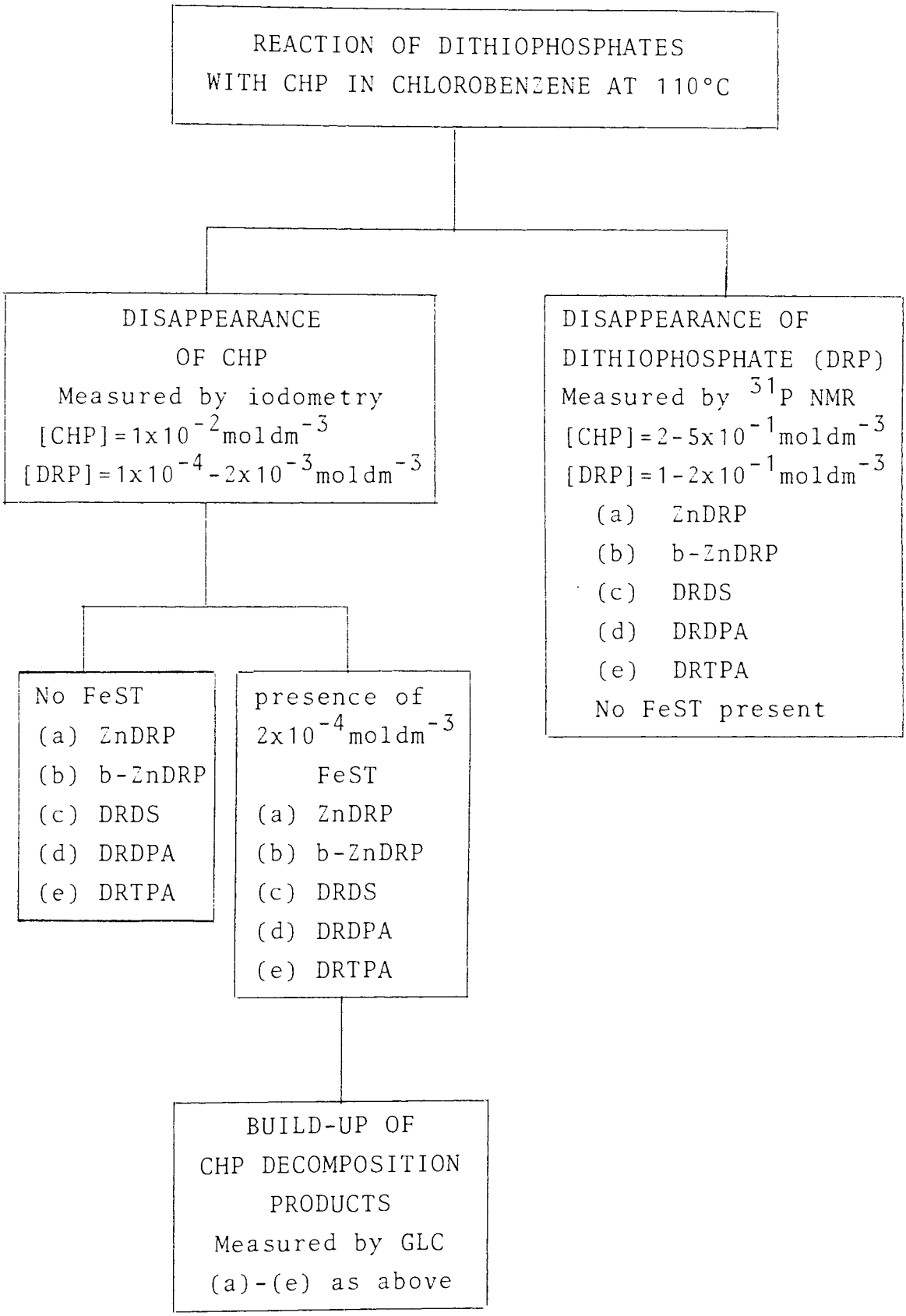

Scheme 5.1. Experiments described in Chapter 5.

the level of α-cumyl alcohol present decreases steadily from its maximum value early in the reaction. At the same time the concentration of α -methyl styrene rises steadily and reaches a level similar to that of the maximum α-cumyl alcohol value. The formation of phenol only occurs in the later stages of the reaction and even then only builds up slowly.

5.2.1.2. DECOMPOSITION OF CHP BY DRDS

The decomposition of $1x10^{-2}moldm^{-3}$ CHP by various concentrations of the isobutyl substituted disulphide (DiBDS) in chlorobenzene at 110°C is shown in Figure 5.4. The reaction took place in two stages, a period of slow decomposition (induction period) being followed by a very rapid disappearance of the CHP. The length of the induction period decreased with increasing DiBDS concentration so that the rapid decomposition step occurred immediately when a DiBDS concentration of $2x10^{-3}moldm^{-3}$ was used. (CHP:DiBDS = 5:1).

5.2.1.3. DECOMPOSITION OF CHP BY DRDPA

The decomposition of $1x10^{-2}moldm^{-3}$ CHP by various concentrations of the n-hexyl substituted dithiophosphoric acid (DnHDPA) in chlorobenzene at 110°C is shown in Figure 5.5. A rapid decomposition was achieved by all concentrations used ($1x10^{-4}$ - $2x10^{-3}moldm^{-3}$, CHP:DnHDPA = 100:1 - 5:1) so that all the CHP had been consumed within 60 minutes.

5.2.1.4. DECOMPOSITION OF CHP BY DRTPA

The decomposition of $1x10^{-2}moldm^{-3}$ CHP by various concentrations of the isobutyl substituted thiophosphoric acid (DiBTPA) in chlorobenzene at 110°C is shown in Figure 5.6. As for DnHDPA (Figure 5.5.), a rapid decomposition of CHP was achieved by all DiBTPA concentrations used. (Figure 5.6.).

5.2.2. DECOMPOSITION OF CHP BY DITHIOPHOSPHATES IN THE PRESENCE OF FeST

5.2.2.1. DECOMPOSITION OF CHP BY FeST

The decomposition of $1x10^{-2}moldm^{-3}$ CHP by $2x10^{-4}moldm^{-3}$ FeST in chlorobenzene at 110°C is shown in Figure 5.7. A gradual disappearance of the CHP occurred so that 75% of the hydroperoxide remained after 5 hours. Also shown in Figure 5.7. is the decomposition of $1x10^{-2}moldm^{-3}$ CHP at 110°C in chlorobenzene in the absence of any additives. No decomposition had occurred after 5 hours.

5.2.2.2. DECOMPOSITION OF CHP BY ZnDRP AND b-ZnDRP

The decomposition of $1x10^{-2}moldm^{-3}$ CHP by various concentrations of ZnDiBP and b-ZnDiBP in the presence of $2x10^{-4}moldm^{-3}$ FeST in chlorobenzene at 110°C is shown in Figures 5.8. and 5.9. The effects of the two types of zinc complex were very similar, although

slightly more CHP was decomposed by ZnDiBP than by b-ZnDiBP at equivalent phosphorus concentrations. At high concentrations of zinc complex a rapid initial decomposition was followed by a much slower disappearance of the CHP. The initial step lasted about 10 minutes for both types of zinc complex. At ZnDiBP concentrations $\leqslant 2.5 \times 10^{-4} moldm^{-3}$ (b-ZnDiBP concentrations $\leqslant 1 \times 10^{-4} moldm^{-3}$) the decomposition proceeded in apparently only one stage, the rate of which was intermediate between those of the fast and slow stages promoted by a high concentration of zinc complex. The rate of this single stage increased with decreasing zinc complex concentration so that in the long-term, i.e. at reaction times in excess of 2 hours, the amount of CHP decomposed was greatest at the lowest concentration used, i.e. $4 \times 10^{-5} moldm^{-3}$ ZnDiBP (CHP:ZnDiBP = 250:1) or $3.3 \times 10^{-5} moldm^{-3}$ b-ZnDiBP (CHP:b-ZnDiBP = 300:1).

Figures 5.10.-5.12. show the build-up of the products derived from $1 \times 10^{-2} moldm^{-3}$ CHP when decomposed by various concentrations of ZnDiBP in the presence of $2 \times 10^{-4} moldm^{-3}$ FeST in chlorobenzene of 110°C. The initial product formed from the decomposition of CHP by ZnDiBP was α-cumyl alcohol. The concentration of α-cumyl alcohol formed was greatest (c. 38%) at the highest ZnDiBP concentration used (Figure 5.10.), and did not vary much after the first 15 minutes. Lower concentrations of ZnDiBP gave lower amounts (6-10%) of α- cumyl alcohol. (Figures 5.11. and 5.12.).

For all concentrations of ZnDiBP studied, the build up of acetophenone occurred from the very early stages and was gradual throughout the reaction. An increase in ZnDiBP concentration led to a slight increase in the amount of acetophenone formed, but in all cases it did not exceed a 15% yield. Although α-methyl styrene was only detected when present in yields above 10%, and was therefore not observed until the later stages of the reactions, its formation also seemed to be slightly favoured by a high concentration of ZnDiBP. (Figure 5.10.).

The build-up of phenol was always delayed until some time into the reaction. Low concentrations of zinc complex led to the highest yields of phenol. (Figures 5.11. and 5.12.). The rate of formation of phenol was particularly fast at a ZnDiBP concentration of $1x10^{-4}moldm^{-3}$ (Figure 5.12.), a yield of 60% was formed in this case. Conversely, very little phenol was formed when a relatively high concentration of $2x10^{-3}moldm^{-3}$ ZnDiBP was used (Figure 5.10.).

Figures 5.13. and 5.14. shown the build up of the products derived from $1x10^{-2}moldm^{-3}$ CHP when decomposed by various concentrations of b-ZnDiBP in the presence of $2x10^{-4}moldm^{-3}$ FeST in chlorobenzene at 110°C. At a high b-ZnDiBP concentration the initial product formed was α-cumyl alcohol, which remained at a constant low concentration (c. 10%) throughout. (Figure 5.13.). The amount of α-cumyl alcohol formed

by a lower b-ZnDiBP concentration (Figure 5.14.) was lower (c. 5%), and built up during the reaction. At this lower concentration of $3.3x10^{-5}moldm^{-3}$ the initial product formed was α-methyl styrene, the level of which remained consistent at 10-13% throughout the reaction. At both b-ZnDiBP concentrations (Figures 5.13. and 5.14.), the formation of acetophenone and phenol was not observed until about 60 minutes into the reaction. Acetophenone built up very slowly in both cases. The build up of phenol was dependent on the b-ZnDiBP concentration, so that a yield of about 40% was obtained from the lower concentration $3.3x10^{-5}moldm^{-3}$ (Figure 5.14.) in the same time that less than 15% was formed when a relatively high concentration ($1x10^{-4}moldm^{-3}$) was used (Figure 5.13.).

5.2.2.3. DECOMPOSITION OF CHP BY DRDS

The decomposition of $1x10^{-2}moldm^{-3}$ CHP by various concentrations of DiBDS in the presence of $1x10^{-4}moldm^{-3}$ FeST in chlorobenzene at 110°C is shown in Figure 5.15. As in the absence of FeST (Figure 5.4.), the decomposition appeared to occur in two stages, although the second, faster stage was not as rapid in the presence of FeST and therefore not as clear as in its absence. The length of the slower initial stage decreased with increasing DiBDS concentration, so that at a concentration of $2x10^{-3}moldm^{-3}$ the disappearance of CHP commenced immediately.

Figures 5.16. - 5.18. show the build up of the products derived from $1x10^{-2}moldm^{-3}$ CHP by various concentrations of DiBDS in the presence of $2x10^{-4}moldm^{-3}$ FeST in chlorobenzene at 110°C. At a high concentration of DiBDS ($2x10^{-3}moldm^{-3}$, Figure 5.1.), a rapid initial build up of α-cumyl alcohol occurred, which reached a maximum value of around 45% after 20 minutes. Subsequent to this time the concentration of α-cumyl alcohol present slowly decreased. Similar behaviour was observed when a lower concentration of DiBDS was used ($5x10^{-4}moldm^{-3}$, Figure 5.17), except that the build-up was much slower, so that the maximum concentration of cumyl alcohol was not reached until 3 hours into the reaction. At the lowest DiBDS concentration of $2.5\ X10^{-4}moldm^{-3}$ (Figure 5.18.), the α-cumyl alcohol build up was even slower so that the concentration was still rising after 5 hours.

The build-up of acetophenone was gradual in each case, but occurred most readily at the highest DiBDS concentration (Figure 5.16.). At low DiBDS concentrations (Figures 5.17. and 5.18.), the formation of phenol was delayed for some time, and the amounts formed even in the later stages were low. At the highest concentration used however ($2x10^{-3}moldm^{-3}$, Figure 5.16.), phenol began to appear after 10 minutes and built up steadily to reach a yield of greater than

50%. The presence of α-methyl styrene was only detected after prolonged reaction times. (not shown on Figures 5.16. - 5.18.).

5.2.2.4. DECOMPOSITION OF CHP BY DRDPA

The decomposition of $1x10^{-2}moldm^{-3}$ CHP by various concentrations of DnHDPA in the presence of $2x10^{-4}moldm^{-3}$ FeST in chlorobenzene at 110°C is shown in Figure 5.19. At all concentrations of DnHDPA used ($1x10^{-4}$ - $2x10^{-3}moldm^{-3}$), a rapid decomposition of CHP occurred immediately. The products of the complete decomposition of CHP by DnHDPA are shown in Table 5.1. At both concentrations of DnHDPA the major product was phenol, but a significant amount of acetophenone was also formed in each case. No α-cumyl alcohol or α-methyl styrene was detected for either DnHDPA concentration used.

Table 5.1. Products of the complete decomposition of CHP by DnHDPA in the presence of $1x10^{-4}moldm^{-3}$ FeST in chlorobenzene at 110°C. Initial CHP concentration = $1x10^{-2}moldm^{-3}$

DnHDPA concentration ($moldm^{-3}$)	Products formed (% yield)			
	αMS	AC	αCA	PH
$2x10^{-3}$	0	22.9	0	67.1
$1x10^{-4}$	0	18.7	0	71.3

5.2.2.5. DECOMPOSITION OF CHP BY DRTPA

The decomposition of $1x10^{-2}moldm^{-3}$ CHP by various concentrations of DiBTPA in the presence of $2x10^{-4}moldm^{-3}$ FeST in chlorobenzene at 110°C is shown in Figure 5.20. Two stages were observed to occur during the decomposition. A slow initial stage was followed by a faster decomposition of CHP. The length of the initial slow stage was shortest and the rate of the subsequent faster stage greatest when a high concentration of DiBTPA ($2x10^{-3}moldm^{-3}$) was used.

The products of the complete decomposition of CHP by DiBTPA are shown in Table 5.2. Despite the differences in the rate of CHP decomposition (Figure 5.20.) the product distributions (Table 5.2.) were remarkably similar. The major product was phenol with smaller amounts of α-methyl styrene and acetophenone also being formed. No α-cumyl alcohol was detected.

Table 5.2. Products of the complete decomposition of CHP by DiBTPA in the presence of $2x10^{-4}moldm^{-3}$ FeST in chlorobenzene at 110°C. Initial CHP concentration = $1x10^{-2}moldm^{-3}$

DiBTPA concentration ($moldm^{-3}$)	Products formed (% yield)			
	αMS	AC	αCA	PH
$2x10^{-3}$	20.1	13.4	0	66.6
$5x10^{-4}$	17.4	14.5	0	68.1

5.2.3. THE PRODUCTS OF THE OXIDATION OF DITHIOPHOSPHATES BY HYDROPEROXIDES

5.2.3.1. OXIDATION OF ZnDRP BY TBH AT 25°C

The phosphorus-containing products formed from the three hour reaction of TBH with excess ZnDiBP (ZnDiBP:TBH > 2:1) in heptane at 25°C as measured by ^{31}P NMR are shown in Table 5.3. At each ZnDiBP:TBH ratio studied, ZnDiBP was oxidised by TBH to give DiBDS and b-ZnDiBP only. The ratio of b-ZnDiBP:DiBDS formed was approximately 1:1, although it was slightly less than this at the highest concentration of TBH used. (Table 5.3.). Virtually all the original ZnDiBP was oxidised when ZnDiBP:TBH $\leqslant$ 3.8:1.

Table 5.3. Products of the oxidation of ZnDiBP ($5x10^{-1}moldm^{-3}$) by TBH in n-heptane at 25°C (δ = ^{31}P chemical shift in ppm).

TBH concentration ($moldm^{-3}$)	phosphorus % yield		
	ZnDiBP (δ=99.6)	b-ZnDiBP (δ=103.0)	DiBDS (δ=85.6)
$6.3x10^{-2}$	43	43	14
$1.3x10^{-1}$	7	70	23
$1.8x10^{-1}$	5	67	27

5.2.3.2. OXIDATION OF ZnDRP by CHP AT 110°C

The distribution of phosphorus-containing products formed during the reaction of ZnDiBP with excess CHP (CHP:ZnDiBP $\geq$ 1:1) in chlorobenzene at 110°C as measured by ^{31}P NMR is shown in Table 5.4., and the peak assignments are given in Table 5.5. along with comments regarding the conditions under which the various products are formed or decomposed. From Table 5.4. it is clear that the reaction of ZnDiBP with CHP leads to the formation of phosphorus-containing compounds having chemical shifts lower than that of the original zinc complex. This is indicative of the formation of highly oxygenated phosphorus species.[45] (Table 5.5.).

At CHP:ZnDiBP ratios of 10:1 and 50:1 a white solid was precipitated (C = 8.7%, H = 2.0%, S = 3.4%), whereas at a ratio of 5:1 a jelly-like material adhering to the reaction vessel was formed.

The decomposition of CHP by ZnDiBP under the same conditions at CHP:ZnDiBP ratios of 5:1 and 10:1 is shown in Figure 5.24. In each case a rapid initial step was followed by a slower decomposition of the CHP.

CHP:ZnDiBP ratio	Reaction time (minutes)	Phosphorus % yield (δvalues = ^{31}P shifts in ppm)																	
		103.0	98.2	94.4	89.7	85.2	84.2	83.8	78.9	64.2	59.7	52.9	48.3	46.3	28.9	24.5	21.0	15.6	-0.9
1:1 [CHP]=$2x10^{-1}moldm^{-3}$ [ZnDiBP]=$2x10^{-1}moldm^{-3}$	0	<1	99						<1					<1					
	30	33	9	1		39	6		4				7	2					
5:1 [CHP]=$0.5moldm^{-3}$ [ZnDiBP=$0.1moldm^{-3}$ (see Figure 5.21.)	0	<1	99						<1					<1					
	4					48	16		8				18	3			7		
	10					45	17		9				16				12		
	60					44	27		12								16		
10:1 [CHP]=$2moldm^{-3}$ [ZnDiBP]=$0.2moldm^{-3}$ (see Figure 5.22.)	0	<1	99						<1					<1					
	5					36	15	11	13			3			2		17	3	
	60			2		34	18	6	10			3			2		9	2	13
50:1 [CHP]=$1moldm^{-3}$ [ZnDiBP]=$2x10^{-2}moldm^{-3}$ (see Figure 5.23.)	0	<1	99						<1					<1					
	10					23	11	14	12			2					31	8	
	180			3	5	14	15		12	16	6	4				12		6	8

Table 5.4. Products of the oxidation of ZnDiBP by CHP in chlorobenzene at 110°C

Table 5.5. Assignments to peaks shown in Table 5.4.

Chemical shift (ppm)	Assignment[47,69]	Comments
103.0	b-ZnDiBP	Only formed when CHP:ZnDiBP = 1:1.
98.2	ZnDiBP	
94.4	$(RO)_2P(S)SR$	Formed in later stages when CHP:ZnDiBP $\geq$ 10:1.
89.7	Unknown	
85.2	DiBDS*	Decreases in yield as CHP excess increases, mainly formed in initial stages then slight decrease with time.
84.2	Tetrasulphide $\{(RO)_2PSS\}_2S_2$	Mainly formed in initial stages and continues to build-up.
83.8	Trisulphide $\{(RO)_2PSS\}_2S$	Only formed when CHP:ZnDiBP $\geq$ 10:1, builds up in initial stages and then decays.

* Note: Although the dithiophosphoric acid (DRDPA) has a very similar chemical shift value to that of DRDS, it is unlikely to be formed here as it is shown in Section 5.2.3.5. that DRDPA is rapidly oxidised to DRDS in the presence of CHP. The addition of a tertiary amine[52] to distinquish between DRDPA and DRDS has found to lead to ambiguous results in the presence of polysulphides.[68]

Table 5.5. (continued)

Chemical shift (ppm)	Assignment[47,69]	Comments
78.9	Monosulphide $\{(RO)_2PS\}_2S$	Formed at all CHP:ZnDiBP ratios, builds up initially and remains.
64.2	$(RO)_3P{=}S$	Only formed in later stages when CHP:ZnDiBP = 50:1.
59.7,52.9	Unknown	
48.3	ZnDRT	Only formed when CHP:ZnDiBP $\leqslant$ 5:1, formed in initial stages then decays.
46.3,28.9	Unknown	
24.5	$(RO)_2(RS)P{=}O$	Only formed when CHP:ZnDiBP = 50:1, and then in later stages.
21.0	DRODS	Formed initially but decays later, especially when CHP:ZnDiBP $\geqslant$ 10:1.
15.6	Unknown	
-0.9	$(RO)_3P{=}O$ or $(RO)_2P(O)OH$	Formed in later stages when CHP:ZnDiBP = 50:1.

5.2.3.3. OXIDATION OF b-ZnDRP BY CHP AT 110°C

The distribution of products formed during the reaction of b-ZnDiBP with excess CHP (CHP:b-ZnDiBP ≥ 1:1) in chlorobenzene at 110°C as measured by ^{31}P NMR is shown in Table 5.6., and the peak assignments are given in Table 5.7. along with comments regarding the conditions under which the various products are formed or decomposed. It is clear from Table 5.6., that even at a CHP:b-ZnDiBP ratio as high as 3:1 not all the b-ZnDiBP has been decomposed, and that extending the reaction time from 2 minutes to 30 minutes has very little effect on the type or distribution of the products formed.

5.2.3.5. OXIDATION OF DRDS BY CHP AT 110°C

The distribution of products formed during the reaction of DiBDS with excess CHP (CHP:DiBDS ≥ 1:1) in chlorobenzene at 110°C as measured by ^{31}P NMR is shown in Table 5.8., and the peak assignments are given in Table 5.9. It is clear from Table 5.8. that DiBDS was resistant to oxidation by CHP at 110°C under the conditions used. In contrast the disappearance of CHP in such systems was very rapid. (Figure 5.25.).

CHP:b-ZnDiBP ratio	Reaction time (minutes)	Phosphorus % yield (6 values in ppm)							
		103.0	98.1	94.4	85.2	84.3	78.9	48.3	46.3
1:1 [CHP] = $2x10^{-1}moldm^{-3}$ [b-ZnDiBP] = $2x10^{-1}moldm^{-3}$	0	90	6					3	
	30	62	9		11	2	3	11	2
3:1 [CHP] = $6x10^{-1}moldm^{-3}$ [b-ZnDiBP] = $2x10^{-1}moldm^{-3}$	0	90	6					3	
	2	10			50	13	10	13	3
	30	10		1	49	11	10	17	1

Table 5.6. Products of the oxidation of b-ZnDiBP by CHP in chlorobenzene at 110°C

Table 5.7. Assignments to peaks shown in Table 5.6.

Chemical shift (ppm)	Assignment[47,69]	Comments
103.0	b-ZnDiBP	Not completely decomposed even at CHP:b-ZnDiBP = 3:1.
98.1	ZnDiBP	Only formed when CHP:b-ZnDiBP = 1:1.
94.4	$(RO)_2P(S)SR$	
85.2	DiBDS*	Yield increases with increasing CHP:b-ZnDiBP ratio.
84.3	Tetrasulphide	
78.9	Monosulphide	
48.3	ZnDRT	Undecomposed.
46.3	Unknown	

* See footnote to Table 5.5.

CHP:DiBDS ratio	Reaction time (minutes)	Phosphorus % yield (δ values in ppm)			
		85.2	84.3	83.8	21.4
1:1 $[CHP]=2\times10^{-1}moldm^{-3}$ $[DiBDS]=2\times10^{-1}moldm^{-3}$	0	100			
	2	100			
	30	96	2	1	1
5:1 $[CHP]=0.5moldm^{-3}$ $[DiBDS]=0.1moldm^{-3}$	0	100			
	2	99	1		
	10	91	6		3
	30	92	6		2

Table 5.8. Products of the oxidation of DiBDS by CHP in chlorobenzene at 110°C.

Table 5.9. Assignments to peaks shown in Table 5.8.

Chemical shift (ppm)	Assignment[47,69]
85.2*	DiBDS
84.3	Tetrasulphide
83.8	Trisulphide
21.4	DRODS

* See footnote to Table 5.5.

5.2.3.5. OXIDATION OF DRDPA BY CHP AT 110°C

The distribution of products formed during the reaction of DnHDPA with excess CHP (CHP:DnHDPA = 2.5:1) in chlorobenzene at 110°C as measured by ^{31}P NMR is shown in Table 5.10., and the peak assignments are given in Table 5.11. The decomposition of CHP occurred rapidly under these conditions (Figure 5.25.).

5.2.3.6. OXIDATION OF DRTPA BY CHP AT 110°C

The distribution of products formed during the reaction of DiBTPA with excess CHP (CHP:DiBTPA = 2.5:1) in chlorobenzene at 110°C as measured by ^{31}P NMR is shown in Table 5.12., and the peak assignments are given in Table 5.13. As a result of the reaction of DiBTPA and CHP the initially clear solution became cloudy. When the reaction was carried out at room temperature the solution quickly became quite warm, indicating that an exothermic process was occurring. The complete decomposition of CHP was readily achieved by DiBTPA at 110°C. (Figure 5.25.).

CHP:DnHDPA ratio	Reaction time (minutes)	Phosphorus % yield (δ values in ppm)				
		85.6	85.0	84.1	24.8	21.5
2.5:1 [CHP]= 0.5moldm^{-3} (DnHDPA] = 0.2moldm^{-3}	0	100				
	2		90	5		5
	12		80	15		5
	30		73	18	4	5

Table 5.10. Products of the oxidation of DnHDPA by CHP at 110°C

Table 5.11. Assignments to peaks shown in Table 5.10.

Chemical shift (ppm)	Assignment[47,69]
85.6	DnHDPA
85.2	DRDS*
84.1	Tetrasulphide
24.8	$(RO)_2P(O)SR$
21.5	DRODS

* See footnote to Table 5.5.

CHP:DiBTPA ratio	Reaction time (minutes)	Phosphorus % yield (δ values in ppm)			
		64.8	63.0	21.0	-0.1
2.5:1 [CHP] = 0.5moldm^{-3} [DiBTPA] = 0.2moldm^{-3}	0		100		
	3			99	1
	20			91	9
	45	3		88	9

Table 5.12. Products of the oxidation of DiBTPA by CHP at 110°C

Table 5.13. Assignments to peaks shown in Table 5.12.

Chemical shift (ppm)	Assignment[47,69]
64.8	$(RO)_3P{=}S$
63.0	DiBTPA
21.0	DRODS
-0.1	$(RO)_3P{=}O$ or $(RO)_2P(O)OH$

5.3. DISCUSSION

5.3.1. DECOMPOSITION OF CHP BY DITHIOPHOSPHATES IN THE ABSENCE OF FeST

5.3.1.1. DECOMPOSITION OF CHP BY ZnDRP AND b-ZnDRP

It is clear from Figures 5.1. and 5.2. that at a temperature of 110°C and in the absence of FeST, both ZnDRP and b-ZnDRP are capable of catalytically decomposing CHP. Both types of zinc complex give two distinct stages during the decomposition of CHP, which is in contrast to the three stage reactions reported by several authors[10,13,17,19,70] to be caused by ZnDRP. The lower reaction temperatures (typically 70°C) used by these workers may account for the more complex type of behaviour observed during their studies. A three stage reaction has also been observed during the decomposition of CHP by NiDRP at 110°C.[30]

The initial fast decomposition promoted by a high concentration of either zinc complex (Figures 5.1. and 5.2.), corresponds to that of the first stage reported by the other authors.[10,13,19] The major products formed during this time, α-cumyl alcohol and acetophenone (Figure 5.3.3), are characteristic of a homolytic decomposition of CHP by ZnDRP. (Scheme 5.2.).[25] The high amount of α-cumyl alcohol formed (> 40%) from the decomposition of CHP by a relatively high concentration of ZnDRP (CHP:ZnDRP = 5:1, Figure 5.3.), is in agreement with previously

reported work.[10,13,19,20,26,71] Interestingly, the yields of acetophenone arising from the use of the zinc complex (Figure 5.3.), are much lower than the high yields of greater than 80% which are given when CHP is decomposed by transition metal dithiophosphates, such as NiDRP[30] or FeDRP (Section 6.2.2.2.), under similar conditions. This illustrates that no single mechanism can fully explain the peroxide decomposing action of MRDP's in general.

The disappearance of α-cumyl alcohol and the building-up of α-methyl styrene and phenol during the slower, second stage (Figure 5.3.), shows that acid catalysed reactions are occurring at this time. Phenol is formed from the ionic decomposition of CHP by a Lewis acid (Schemes 5.2.[25] and 5.4.[8]), and α-methyl styrene arises from the dehydration of cumyl alcohol, also catalysed by an acidic species. (Schemes 5.2.[25] and 5.3.[72]). The nature of this acid is controversial. Sulphuric acid[19,22] or dialkyldithiophosphoric acid[14,25,26] (DRDPA) are favoured by different groups of workers. The nature of the acidic species formed by the reaction of ZnDRP or b-ZnDRP with CHP is discussed in Sections 5.3.3.2. and 5.3.3.3.

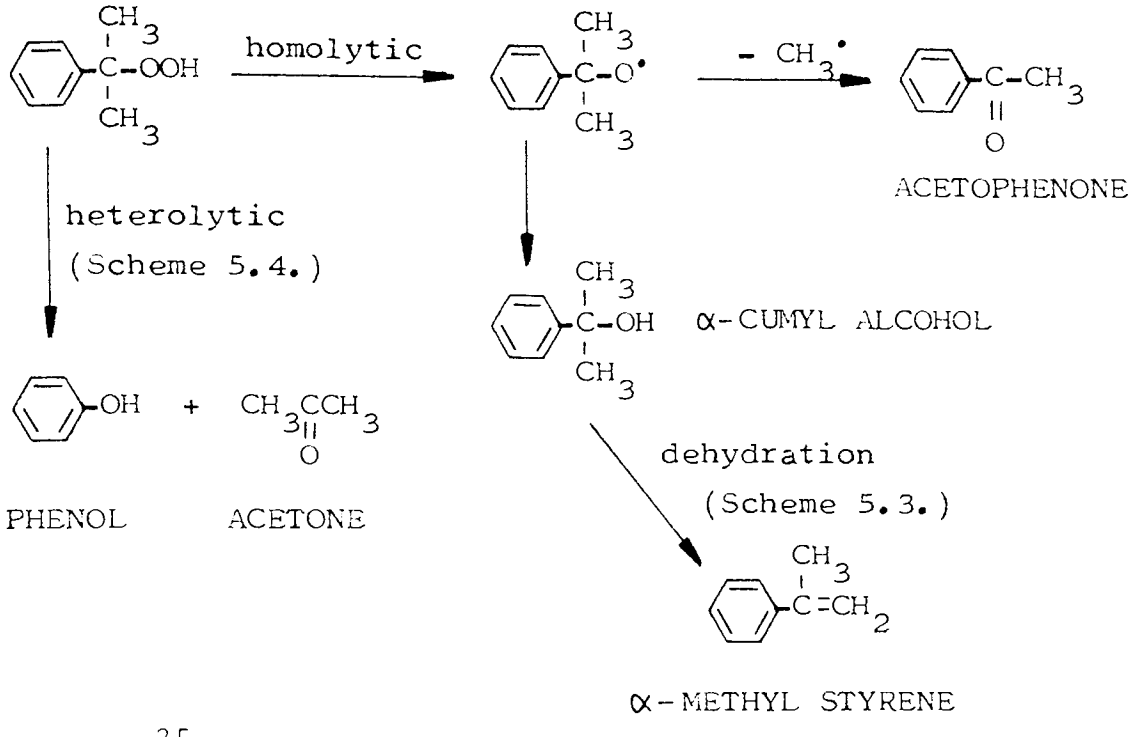

Scheme 5.2.[25] Homolytic and heterolytic mechanisms of CHP decomposition

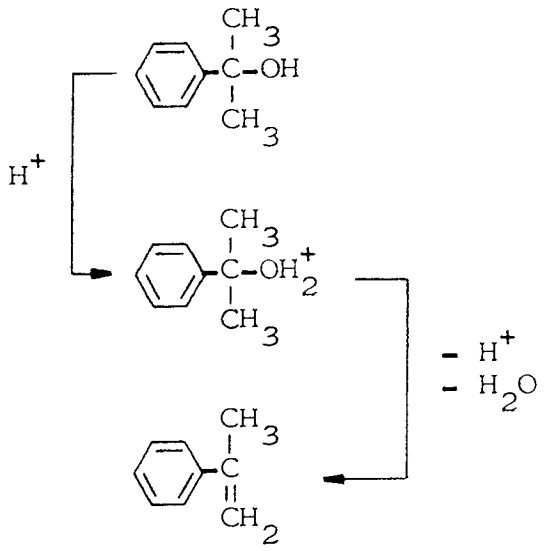

Scheme 5.3.[72] Dehydration of α-cumyl alcohol by Lewis acids

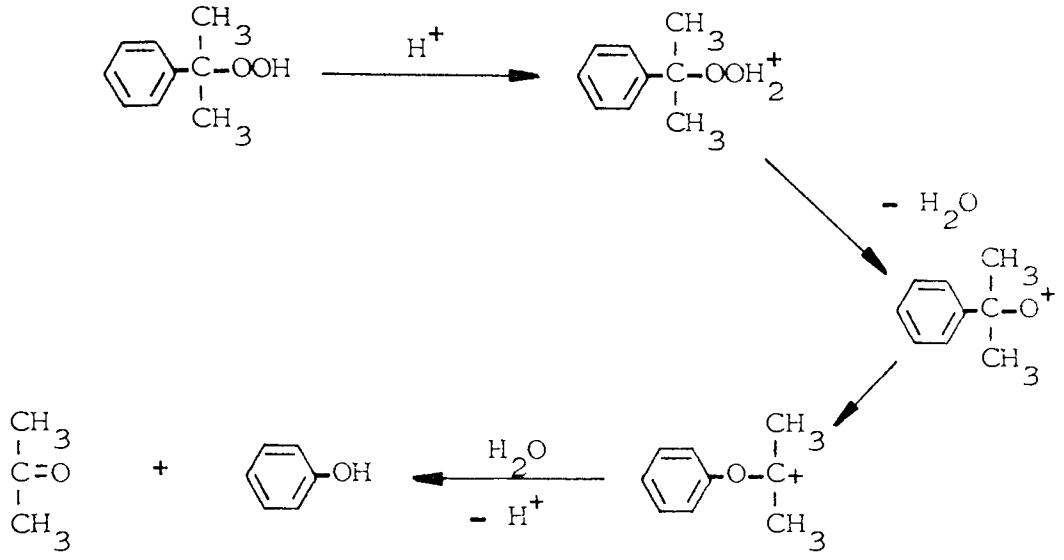

Scheme 5.4.[8] Lewis acid catalysed ionic decomposition of CHP

The hydroperoxide decomposing behaviour exhibited by ZnDRP and b-ZnDRP (Figures 5.1. and 5.2.) accounts for the type of inhibition of oxidation caused by the zinc compleses in the presence of excess CHP. (Section 3.3.2.1., Figures 3.10 and 3.11.). The initial homolytic decomposition, leading to the generation of free radicals, is responsible for the initial pro-oxidant stage observed at high ZnDRP and b-ZnDRP concentrations (Figures 3.10 and 3.11.). The subsequent effective auto-retarding inhibition is caused by ionic decomposition of hydroperoxides by sulphur acids formed by the interaction of ZnDRP and CHP during the first stage. Low concentrations of ZnDRP (e.g. $1x10^{-4}moldm^{-3}$), not being able to decompose

hydroperoxide other than by the first stage radical generating mechanism (Figure 5.1.), are unable to inhibit the CHP initiated oxidation of hydrocarbons. (Figure 5.11.).

5.3.1.2. DECOMPOSITION OF CHP BY DRDS

The inability of low concentrations of DRDS (CHP:DRDS $\geq$ 20:1) to decompose CHP until a considerable induction period has elapsed (Figure 5.4.), shows that it needs to be oxidised by the CHP before an effective peroxide decomposing species is present in the system. The two stage behaviour observed in Figure 5.4. has been reported to occur when DRDS is present in catalytic quantities by Rossi and Imperato,[10] and also by Burn and co-workers.[13] Under these conditions, both ionic and free radical decomposition of CHP has been shown to be occurring. As for the zinc complexes (Section 5.3.1.1.), the nature of the peroxide decomposing species formed is controversial.[22,25,73]

The immediate and rapid decomposition of CHP promoted by a concentration of $2x10^{-3}moldm^{-3}$ DRDS (Figure 5.4., CHP:DRDS = 5:1) shows that, when present in a high concentration, the disulphide can itself act as a hydroperoxide decomposer without needing to first be oxidised through to an acidic species. Similar behaviour has been observed at a high DRDS concentration by Ohkatsu and co-workers[19] and Burn and co-workers.[13] The ability of DRDS to decompose CHP without needing to first be oxidised is further demonstrated in Section 5.3.3.4.

The inability of a low concentration of DRDS to initially decompose CHP (Figure 5.4) accounts for the rapid initial oxidation of hydrocarbons in the presence of DRDS and excess CHP (Section 3.3.2.2., Figures 3.13 and 3.14.). The auto-retarding inhibition observed during the later stages when a high concentration of DRDS is used (Figures 3.13 and 3.14.), is caused by ionic hydroperoxide decomposition promoted by the sulphur acids formed from the DRDS/CHP interaction. (see Section 5.3.3.4.).

5.3.1.3. DECOMPOSITION OF CHP BY DRDPA

The rapid disappearance of CHP caused by all concentrations of DRDPA used (Figure 5.5.) is further evidence that the reaction of DRDS and CHP must lead to the rapid formation of extremely powerful antioxidant species. (see reaction 40, Section 3.3.2.3.). The DRDPA/CHP reaction is further discussed in Section 5.3.3.5.. Although it has been reported by Johnson and co-workers[27] and Grishina and co-workers[26] that the interaction of DRDPA and CHP leads to the formation of DRDS, the rapid disappearance of CHP observed (Figure 5.5.) cannot be caused by the disulphide alone, as it is shown in Section 5.3.1.2. that a low concentration of DRDS needs to be oxidised further to sulphur acids before hydroperoxide decomposition can take place.

Although Bridgewater and co-workers[25] report that the decomposition of CHP by DRDPA requires a higher temperature than that needed when DRDS is used as the hydroperoxide decomposer, this has clearly not been found to be true in the present work.

The very effective inhibition of CHP initiated oxidation of hydrocarbons shown by DRDPA (Section 3.3.2.3., Figures 3.15. and 3.16.) is clearly due to the ionic decomposition of CHP by the sulphur acids formed in the DRDPA/CHP interactions (reaction 40, Section 3.3.2.3.).

5.3.1.4. DECOMPOSITION OF CHP BY DRTPA

The decomposition of CHP by DRTPA (Figure 5.6.) shows great similarity to that caused by DRDPA (Figure 5.5.), and it is therefore very probable that the mechanism of hydroperoxide decomposition by DRTPA is closely related to that discussed in Section 5.3.1.3. to account for the behaviour of DRDPA. The reaction of DRTPA with CHP, leading to the formation of the phosphoryl disulphide, DRODS (See Scheme 3.2., Section 3.3.1.4.), along with sulphur acids, is discussed in Section 5.3.3.6.

5.3.2. DECOMPOSITION OF CHP BY DITHIOPHOSPHATES IN THE PRESENCE OF FeST

5.3.2.1. DECOMPOSITION OF CHP BY FeST

Comparison of Figure 5.7. with Figures 5.1. and 5.4. shows that FeST is an effective hydroperoxide decomposer compared with ZnDRP or DRDS. This is not however a desirable effect as the mode of decomposition is entirely homolytic.[12] (Section 4.3.1.). It is the decomposition of hydroperoxides by FeST to free radicals that is responsible for the catalysis of hydrocarbon oxidation that is observed in the presence of FeST (Section 4.3.1., Figures 4.1. and 4.2.). Reactions (8) and (9) (Sections 1.2. and 4.3.1.) explain the fairly constant rate of decomposition, without pronounced fast or slow stages, which is observed. (Figure 5.7.).

5.3.2.2. DECOMPOSITION OF CHP BY ZnDRP AND b-ZnDRP

The very effective decomposition of CHP achieved by a concentration of $1x10^{-4}moldm^{-3}$ ZnDRP (CHP:ZnDRP = 100:1, Figure 5.8.) is largely due to an ionic reaction leading to a very high yield of phenol (Figure 5.12.), and is characteristic of the formation of powerful acidic species. The same concentration of ZnDRP is however virtually inactive as a hydroperoxide decomposer in the absence of FeST (Figure 5.1.), so it is clear that the FeST is having a dramatic effect under these conditions. The possibility of a direct reaction between ZnDRP and FeST being responsible for the observed behaviour is unlikely however, for two reasons. Firstly, the reaction

of ZnDRP and FeST is shown in Section 6.3.3.2. to proceed slowly, even at a temperature of 130°C. Secondly, the presence of a 100 fold excess of CHP over ZnDRP will ensure that all the zinc complex is destroyed very quickly, before it can possibly react with FeST. In Section 5.3.3.2., it is demonstrated that a CHP:ZnDRP ratio of 5:1 is sufficiently high to destroy all the zinc complex within four minutes. It is therefore clear that the FeST must be exerting an effect by reaction with one or more of the oxidation products of ZnDRP to form an extremely powerful hydroperoxide decomposer.

The identity of this species is unclear, but it must possess exceptional hydroperoxide decomposing ability as it can only be formed in very small amounts. Although very efficient ionic decomposition of hydroperoxides is achieved by the use of a small amount of ZnDRP in the presence of FeST in an inert system (Figure 5.8.), the results obtained in an oxidisable medium are very disappointing. (Section 4.3.2.1., Figures 4.11. and 4.112.). Catalysis of oxidation of FeST must be completely overriding the effect of any antioxidant species formed in an oxidisable substrate.

The use of a high concentration of ZnDRP ($2x10^{-3}moldm^{-3}$) to decompose CHP leads to very similar results in both the presence (Figure 5.8.) and absence (Figure 5.1.) of FeST, i.e. a fast free radical stage followed by

a slower ionic step. (Figure 5.3. and 5.10.). This suggests that the mechanism used to explain the decomposition of CHP by ZnDRP in the absence of FeST (Section 5.3.1.1.) is still predominant for high concentrations of ZnDRP in the presence of FeST. The appearance of phenol is slightly delayed in the presence of FeST however (compare Figures 5.3. and 5.10.), and this may reflect the reaction of FeST with some of the sulphur containing acids resulting from the ZnDRP/CHP interaction. It is clear that the species responsible for the rapid, ionic decomposition of CHP observed when a very low concentration of $1x10^{-4}moldm^{-3}$ ZnDRP is used is not being formed when a higher concentration of $2x10^{-3}moldm^{-3}$ zinc complex is employed, as the ionic hydroperoxide decomposition stage is relatively slow under these conditions. (Figure 5.8.).

The rapid iron catalysed oxidation of hydrocarbons observed when a low concentration of $5x10^{-4}moldm^{-3}$ or less ZnDRP is used (Section 4.3.2.1., Figures 4.11. and 4.12.), indicates that under conditions where iron deactivation, if occurring, would be expected to make its greatest contribution to the overall antioxidant activity of ZnDRP (i.e. ZnDRP:FeST < 2.5.:1), close to stoichiometric), little stabilisation is achieved. It is therefore likely that inhibition of hydrocarbon oxidation by ZnDRP in the presence of FeST, which is only observed

when a relatively high level of ZnDRP is present (Figures 4.11. and 4.12.), is occurring primarily by the same mechanism as that established to account for the inhibition of corresponding oxidations in the absence of FeST. (Section 5.3.1.1.).

The similar effect given by both ZnDRP and b-ZnDRP (compare Figures 5.8. and 5.9.) shows that the two types of zinc complex act by the same mechanism.

5.3.2.3. DECOMPOSITION OF CHP BY DRDS

Comparison of Figures 5.4. and 5.15. shows that, as observed for the zinc complexes (Section 5.3.2.2.), the effect of $2x10^{-4}moldm^{-3}$ FeST on the hydroperoxide decomposing activity of DRDS has its greatest effect when a low initial concentration of the disulphide is present. The rapid and immediate decomposition of CHP achieved by a high concentration of $2x10^{-3}moldm^{-3}$ DRDS (Figure 5.15.) is very similar to that observed in the absence of FeST (Figure 5.4.), which suggests that a direct reaction between FeST and DRDS is not occurring. Further evidence for this is provided in Section 6.3.3.2. where it is shown that such a reaction does not take place in the absence of CHP.

The lack of any induction period before decomposition (Figure 5.15.) again suggests that a high concentration of DRDS is in some way able to itself decompose CHP.

The high yield of α-cumyl alcohol formed in the early stages of the reaction (Figure 5.16.), shows that this decomposition process is initially homolytic in nature. The ionic decomposition of CHP which subsequently occurs and results in the formation of phenol must be due to the action of sulphur acids formed during the first stage of hydroperoxide decomposition. It is the presence of these species that is responsible for the eventual inhibition of iron catalysed oxidation in the presence of a high DRDS concentration. (Section 4.3.2.2., Figures 4.14. and 4.15.). The existence of both free radical and ionic processes during the decomposition of CHP by DRDS in the absence of FeST has been demonstrated by Ohkatsu.[73]

As mentioned above, the presence of FeST has the greatest effect when a low concentration of DRDS ($\leqslant 5\times10^{-4}$moldm^{-3}) is used, i.e. at DRDS:FeST ratios of $\leqslant$ 2.5.:1. The presence of two stages during the decomposition (Figure 5.15.) suggests that a similar process to that used to account for the action of a catalytic amount of DRDS as a hydroperoxide decomposer in the absence of FeST (Section 5.3.1.2.) is again occurring. The much reduced rate at which the relatively fast decomposition stage occurs in the presence of FeST (compare Figures 5.4. and 5.15.), along with the rather slow build-up of phenol (Figures 5.17. and 5.18.), does

suggest however that the effectiveness of any sulphur acids formed is severely reduced, presumably by reaction with the FeST. The greatest effect is seen at lower DRDS concentrations, at which smaller amounts of such acids are likely to be formed and may largely be consumed by reaction with FeST. The use of a much higher DRDS concentration will result in the formation of a much greater level of acids which may only partially be used up by the FeST, leaving the remainder free to continue hydroperoxide decomposition.

The involvement of FeST in the reaction of DRDS with CHP is therefore shown to only be important when a low concentration of DRDS is present. At these concentrations the disulphide is shown in Section 4.3.2.2. to be unable to provide inhibition of iron catalysed oxidation. (Figures 4.14. and 4.15.). The inhibition of such an oxidation only occurs when the concentration of DRDS is at levels where iron deactivation is not making a significant contribution. It is therefore apparent that effective inhibition of iron catalysed oxidation by DRDS is not occurring via iron deactivation. A similar conclusion regarding the action of ZnDRP was made in Section 5.3.2.2.

5.3.2.4. DECOMPOSITION OF CHP BY DRDPA

The rapid, ionic decomposition of CHP achieved by all DRDPA concentrations used (Figure 5.19., Table 5.1.) indicates that the generation of extremely powerful hydroperoxide decomposing species from the reaction of DRDPA and CHP (see Sections 3.3.2.3. and 5.3.1.1.) is still occurring, even in the presence of FeST. The stabilisation given by the addition of CHP to iron catalysed hydrocarbon oxidation in the presence of DRDPA (compare Figures 4.9. and 4.17., Chapter 4.), is readily explained by the formation of such species. The build-up of the green colouration of FeDRP shows that there is competition between FeST and CHP for the DRDPA. (see Scheme 4.2., Section 4.3.2.3.). The subsequent disappearance of the iron complex is not surprising, as it is shown in Section 6.3.2. that FeDRP is rapidly oxidised by CHP. The maximum concentration of FeDRP that can be formed under these conditions is only $2 \times 10^{-4} moldm^{-3}$ which, again in Section 6.3.2., is shown to lead to the ionic decomposition of CHP to phenol. The formation of FeDRP, despite consuming some of the original DRDPA present, does not therefore lead to a marked reduction in the hydroperoxide decomposing activity of the system. The significant yields of acetophenone formed (Table 5.1.) do show that some homolytic CHP decomposition is occurring, although the predominant mechanism is clearly ionic.

5.3.2.5. DECOMPOSITION OF CHP BY DRTPA

Although the ability of a high concentration of $2x10^{-3}moldm^{-3}$ DRTPA to decompose CHP is largely unaffected (compare Figures 5.6. and 5.20.), it is clear that at a lower concentration a considerable reduction in the effectiveness of the acid is caused by the presence of FeST. Competition between CHP and FeST for the DRTPA, similar to that occurring with DRDPA, (Section 5.3.2.4.) is again apparent as evidenced by the appearance of the orange/red colouration of iron dialkylthiophosphate (FeDRT). Although the hydroperoxide decomposing ability of FeDRT has not yet been evaluated, it is probable that it is not as powerful as its dithiophosphate analogue, FeDRP, due to its lower sulphur content. The effect of FeST may therefore be to consume some of the DRTPA, thereby reducing the amount of the powerful antioxidant species formed from the DRTPA/CHP interaction. (Section 3.3.2.4.). This would have its greatest effect on a relatively low concentration of DRTPA as is observed in Figure 5.20.

The lower hydroperoxide decomposing ability of DRTPA in the presence of FeST compared to that of DRDPA under similar conditions is reflected in the relative degree of inhibition of iron catalysed hydrocarbon oxidation achieved by the two acids. (Figures 4.17. and 4.18., Chapter 4.).

5.3.3. THE PRODUCTS OF THE OXIDATION OF DITHIOPHOSPHATES BY HYDROPEROXIDES

5.3.3.1. OXIDATION OF ZnDRP BY TBH AT 25°C

The reaction of excess ZnDRP with hydroperoxides leading to the formation of DRDS and b-ZnDRP (reaction 43), was demonstrated by Rossi and Imperato.[10] (see also Scheme 1.5.).

$$4\left\{(RO)_2PSS\right\}_2Zn + RO_2H \longrightarrow \left\{(RO)_2PSS\right\}_6Zn_4O + \left\{(RO)_2PSS\right\}_2 + ROH \qquad (43)$$

5.3.3.2. OXIDATION OF ZnDRP by CHP AT 110°C

The wide variety of phosphorus containing products formed from the reaction of ZnDRP with excess CHP (Table 5.4.), illustrates that a very complex series of reactions is occurring. It may be seen from Table 5.4. that the type and amount of products formed is dependent on both the initial CHP:ZnDRP ratio and the reaction time.

When a relatively high concentration of ZnDRP is used (CHP:ZnDRP = 1:1), many of the products formed still contain zinc. The oxidation of ZnDRP by hydroperoxides, as shown in reaction 43, would appear to be the initial reaction occurring under these conditions as high yields of b-ZnDRP and DRDS are formed. (Table 5.4.). The presence of apparently unreacted ZnDRP is probably due to the decomposition by CHP of some of the b-ZnDRP formed in the initial reaction. (Section 5.3.3.3.).

From Tables 5.4. and 5.5. it is clear that at a CHP:ZnDRP ratio of 5:1 or greater, no ZnDRP or b-ZnDRP remains, even after a reaction time as short as four minutes. The only zinc containing species observed when CHP:ZnDRP = 5:1 is zinc dialkylthiophosphate, (ZnDRT, δ= 48.3 ppm). Even this species, which has been observed by Sher,[24] is only stable during the very early stages of the reaction and is rapidly lost, so that by 60 minutes no soluble zinc containing compounds are present in the system. The formation of an insoluble zinc containing precipitate has been observed by several authors.[10,13,17,19,70] The composition of the white precipitate isolated in the present work indicates that it is not a simple inorganic salt but is probably a polymeric material.

The amount of DRDS formed stays reasonably constant up to a reaction time of 60 minutes when CHP:ZnDRP = 5:1, demonstrating the considerable resistance of the disulphide to oxidation by CHP at 110°C (see Section 5.3.3.3.). The formation of the phosphoryl disulphide (DRODS; δ= 21.0, Table 5.4.) from the reaction of ZnDRP with excess CHP has been shown by various groups of workers.[10,20]

From Table 5.4. it is clear that most of the DRODS must be formed from ZnDRT, this in turn being derived from b-ZnDRP. This is in agreement with Rossi and Imperato[10] who have shown that DRODS is formed from b-ZnDRP. They have not however demonstrated the intermediate

formation of ZnDRT in the process. Bridgewater and co-workers[25] have proposed that the oxidation of ZnDRT by CHP leads to DRTPA. Further reaction of this (Scheme 3.2.) would then give DRODS. The formation of DRODS from the oxidation of the DRDS (Schemes 1.4.[20] and 1.7.) must also be occurring to some extent as not all of it can be attributed to the oxidation of ZnDRT. (Table 5.4.).

The build-up of the monosulphide and the tetrasulphide during the oxidation at all CHP:ZnDRP ratios studied (1:1 - 50:1) shows that, like DRDS, these are highly resistant to further oxidation once formed. In contrast, the trisulphide, formed only when CHP:ZnDRP $\geqslant$ 10:1, is not stable and undergoes further reaction. Despite being stable when a small excess of CHP is present, (CHP:ZnDRP $\leqslant$ 5:1) DRODS is clearly not stable in the presence of a larger excess of CHP (CHP:ZnDRP > 10:1). The formation of dialkyl phosphoric acid, $(RO)_2P(O)OH$, (see Scheme 3.2.) only accounts for some of the original DRODS, the remainder being oxidised to isomeric esters of thiophosphoric acid, $(RO)_2P(S)OR'$ (δ= 64.2) and $(RO)_2P(O)SR$ (δ= 24.5). Esters of this type have been shown to be able to further react with CHP.[74] The formation of highly oxygenated species as a result of the use of ZnDRP as a lubricating oil antioxidant in engine tests has been observed by Marshall[45] and Barber and Yamaguchi.[46]

Although small amounts of a number of other, mainly unidentified, phosphorus containing compounds have also been observed to result from the ZnDRP/CHP interaction (See Table 5.4.), it is the products outlined above that appear to be the most important species formed from the interaction of ZnDRP and CHP. The various reactions taking place during the oxidation of ZnDRP by CHP are summarised in Scheme 5.5.

The species formed in the early stages, especially when the CHP:ZnDRP ratio is relatively low, i.e. $\leqslant$ 5:1, are those which are products of the free radical stage of hydroperoxide decomposition (Section 5.3.1.1.), which is responsible for the pro-oxidant step observed during the oxidation of hydrocarbons in the presence of both CHP and ZnDRP. (Section 3.3.2.1., Figures 3.10. and 3.11.). In contrast, those species formed only after prolonged oxidation, especially by a large excess of CHP (CHP:ZnDRP $\geqslant$ 10:1), must be the products of reactions associated with the ionic decomposition of CHP, which is responsible for the slow, auto-retarding step that occurs in the later stages of the same hydrocarbon oxidations. (Figures 3.10. and 3.11.). The formation of DRODS from DRDS, and dialkyl phosphoric acid from DRODS are both associated with the evolution of sulphur dioxide from unstable intermediates. (see Schemes 1.7. and 3.2.). Thus although the sulphur acids cannot be detected by ^{31}P NMR, the formation of DRODS and dialkylphosphoric acid is evidence that they are produced.

It is also possible that very small amounts of extremely powerful phosphorus containing sulphur acids may be formed during the oxidation of ZnDRP by CHP. It is shown in Section 5.3.1.3. that as little as $1x10^{-4}moldm^{-3}$ hydroperoxide decomposer can be active, whereas the minimum concentration of phosphorus species detectable by ^{31}P NMR is around $1x10^{-3}moldm^{-3}$ (Section 2.2.5.). Unfortunately the products of the oxidation of ZnDRP or other dithiophosphates in the presence of FeST could not be determined, due to the highly paramagnetic nature of iron (III) compounds. (Section 2.2.2.5.).

5.3.3.3. OXIDATION OF b-ZnDRP BY CHP

Comparison of Tables 5.4. and 5.6. indicates that a much greater amount of CHP is needed to completely break down b-ZnDRP than is required to destroy the same molar concentration of ZnDRP. This is due to the fact that b-ZnDRP has three times as many thiophosphoryl ligands than ZnDRP. The formation of ZnDRT from the interaction of b-ZnDRP with CHP demonstrates that the build-up of ZnDRT during the early stages of the oxidation of ZnDRP by CHP (Section 5.3.3.2.) must be occurring via the basic zinc complex. The excess of CHP used in the present work is however insufficient to further oxidise the ZnDRT.

The appearance of the monosulphide and tetrasulphide as a result of the oxidation of b-ZnDRP by CHP (Table 5.6.) suggests that the formation of these products from ZnDRP (Section 5.3.3.2.) is also through the intermediate production of b-ZnDRP. A substantial proportion of the DRDS observed to result from the the reaction of ZnDRP and CHP (Table 5.4.) must also be formed via breakdown of b-ZnDRP, although it is shown in Sections 5.3.3.1. and 5.3.3.2. that some of it arises form the original ZnDRP/CHP reaction.

The reactions taking place during the oxidation of b-ZnDRP by CHP are summarised within Scheme 5.5.

5.3.3.4. OXIDATION OF DRDS BY CHP

The lack of any induction period preceding the rapid disappearance of CHP in the presence of DRDS (CHP:DRDS = 5:1, Figure 5.25.) provides further evidence that a high concentration of the disulphide is able to decompose hydroperoxides without needing to first be oxidised through to sulphur containing acids. Hydroperoxide decomposition under similar conditions is shown in Section 5.3.2.3. to be homolytic, with ionic breakdown only occurring in the later stages of the reaction. From Table 5.8. it is clear that, despite the rapid decomposition of CHP that occurs (Figure 5.25.), the disappearance of DRDS is very slow. It would therefore appear that a high concentration

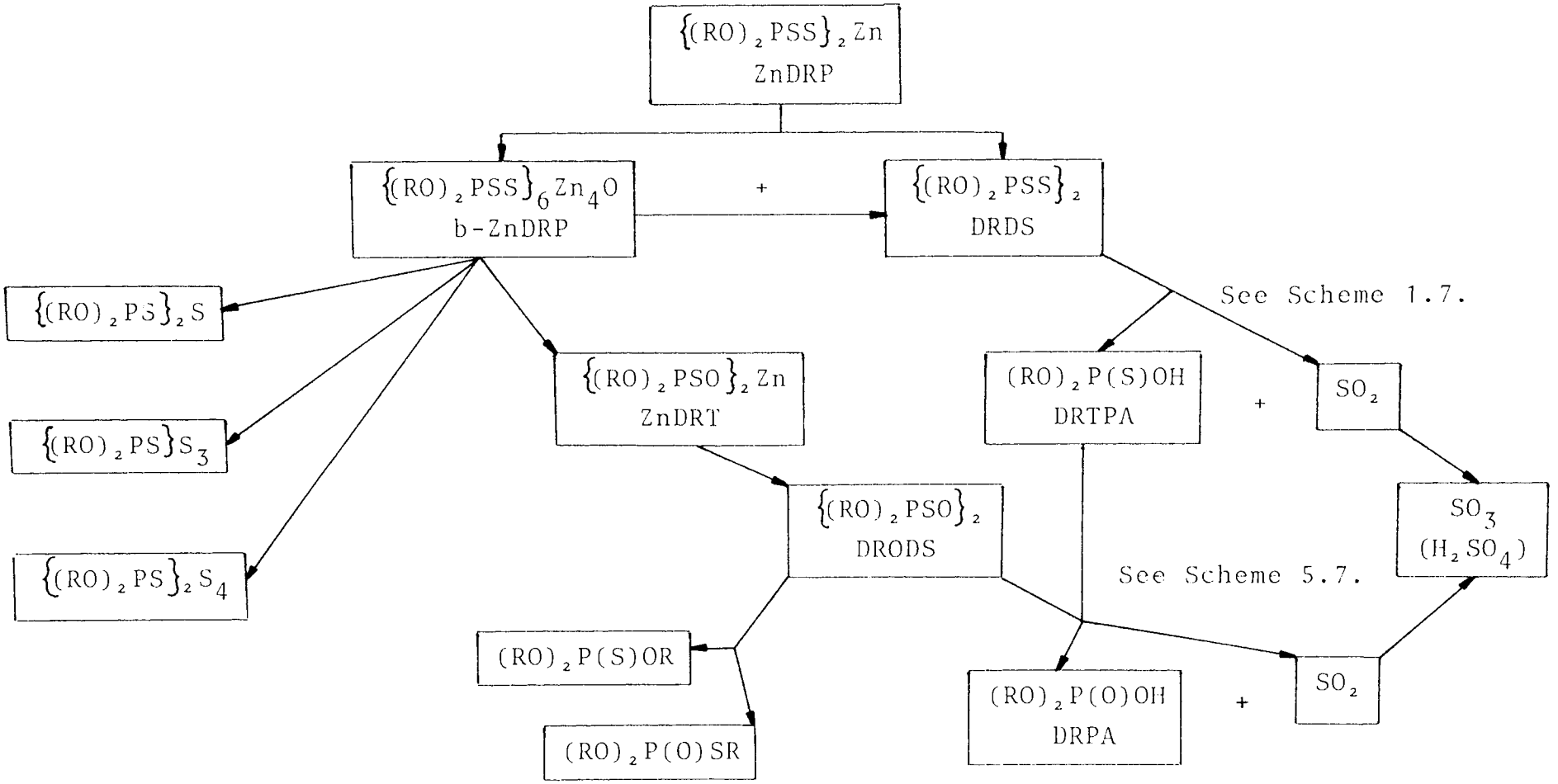

Scheme 5.5. Oxidation of ZnDRP by CHP

of DRDS is itself able to decompose hydroperoxides by a free radical mechanism in which the disulphide is, to a large extent, not consumed. Grishina and co-workers[21] have similarly shown that the oxidation of DRDS when CHP:DRDS = 20:1 also proceeds slowly. Under these conditions the main products were found to be triesters of thiophosphoric acid.

The appearance of DRODS (δ = 21.0, Table 5.8.) in the later stages of the reaction of DRDS and CHP is evidence for the formation of sulphur containing acids on prolonged oxidation of the disulphide. (See Schemes 1.7. and 3.2.). Such acids have been shown by Al-Malaika and Scott[22] to build-up rapidly during the oxidation of DRDS by a large excess of CHP (CHP:DRDS > 75:1), and their formation is responsible for the rapid ionic stage of CHP decomposition observed in the presence of low concentrations of DRDS (CHP:DRDS $\geqslant$ 20:1, Figure 5.4.). A study of the products derived when DRDS is oxidised by a high concentration of CHP was not possible, owing to the very high accumulation time needed to obtain the ^{31}P NMR spectrum when a sample of very low phosphorus content is scanned. (see Section 2.2.5.).

5.3.3.5. OXIDATION OF DRDPA BY CHP

The oxidation of DRDPA by CHP has been shown by Johnson and co-workers,[27] and Grishina and co-workers,[26] to lead to the formation of DRDS (reaction 39,

Section 3.3.1.3.). Although a high yield of disulphide is indeed found, (Table 5.10) the formation of several other products shows that side reactions are also occurring. It is shown in Section 5.3.1.3. that a very low concentration of DRDPA can rapidly decompose CHP by an ionic mechanism. A similar concentration of DRDS is however initially inactive. This demonstrates that the formation of products other than DRDS must be responsible for the hydroperoxide decomposition observed in the presence of DRDPA. (Figure 5.5.). The direct oxidation of DRDPA to DRODS, analogous to that shown to be occurring to DRDS (Scheme 1.7,), would account for the formation of DRODS along with SO_2. (Scheme 5.6.).

The rapid oxidation of DRDPA by CHP means that even if the acid is formed during the reaction of ZnDRP with excess CHP (Section 5.3.3.2.), its existence will only be transitory and it will not be detected. Only when no hydroperoxide is present can DRDPA be expected to remain as a stable species. (se Section 6.3.2.3.).

The mechanism by which the considerable amount of tetrasulphide is formed (Table 5.10.) is not clear.

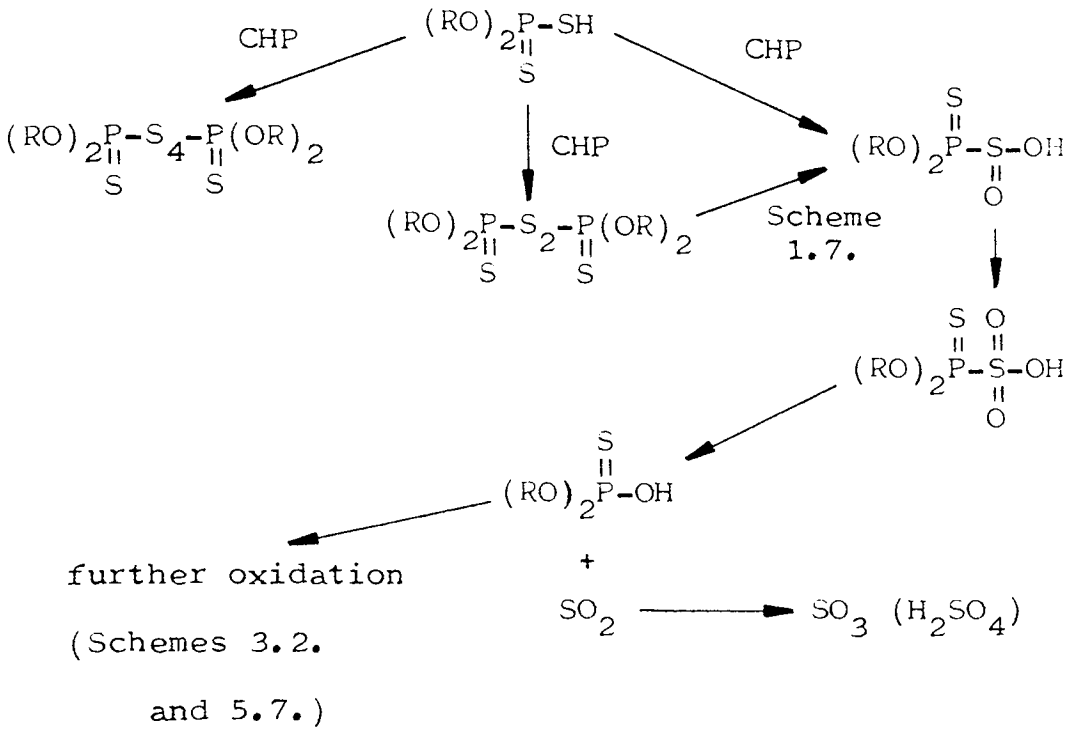

Scheme 5.6. The oxidation of DRDPA by CHP

5.3.3.6. OXIDATION OF DRTPA BY CHP

The oxidation of DRTPA by CHP (Scheme 3.2.) is similar to that of DRDPA (Section 5.3.3.5.), in that the disulphide is the major product. Although no work has been carried out to determine the hydroperoxide decomposing ability of DRODS, it is likely to be no more powerful than DRDS, and hence cannot be responsible for the very effective ionic destruction of CHP observed in the presence of DRTPA. (Figure 5.6., Tables 5.2.). It is therefore clear that other side reactions must also be occurring during the oxidation of DRTPA by CHP, which result in the formation of strong antioxidant species. The direct oxidation of some of the DRTPA by CHP to give SO_2 and dialkyl phosphoric acid would therefore appear

to be likely. (Scheme 5.7.). Oxidation of the DRODS formed from the remainder of the DRTPA (i.e. by Scheme 3.2.) would result in the same products. (Scheme 5.7.). Dialkyl phosphoric acids have been shown to be inactive towards CHP[75] and may therefore be considered as a final product of the interaction of thio- or dithiophosphates with hydroperoxides.

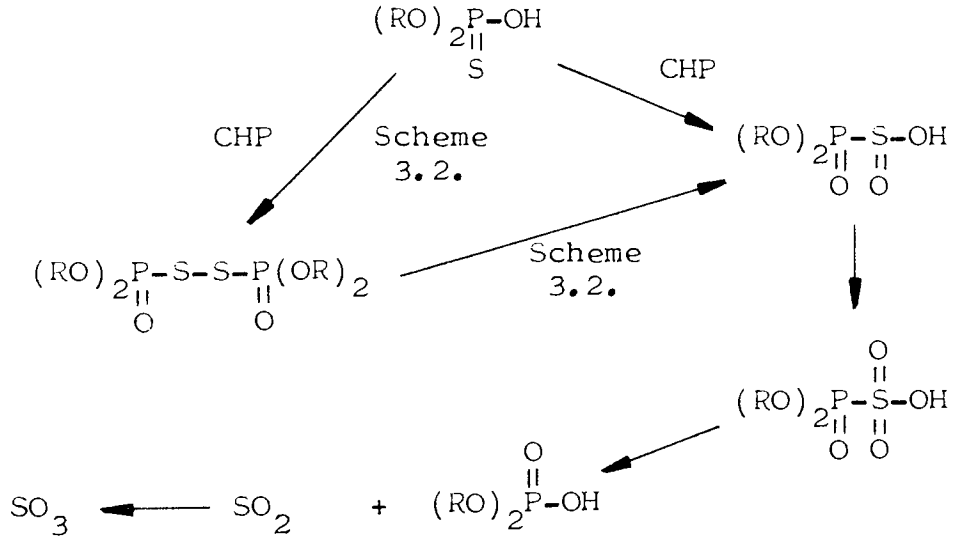

Scheme 5.7. Oxidation of DRTPA by CHP

5.4. SUMMARY OF CHAPTER FIVE

The decomposition of CHP by ZnDRP at 110°C proceeds in two steps. (Figure 5.1.). An initial homolytic decomposition process, which is favoured by the use of a high concentration of ZnDRP, leads to the formation of b-ZnDRP, DRDS and α-cumyl alcohol. (Figure 5.3., Tables 5.3. and 5.4.). Further rapid oxidation of the b-ZnDRP leads to the formation of ZnDRT and then DRODS. (Table 5.4.). Oxidation of the DRDS formed in the first stage leads to the build-up of DRODS, along with sulphur acids, e.g. SO_2, SO_3, which are responsible for the ionic decomposition stage observed during the latter stages of the ZnDRP/CHP reaction. (Figures 5.1. and 5.3.). Although a low concentration of DRDS is inactive towards hydroperoxides until it has been oxidised through to sulphur acids (Figure 5.4.), it is apparent that a high concentration of disulphide can itself promote hydroperoxide decomposition. (Figures 5.4. and 5.24.). Under these conditions sulphur acids are still formed, but only in the later stages of the reaction. (Table 5.8.).

Hydroperoxide decomposition is very rapid in the presence of DRDPA even when a very low concentration of acid is present. (Figure 5.5.). This is a result of the formation of small amounts of sulphur containing acids from the oxidation of DRDPA

by CHP. (Table 5.10). The major product of the oxidation is DRDS which, on further oxidation, leads to the generation of more sulphur acids. The effective decomposition of CHP by DRTPA (Figure 5.6.) takes place by a similar mechanism as that occurring for DRDPA. The oxidation of DRTPA leads to the formation of DRODS and sulphur acids. (Table 5.12.). Additional amounts of acid arise from the further oxidation of DRODS by CHP. The latter reaction takes place on prolonged oxidation of ZnDRP by a large excess of CHP, (Table 5.4.) thus supplementing the acids formed from DRDS.

The extent of CHP decomposition achieved by a very low concentration of ZnDRP is greatly increased in the presence of FeST. (ZnDRP:FeST = 1:2, Figure 5.8.). The reaction is ionic and is presumably due to the formation of an iron-containing complex from FeST and an oxidation product of ZnDRP. Th decomposition of CHP by a high concentration of ZnDRP proceeds in much the same way in the presence of FeST (ZnDRP:FeST = 10:1, Figure 5.8.) as in its absence (Figure 5.1.), although some of the sulphur acids formed from the CHP/ZnDRP interaction may be consumed by reaction with the FeST. The direct reaction of FeST with ZnDRP does not occur in the presence of CHP.

The presence of FeST has its greatest effect on the decomposition of CHP by DRDS when a low concentration of disulphide is used. (DRDS:FeST < 2.5:1, Figure 5.15.). The curtailment of the ionic destruction of CHP observed in the absence of FeST (Figure 5.4.) is indicative of the partial consumption of the sulphur acids formed by the oxidation of DRDS. The ability of a high concentration of DRDS to itself decompose CHP, initially by a homolytic mechanism, is largely unaffected by the presence of FeST. (DRDS:FeST = 10:1, Figure 5.15.) As for ZnDRP, the direct reaction of DRDS with FeST does not occur in the presence of CHP.

Although the rapid ionic hydroperoxide decomposition promoted by DRDPA is not significantly restricted by the presence of FeST, (Figure 5.19.), the direct reaction of FeST with DRDPA is occurring. Hydroperoxide decomposition by the FeDRP so formed is however sufficiently effective to compensate for any reduction in the yield of sulphur acids formed from the DRDPA/CHP reaction. The corresponding reaction of DRTPA with FeST leads to the formation of FeDRT. Although hydroperoxide decomposition in the presence of a high concentration of DRTPA (DRTPA:FeST = 10:1, Figure 5.20) is largely unaffected by the occurrence of such a reaction, the activity of a low concentration (DRTPA:FeST = 2.5:1) is severely reduced. The relative

inability of FeDRT to decompose CHP would explain this behaviour as, at low DRTPA concentrations, all the acid may be consumed by reaction with FeST, leaving none available to be oxidised to sulphur acids.

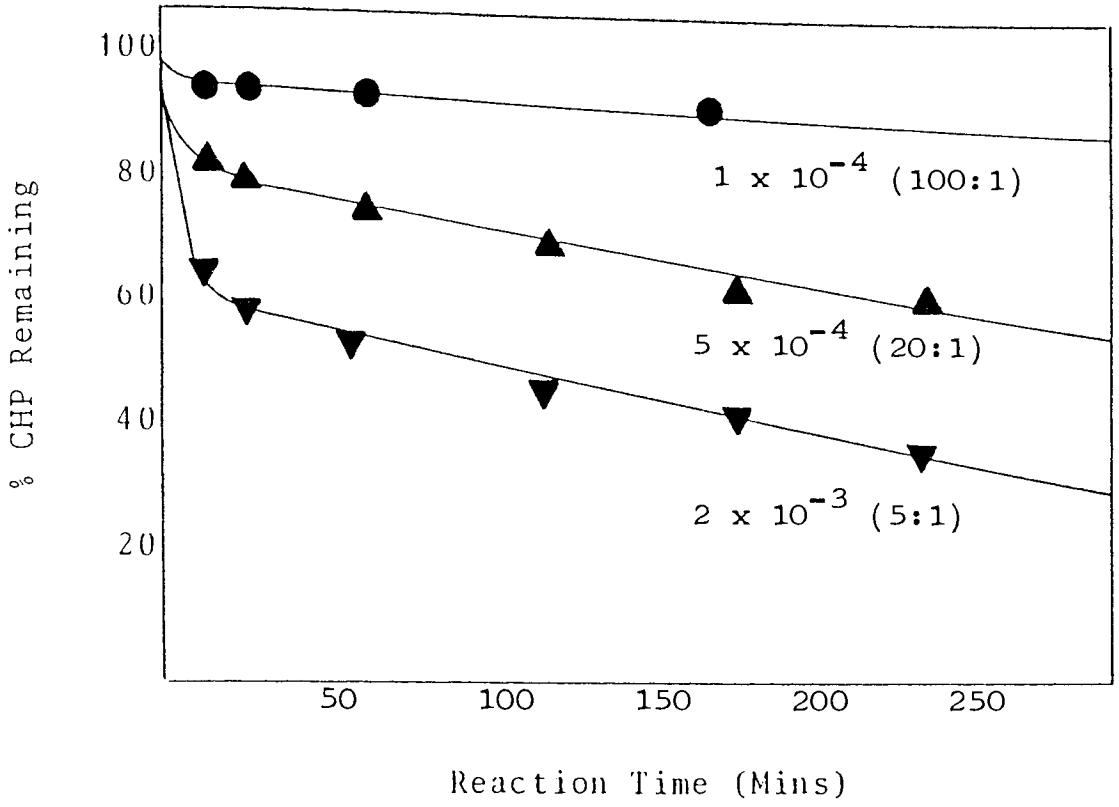

Figure 5.1. Decomposition of 1 x 10^{-2}moldm^{-3} CHP by ZnDiBP at 110°C. Numbers on Curves are ZnDiBP Concentrations in moldm^{-3}.

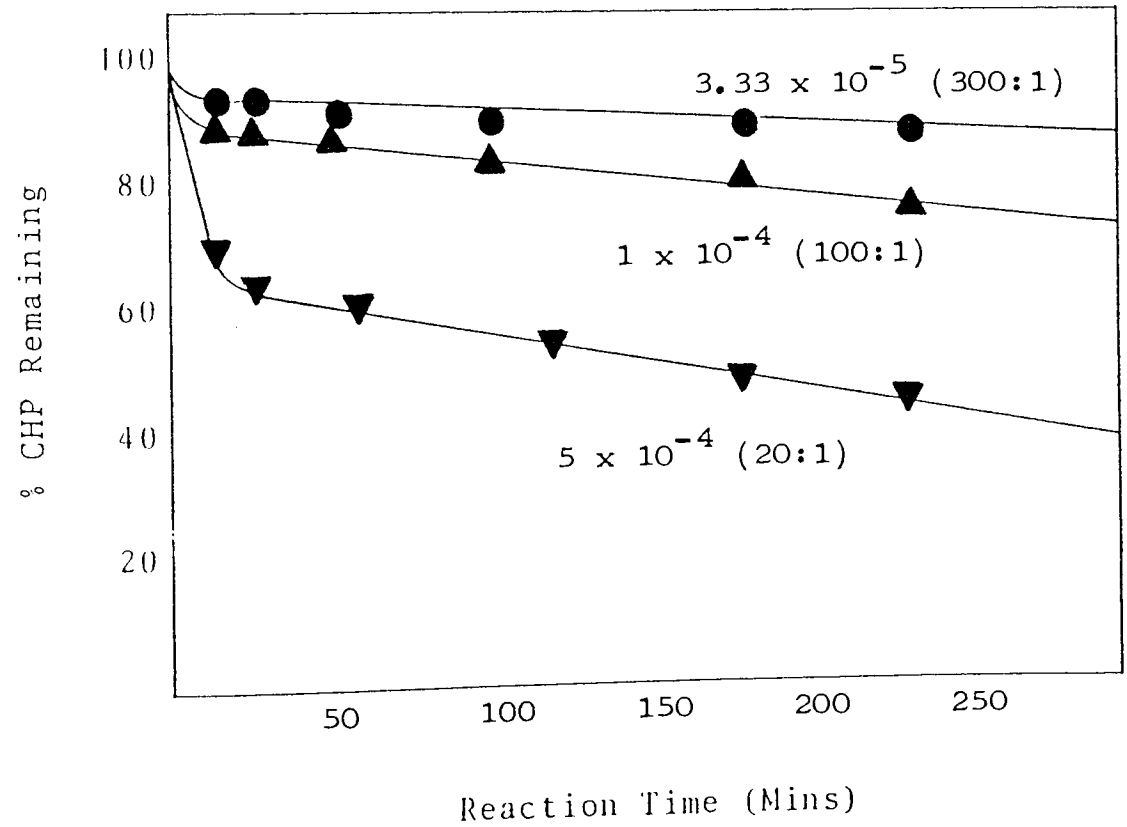

Figure 5.2. Decomposition of 1 x 10^{-2}moldm^{-3} CHP by b-ZnDiBP at 110°C. Numbers on Curves are b-ZnDiBP Concentrations in moldm^{-3}.

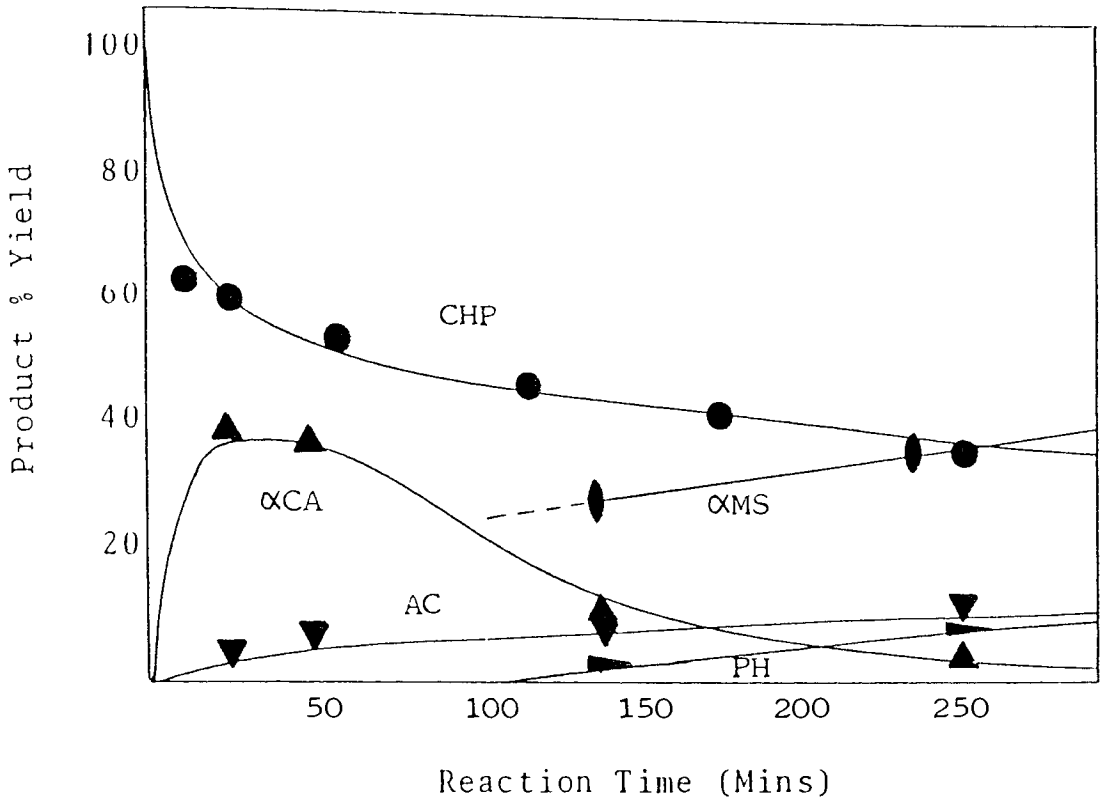

Figure 5.3. Products of Decomposition of 1 x 10^{-2}moldm^{-3} CHP by 2 x 10^{-3}moldm^{-3} ZnDiBP at 110°C. (CHP:ZnDiBP = 5:1)

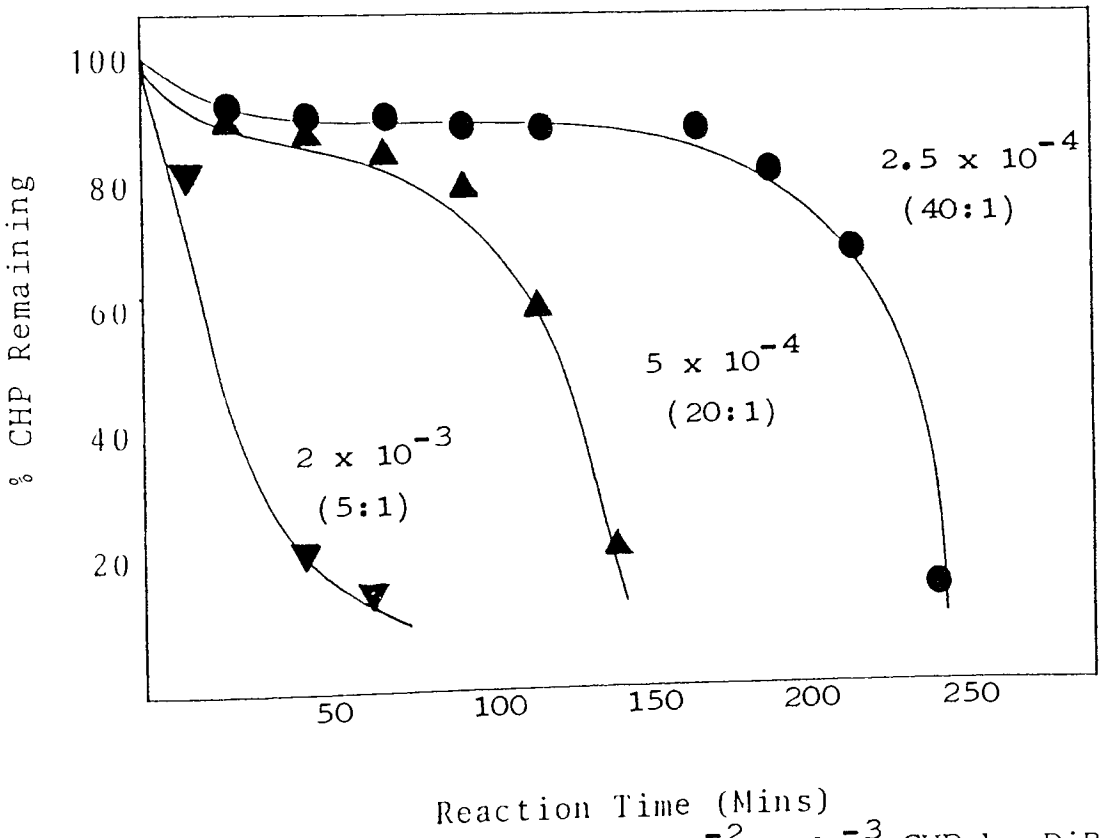

Figure 5.4. Decomposition of 1 x 10^{-2}moldm^{-3} CHP by DiBDS at 110°C. Numbers on Curves are DiBDS Concentrations in moldm^{-3}.

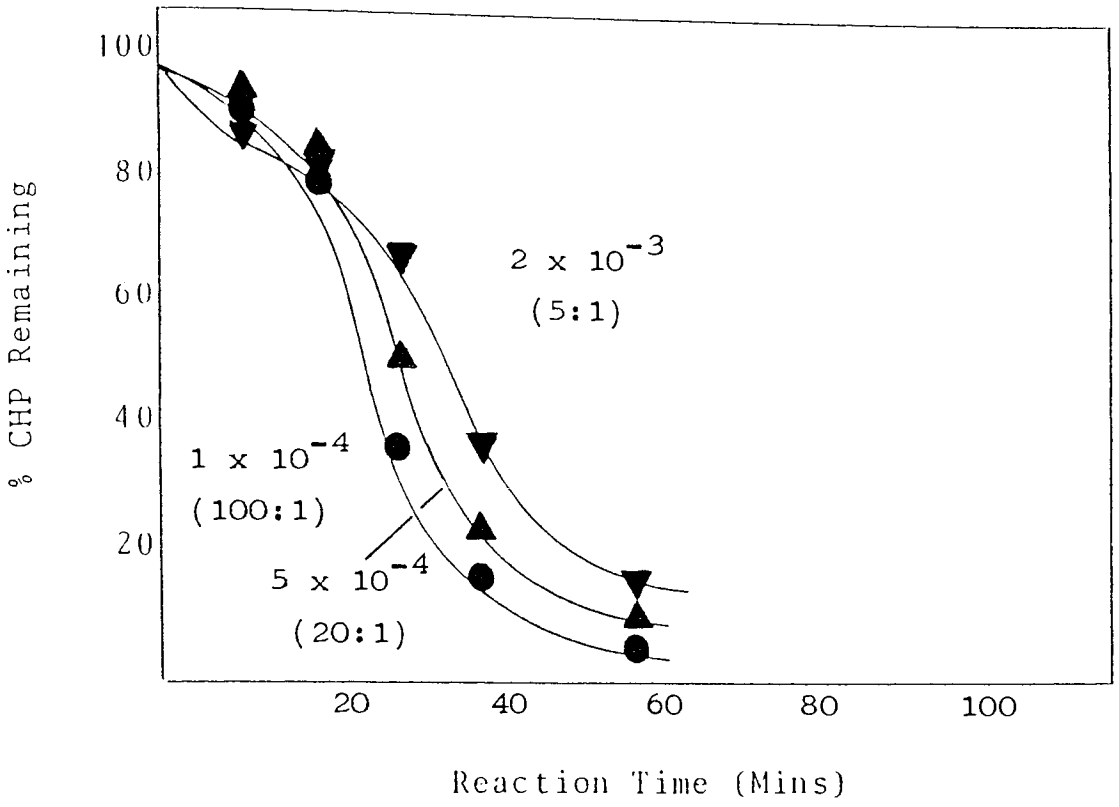

Figure 5.5. Decomposition of 1 x 10^{-2}moldm^{-3} CHP by DnHDPA at 110°C. Numbers on Curves are DnHDPA Concentrations in moldm^{-3}.

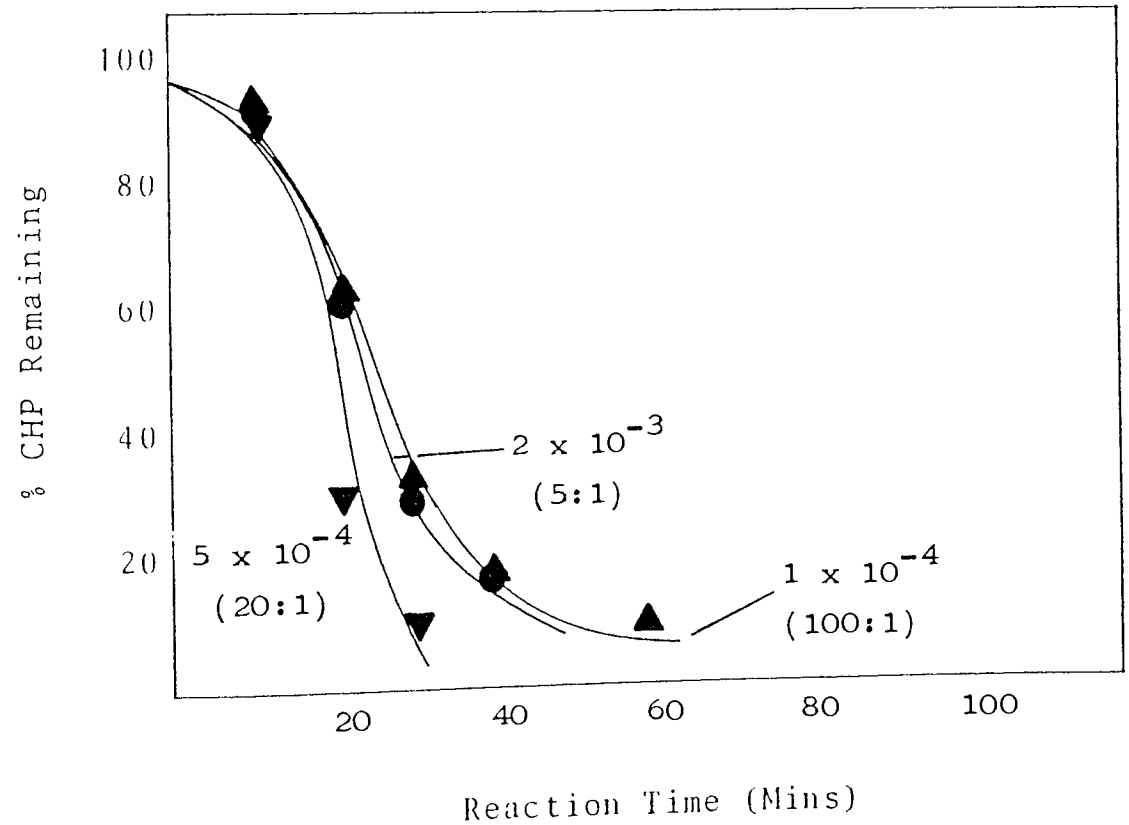

Figure 5.6. Decomposition of 1 x 10^{-2}moldm^{-3} CHP by DiBTPA at 110°C. Numbers on Curves are DiBTPA Concentrations in moldm^{-3}.

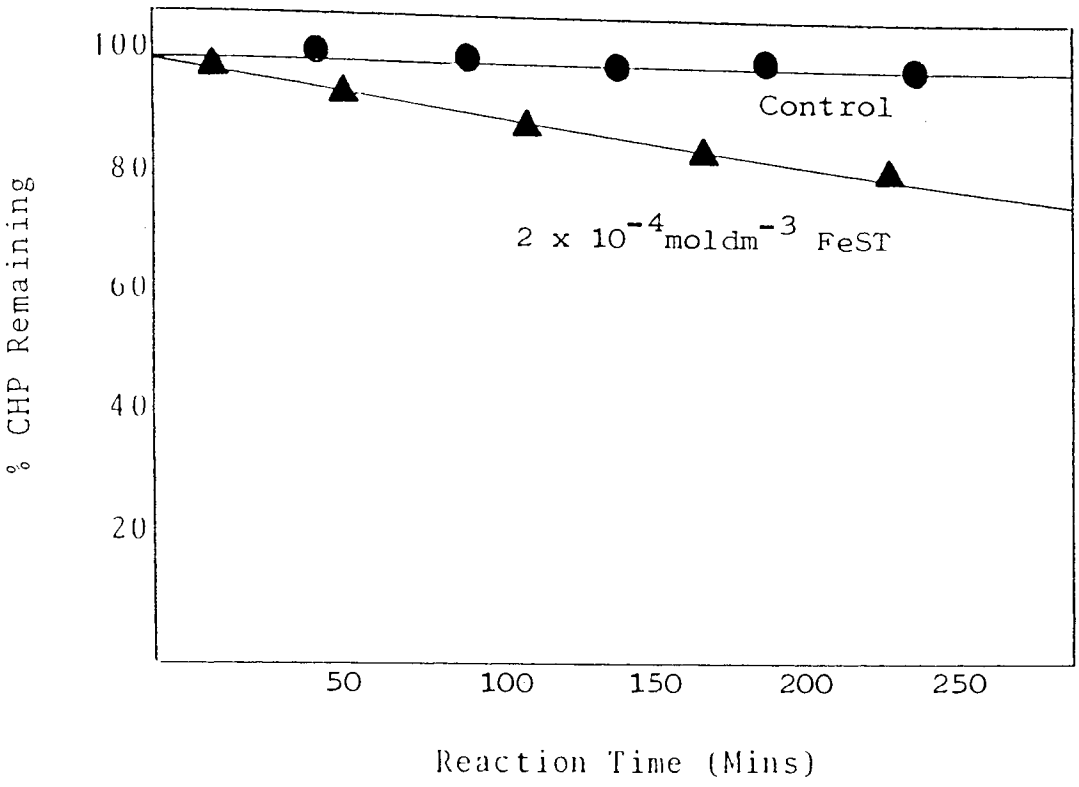

Figure 5.7. Decomposition of 1 x 10^{-2}moldm^{-3} CHP by FeST at 110°C.

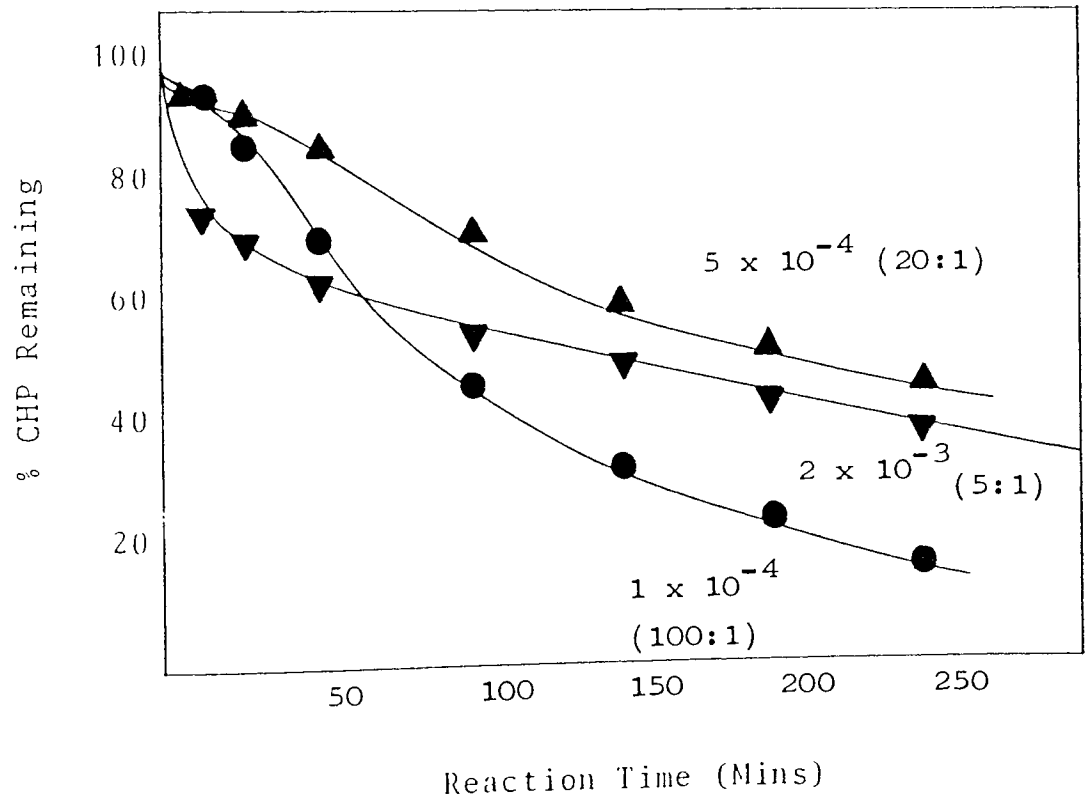

Figure 5.8. Decomposition of 1 x 10^{-2}moldm^{-3} CHP by ZnDiBP at 110°C in the Presence of 2 x 10^{-4}moldm^{-3} FeST. Numbers on Curves are Concentrations in moldm^{-3}.

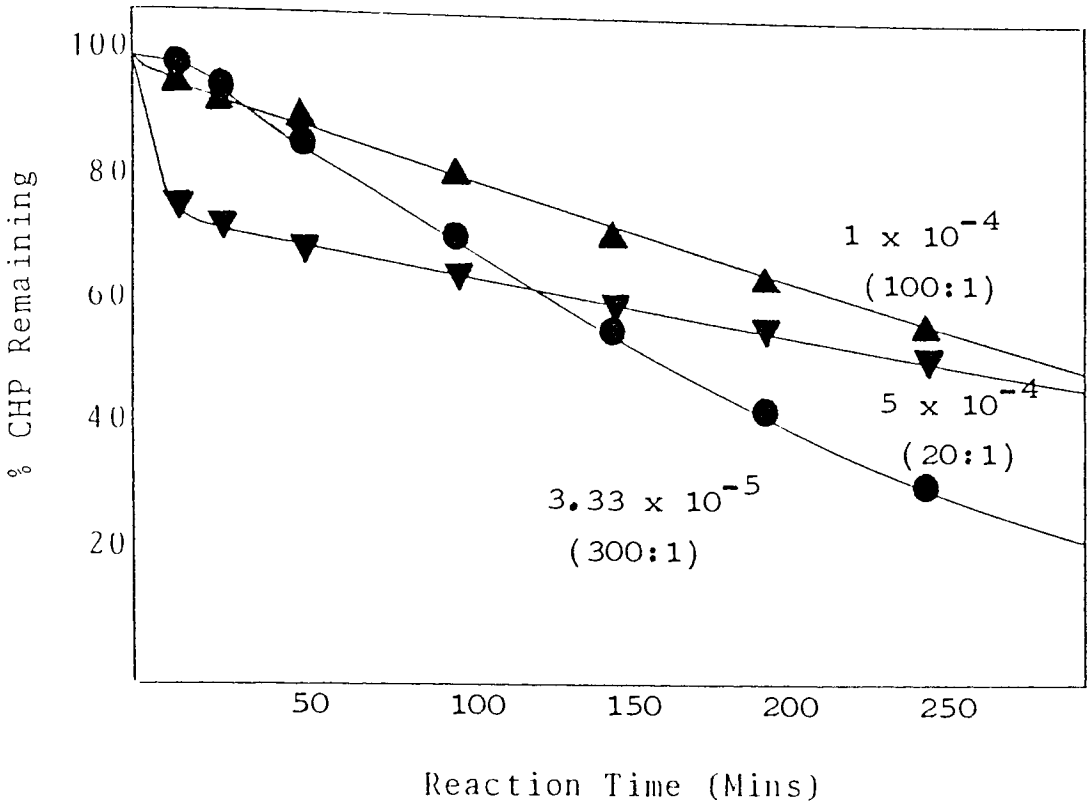

Figure 5.9. Decomposition of 1 x 10^{-2}moldm^{-3} CHP by b-ZnDiBP at 110°C in the Presence of 2 x 10^{-4}moldm^{-3} FeST. Numbers on Curves are b-ZnDiBP Concentrations in moldm^{-3}.

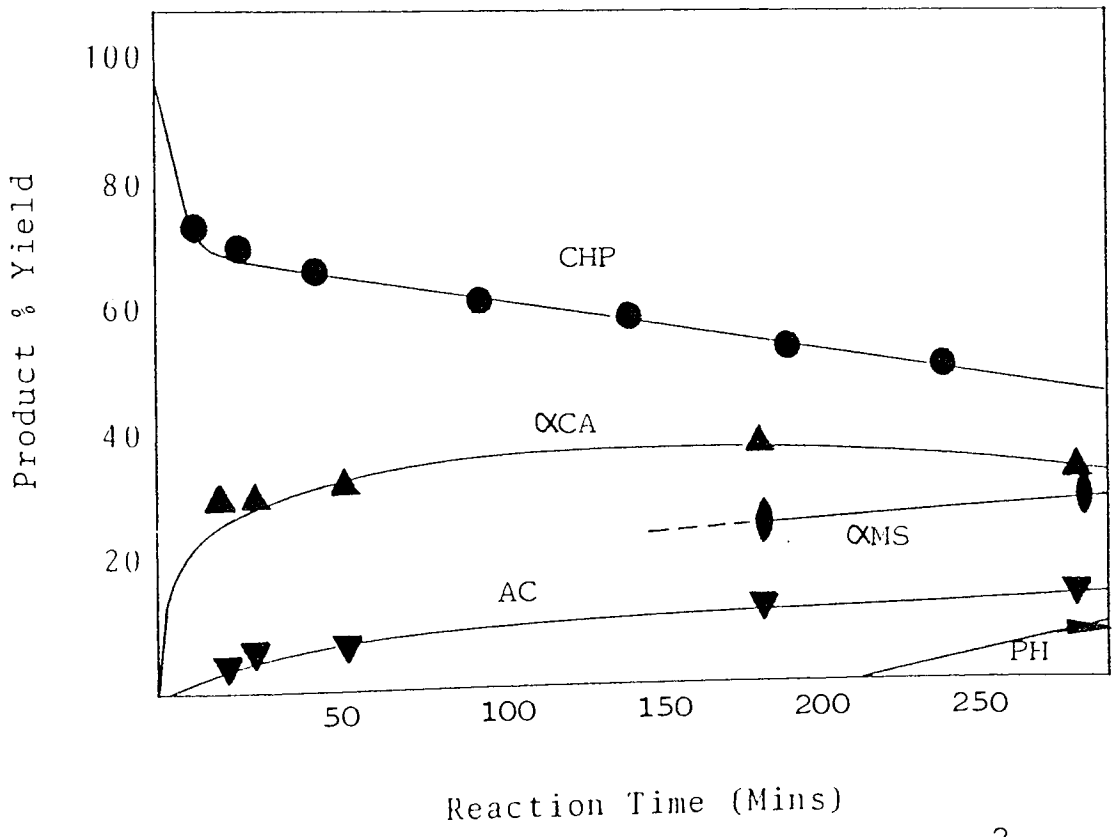

Figure 5.10. Products of Decomposition of 1 x 10^{-2}moldm^{-3} CHP by 2 x 10^{-3}moldm^{-3} ZnDiBP at 110°C in the Presence of 2 x 10^{-4}moldm^{-3} FeST.

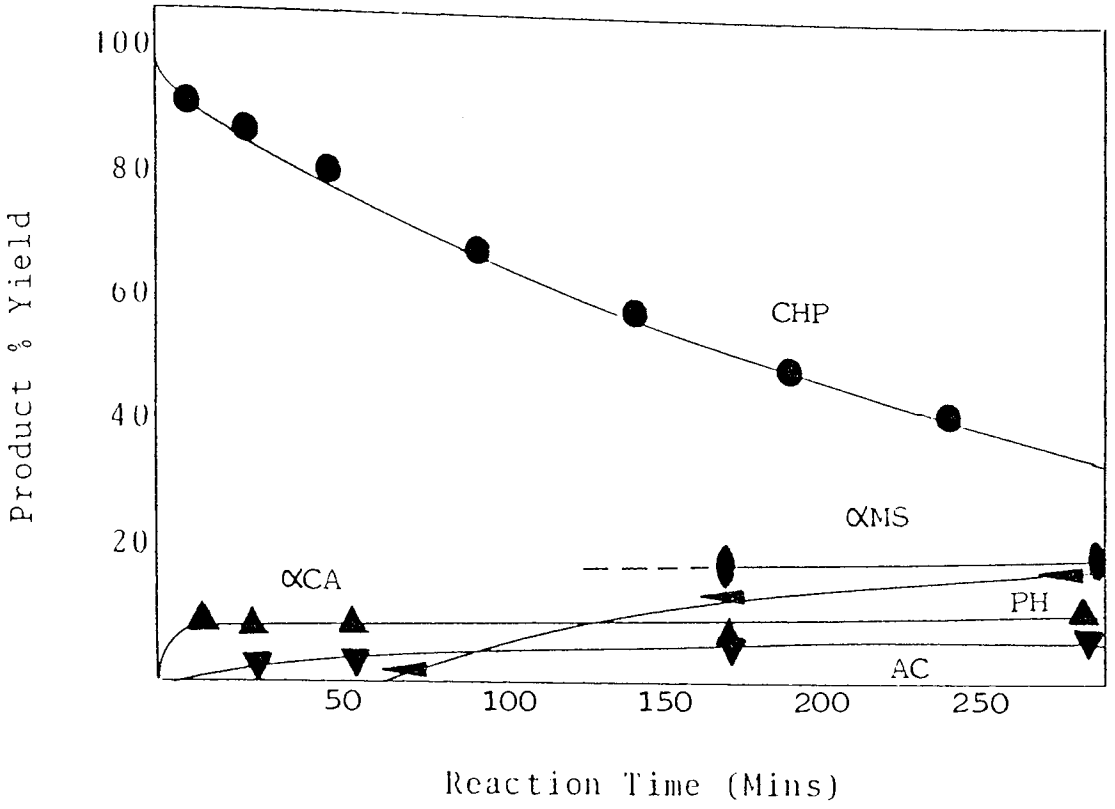

Figure 5.11. Products of Decomposition of 1 x 10^{-2}moldm^{-3} CHP by 5 x 10^{-4}moldm^{-3} ZnDiBP at 110°C in the Presence of 2 x 10^{-4}moldm^{-3} FeST.

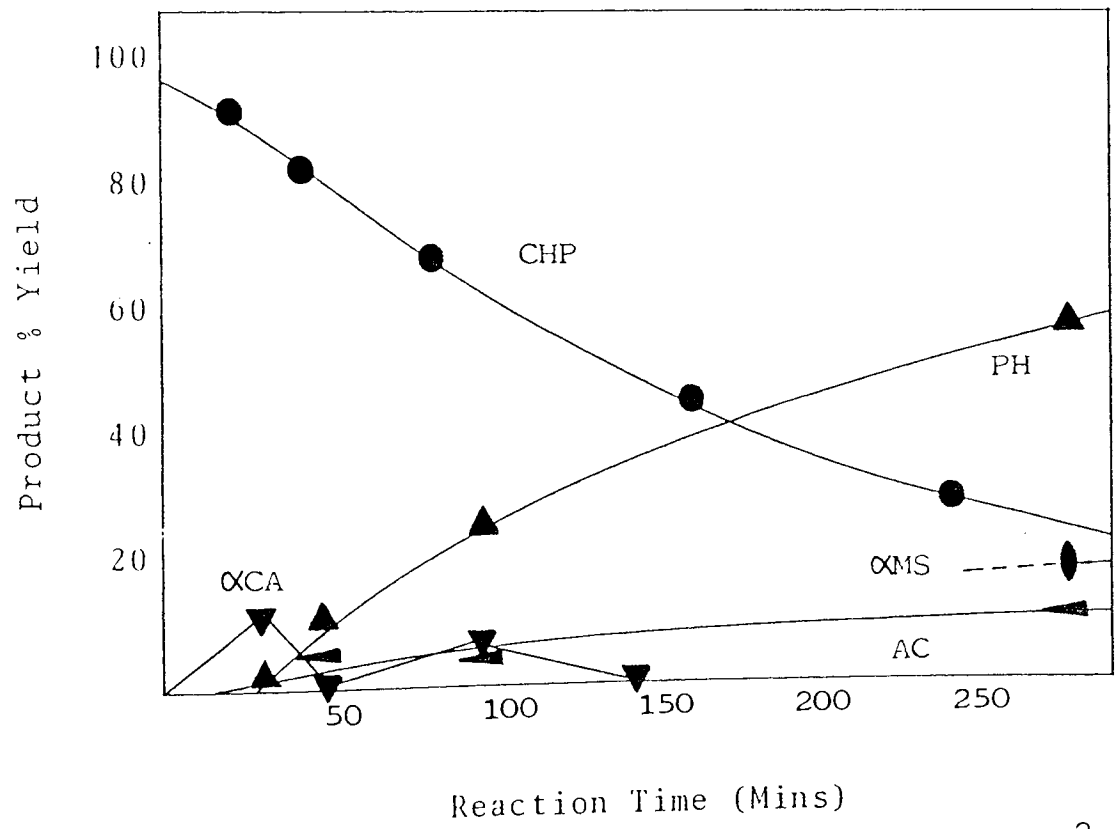

Figure 5.12. Products of the Decomposition of 1 x 10^{-2} moldm^{-3} CHP by 1 x 10^{-4}moldm^{-3} ZnDiBP at 110°C in the Presence of 2 x 10^{-4}moldm^{-3} FeST.

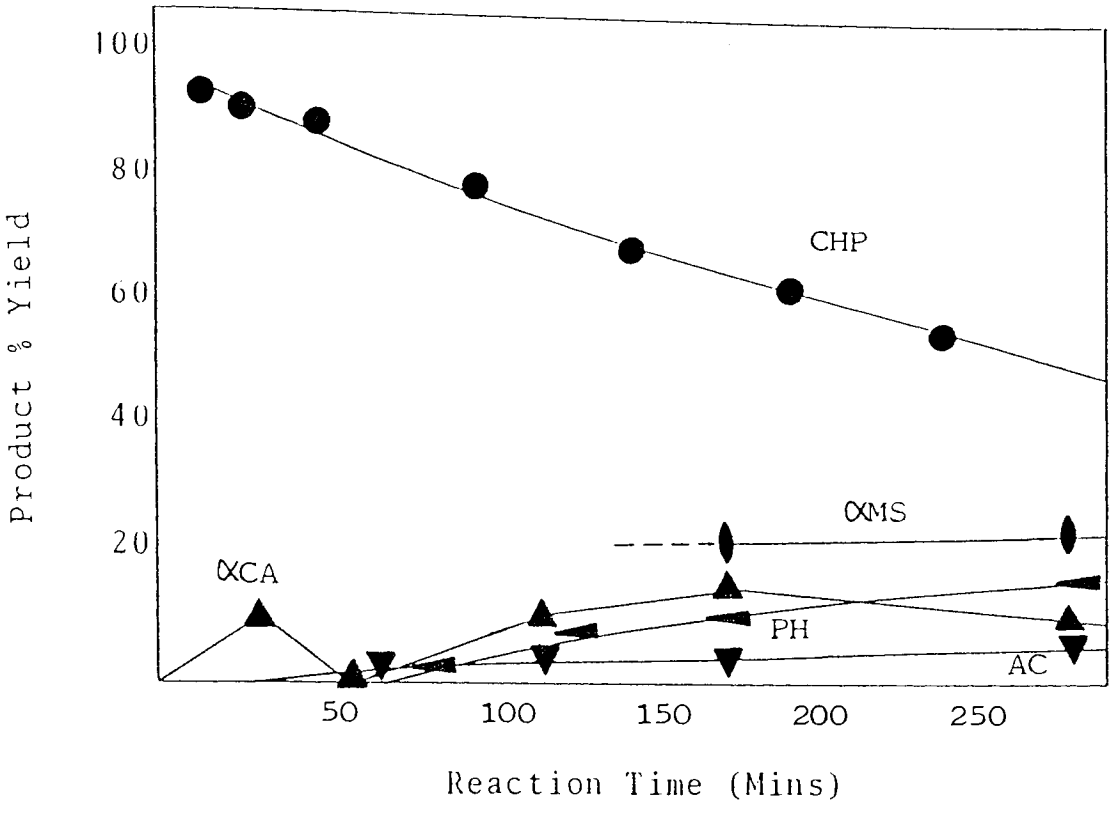

Figure 5.13. Products of Decomposition of 1 x 10^{-2}moldm^{-3} CHP by 1 x 10^{-4}moldm^{-3} b-ZnDiBP at 110°C in the Presence of 2 x 10^{-4}moldm^{-3} FeST.

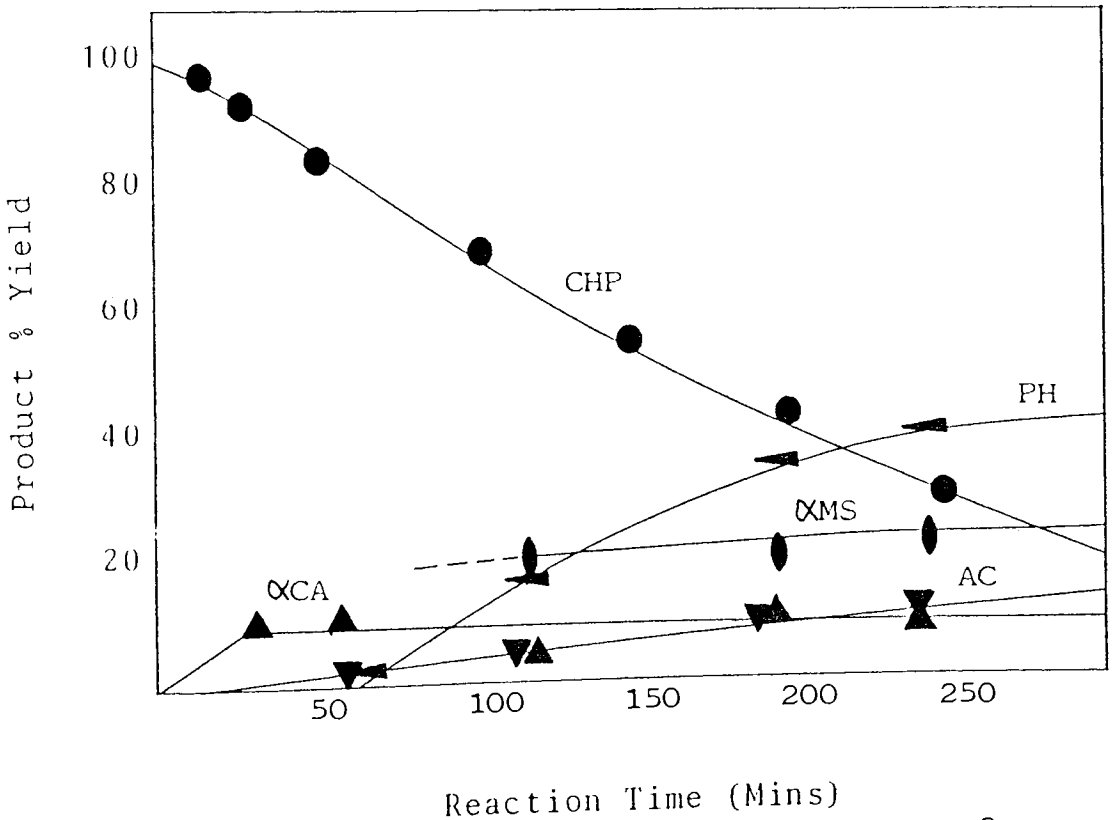

Figure 5.14. Products of Decomposition of 1 x 10^{-2}moldm^{-3} CHP by 3.33 x 10^{-5}moldm^{-3} b-ZnDiBP at 110°C in the Presence of 2 x 10^{-4}moldm^{-3} FeST.

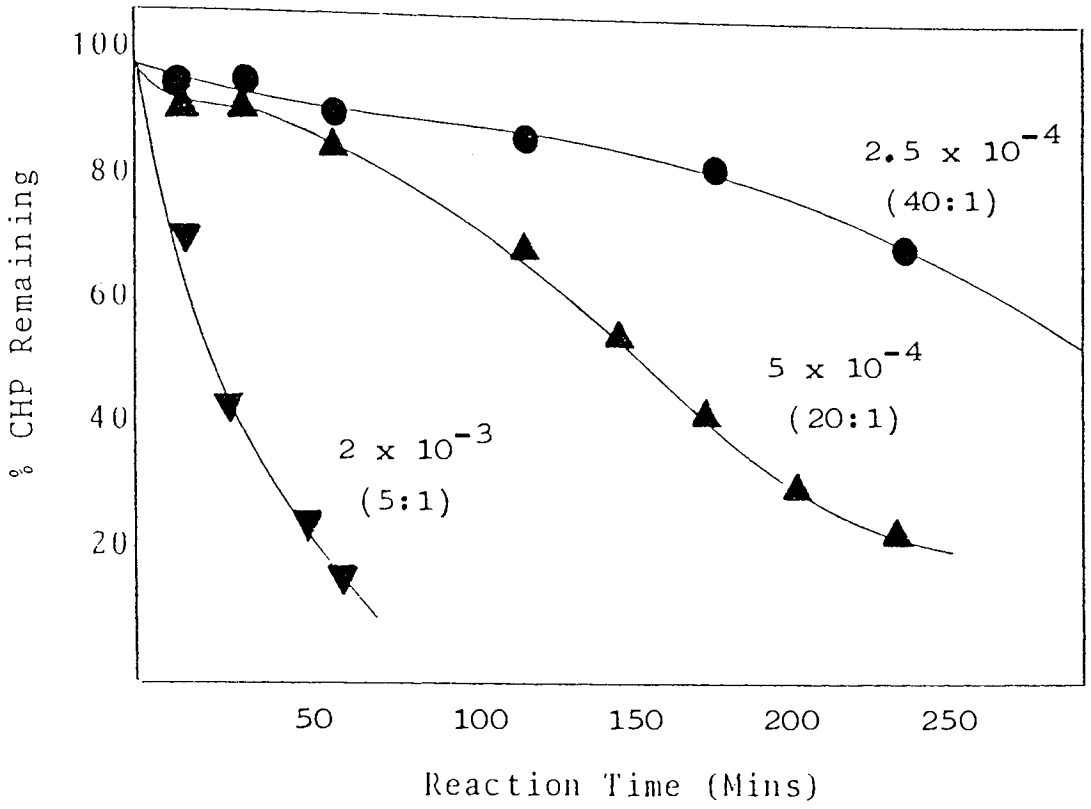

Figure 5.15. Decomposition of 1 x 10^{-2}moldm^{-3} CHP by DiBDS at 110°C in the Presence of 2 x 10^{-4}moldm^{-3} FeST. Numbers on Curves are DiBDS Concentrations in moldm^{-3}.

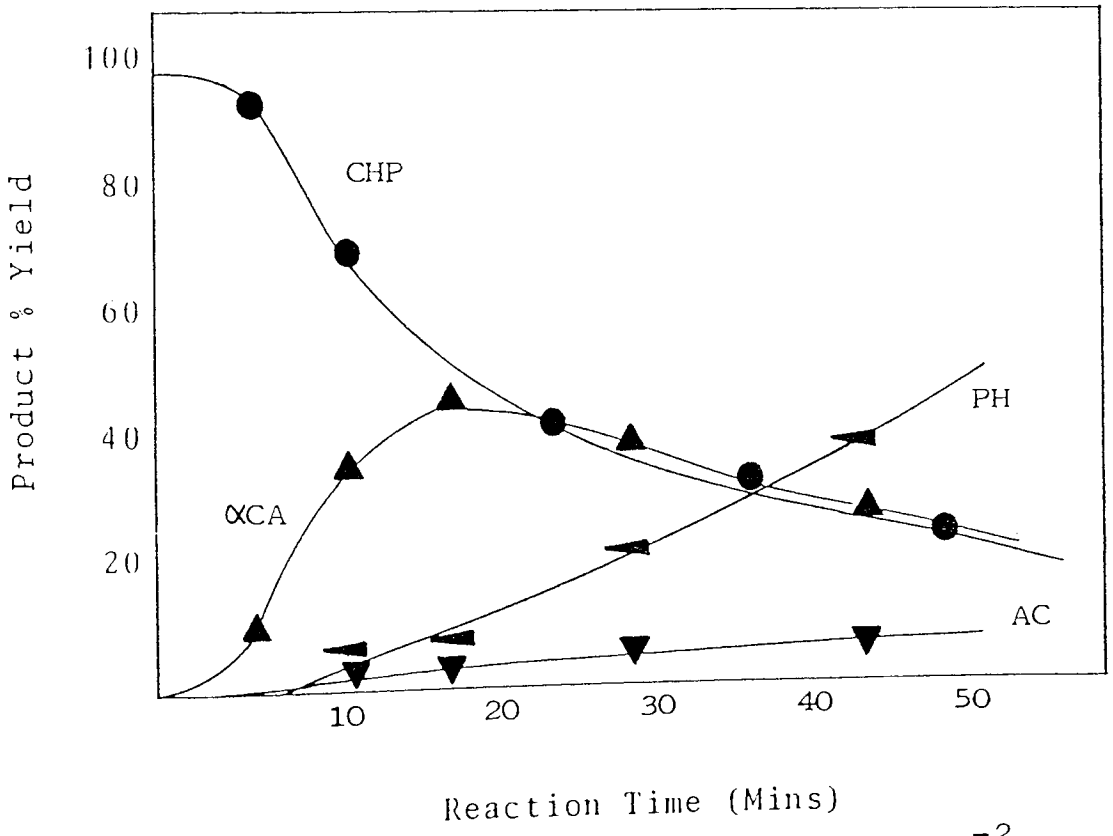

Figure 5.16. Products of Decomposition of 1 x 10^{-2}moldm^{-3} CHP by 2 x 10^{-3}moldm^{-3} DiBDS at 110°C in the Presence of 2 x 10^{-4} moldm^{-3} FeST.

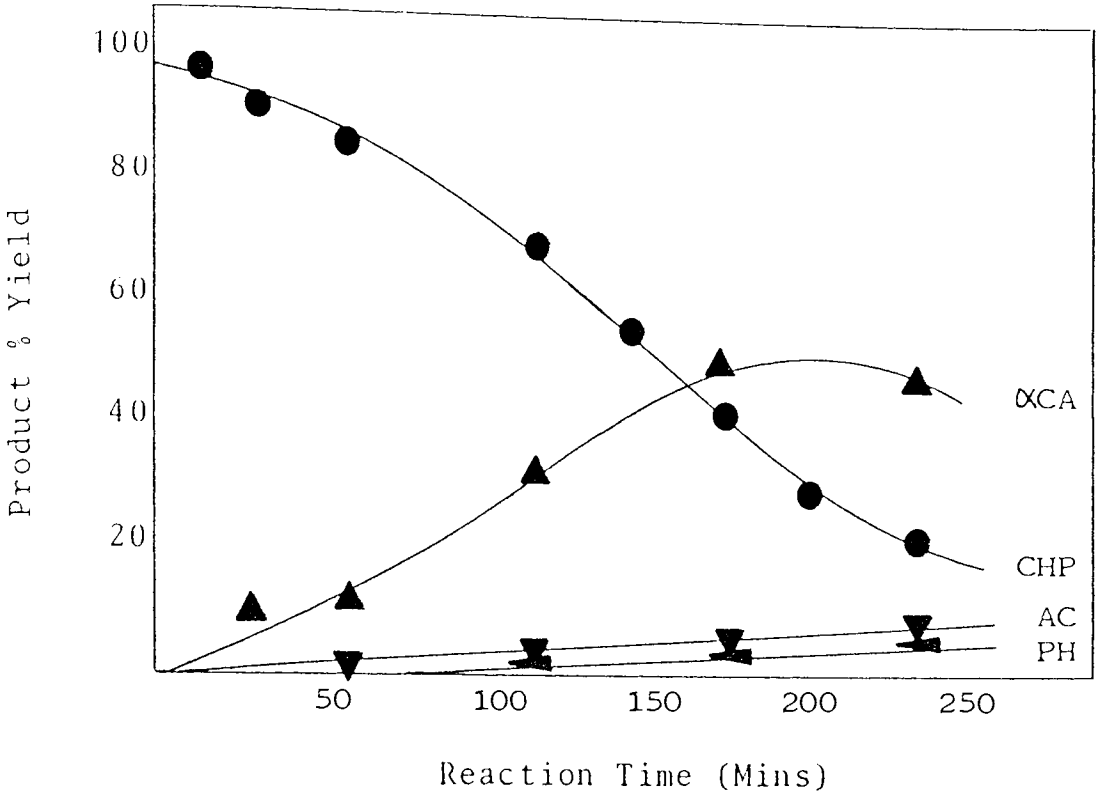

Figure 5.17. Products of Decomposition of 1 x 10^{-2}moldm^{-3} CHP by 5 x 10^{-4}moldm^{-3} DiBDS at 110°C in the Presence of 2 x 10^{-4}moldm^{-3} FeST.

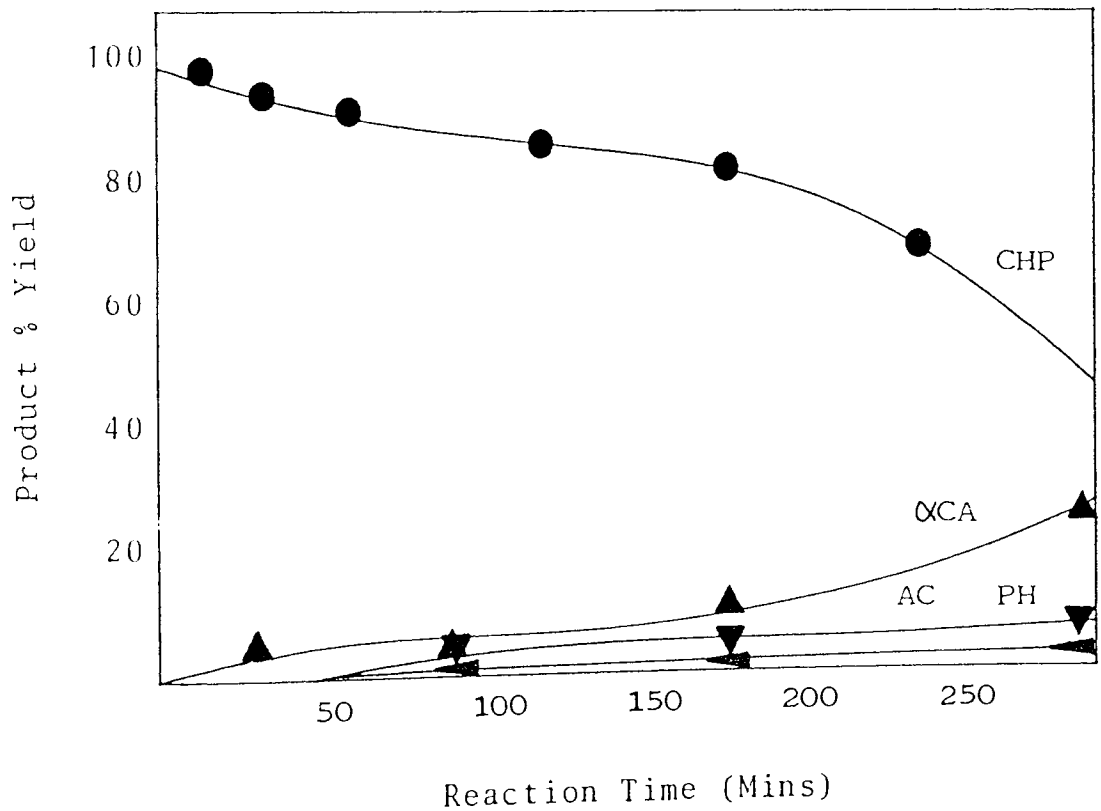

Figure 5.18. Products of Decomposition of 1 x 10^{-2}moldm^{-3} CHP by 2.5 x 10^{-4}moldm^{-3} DiBDS at 110°C in the Presence of 2 x 10^{-4}moldm^{-3} FeST.

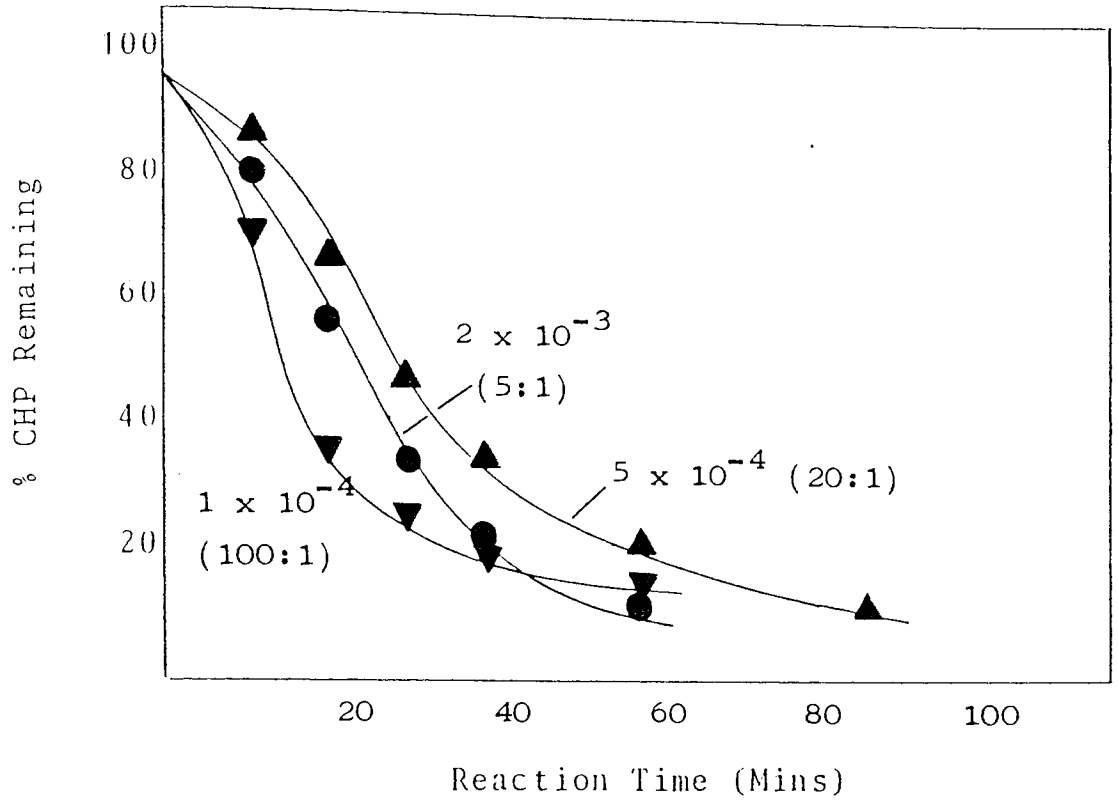

Figure 5.19. Decomposition of 1 x 10^{-2}moldm^{-3} CHP by DnHDPA at 110°C in the Presence of 2 x 10^{-4}moldm^{-3} FeST. Numbers on Curves are Concentrations of DnHDPA in moldm^{-3}.

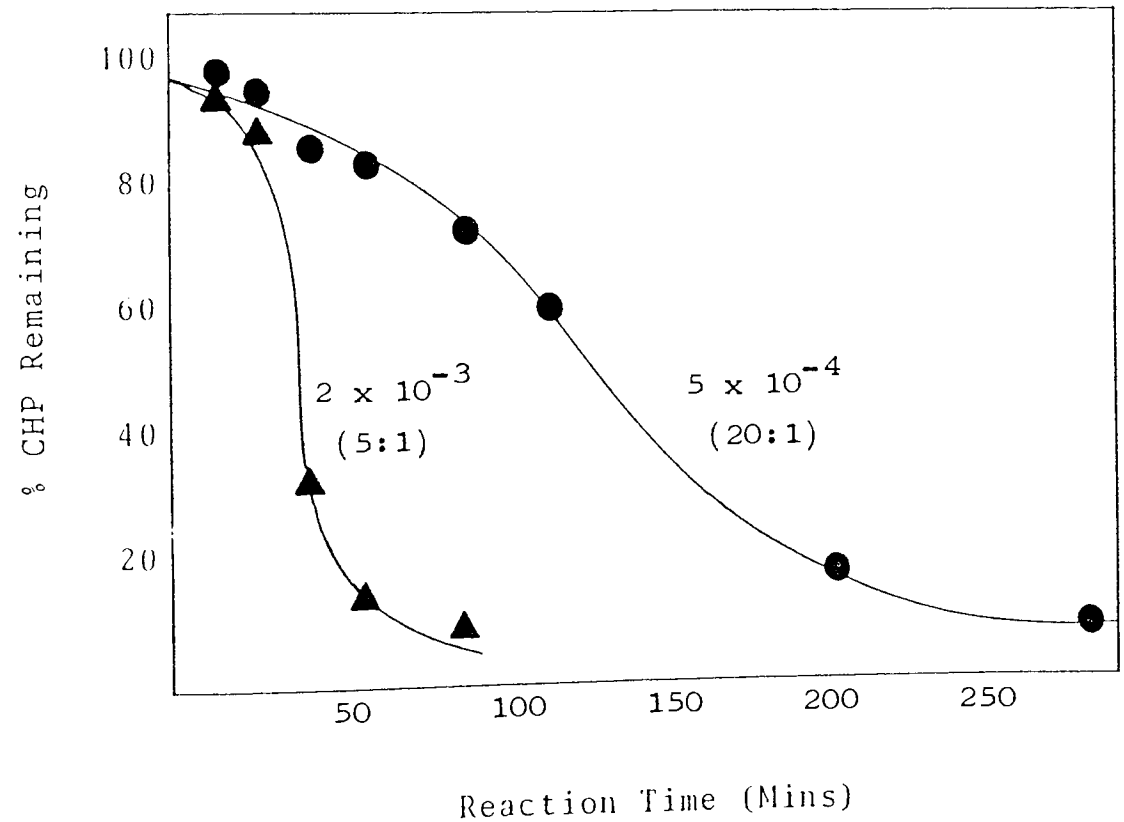

Figure 5.20. Decomposition of 1 x 10^{-2}moldm^{-3} CHP by DiBTPA at 110°C in the Presence of 2 x 10^{-4}moldm^{-3} FeST. Numbers on Curves are Concentrations of DiBTPA in moldm^{-3}.

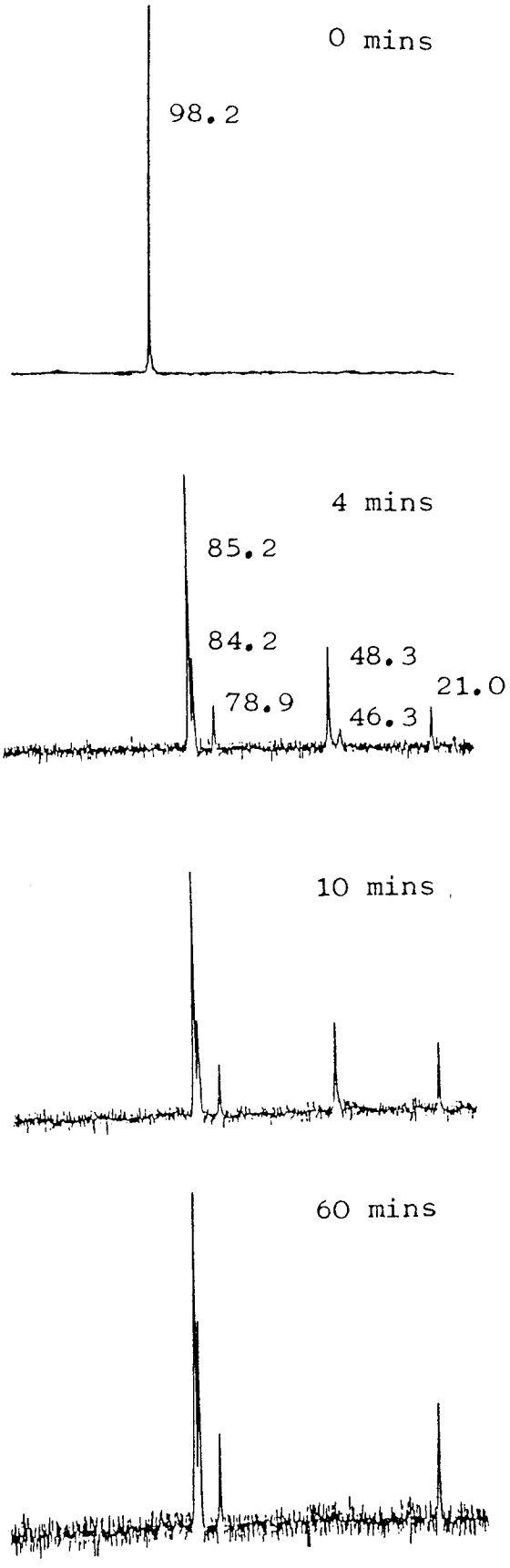

Figure 5.21. Changes in ^{31}P NMR Spectrum During Reaction of ZnDiBP and CHP at 110°C. (CHP:ZnDiBP = 5:1)

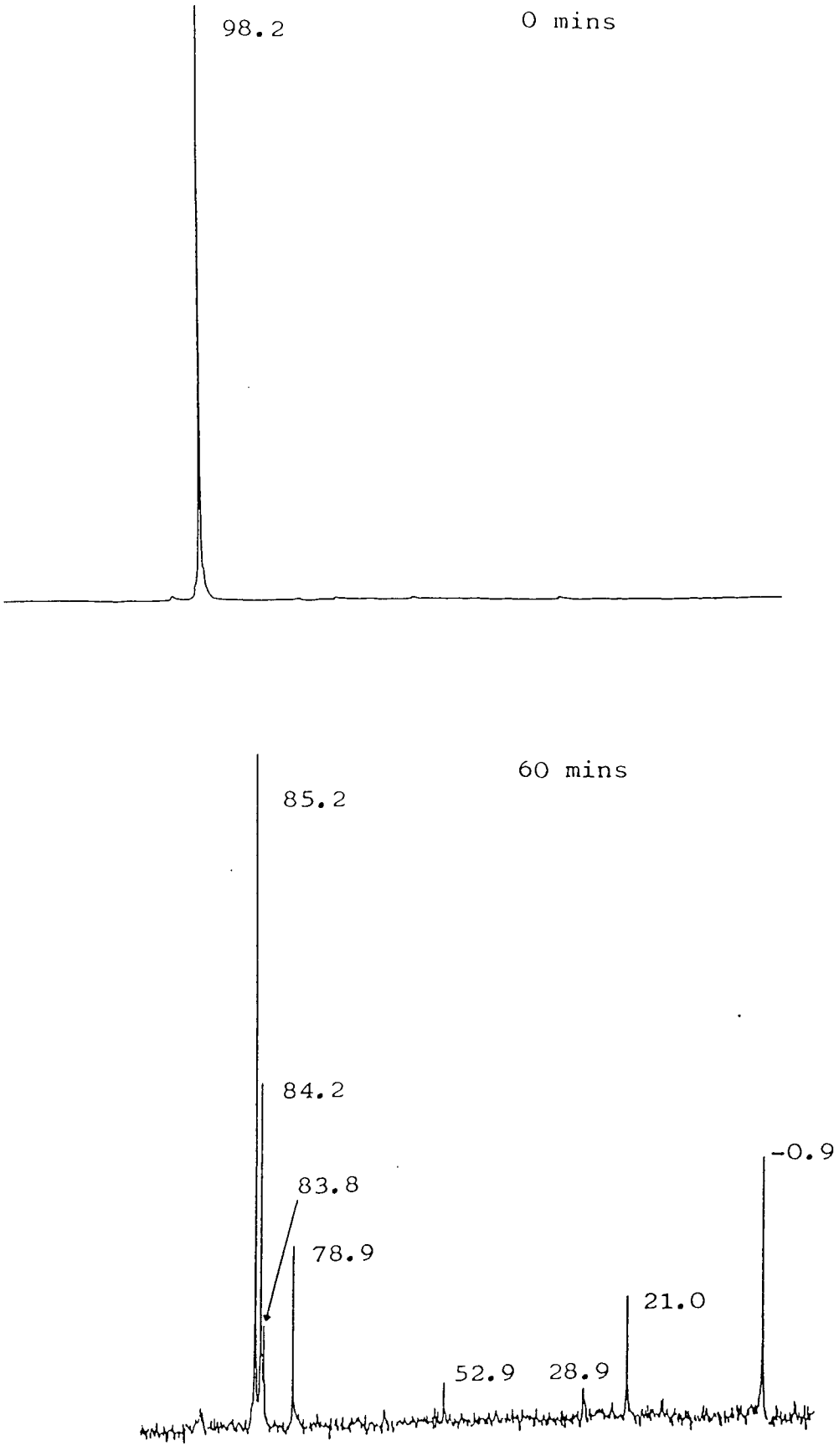

Figure 5.22. Changes in ^{31}P NMR Spectrum During Reaction of ZnDiBP and CHP at 110°C. (CHP:ZnDiBP = 10:1)

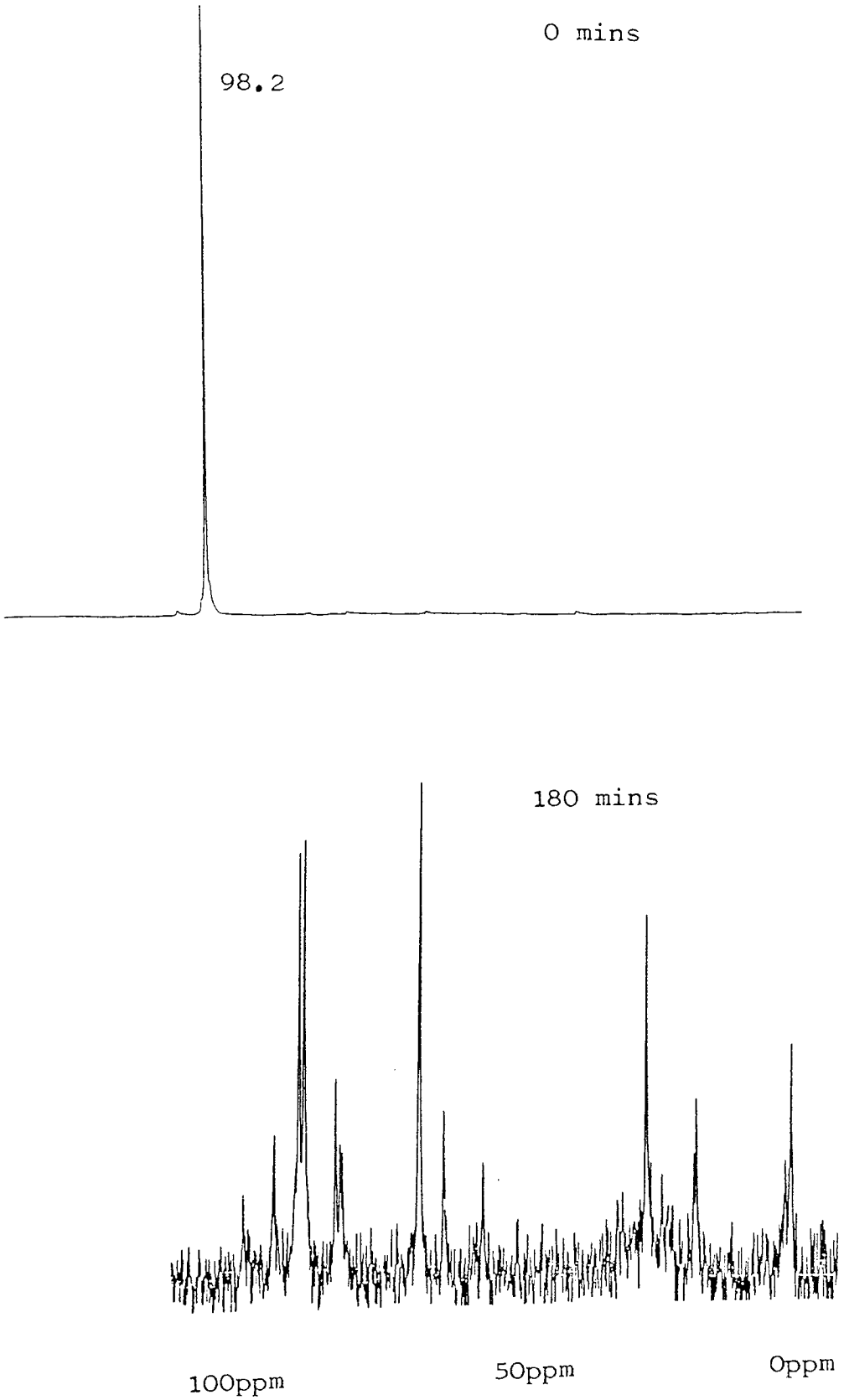

Figure 5.23. Changes in ^{31}P NMR Spectrum During Reaction Between ZnDiBP and CHP at 110°C. (CHP:ZnDiBP = 50:1)

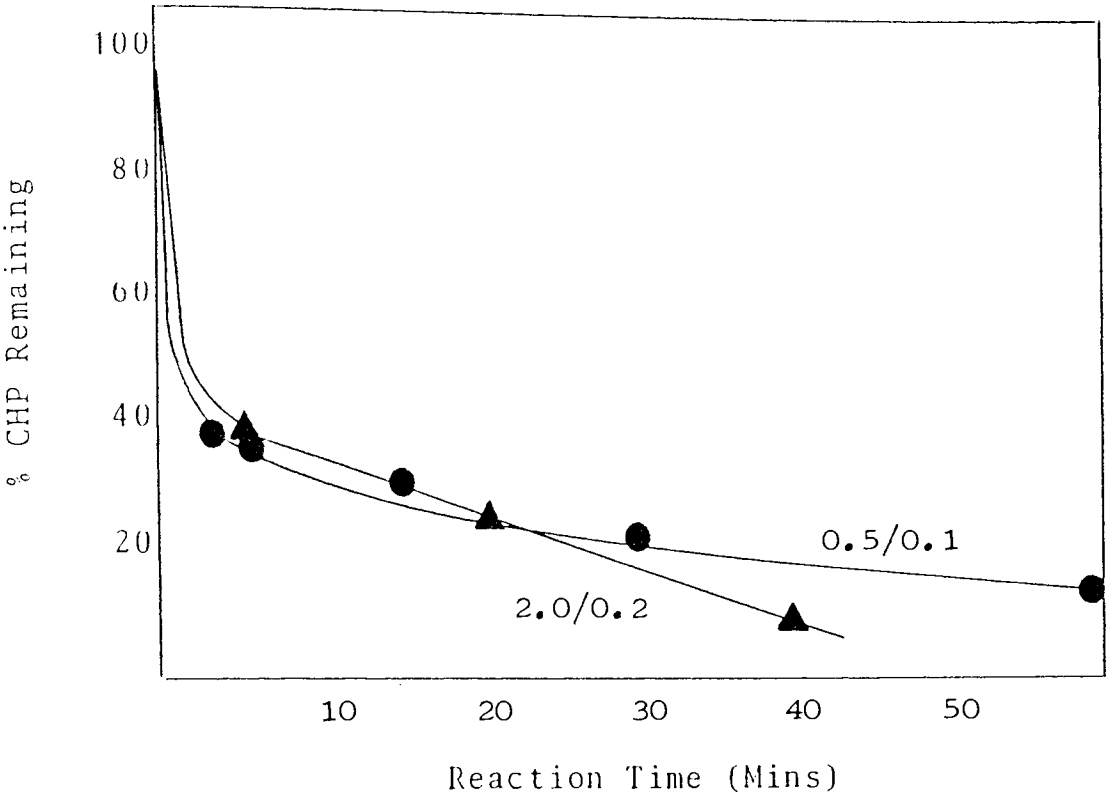

Figure 5.24. Decomposition of CHP by ZnDiBP at 110°C. Numbers on Curves are Concentration of CHP/Concentration of ZnDiBP.

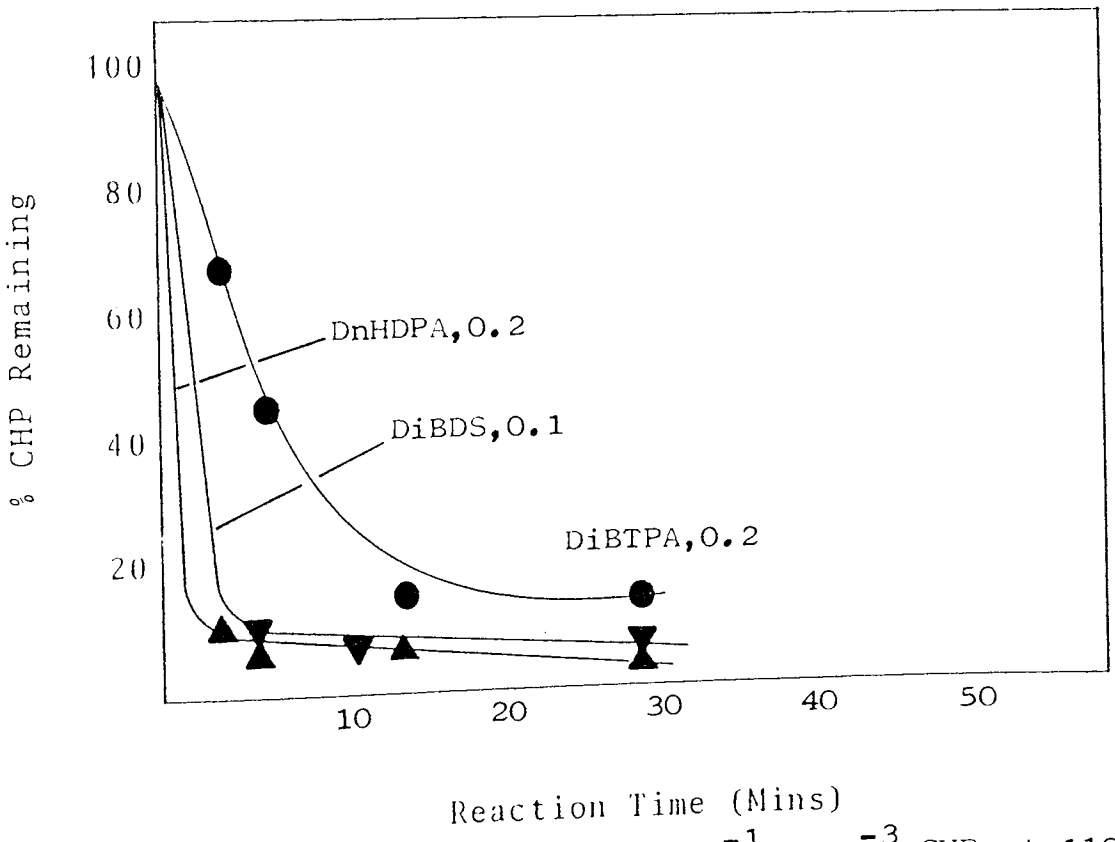

Figure 5.25. Decomposition of 5 x 10^{-1}moldm^{-3} CHP at 110°C by Various Phosphorus Containing Additives. Numbers on Curves are Concentrations in moldm^{-3}.

CHAPTER SIX

THE ACTIVITY OF IRON (III) DIALKYLDITHIOPHOSPHATE AS AN ANTIOXIDANT

6.1. OBJECT

Although the recent literature contains several references[40,76] to the preparation of iron (III) complexes of dialkyldithiophosphoric acid, little work has previously been carried out on the effect of such compounds as antioxidants, or on their reaction with hydroperoxides. The main reason for the lack of study in this field is probably the reported[40,76] instability of the iron complexes, decomposition occurring over a period of weeks or months. This instability may have been due to the presence of traces of hydrogen chloride, derived from iron (III) chloride which is employed in their preparation (reaction 44).

$$FeCl_3 + 3(RO)_2PSSNa \longrightarrow \{(RO)_2PSS\}_3Fe + 3NaCl \qquad (44)$$

Recently, however, a successful route to the preparation of stable iron (III) dialkyl dithiophosphates (FeDRP) has been developed by workers at Reading University.[77] This was achieved by using an acid-base neutralisation reaction (reaction 33), similar to that employed for the preparation of zinc dialkyldithiophosphate (ZnDRP) described in

Section 2.1.1.8. The preparation of FeDRP by this method has successfully been repeated here. (Section 2.1.1.1.16).

$$6(RO)_2PSSH + Fe_2O_3 \longrightarrow 2\{(RO)_2PSS\}_3Fe + 3H_2O \qquad (33)$$

In this chapter, work will be presented using FeDRP prepared by two methods, i.e. "in-situ", via reaction of iron (III) chloride and ZnDRP, (reaction 32), and in its pure crystalline form, as prepared by reaction (33), at Reading University.

$$3\{(RO)_2PSS\}_2Zn + 2FeCl_3 \longrightarrow 2\{(RO)_2PSS\}_3Fe + 3ZnCl_2 \qquad (32)$$

The effectiveness of FeDRP as an antioxidant is evaluated by the oxygen absorption technique. (Section 2.2.1.). Decalin is used as the oxidisable substrate and the temperature used is again 130°C, so that a direct comparison of FeDRP with the other dithiophosphates studied in Chapter 3 can be made. The effect of FeDRP as an antioxidant in the presence of a fixed concentration of cumene hydroperoxide (CHP) is also studied by oxygen absorption using similar conditions. A number of different FeDRP concentrations are used, both in the presence and absence of CHP.

The reaction of FeDRP with hydroperoxides is studied in several ways. The disappearance of CHP in the presence of FeDRP is followed, as a function of time, using the hydroperoxide decomposition technique described in Section 2.2.2., and previously used to determine the hydroperoxide decomposing ability of ZnDRP and related compounds (Section 5.1.). The reactions are carried out at 110°C in chlorobenzene under nitrogen, so that inert conditions are achieved. In all experiments the CHP concentration is fixed at $1x10^{-2}moldm^{-3}$, and the FeDRP concentration is varied between $1x10^{-4}moldm^{-3}$ and $2x10^{-3}moldm^{-3}$, so that the effects of stoichiometric and catalytic amounts of iron complex can be observed.

Samples removed from the above experiments at suitable time intervals are analysed by gas-liquid chromatography (GLC) to determine qualitatively and quantitatively the decomposition products derived from the CHP, in order to establish the relative contributions of the free radical and ionic decomposition mechanisms (see Section 5.3.1.1.) towards the overall decomposition of hydroperoxides by FeDRP.

The decomposition of FeDRP in the presence of hydroperoxides is studied by ultra-violet/visible (UV-VIS) spectroscopy at 25°C and 50°C. Spectroscopic grade cyclohexane is used as the substrate at 25°C, and puriss grade n-dodecane is used at 50°C.

The hydroperoxide used is t-butyl hydroperoxide (TBH). A fixed initial concentration of $2.5 \times 10^{-4} moldm^{-3}$ FeDRP is used in all experiments and the TBH concentration is varied from $1 \times 10^{-4} moldm^{-3}$ to $1 \times 10^{-2} moldm^{-3}$. The disappearance of the FeDRP and the build-up of decomposition products are followed by monitoring the intensities of the 596nm and 260nm absorption bands respectively as a function of time.

The phosphorus containing products of the reaction between FeDRP and hydroperoxides are identified by phosphorus-31 nuclear magnetic resonance spectroscopy. (^{31}P NMR). Finally, the reactions between several dithiophosphates (ZnDRP, DRDS and DRDPA) and a number of iron containing compounds are studied, primarily by UV-VIS spectroscopy, in order to determine the conditions under which FeDRP may be formed.

Scheme 6.1. summarises the work carried out in the present chapter.

6.2. RESULTS

6.2.1. OXIDATION OF DECALIN IN THE PRESENCE OF FeDRP

6.2.1.1. OXIDATION IN ABSENCE OF HYDROPEROXIDES

The oxidation of decalin at 130°C in the presence of FeDRP is shown in Figure 6.1. At the two lower concentrations, the isobutyl substituted iron complex, FeDiBP, was prepared "in-situ", by the action of excess aqueous iron (III) chloride on a solution of zinc di-isobutyldithiophosphate, (ZnDiBP), in decalin. (See Section 2.1.1.15. for preparative details). The initial induction period, which increases with concentration of the iron complex, was followed by an autoaccelerating stage, evident from the rapid uptake of oxygen which shows no tendency to retard at high levels of oxidation.

The isopropyl substituted iron complex, FeDiPP, which was prepared by reaction (33) and subsequently dissolved in decalin, was used at a concentration of $5 \times 10^{-3} moldm^{-3}$ and its effect is also shown in Figure 6.1. It is clear that under these conditions there is a longer induction period, which is followed by an accelerating oxygen uptake stage which is far less steep than that observed at the lower concentrations when "in-situ" FeDiBP was used.

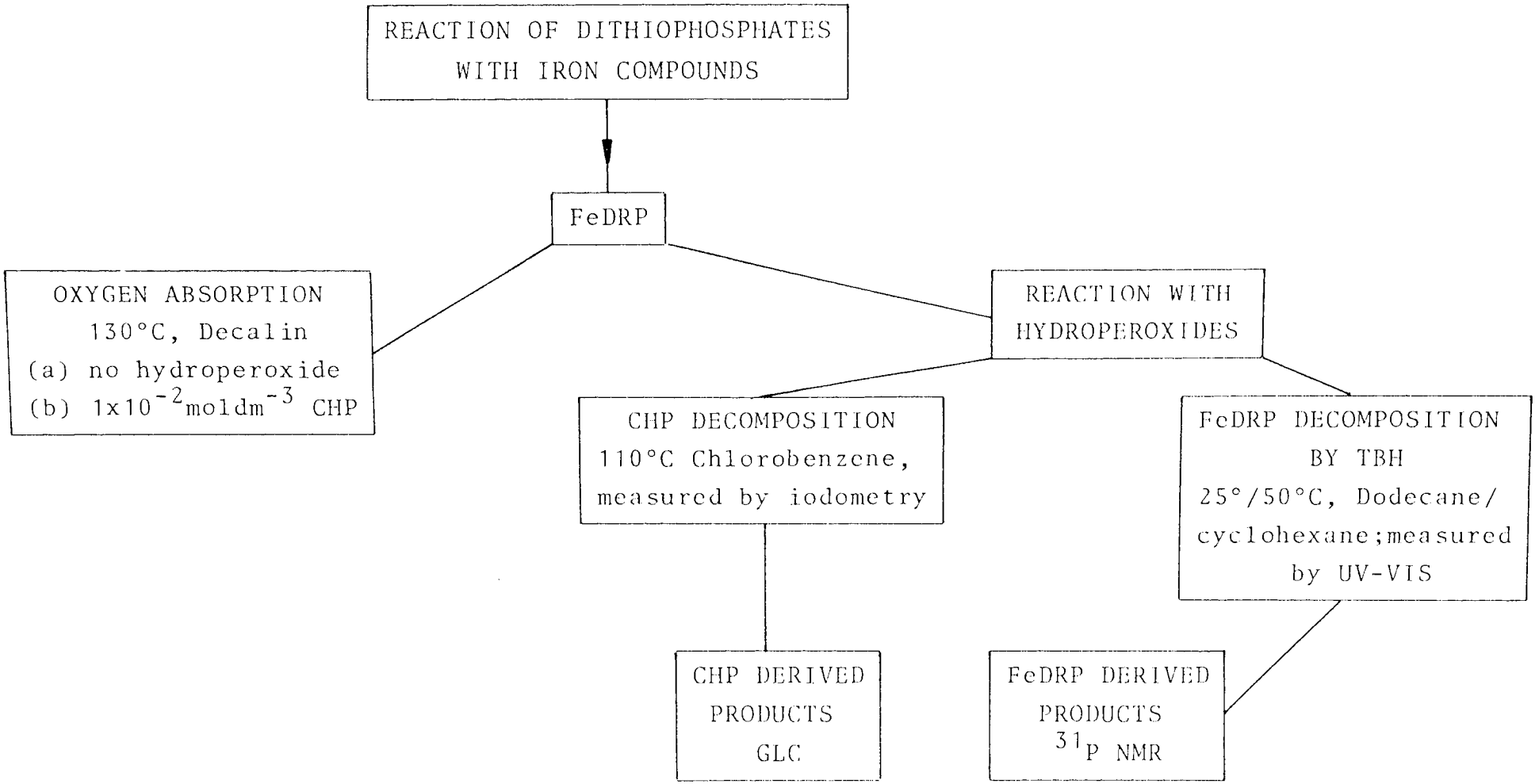

Scheme 6.1. Experiments described in Chapter 6.

6.2.1.2. OXIDATION IN THE PRESENCE OF CHP

The effect of $1x10^{-2}moldm^{-3}$ CHP on the oxidation of decalin at 130°C in the presence of FeDIBP is shown in Figure 6.2. The iron complex was prepared "in-situ" as above. The induction periods observed in the absence of CHP (see Figure 6.1.) were greatly reduced, such that severe oxidation occurs within 5-6 hours of the beginning of the experiment.

6.2.2. REACTION OF FeDRP WITH HYDROPEROXIDES

6.2.2.1. DECOMPOSITION OF CHP BY FeDRP

The decomposition of CHP by FeDiPP in chlorobenzene at 110°C is shown in Figure 6.3. The reactions were carried out under nitrogen. The concentration of CHP was fixed at $1x10^{-2}moldm^{-3}$, and the concentration of FeDiPP was varied from $1x10^{-4}$ - $2x10^{-3}moldm^{-3}$. Figure 6.3. shows that at all concentrations studied a complete decomposition of CHP by FeDiPP was readily achieved. At the highest concentration a rapid initial reaction was followed by a slower subsequent stage, whereas the reverse was true at the lowest concentration, with an intermediate behaviour at a FeDiPP concentration of $5x10^{-4}moldm^{-3}$. In each case the initially dark green solution became orange within 6 minutes, i.e. by the time the first sample for analysis was withdrawn from the reaction vessel.

On standing for several hours after the completion of each experiment an orange/brown precipitate settled out below a colourless solution.

Although not shown, the results obtained when the iron complex (FeDiBP) was prepared "in-situ" were very similar to thos presented in Figure 6.3. using the pure crystalline FeDiPP.

In order to try to identify the orange/brown precipitate, the reaction of FeDiPP with hydroperoxide was carried out on a larger scale. An initially dark green solution of $5x10^{-2}moldm^{-3}$ FeDiPP in chlorobenzene was violently decomposed by the addition of a solution of $2.5x10^{-1}moldm^{-3}$ TBH in chlorobenzene at 110°C. (FeDiPP:TBH = 1:5). Within 5 minutes the solution had become orange, and on standing at room temperature for 30 minutes an orange/brown precipitate settled out below a pale yellow solution.

The mass of solid isolated by filtration was 8.5% of the original mass of FeDiPP used. The precipitate was found to be insoluble in water or organic solvents, but readily soluble in dilute hydrochloric acid, had a high melting point (> 250°C) and was resistant to pyrolysis. An attempt to characterise it by X-ray diffraction was unsuccessful. Although it was not possible to positively identify the brown precipitate, it is highly likely that it is a form

of iron (III) oxide. The reasons for this conclusion are outlined in Section 6.3.2.1.

The major phosphorus-containing constituent of the soluble fraction was identified by ^{31}P NMR as di-isopropyl thiophosphoryl disulphide. (DiPDS, δ= 80.8ppm). Less than 1% insoluble material was obtained when a solution of FeDiPP was heated in chlorobenzene alone at 110°C for 3 hours.

For each of the three concentrations of iron complex used above inthe hydroperoxide decomposition experiments (see Figure 6.3.), the products arising from the CHP were qualitatively and quantitiatively identified by GLC. Figures 6.4., 6.5. and 6.6. show the kinetics of product build up for each concentration of iron complex used.

Several distinct trends may be observed. Firstly, the amount of acetophenone formed was greatest at high FeDiPP concentrations (Figure 6.4.), whilst the amount of phenol formed was greatest at lower iron concentrations. (Figures 6.5. and 6.6.). Figure 6.7. shows this concentration dependence quite clearly. At all concentrations of FeDiPP most of the acetophenone formed built up in the first 5-10 minutes of the reaction. Conversely, the formation of significant amounts of phenol was always delayed until after this time. Finally, the amounts of α-methylstyrene

and α-cumyl alcohol formed were low at all concentrations of FeDiPP studied. (In fact no α-cumyl alcohol was found, but see Section 2.2.3.).

6.2.2.2. DECOMPOSITION OF FeDRP BY TBH

The decomposition of FeDiPP by TBH in cyclohexane at 25°C was followed by UV-VIS spectroscopy. In all studies the initial concentration of the iron complex was set at $2.5 \times 10^{-4} mol dm^{-3}$.

Two types of behaviour, dependent on the initial TBH concentration, were observed on addition of the TBH. At TBH:FeDiPP ratios above 4:1, the bands characteristic of the original iron complex completely disappeared after a very short period of the reaction. (Figures 6.8a. and 6.8b.). At ratios less than 1:1 however, these bands initially reduced in intensity (Figure 6.9a.), but reached a minimum absorbance value after 6-12 minutes and thereafter increased again. The "final" intensities did not recover to the initial values, but levelled off after 20-25 minutes. (Figures 6.9b. and 6.9c.).

This behaviour is shown more clearly in Figure 6.10., which shows the changes in absorbance of the 596nm band of the iron complex with time at different TBH concentrations, as measured continuously and directly by the spectrophotometer using the kinetic facility. This confirms that the observed increase

in absorbance (Figures 6.9b. and 6.9c.) is a genuine one, and not a consequence of the experimental technique. Similar effects had been observed in this work when conducting preliminary experiments using dodecane at 25°C.

The initial rate of decomposition of FeDiPP increased with increasing TBH concentration. (Table 6.1.). When no hydroperoxide was added the absorbance at 596nm remained constant over a period of 90 minutes.

At the same time as the bands in the 300-700 m region decreased, so the absorbance in the 200-300 nm range increased. (Figure 6.11). The initial rate of product build up, as measured by the increase in absorbance of the 260nm band, increased with increasing TBH concentration. (Table 6.1.).

Similar behaviour was observed when the decomposition was carried out in dodecane at 50°C. (Figures 6.12. and 6.13.). The rates of FeDiPP decomposition and product formation were greater than at 25°C. (Table 6.2.). Consequently the time taken for the absorbance to reach a minimum at the lower TBH concentrations was reduced at this higher temperature. (Figure 6.12.). At 50°C the absorbance of the 596nm band again remained constant when no hydroperoxide was present.

TBH concentration ($moldm^{-3}$) (molar ratio TBH:FeDiPP)	Δ absorbance (min^{-1})*	$\frac{\Delta absorbance\ (260nm)}{\Delta absorbance\ (596nm)}$
$1x10^{-4}$ (0.4:1)	+ 0.072 (260nm) - 0.049 (596nm)	1.47
$2.5x10^{-4}$ (1:1)	+ 0.120 (260nm) - 0.066 (596nm)	1.82
1x10-3 (4:1)	+ 0.224 (260nm) - 0.110 (596nm)	2.04
$5x10^{-3}$ (20:1)	+ 0.246 (260nm) - 0.120 (596nm)	2.05

* Δabsorbance = initial rate of change of absorbance per minute calculated from Figures 6.10. and 6.11.

Table 6.1. Initial rates of decomposition of FeDiPP in cyclohexane at 25°C

TBH concentration ($moldm^{-3}$) (molar ratio TBH:FeDiPP)	△absorbance (min^{-1})*	$\frac{\triangle absorbance\ (260nm)}{\triangle absorbance\ (596nm)}$
$1x10^{-4}$ (0.4:1)	+ 0.130 (260nm) - 0.073 (596nm)	1.78
$2.5x10^{-4}$ (1:1)	+ 0.260 (260 nm) - 0.243 (596 nm)	1.07
$1x10^{-3}$ (4:1)	+ 0.617 (260nm) - 0.347 (596nm)	1.78
$5x10^{-3}$ (20:1)	+ 1.053 (260 nm) - 0.567 (596nm)	1.86

* △absorbance = initial rate of change of absorbance per minute calculated from Figures 6.12. and 6.13.

Table 6.2. Initial rates of decomposition of FeDiPP in n-dodecane at 50°C

The products of the decomposition of $4x10^{-1}moldm^{-3}$ FeDiPP by $2moldm^{-3}$ TBH in chlorobenzene at 25°C (FeDIPP:TBH = 1:5) were identified by ^{31}P NMR. An immediate, exothermic reaction led to the rapid disappearance of the dark green colour of the FeDiPP within 5 minutes, giving an orange precipitate and a yellow solution. The soluble products of the decomposition gave the ^{31}P NMR spectrum shown in Figure 6.14.; the proposed assignments[47,69] are given in Table 6.3.

6.2.3. FeDRP AS A PRODUCT OF THE REACTION OF DITHIOPHOSPHATES AND IRON COMPOUNDS

The reaction of three dithiophosphates i.e. n-hexyl dithiophosphoric acid (DnHDPA), di-isobutyl thiophosphoryl disulphide (DiBDS) and ZnDiBP, with various iron containing compounds was studied to see if FeDRP was formed.

6.2.3.1. REACTION OF DITHIOPHOSPHATES WITH IRON (III) CHLORIDE ($FeCl_3$)

Addition of an aqueous solution of $FeCl_3$ to a solution of ZnDiBP in chlorobenzene or decalin at 25°C led to the immediate formation of the characteristic black colouration of FeDRP. This also occurred when DnDHPA or DiBDS were used.

Table 6.3. Products of the decomposition of FeDiPP by TBH at 25°C, as measured by ^{31}P NMR. (Figure 6.14.)

Chemical shift	Phosphorus % yield	Assignment[47,69]
90.9	5	$(RO)_2PSSR$ ⎫ R=s-alkyl
		R'=t-alkyl
87.3	20	$(RO)_2PSSR'$ ⎭
81.0	41	DRDS
75.3	14	$\{(RO)_2PS\}_2S$
18.0	19	DRODS

In addition to the above, several small peaks were observed.

Chemical shift (ppm)	Assignment[47,69]
72.8	Unknown
49.4-56.8	Unknown
12.3	Unknown
-3.4	$(RO)_3P{=}O$ or $(RO)_2P(O)OH$

6.2.3.2. REACTION OF DITHIOPHOSPHATES WITH IRON (III) STEARATE (FeST)

The reaction between ZnDIBP and FeST was studied at 25°C and 130°C in chlorobenzene. After 3 hours, thin layer chromatography (TLC) showed little reaction had occurred at either temperature, although some DiBDS had formed at 130°C. In both cases, the residue left after filtration and removal of the solvent had a slight greenish-brown colouration. When the reaction was repeated on a larger scale at 25°C for 4 hours, the UV-VIS spectrum of the solution indicated that less than 2% of the ZnDiBP had been converted into FeDRP (ZnDiBP:FeST = 3:2.). The formation of FeDRP from DnHDPA and FeST in decalin at 25°C was observed during oxygen absorption studies. (Section 4.2.1.3.). FeDRP was not formed at all by the reaction of DiBDS with FeST after 3 hours at 25°C in cyclohexane.

6.2.3.3. REACTION OF DITHIOPHOSPHATES WITH IRON METAL. (Fe)

The reaction of DiBDS and ZnDiBP with powdered iron metal at 130°C in chlorobenzene was studied by TLC. No reaction was observed in either case after 2 hours. In contrast, the reaction between iron metal and DnHDPA in cyclohexane at 25°C occurred rapidly giving the black FeDRP.

6.2.3.4. REACTION OF DITHIOPHOSPHATES WITH IRON (III) OXIDE (Fe_2O_3)

The preparation of FeDRP by the action of DRDPA on Fe_2O_3 at 70°C in hexane has been described in Section 2.1.1.16. Studies of the reaction at 25°C in cyclohexane were carried out using UV-VIS spectroscopy. Two types of Fe_2O_3 were used; firstly the commercially available material previously used in the bulk preparation of FeDRP (Section 2.1.1.16.), and secondly the orange/brown precipitate formed when FeDiPP was decomposed by TBH at 25°C. (see Section 6.2.2.1.). After 3 hours stirring at 25°C the UV-VIS spectra of the filtered solutions were measured. A considerable difference in the reactivity of the two types of Fe_2O_3 was observed. (Figures 6.15. and 6.16.). By measuring the absorbance of the 596nm band, the approximate amounts of FeDRP formed from the reaction of DnHDPA with Fe_2O_3 were found to be 6% (commercial Fe_2O_3) and 83% (prepared Fe_2O_3). Figures 6.15. and 6.16. also show that a reaction between DiBDS and the two types of Fe_2O_3 to give FeDRP did not occur within 3 hours in cyclohexane at 25°C. Similarly, no FeDRP was formed in the reaction of ZnDiBP with either type of Fe_2O_3 after 3 hours in cyclohexane at 25°C.

6.3. DISCUSSION

6.3.1. OXIDATION OF DECALIN IN THE PRESENCE OF FeDRP

The trend of the increasing length of the induction period with increasing concentration of FeDRP (Figure 6.1.), shows that the iron complex does act as an inhibitor of the non-catalysed oxidation of decalin at 130°C. (It should be noted that the alkyl group used at the lower concentrations is a primary isobutyl, while a secondary isopropyl was used at the highest concentration.)

The type of inhibition exhibited by the iron complex in the absence of CHP (Figure 6.1.) is similar to that shown by the analogous zinc complex, ZnDRP. (Section 3.2.1.1., Figure 3.4.). The length of the induction periods observed under all concentrations tested show that the iron complex is rather less effective than the zinc analogue, in spite of the fact that the FeDRP molecule has three ligands compared to only two in the case of ZnDRP. Burn[33,34] has studied the effect of metal dialkyldithiophosphates (MDRP) on AZBN catalysed oxidation of cumene at 60°C. It was shown that at low concentrations[34] ZnDRP offered a better inhibition activity than FeDRP, but at a higher concentration[33] the reverse was true. (R = isopropyl in each case). The author therefore concluded[33,34] that FeDRP is a good trapping agent for peroxyl radicals.

It is clear from Figure 6.2. that FeDRP has very little inhibitory effect on the oxidation of decalin initiated by CHP at 130°C. Burn[34] found that the effectiveness of FeDRP as an antioxidant for cumene was seriously affected by the presence of hydroperoxides. This could be due to:-

(a) The inability of FeDRP to decompose hydroperoxides.

(b) The decomposition of hydroperoxides by FeDRP to give free radical species capable of chain propagation.

(c) The formation of an inactive species from the reaction of FeDRP with hydroperoxides.

The reaction of FeDRP with hydroperoxides is discussed in Section 6.3.2.

6.3.2. REACTION OF FeDRP WITH HYDROPEROXIDES

6.3.2.1. DECOMPOSITION OF CHP BY FeDRP

The iron complex behaves in a similar way to other metal dithiolates,[13,19,30] in that its decomposition of CHP takes place by more than one step. There are however some differences between FeDRP and other MRDPs. The nickel[30] and zinc dithiophosphates[13,19] are both responsible for a three step decomposition, with FeDRP there appears to be two stages. (Figure 6.3.). The relative importance of each stage is dependent on the initial FeDRP:CHP molar ratio.

The initial stage, lasting about 10 minutes and favoured by a high concentration of FeDRP, represents a free radical decomposition of CHP (Scheme 5.2., Section 5.3.1.1.), which gives acetophenone as the major product and is best seen in Figure 6.4. The large yields of acetophenone obtained with FeDRP (Figure 6.4.) are comparable to those observed when CHP was decomposed by NiDRP.[30] Under identical conditions, the use of a non-transition metal dithiophosphate, ZnDRP, is shown in Section 5.3.1.1. to lead to yields of acetophenone of only 10%.

The observed colour change from green to orange during the first stage of the FeDRP/hydroperoxide reaction shows that all the iron complex is destroyed in this time. Although it has not been possible to positively identify the orange/brown precipitate which is formed, the available evidence suggests that it is a form of iron (III) oxide. The colour and yield of the precipitate show that it cannot be a sulphate or sulphide of iron, leaving iron (III) oxide as the only possibility. (Table 6.4.).

Iron compound (Fe_nX_m)	Colour	% yield*
FeO	black	10.6
Fe_2O_3	brown	11.5
FeS	grey	12.7
Fe_2S_3	black	15.0
$FeSO_4$	pale green	21.9
$Fe_2(SO_4)_3$	pale pink	28.8
precipitate from FeDiPP/TBH reaction	orange/brown	8.4

* Theoretical yield of Fe_nX_m obtained if the iron present in the FeDiPP is, on complete destruction of the original iron complex by TBH, all now contained as Fe_nX_m.

Table 6.4. Comparison of precipitate formed in FeDiPP/TBH reaction, with inorganic iron compounds

No α-cumyl alcohol is detected when CHP is decomposed by FeDRP. (Figures 6.4., 6.5. and 6.6.). The possibility that this is due to the instantaneous oxidation of any α-cumyl alcohol initially formed to acetophenone, by the iron complex may be rejected, because of the lack of any reaction between FeDRP and α-cumyl alcohol in chlorobenzene

at 110°C. Thus the acetophenone must arise from the reaction of cumyloxyl radicals formed by the homolytic decomposition of CHP. (reaction 45).

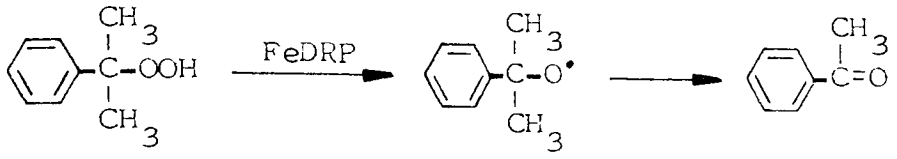

(45)

The free radical nature of the first stage decomposition of CHP by FeDRP (Figures 6.4., 6.5. and 6.6.), explains why the iron complex is unable to prevent the oxidation of decalin in the presence of CHP. (Figure 6.2.). At the CHP:FeDRP ratios of < 5:1 used in the oxidation studies, virtually all of the CHP would be decomposed via free radical processes.

The second step of CHP decomposition by FeDRP (Figure 6.3.) is ionic (Scheme 5.4., Section 5.3.1.1.), as evidenced by a high yield of phenol, (Figures 6.5 and 6.6), especially at low concentrations of iron complex. (CHP:FeDRP $\geqslant$ 20:1) Holdsworth and co-workers[12] found a high yield of phenol when CHP was decomposed by FeDRP at 25°C. (CHP:FeDRP = 100:1). This ionic stage is caused by the decomposition products of the FeDRP, because the dark green colouration characteristic of the original iron complex has

disappeared by the end of the first stage of CHP decomposition. Several phosphorus containing products have been found to be formed during the first stage of the reaction between FeDRP and TBH, (Figure 6.14., TBH:FeDRP = 5:1), and are discussed further in Section 6.3.2.2. Both acetophenone and phenol are formed to some extent at each FeDRP concentration used (see Figure 6.7.), showing that both free radical and ionic CHP decomposition pathways occur at all CHP:FeDRP ratios.

Despite the peculiarities discussed above, the way in which FeDRP decomposes CHP follows a similar pattern to that established for other metal dithiolates, especially ZnDRP[13,19] and NiDRP.[30] An initial reaction leads to the decomposition of some of the CHP via a homolytic mechanism, and the simultaneous breakdown of the metal complex to products which can then be further oxidised to species capable of decomposing the remaining CHP by a heterolytic ionic mechanism. The lack of an observable induction period (Figure 6.3.) between the two stages of CHP decomposition by FeDRP, suggests that the formation of the catalyst(s) for ionic CHP decomposition is very rapid. (Section 6.3.2.2.).

6.3.2.2. DECOMPOSITION OF FeDRP BY TBH

When an excess of TBH is present the FeDRP is decomposed very quickly (Figures 6.8a., 6.8b. and 6.10.), proving that only the initial stages of CHP decomposition by FeDRP (Figure 6.3., discussed in Section 6.3.2.1.) can be attributed to the original iron complex. A TBH:FeDRP ratio of 4:1 is sufficient to provide this excess.

It is when there is an excess of FeDRP that the behaviour observed is most interesting. (Figures 6.9a., 6.9b., 6.9c. and 6.10.). By measuring the loss of FeDRP in the presence of TBH (Figure 6.10., Table 6.5.), it is found that each mole of TBH can decompose 0.5-0.7 moles of FeDRP at 25°C when FeDRP is present in excess. The subsequent increase of the absorbance of the 596nm band (Figure 6.10.) can only be due to a regeneration of the FeDRP. From Figure 6.10 it is found that 6-8% of the initial FeDRP concentration is regenerated at 25°C, this represents 11-21% of the amount decomposed. At 50°C in dodecane the rates of decomposition and regeneration of the FeDRP were higher. (Figure 6.12., Table 6.2.) 18-24% of the amount of FeDRP decomposed was regenerated.

$[TBH]_0$	$[TBH]_{min}$	$\triangle[TBH]$	$[FeDiPP]_0$	$[FeDiPP]_{min}$	$\triangle[FeDiPP]$	$\frac{\triangle[FeDiPP]}{\triangle[TBH]}$
$1x10^{-4}$	0	$1x10^{-4}$	$2.5x10^{-4}$	$1.8x10^{-4}$	$7x10^{-5}$	0.7
$2.5x10^{-4}$	0	$2.5x10^{-4}$	$2.5x10^{-4}$	$1.2x10^{-4}$	$1.3x10^{-4}$	0.5

$[TBH]_0$ = initial concentration of TBH

$[TBH]_{min}$ = final concentration of TBH = 0

$[FeDiPP]_0$ = initial concentration of FeDiPP

$[FeDiPP]_{min}$ = minimum concentration of FeDiPP reached during reaction. (see Figure 6.10).

All concentrations in $moldm^{-3}$

Table 6.5. Decomposition of FeDiPP by TBH in cyclohexane at 25°C

Reaction of the decomposition products of FeDRP back to the iron complex must be occurring from the time that the system is free of hydroperoxide, i.e. when the minimum concentration of FeDRP is reached. (Figure 6.10.). Fe_2O_3 has been isolated as a product of the complete decomposition of FeDRP by TBH (Section 6.2.2.1.), and it is likely that this is reacting with one or more of the decomposition products formed as a result of the reaction of TBH and FeDRP. Unfortuantely these products could not be identified by ^{31}P NMR whilst some of the original iron complex (having 5 unpaired electrons) remained undecomposed, because the technique is not possible when highly paramagnetic species are present. (Section 2.2.5.). Instead, the FeDRP was completely decomposed by adding a slight excess of TBH. Subsequent removal by filtration of the precipitate of Fe_2O_3 formed allowed the measurement of the ^{31}P NMR spectrum.

A number of phosphorus containing species are formed when FeDRP reacts with TBH. (Figure 6.14., Table 6.3.). This is similar to the case when ZnDRP is decomposed by CHP. (Section 5.2.3.2., Tables 5.4. and 5.5.). If it is assumed that the products of the partial decomposition of FeDRP are the same as those of the complete decomposition, then only three of the products, i.e. the monosulphide, the

triester [$(RO)_2P(S)SR$], or the disulphide, (DRDS), could be capable of reforming the iron complex. No reaction occurs between DRDS and Fe_2O_3 (Section 6.2.3.4.), and it would also seem unlikely that any would occur with the neutral triester or monosulphide.

Thus the earlier assumption that the products of the partial decomposition of FeDRP by TBH are the same as those of the complete decomposition does not appear to be valid. It is possible that the dialkyldithiophosphoric acid (DRDPA) could be formed in a system where hydroperoxides are deficient. The reaction between DRDPA and Fe_2O_3 does give the iron complex, FeDRPA. (Section 6.2.3.4.). DRDPA cannot however exist in systems where excess hydroperoxide is present, and is rapidly oxidised to DRDS. (Section 5.3.3.5.). This would explain why no regeneration of FeDRP occurs at TBH:FeDRP ratios greater than 1:1. (Figures 6.8a., 6.8b. and 6.10.). The range of sulphur containing products formed by the action of TBH on FeDRP (Table 6.3.) explains the width of the band which builds up in the 200-300nm region of the UV-VIS spectrum. (Figures 6.8. and 6.9.).

The phosphorus containing products observed in Figure 6.14. (TBH:FeDRP = 5:1) are those which

are formed during the initial homolytic reaction of FeDRP and hydroperoxides. (Section 6.3.2.1.). Further reaction of these products to give powerful hydroperoxide decomposing antioxidants must occur, in order to explain the ionic decomposition of CHP that is observed during the later stages of the above reaction. (Figures 6.3.-6.6.). Although it has not been possible in this work to identify the products formed when FeDRP is oxidised by a much greater excess of hydroperoxide (TBH:FeDRP $\geq$ 50:1). it is likely that sulphur acids such as SO_2, SO_3 and H_2SO_4 are being formed from the further oxidation of the initial decomposition products of FeDRP. DRDS and DRODS, which are both formed in the initial stages of the FeDRP/TBH reaction (Figure 6.14., Table 6.3.), are shown in Sections 5.3.3.4. and 5.3.3.5.) to be oxidised to sulphur acids by excess hydroperoxide.

The reaction of FeDRP with hydroperoxides is summarised in Scheme 6.2.

6.3.3. FeDRP AS A PRODUCT OF THE REACTION OF DITHIOPHOSPHATES AND IRON COMPOUNDS

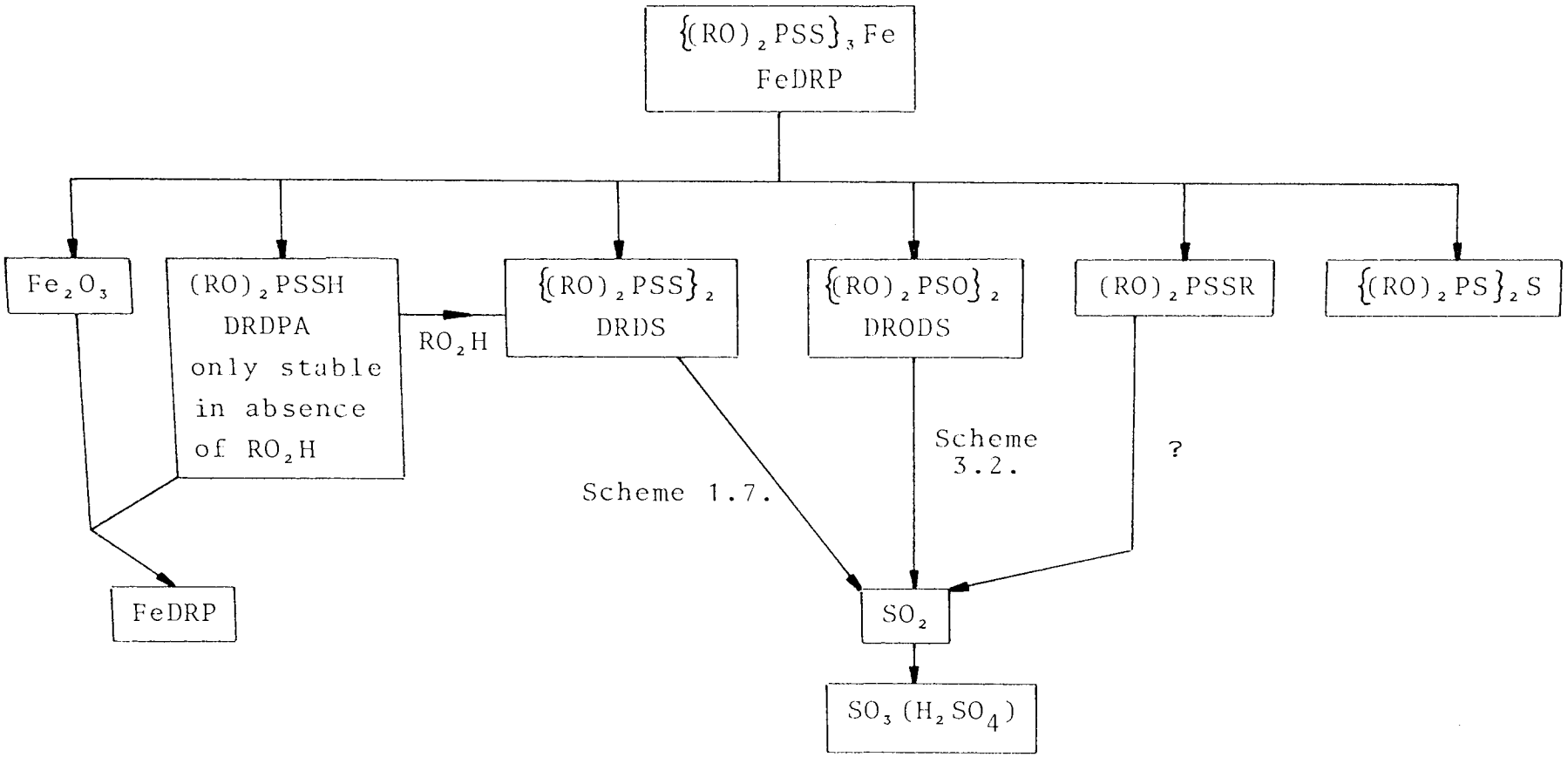

Scheme 6.2. Reaction of FeDRP with hydroperoxides

6.3.3.1. REACTION OF DITHIOPHOSPHATES WITH IRON (II) CHLORIDE, ($FeCl_3$)

All three dithiophosphates studied, i.e. ZnDRP, DRDS and DRDPA, react readily with $FeCl_3$ to give FeDRP. This would suggest that the replacement of zinc by iron is easier under acidic conditions than in the neutral media studied in Sections 6.3.3.2.-6.3.3.4. The extraction of Fe^{3+} ions from acidic aqueous solutions by DRDPA has been reported[78] to form FeDRP.

6.3.3.2. REACTION OF DITHIOPHOSPHATES WITH IRON (III) STEARATE. (FeST)

The formation of FeDRP, characterised by the appearance of a dark green colouration, has been observed during the studies of DRDPA in the presence of FeST. (see Section 4.2.1.3.). The formation of the iron complex from the reaction of DRDPA and FeST is predictable, as a strong acid such as DRDPA would be expected to liberate the weaker stearic acid from its salt (FeST), according to reaction (41).

$$3(RO)_2PSSH + (C_{17}H_{35}COO)_3Fe \rightarrow \{(RO)_2PSS\}_3Fe + 3C_{17}H_{35}COOH \quad (41)$$

The zinc-iron exchange reaction that occurs in acidic media (Section 6.3.3.1.), does not occur

readily between ZnDRP and FeST under neutral conditions. (Section 6.2.3.1.). It is not clear whether the small amounts of FeDRP formed are from a direct interaction between the two species, or whether it is necessary for the ZnDRP to undergo decomposition (possibly to DRDPA?) before a reaction can occur. The neutral thiophosphoryl ligand (in the form of DRDS) does not react at all with FeST. (Section 6.2.3.1.).

Thus the order of reactivity of the dithiophosphates towards FeST decreases in the order:-

DRDPA >> ZnDRP > DRDS

6.3.3.3. REACTION OF DITHIOPHOSPHATES WITH IRON METAL (Fe).

The reaction of DRDPA with Fe metal to give FeDRP (Section 6.2.3.3.) is typical of the action of a strong acid on a metal. (reaction 46).

$$6(RO)_2PSSH + 2Fe \longrightarrow 2\{(RO)_2PSS\}_3Fe + 3H_2 \qquad (46)$$

The inability of either ZnDRP or DRDS to produce FeDRP from their reaction with Fe (Section 6.2.3.3.), is further evidence that the iron complex is not readily formed under neutral conditions.

Previous work on the reaction of ZnDRP with Fe powder is contradictory. Homan and co-workers[41,42] observed the formation of FeDRP from the reaction of ZnDRP with iron metal, whilst Bovington and Dacre[79] found DRDPA to be the main product, along with a little DRDS. The existence of DRDPA in a system containing an excess of Fe powder is very surprising, in view of the ease with which reaction (46) takes place. Georges and co-workers[43] have also speculated that FeDRP is formed as a result of the reaction of ZnDRP with a steel surface.

6.3.3.4. REACTION OF DITHIOPHOSPHATES WITH IRON (III) OXIDE (Fe_2O_3)

The rate of reaction of Fe_2O_3 with DRDPA (reaction 33) seems to be dependent on the origin of the Fe_2O_3. (Compare Figures 6.15. and 6.16.). The commercial material is dark red and somewhat coescent, whereas the product obtained form the reaction of FeDRP with TBH, (Section 6.2.2.1.) is a finely divided orange powder. The greater reactivity of the latter may be due to its larger surface area.

$$Fe_2O_3 + 6(RO)_2PSSH \longrightarrow 2\{(RO)_2PSS\}_3Fe + 3H_2O \qquad (33)$$

Neither type of Fe_2O_3 reacts with ZnDRP or DRDS. (Section 6.2.3.4.). It is therefore clear that the regeneration of FeDRP observed in Section 6.2.2.2. cannot be due to a reaction between DRDS and Fe_2O_3. (reaction 47).

$$Fe_2O_3 + \{(RO)_2PSS\}_2 \longrightarrow \{(RO)_2PSS\}_3Fe \qquad (47)$$

6.4. SUMMARY OF CHAPTER SIX

FeDRP is a reasonably good inhibitor of the oxidation of decalin at 130°C in the absence of added hydroperoxides (Figure 6.1.), but is totally ineffective when excess CHP is present. (Figure 6.2.). Two steps are observed when CHP is decomposed by FeDRP at 110°C. (Figure 6.3.). An initial homolytic destruction of CHP is followed by an ionic decomposition stage. The first stage predominates when a high concentration of FeDRP is present (Figure 6.4.), and the formation of free radicals during this process must be responsible for the inability of the iron complex to act as an inhibitor in the presence of CHP. (Figure 6.2.). During the initial stage, the FeDRP is rapidly oxidised and a brown precipitate, thought to be iron (III) oxide, separates out. DRDS has been identified as the major phosphorus containing product formed at this time.

The second stage assumes greatest importance when a low concentration of FeDRP is used. The ionic decomposition of CHP, shown to be occurring in this step (Figure 6.6.), must be caused by sulphur acids formed by the rapid oxidation of the first stage products.

The oxidation of FeDRP by TBH is very rapid even at 25°C, complete destruction of the iron complex being readily achieved when the TBH:FeDRP molar ratio exceeds 4:1. When the FeDRP is in excess, however, the decomposition of the iron complex is only partially achieved and is followed by the regeneration of some of the FeDRP. This is probably due to the reaction of iron (III) oxide and DRDPA formed as a result of the initial oxidation of the iron complex, and can only occur under conditions where no hydroperoxide is present.

The reaction of ZnDRP or DRDS with iron compounds occurs readily under acidic conditions to give FeDRP, but very little or no iron complex is formed from ZnDRP or DRDS by reaction with FeST, iron metal or iron (III) oxide in a neutral medium. DRDPA reacts readily with the above iron compounds to give FeDRP.

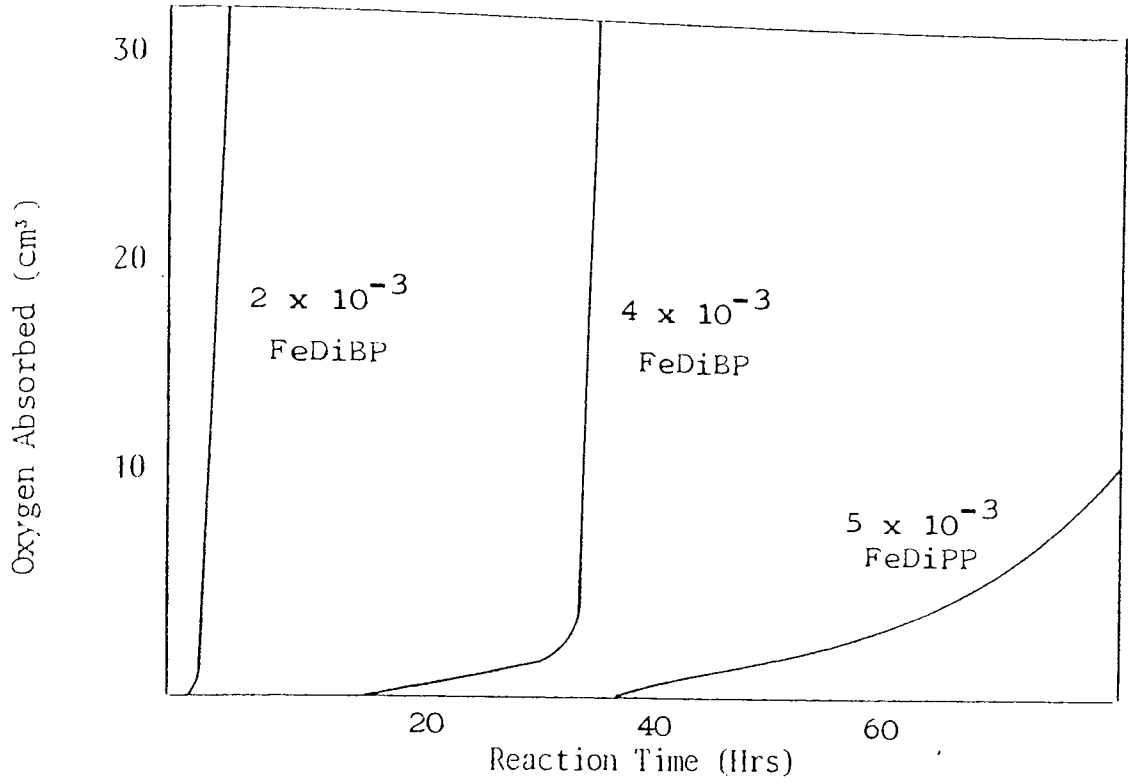

Figure 6.1. Effect of FeDRP on Oxidation of Decalin at 130°C. Numbers on Curves are Concentrations of FeDRP in moldm^{-3}.

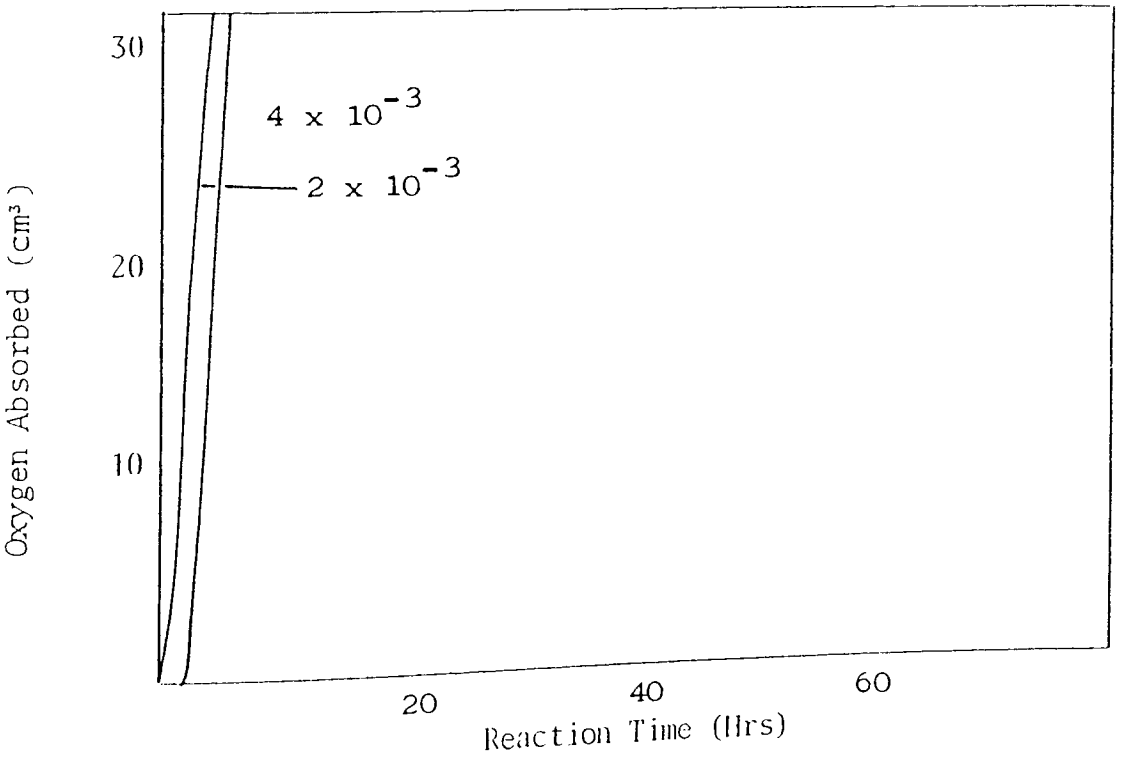

Figure 6.2. Effect of FeDiBP on the Oxidation of Decalin at 130°C in the Presence of 1 x 10^{-2}moldm^{-3} CHP. Numbers on Curves are Concentrations of FeDiBP in moldm^{-3}.

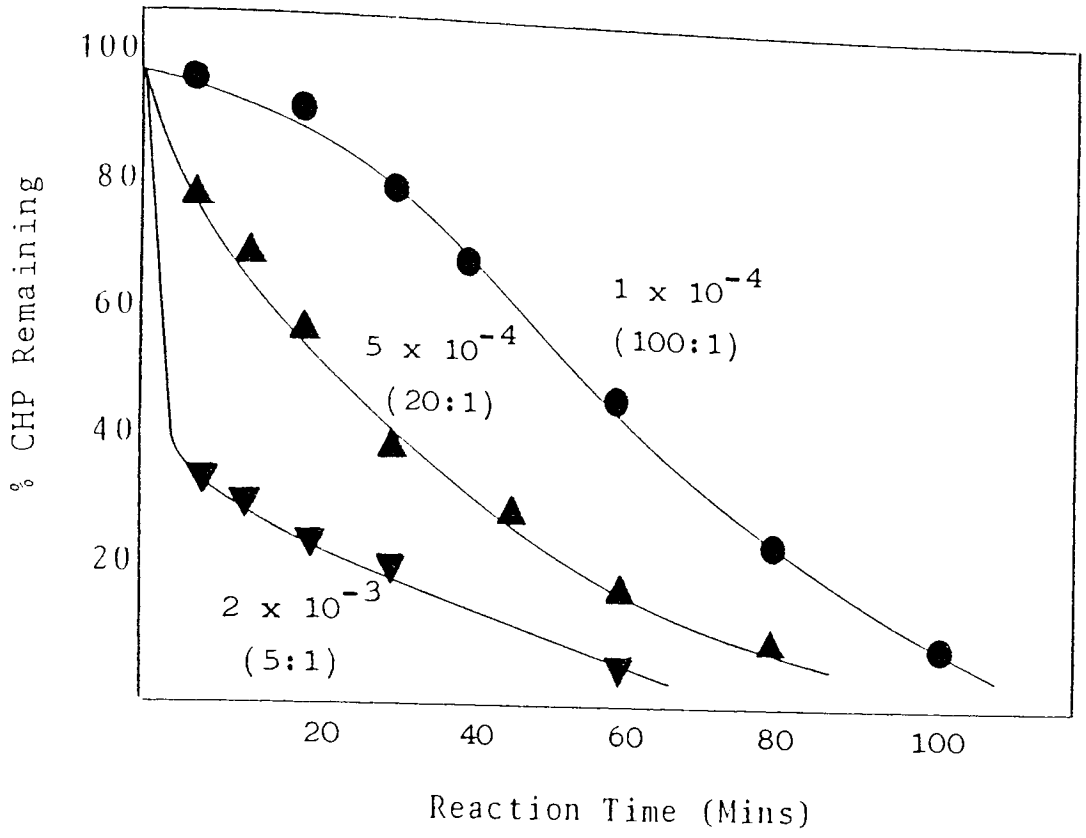

Figure 6.3. Decomposition of 1 x 10^{-2}moldm^{-3} CHP by FeDiPP at 110°C. Numbers on Curves are Concentrations of FeDiPP in moldm^{-3}.

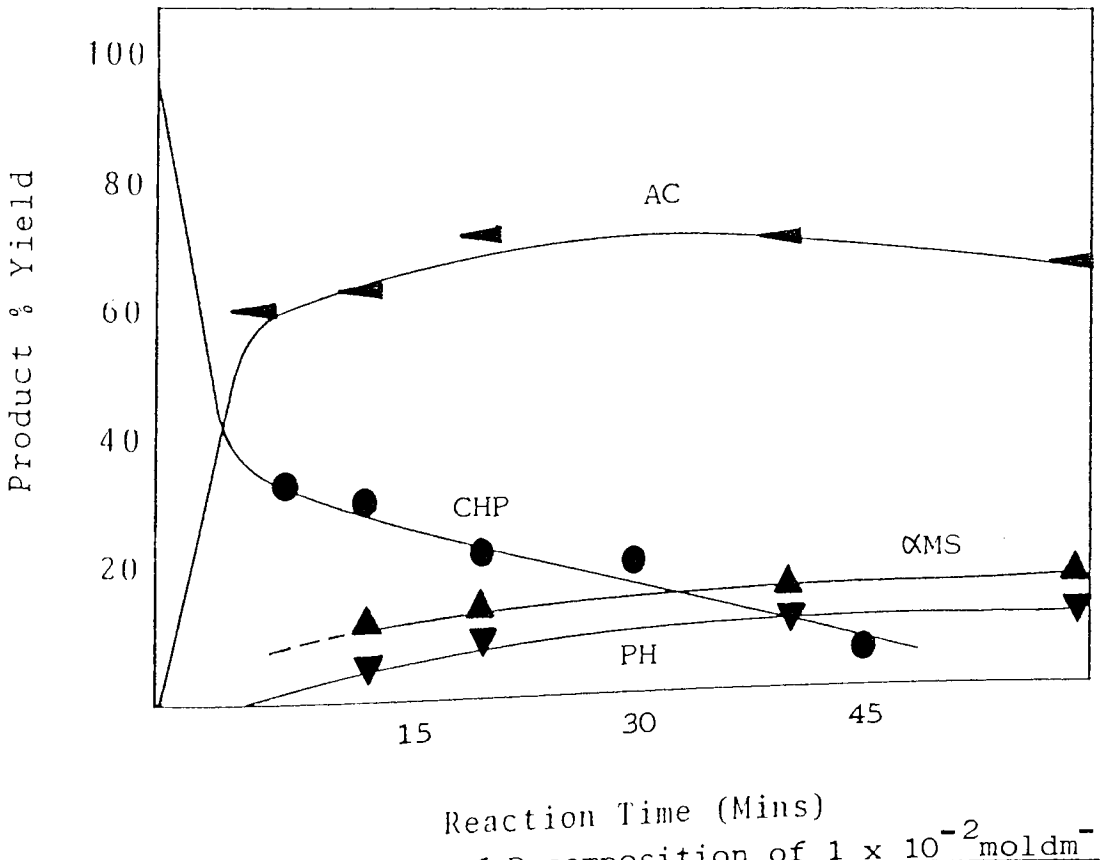

Figure 6.4. Products of Decomposition of 1 x 10^{-2}moldm^{-3} CHP by 2 x 10^{-3}moldm^{-3} FeDiPP at 110°C. (CHP:FeDiPP = 5:1)

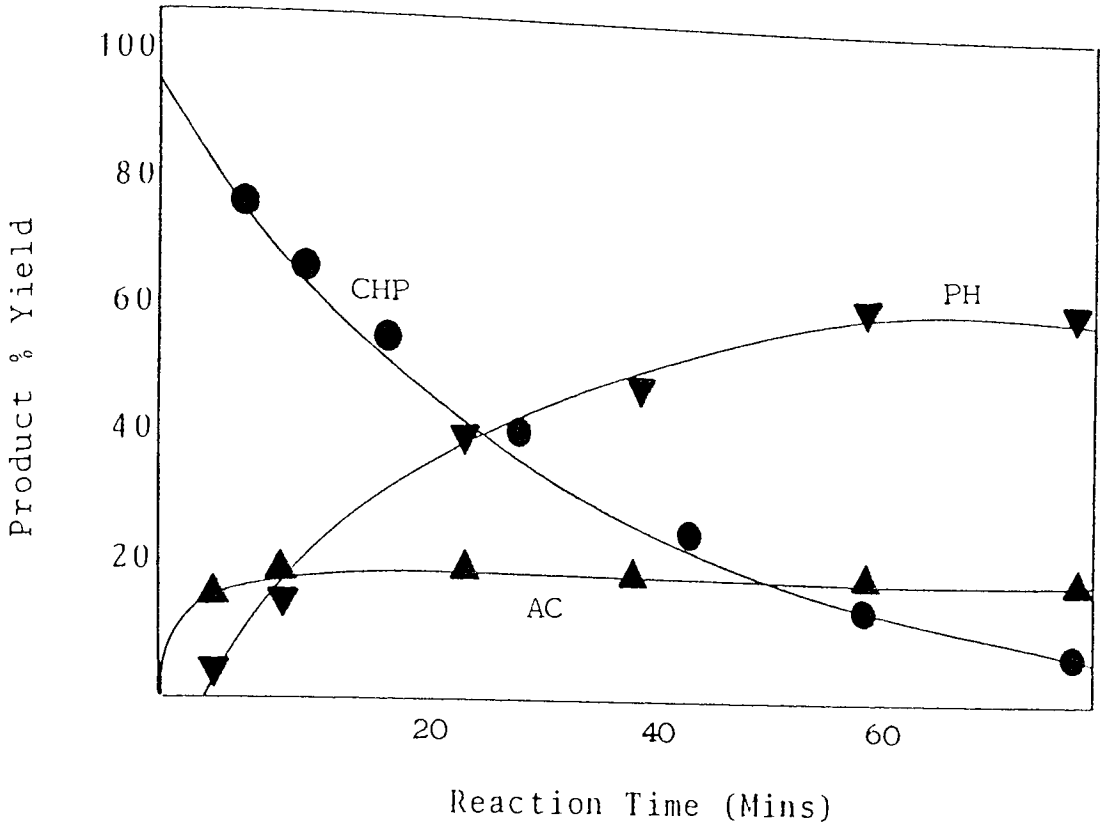

Figure 6.5. Products of Decomposition of 1 x 10^{-2}moldm^{-3} CHP by 5 x 10^{-4}moldm^{-3} FeDiPP at 110°C. (CHP:FeDiPP = 20:1)

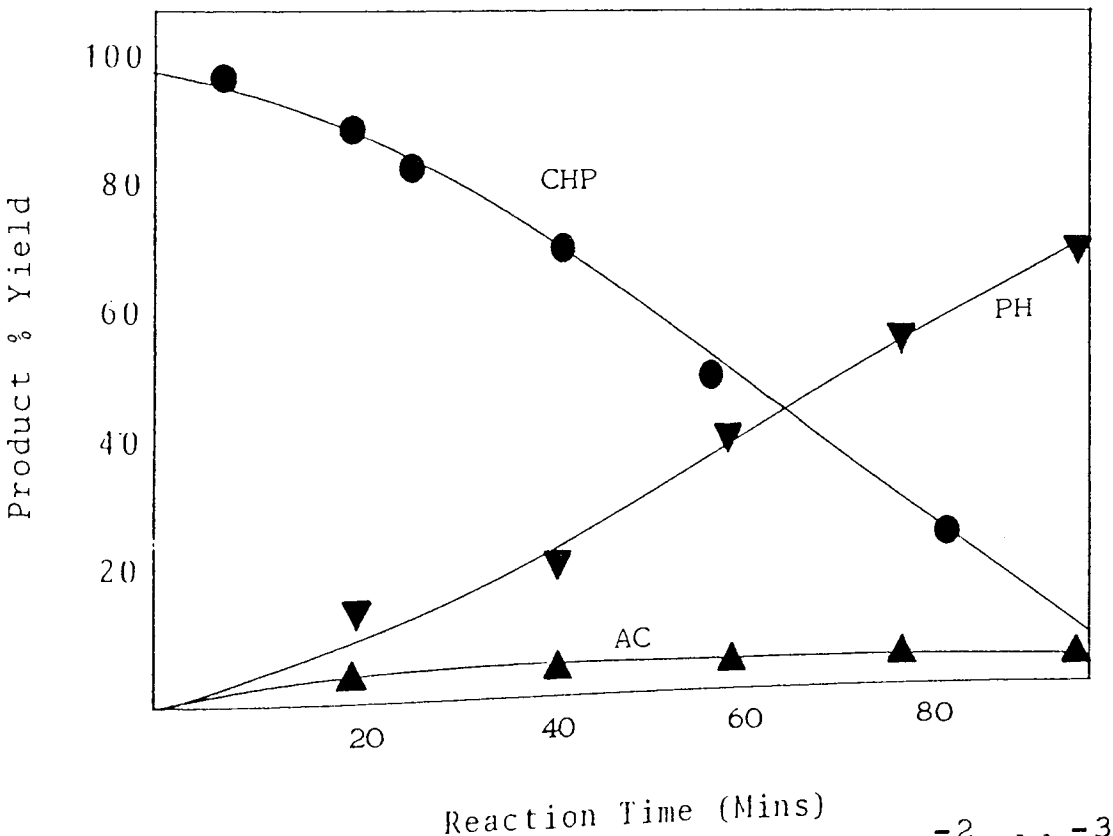

Figure 6.6. Products of Decomposition of 1 x 10^{-2}moldm^{-3} CHP at 110°C by 1 x 10^{-4}moldm^{-3} FeDiPP.(CHP:FeDiPP = 100:1)

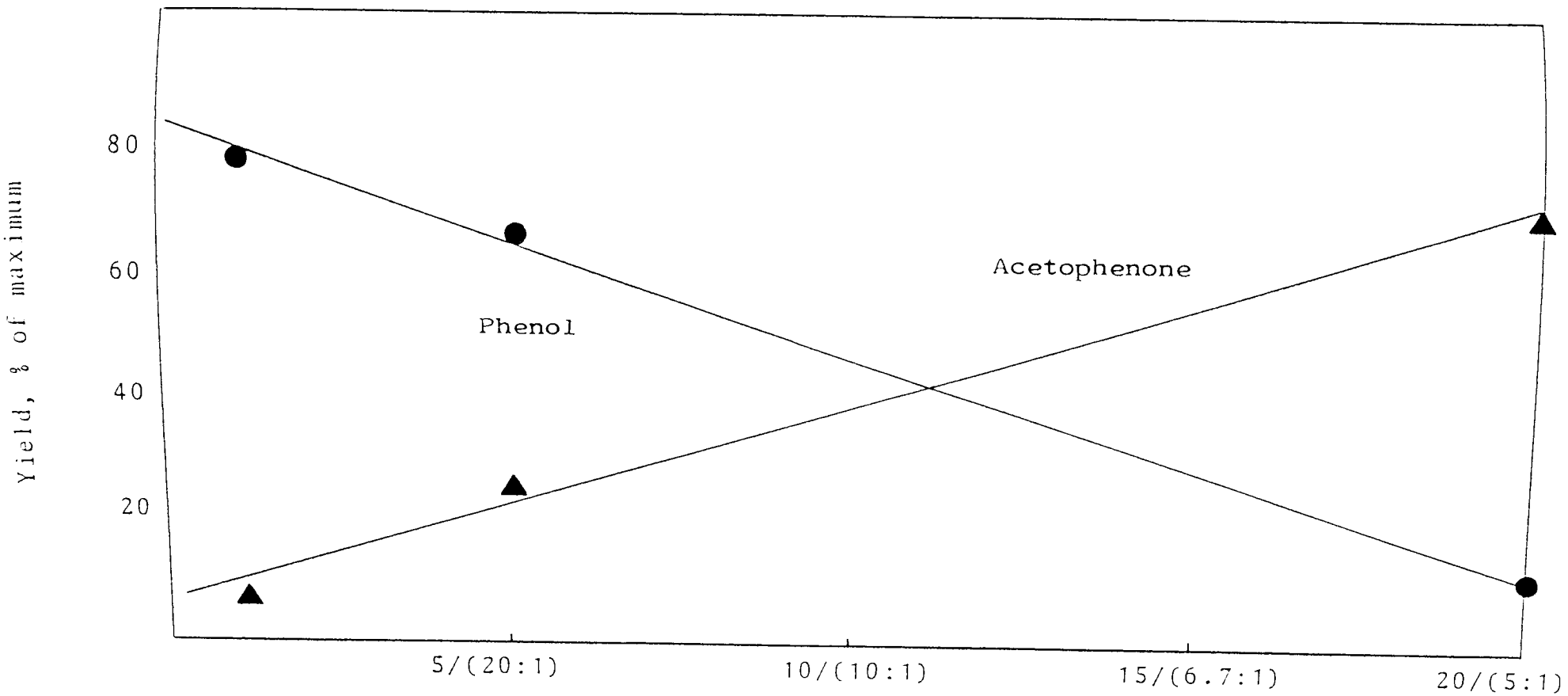

Figure 6.7. Variation in Products Formed at 110°C as a Result of the Complete Decomposition of CHP by FeDiPP, with Initial CHP:FeDiPP Ratio.

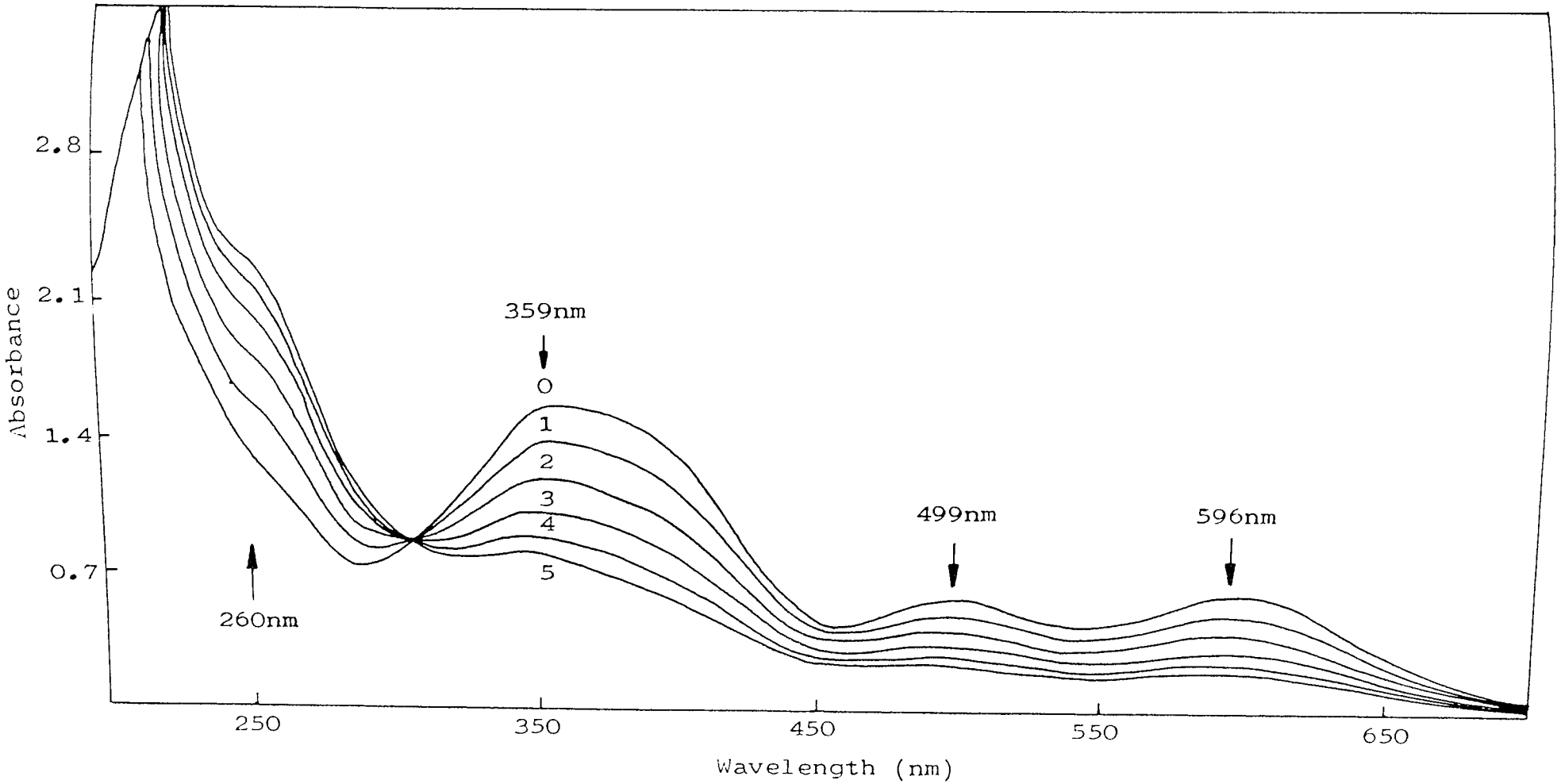

Figure 6.8a. Initial Changes in the UV-VIS Spectrum of 2.5×10^{-4} moldm^{-3} FeDiPP when Decomposed by 5×10^{-3} moldm^{-3} TBH in cyclohexane at 25°C. (TBH:FeDiPP = 20:1) Numbers on Curves are Reaction Times in Minutes, Arrows show the Direction of Change in Absorbance.

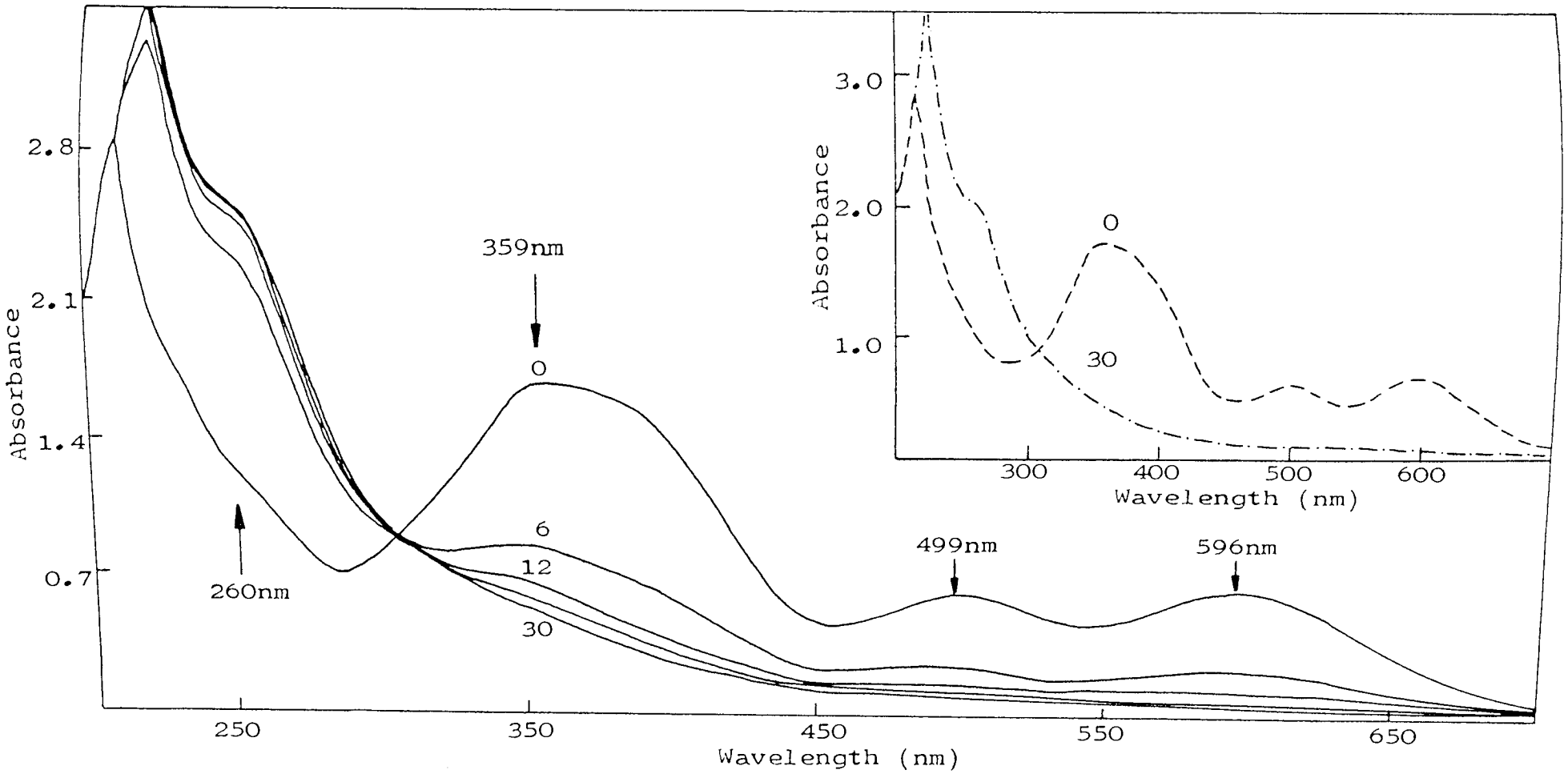

Figure 6.8b. Changes in the UV-VIS Spectrum of 2.5×10^{-4}moldm^{-3} FeDiPP at Prolonged Reaction Times when Decomposed by 5×10^{-3}moldm^{-3} TBH in cyclohexane at 25°C. Numbers on Curves are Reaction Times, Arrows show the Direction of Change in Absorbance.

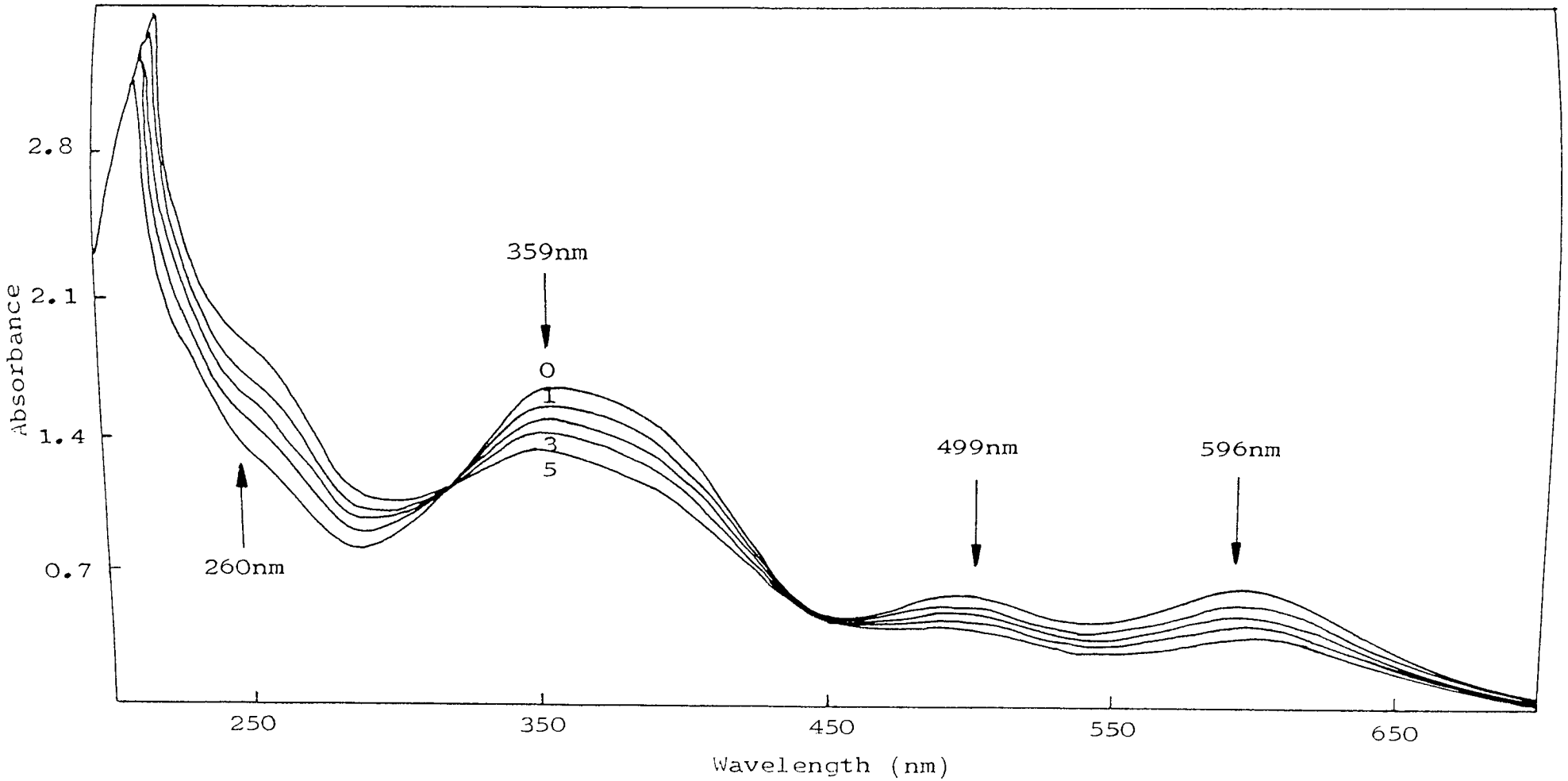

Figure 6.9a. Initial Changes in the UV-VIS Spectrum of 2.5×10^{-4}moldm^{-3} FeDiPP when Decomposed by 2.5×10^{-4}moldm^{-3} TBH in cyclohexane at 25°C. (TBH:FeDiPP = 1:1) Numbers on Curves are Reaction Times in Minutes, Arrows show the Direction of Change in Absorbance.

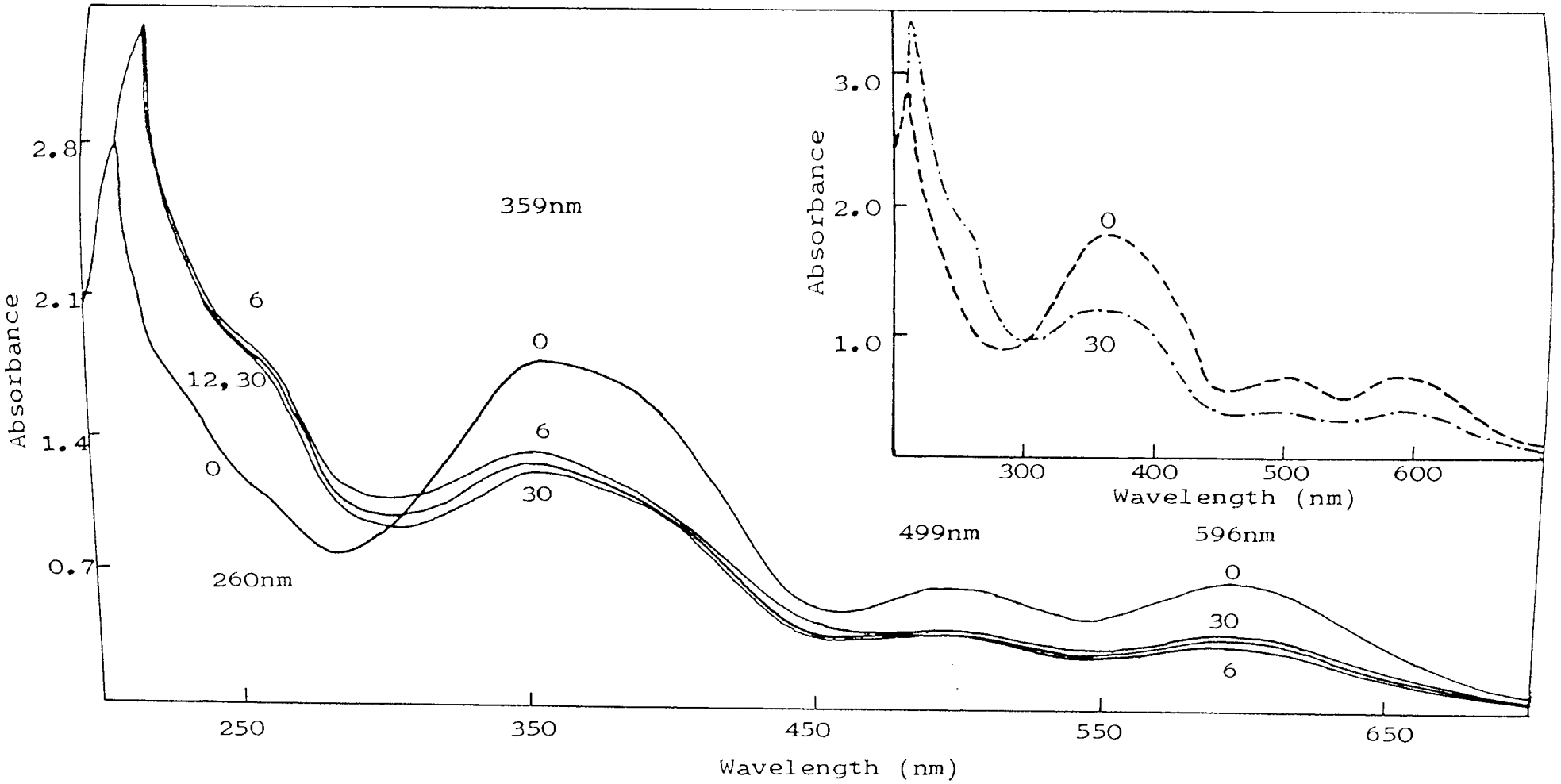

Figure 6.9b. Changes in the UV-VIS Spectrum of 2.5×10^{-4} moldm^{-3} FeDiPP at Prolonged Reaction Times when Decomposed by 2.5×10^{-4} moldm^{-3} TBH in Cyclohexane at 25°C. (TBH:FeDiPP = 1:1) Numbers on Curves are Reaction Times in Minutes.

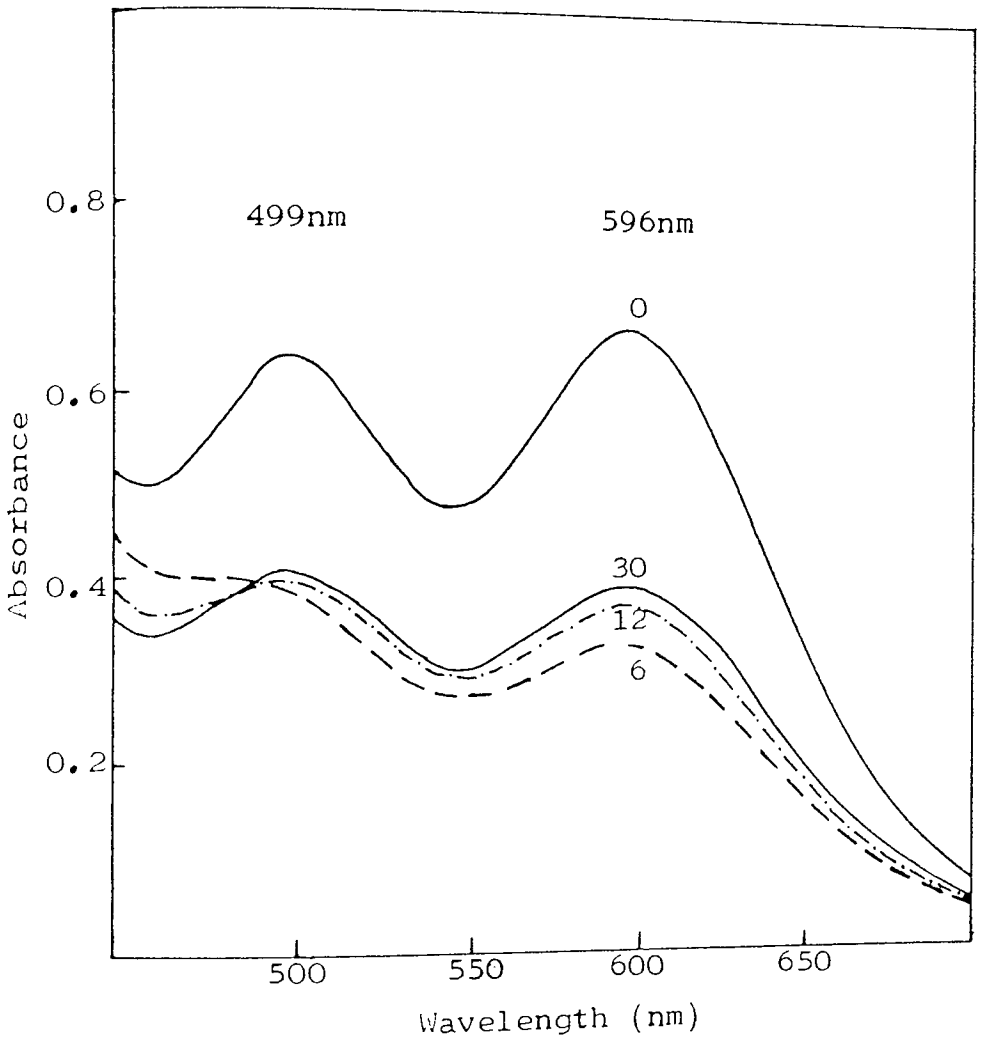

Figure 6.9c. Enlargement of Figure 6.9b. in the Region 450 - 700nm. Numbers on Curves are Reaction Times in Minutes.

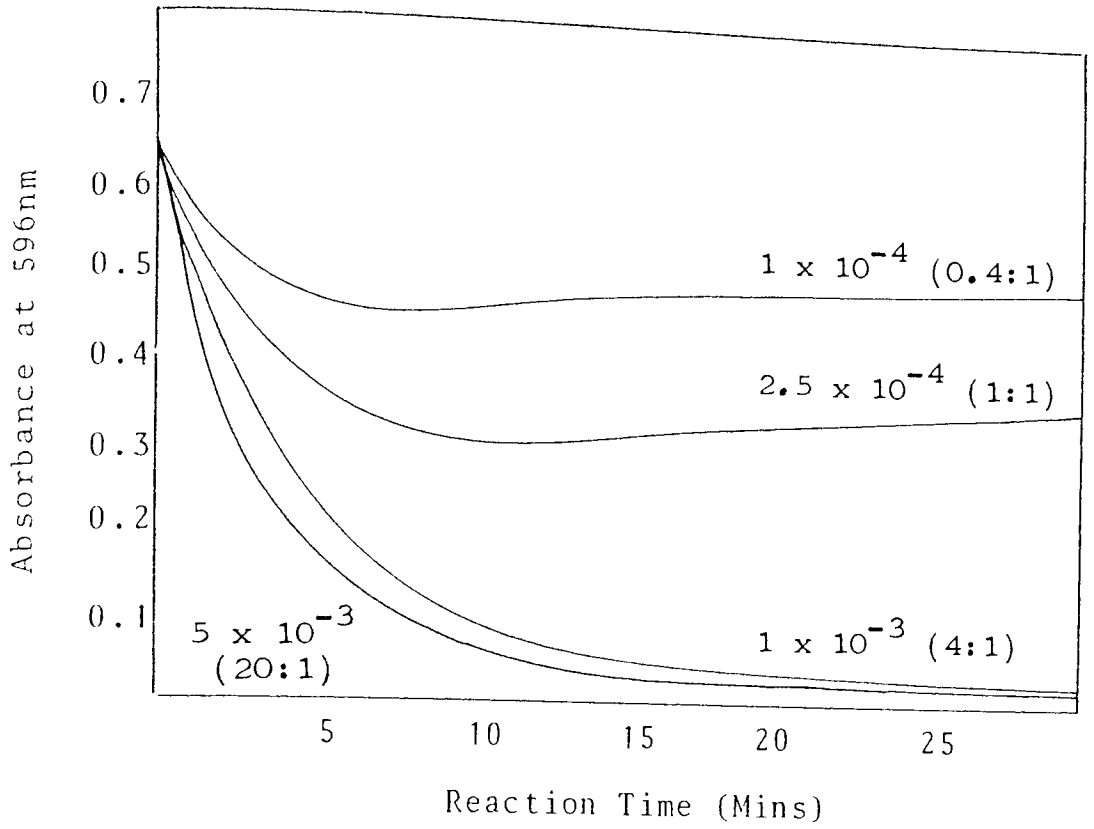

Figure 6.10. Decomposition of 2.5×10^{-4} moldm^{-3} FeDiPP by TBH in Cyclohexane at 25°C. Numbers on Curves are Concentrations of TBH in moldm^{-3}.

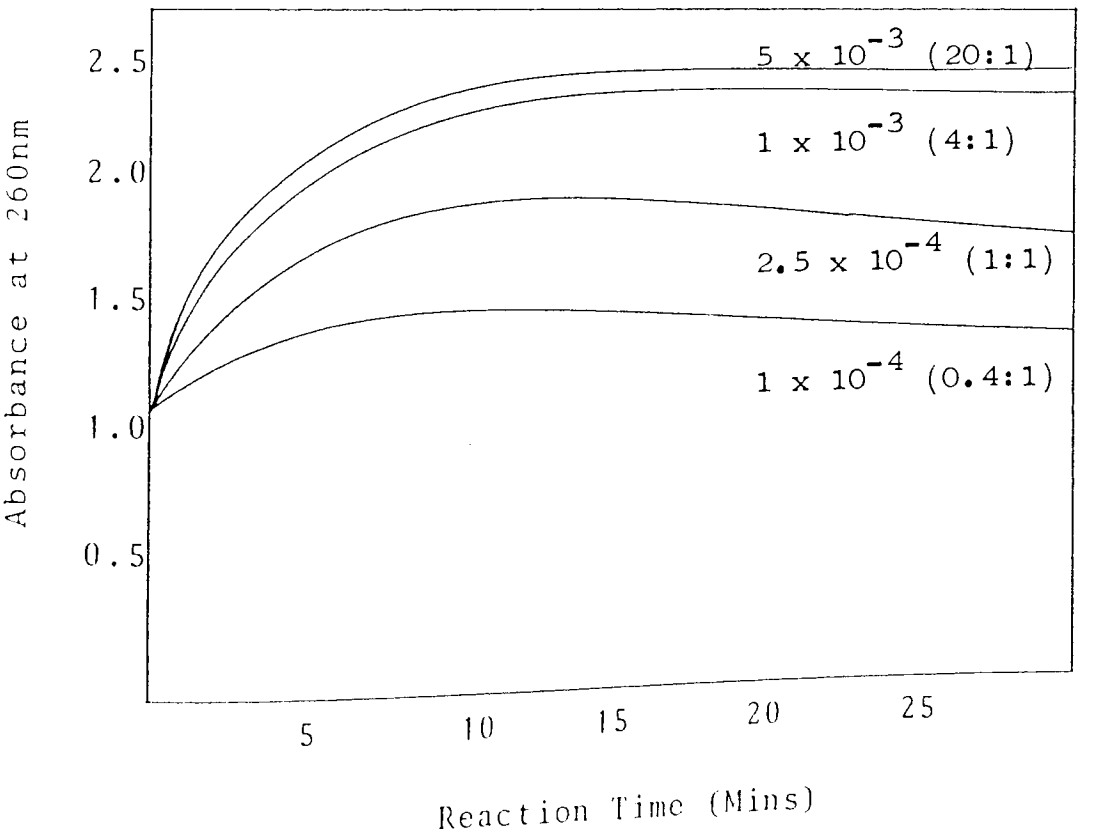

Figure 6.11. Build-up of Products of Reaction between 2.5×10^{-4} moldm^{-3} FeDiPP and TBH in Cyclohexane at 25°C. Numbers on Curves are Concentrations of TBH in moldm^{-3}.

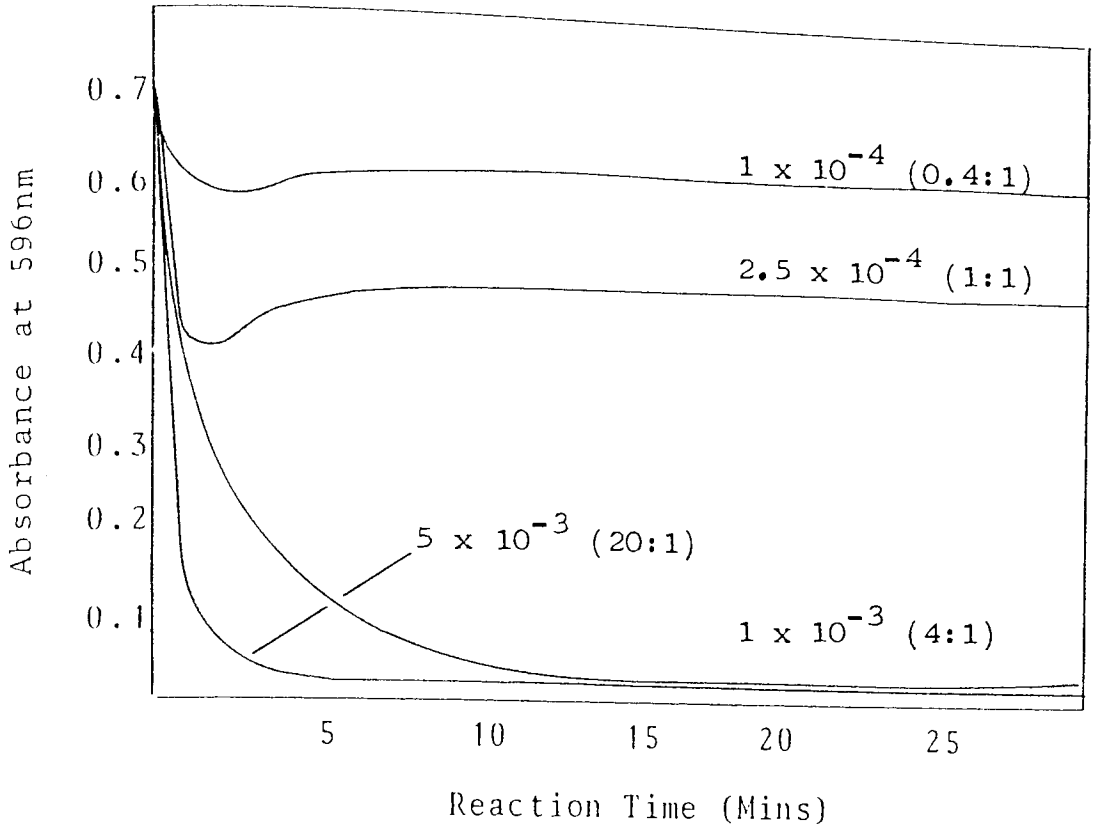

Figure 6.12. Decomposition of 2.5×10^{-4} moldm^{-3} FeDiPP by TBH in Dodecane at 50°C. Numbers on Curves are Concentrations of TBH in moldm^{-3}.

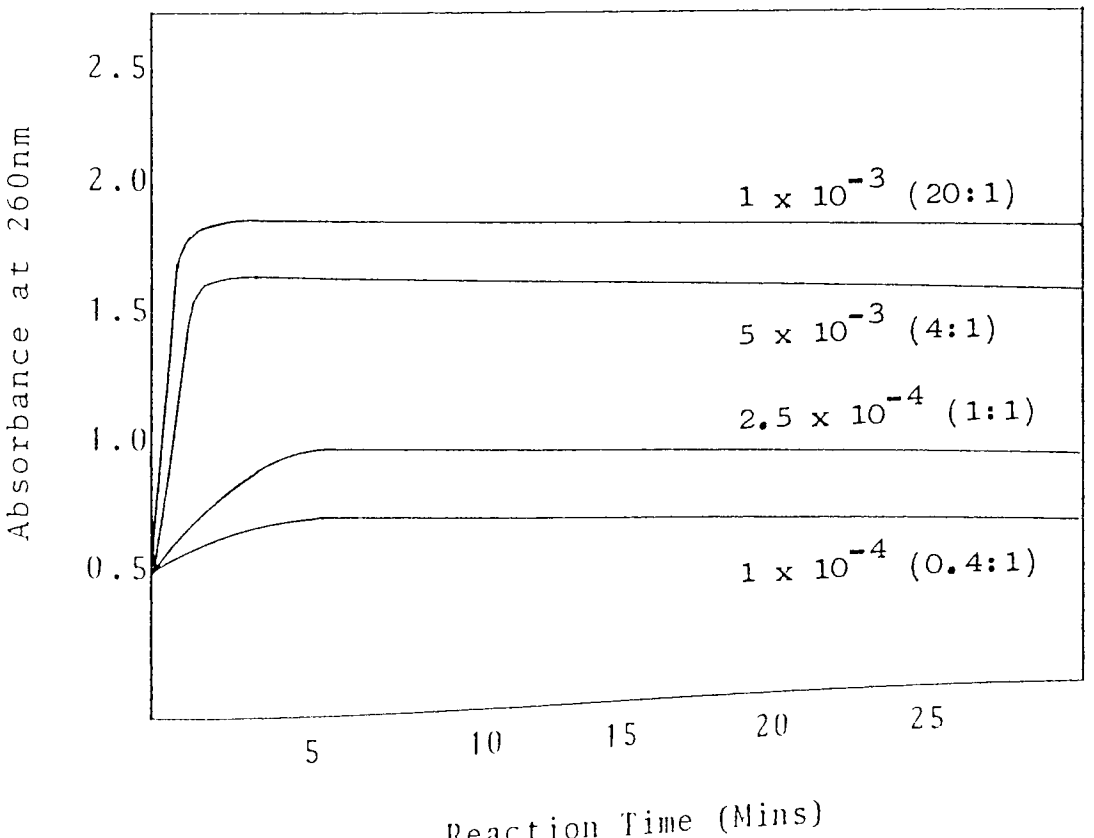

Figure 6.13. Build-up of Products of Reaction between 2.5×10^{-4} moldm^{-3} FeDiPP and TBH in Dodecane at 50°C. Numbers on Curves are Concentrations of TBH in moldm^{-3}.

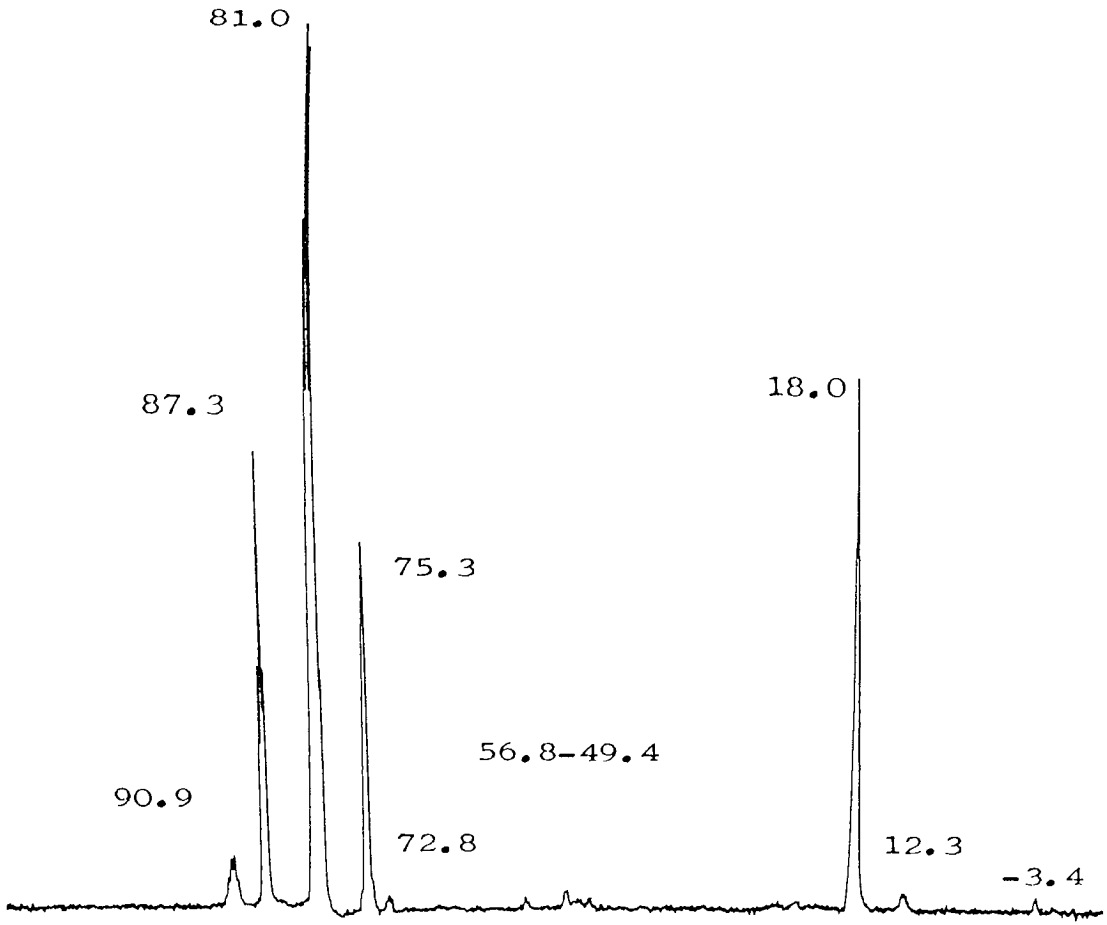

Figure 6.14. ^{31}P NMR Spectrum Showing Products of Reaction of FeDiPP with TBH at 25°C.

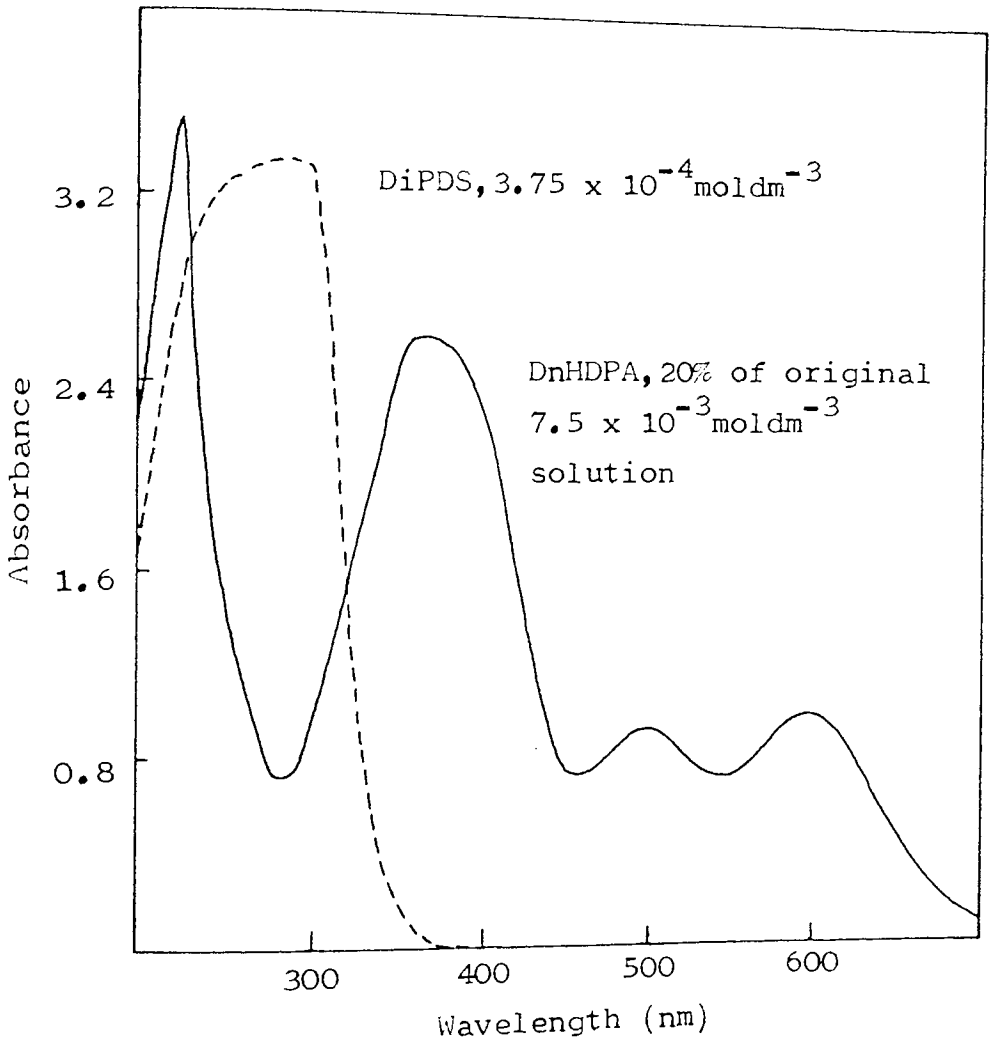

Figure 6.16. Products of Reaction of Iron (III) Oxide (isolated from reaction of FeDiPP and TBH) and Thiophosphoryl Compounds in Cyclohexane at 25°C. "Concentration" of Iron (III) Oxide = 5 x 10^{-2}moldm^{-3}.

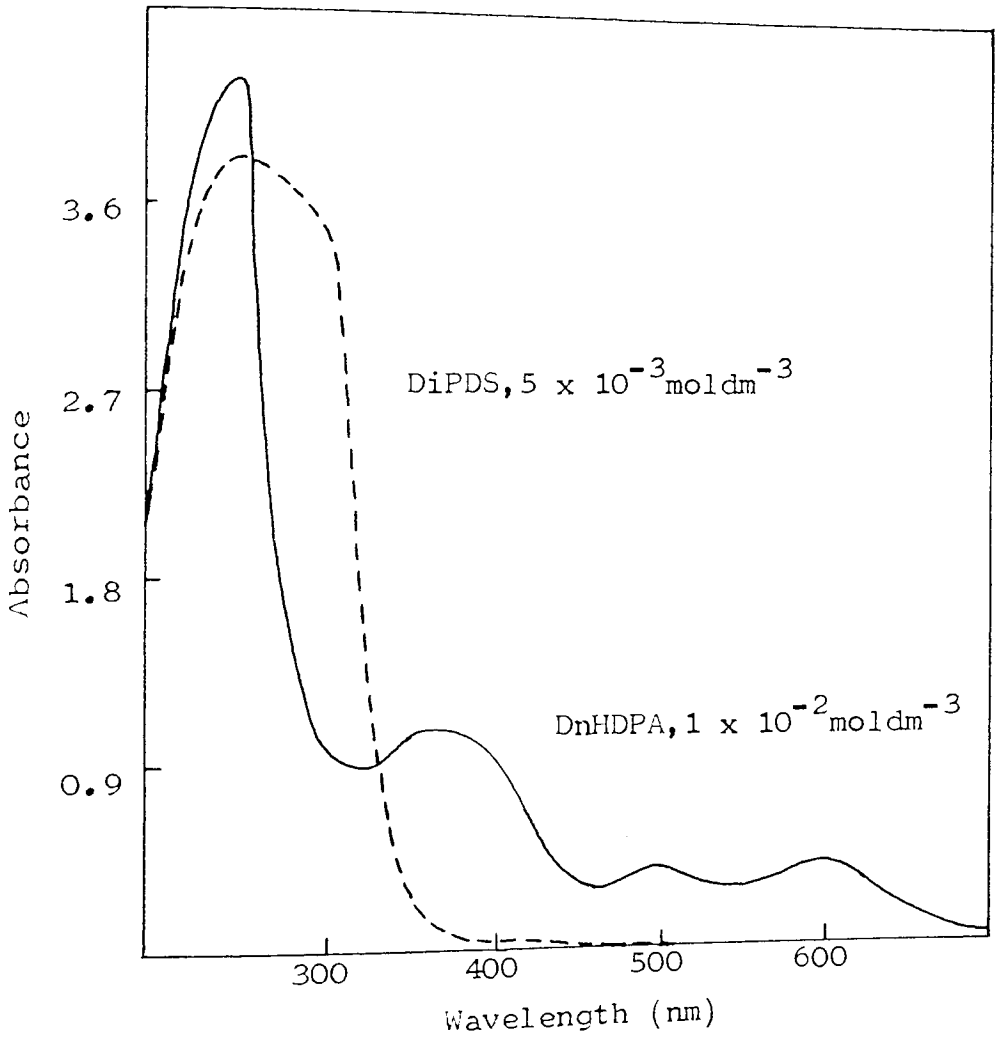

Figure 6.15. Products of Reaction of Iron (III) Oxide (ex BDH) and Thiophosphoryl Compounds in Cyclohexane at 25°C. "Concentration of Iron (III) Oxide = 5 x 10^{-2} moldm^{-3}.

CHAPTER SEVEN

CONCLUSIONS AND SUGGESTIONS FOR FURTHER WORK

7.1. CONCLUSIONS

1. Each of the additives studied (ZnDRP, b-ZnDRP, DRDS, DRDPA and DRTPA) provides effective stabilisation against the thermal oxidation of hydrocarbons at 130°C in the absence of added hydroperoxides. The existence of induction periods prior to oxidation when the above inhibitors are used indicates that they are themselves capable of acting as antioxidants under relatively mild conditions. This is especially so for the two types of zinc complex, both of which give particularly long induction periods.

   The slow auto-retarding inhibition provided by each of the above additives when present in high concentrations shows that the products formed during the induction periods also have antioxidant activity. When low additive concentrations are used, however, the amount of these oxidation products formed may be too low for any inhibition to be achieved after the end of the induction period.

2. The antioxidant activity of the above additives is severely affected by the initial presence of added hydroperoxides. ZnDRP is rapidly oxidised by CHP to give b-ZnDRP and DRDS. At the same time the hydroperoxide is decomposed to free radicals, which are responsible for the pro-oxidant effects observed in oxidisable substrates.

Oxidation of the b-ZnDRP results in the formation of DRODS. The formation of sulphur acids, notably sulphuric acid, from the further oxidation of the DRDS and DRODS formed during the initial stages, is responsible for the very effective auto-retardation observed in the later stages of hydrocarbon oxidation in the presence of both ZnDRP and CHP. The inhibition observed during this time is due to the ionic decomposition of hydroperoxide to products that cannot propagate the oxidative chain reaction.

The initial inactivity of DRDS as an inhibitor of hydrocarbon oxidation in the presence of CHP is due to two factors. Low concentrations of DRDS are unable to decompose the hydroperoxide

until the disulphide has been oxidised through to sulphur acids, and although a high concentration of DRDS is itself able to decompose CHP this initially occurs via a free radical mechanism leading to a pro-oxidant effect in an oxidisable substrate. The formation of sulphur acids from DRDS during the later stages of oxidation is evident from the slow auto-retarding uptake of oxygen observed.

The oxidation of DRDPA by hydroperoxide, in addition to giving DRDS, also results in the formation of sulphur acids, which are responsible for the extremely effective inhibition of hydrocarbon oxidation achieved by the dithiophosphoric acid in the presence of added CHP. The generation of sulphur containing acids from DRDPA must occur extremely readily in order to explain the rapid decomposition of CHP achieved even in the presence of a very low DRDPA concentration, and occurs without the initial homolytic reaction (s) which take place during their formation from DRDS.

The mechanism of hydroperoxide decomposition by DRTPA parallels that described above for DRDPA. Sulphur containing acids are generated

both during the initial DRTPA/hydroperoxide interaction, and by the further oxidation of DRODS which is formed in the early stages of the reaction. The final phosphorus containing product formed by the oxidation of thio- or dithio-phosphates by hydroperoxides is DRPA.

3. The presence of $2x10^{-4}moldm^{-3}$ FeST has a severe effect on the antioxidant activity of each of the inhibitors studied, (ZnDRP, b-ZnDRP, DRDS, DRDPA and DRTPA), especially at low concentrations in the absence of added hydroperoxide. Auto-retardation is only observed after a high degree of oxidation has taken place; this is particularly so for DRDPA and DRTPA. The reaction of DRDPA with FeST leads to the formation of FeDRP, similarly FeDRT is formed from DRTPA. FeST does not react with DRDS and only very slowly with ZnDRP.

The initial presence of added CHP leads to an improvement in the effectiveness of each of the above compounds as inhibitors of FeST catalysed oxidation. FeST has the greatest effect on the reaction of ZnDRP with CHP when a low concentration of the zinc complex is present. Although a rapid, ionic decomposition of CHP is achieved under these conditions

in an inert medium, no stabilisation is given in an oxidisable system because of the very low concentration of antioxidant present. At concentrations of ZnDRP where effective inhibition of hydrocarbon oxidation is observed, the mechanism of hydroperoxide decomposition is very similar to that occurring in the absence of FeST, i.e. an initial, fast, free radical reaction followed by a slower ionic step. The slow auto-retarding uptake of oxygen observed during the oxidation of hydrocarbon substrates is further evidence that sulphur containing acids are still being formed from the ZnDRP/CHP interaction, despite the presence of FeST.

The partial removal of these species by reaction with the FeST is apparent from the effect of FeST on the rate of the fast, ionic stage of CHP decomposition promoted by DRDS. The disulphide is not itself able to inhibit iron catalysed oxidation until it has been oxidised to sulphur acids, but when present in a sufficiently high concentration does retain its ability to decompose hydroperoxides homolytically even in the presence of FeST.

In the presence of CHP, DRDPA and DRTPA still react with FeST to form the corresponding iron complexes, FeDRP and FeDRT, but these are rapidly oxidised by the hydroperoxide. The direct oxidation of the remainder of the DRDPA and DRTPA to sulphur acids is still occurring and results in effective exhibition The ability of DRDPA to decompose hydroperoxides ionically is not significantly affected by the presence of FeST, although that of DRTPA is somewhat reduced at low concentrations, probably because the FeDRT formed by the reaction of DRTPA and FeST is less active as a hydroperoxide decomposer than the parent acid.

4. The direct reaction of ZnDRP and FeST to give FeDRP occurs very slowly in the absence of hydroperoxide, and not at all in the presence of added CHP owing to the rapid oxidation of the zinc complex by the CHP. Although it is possible that DRDPA may be formed from the ZnDRP/CHP reaction and that this could then react with FeST to form FeDRP, it is not possible to demonstrate the formation of either acid or the iron complex, due to their rapid reaction with hydroperoxides.

The decomposition of CHP by FeDRP is similar to that promoted by ZnDRP and other metal dithiophosphates, in that both homolytic and ionic mechanisms are possible, depending on the CHP:FeDRP molar ratio used. An initial homolytic reaction, which is favoured by a high FeDRP concentration, leads to the rapid destruction of the FeDRP and the formation of DRDS, DRODS and several other phosphorus containing products, along with a precipitate of iron (III) oxide. Further oxidation of the DRDS and DRODS to sulphur acids is achieved rapidly, so that ionic decomposition of the remainder of the CHP occurs without an observable induction period. DRDPA is a product of the reaction, but is not stable in the presence of hydroperoxides and is oxidised to DRDS. Under conditions where FeDRP is present in excess however, all the hydroperoxide is destroyed, allowing the DRDPA formed to regenerate some of the original iron complex by reaction with iron (III) oxide.

Although FeDRP is a reasonable inhibitor of decalin oxidation at 130°C, the free radicals generated by the FeDRP/hydroperoxide interaction result in a pro-oxidant step in the presence of added CHP.

7.2. SUGGESTIONS FOR FURTHER WORK

1. Of the two types of antioxidant behaviour known to be exhibited by zinc dialkyldithiophosphate, i.e. radical trapping and hydroperoxide decomposition, only the latter has been studied in the present work. The radical trapping ability of ZnDRP and related compounds therefore needs to be established, firstly in pure hydrocarbon substrates and then in the presence of added FeST. In this way it should be possible to discover to what extent radical scavenging by the dithiophosphates is affected by the presence of FeST. No major adjustment to the oxygen absorption technique would be required to obtain the necessary results, the source of free radicals being from the thermal decomposition of an initiator, such as AZBN, predissolved in the hydrocarbon substrate.

2. Although ^{31}P NMR studies have been very useful in establishing which phosphorus containing decomposition products may be formed from the dithiophosphates in the absence of FeST, it has not been possible to use the technique to identify the corresponding species formed when iron (III) compounds are present. With

the exception of FeDRP, which has been observed by the use of UV-VIS, any iron containing oxidation products of the dithiophosphates formed as a result of the presence of FeST will therefore have remained undetected in the present work. The use of high performance liquid chromatography (HPLC) may lead to the detection and identification of any iron containing species, if indeed they are formed.

3. The phosphoryl disulphide, DRODS, has been identified as an important intermediate species formed during the oxidation of ZnDRP by hydroperoxide. A detailed evaluation of its antioxidant activity is therefore required, similar to that carried out for the additives studied in the present work. This would entail oxygen absorption and hydroperoxide decomposition studies, along with the identification of phosphorus containing species arising from the oxidation of DRODS by CHP.

4. A limitation of the present work is the difficulty in accurately correlating results obtained from different types of experiment, owing to the necessary variations in conditions

from technique to technique. A particular problem lies in the concentration of additive used. It has been desirable to use a relatively low concentration of inhibitor for the oxygen absorption studies in order to ensure a reasonably short reaction time, i.e. no more than 3 days, but unfortunately these same concentrations of additive have proved far too low for detection by ^{31}P NMR. A technique of much greater sensitivity, probably HPLC, would be able to detect very low levels of antioxidant and derived oxidation products, so that a direct correlation between the type of oxidation occurring and the build-up or decay of particular compounds may be made with greater confidence.

APPENDIX 1

CHEMICAL STRUCTURES AND CODES OF COMPOUNDS USED

CHEMICAL NAME	CODE	STRUCTURE
Zinc Dialkyldithiophosphate	ZnDRP	$\{(RO)_2PSS\}_2Zn$
Basic Zinc Dialkyldithiophosphate	b-ZnDRP	$\{(RO)_2PSS\}_6Zn_4O$
Dialkylthiophosphoryl Disulphide	DRDS	$\{(RO)_2PSS\}_2$
Dialkyldithiophosphoric Acid	DRDPA	$(RO)_2P(S)SH$
Dialkylthiophosphoric Acid	DRTPA	$(RO)_2P(S)OH$

For each of the above the R may be replaced by another letter when a specific compound is being described.

iP	isopropyl	iB	isobutyl
sB	s-butyl	nH	n-hexyl

CHEMICAL NAME	CODE	STRUCTURE
Metal Dialkyldithiophosphate	MDRP	$\{(RO)_2PSS\}_xM$
Iron (III) Dialkyldithiophosphate	FeDRP	$\{(RO)_2PSS\}_3Fe$

CHEMICAL NAME	CODE	STRUCTURE
Copper (I) Dialkyldithio-phosphate	CuDRP	$\{(RO)_2PSS\}_4Cu_4$
Nickel Dialkyldithio-phosphate	NiDRP	$\{(RO)_2PSS\}_2Ni$
Zinc Dialkylthiophosphate	ZnDRT	$\{(RO)_2PSO\}_2Zn$
Iron (III) Dialkylthio-phosphate	FeDRT	$\{(RO)_2PSO\}_3Fe$
Dialkylphosphoric Acid	DRPA	$(RO)_2P(O)OH$
Dialkylphosphoryl Disulphide	DRODS	$\{(RO)_2P(O)S\}_2$
Zinc Dialkyldithio-carbamate	ZnDMC	$(R_2NCSS)_2Zn$
Cumene Hydroperoxide	CHP	$C_6H_5C(CH_3)_2OOH$
t-Butyl Hydroperoxide	TBH	$(CH_3)_3COOH$
Azo Bisisobutyronitrile	AZBN	$\{(CH_3)_2C(CN)N\}_2$
Iron (III) Stearate	FeST	$(C_{17}H_{35}COO)_3Fe$
α-Methyl Styrene	αMS	$C_6H_5C(CH_3)_2=CH_2$
Phenol	PH	C_6H_5OH
α-Cumyl Alcohol	αCA	$C_6H_5C(CH_3)_2OH$
Acetophenone	AC	$C_6H_5C(O)CH_3$

APPENDIX 2

SPECTROSCOPIC DATA OF COMPOUNDS

SYNTHESISED IN CHAPTER TWO

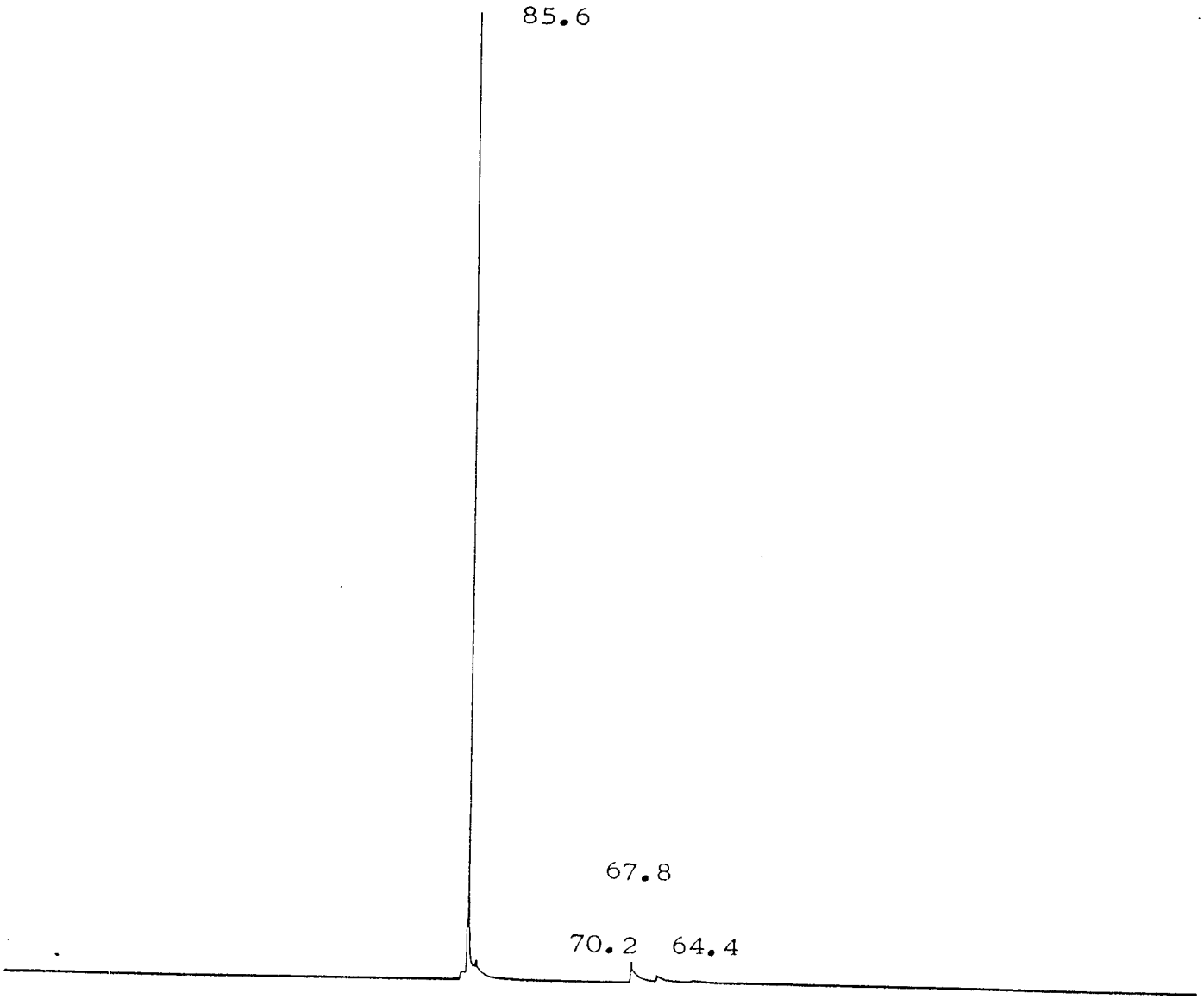

Figure A.1. ^{31}P NMR Spectrum of DiBDPA.

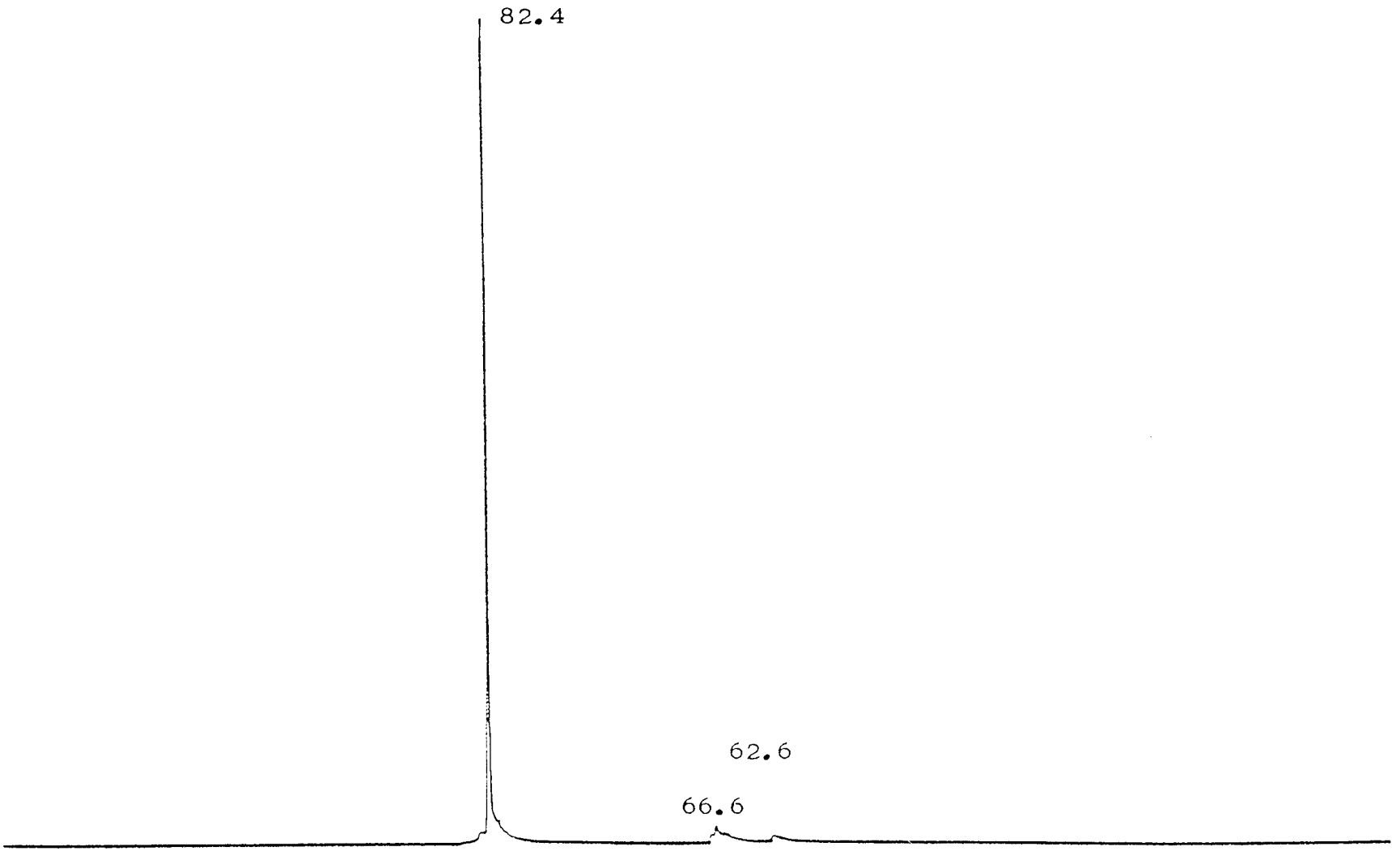

Figure A.2. ^{31}P NMR Spectrum of DsBDPA

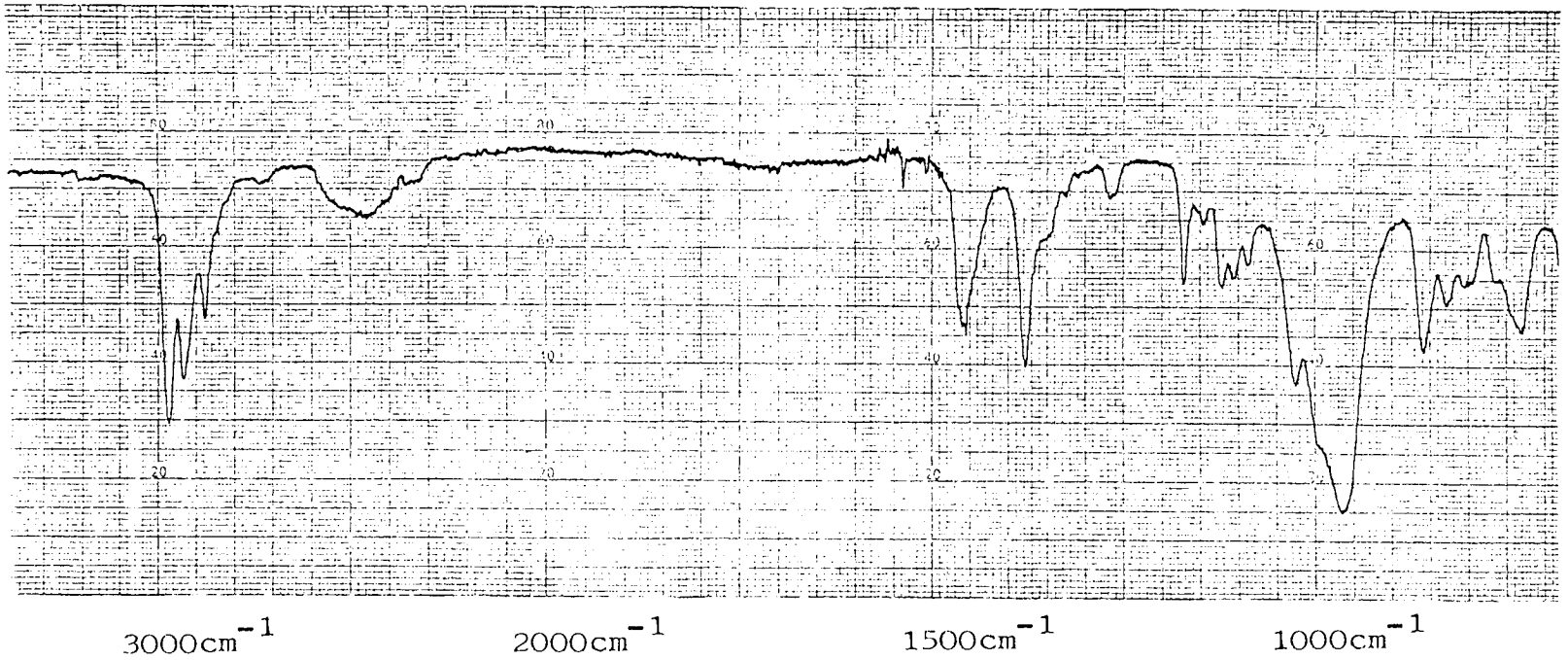

Figure A.3. IR Spectrum of DsBDPA (Liquid film).

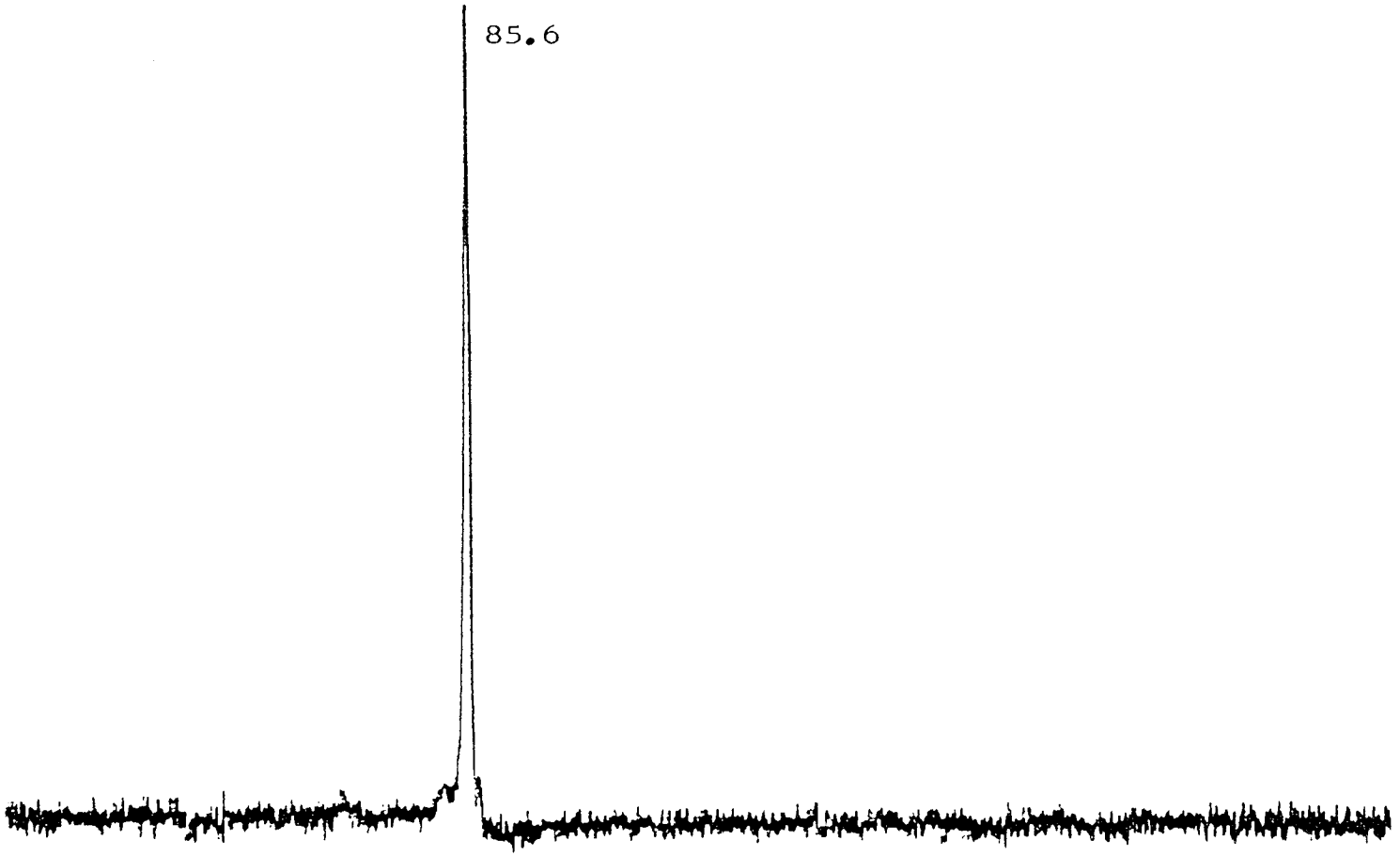

Figure A.4. ^{31}P NMR Spectrum of DnHDPA.

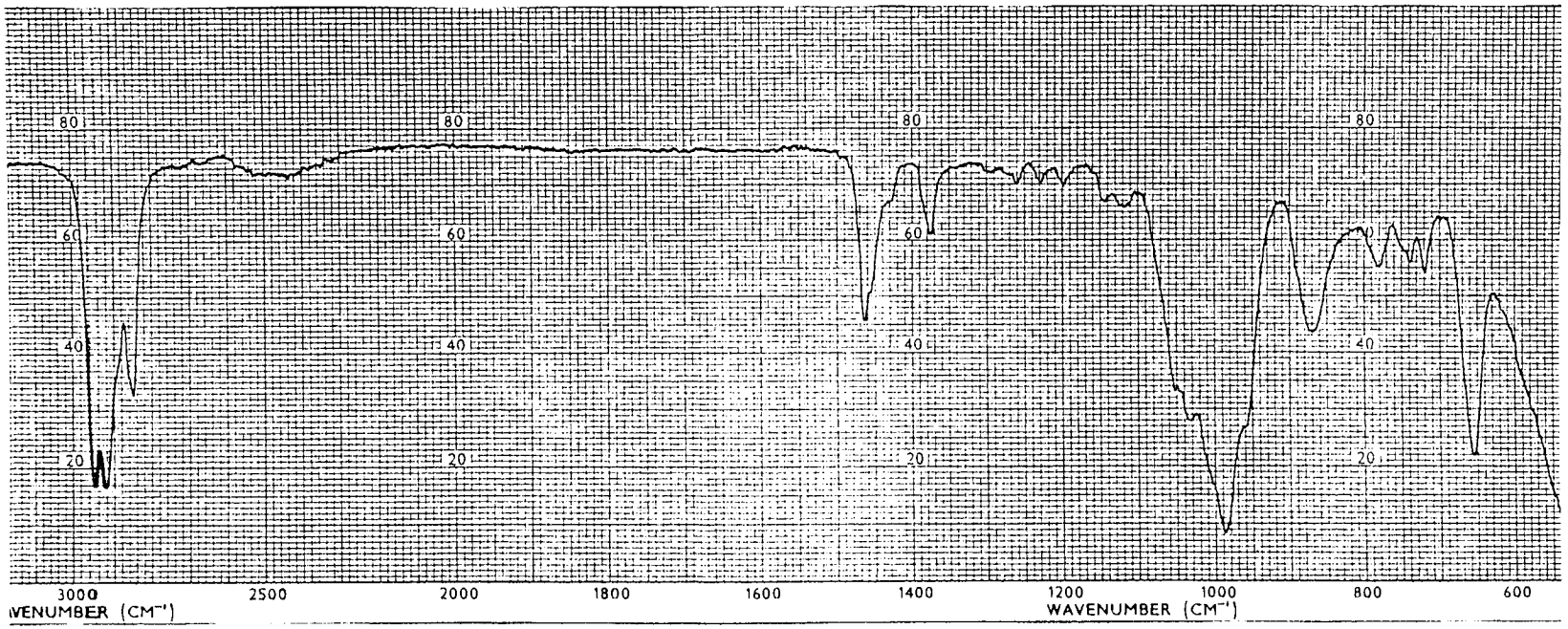

Figure A.5. IR Spectrum of DnHDPA (Liquid film).

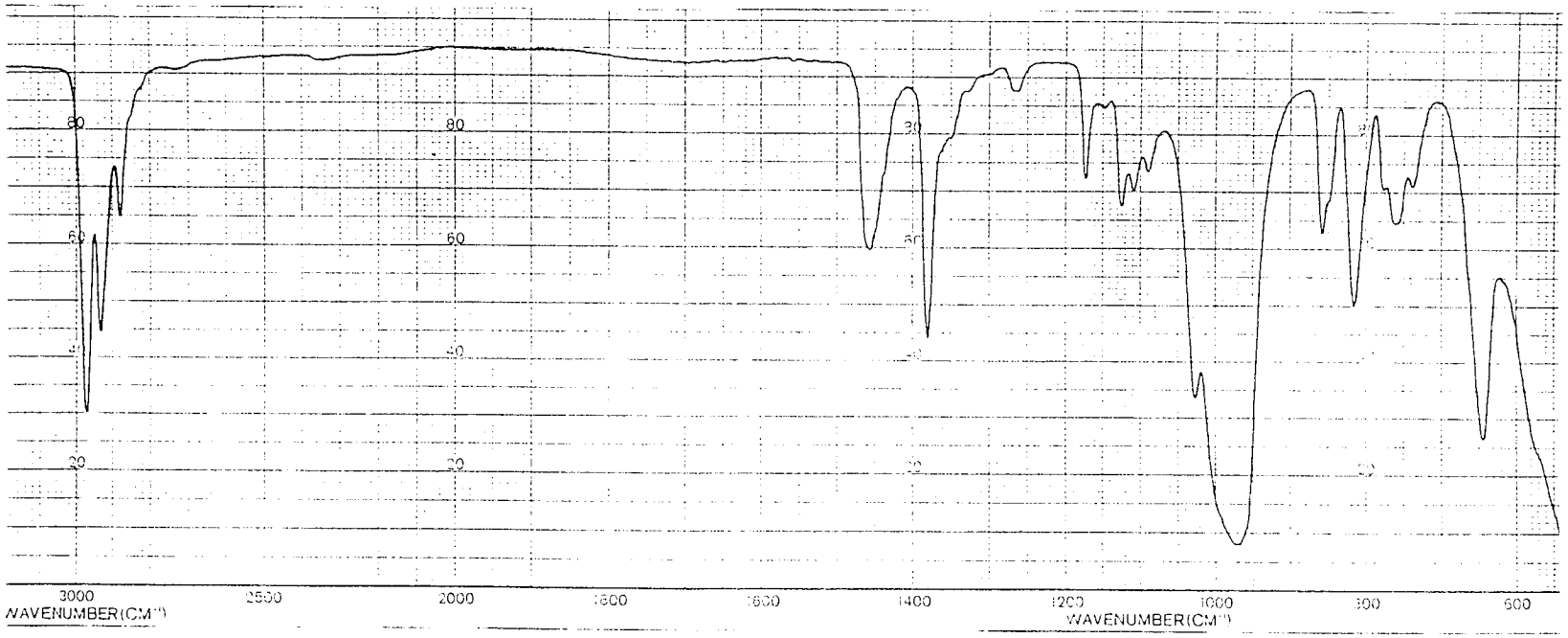

Figure A.6. IR Spectrum of DsBDS (Liquid film).

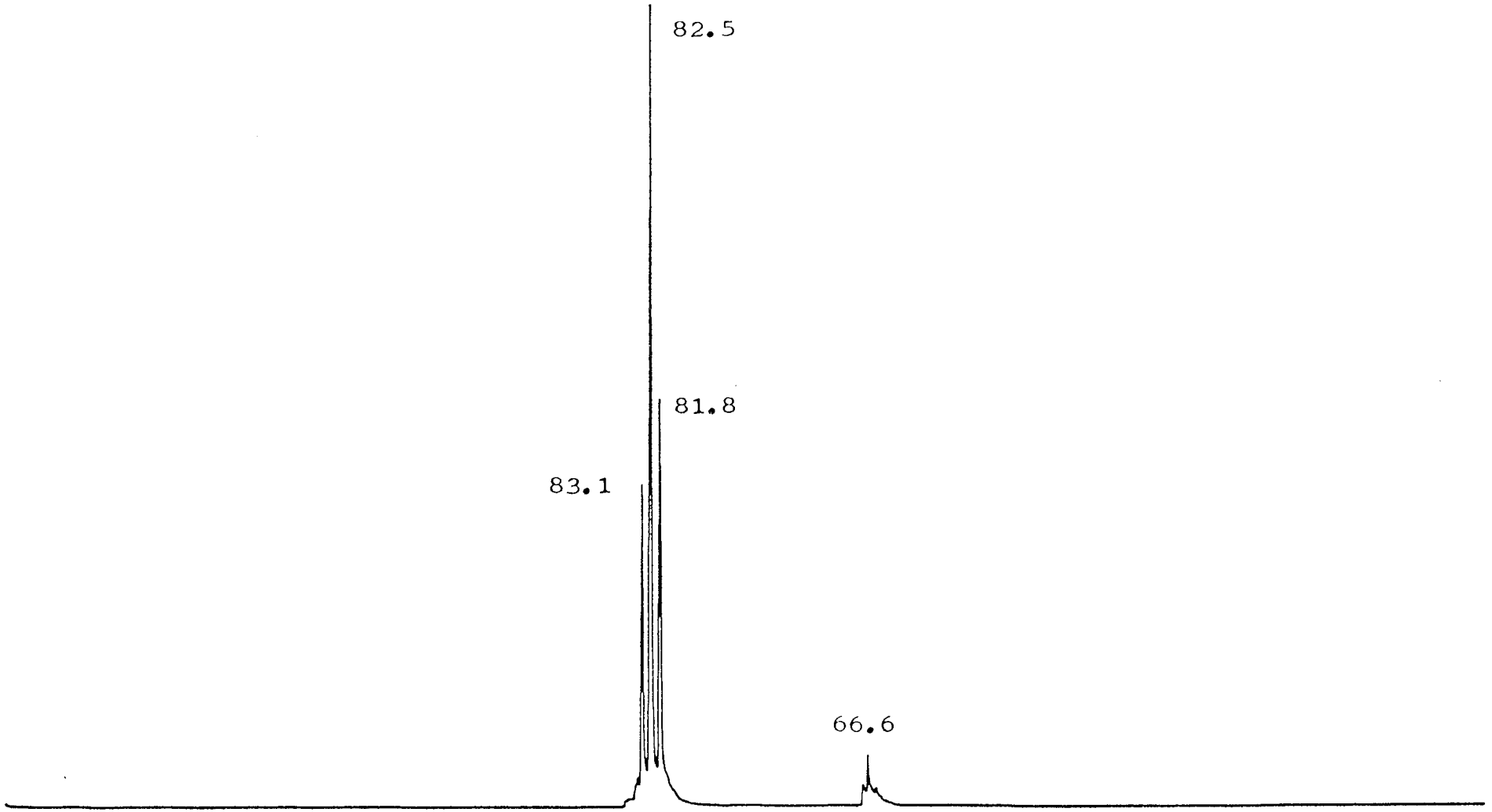

Figure A.7. ^{31}P NMR Spectrum of DsBDS.

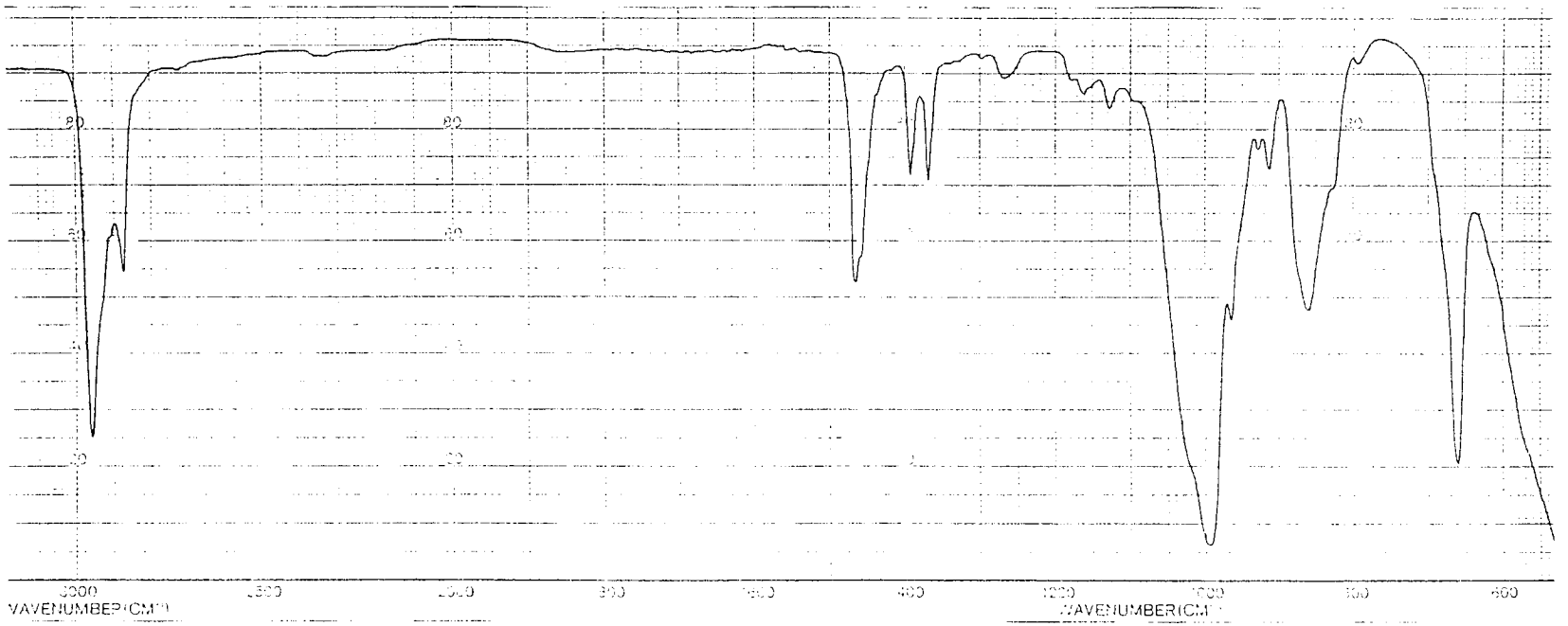

Figure A.8. IR Spectrum of DiBDS (Liquid film).

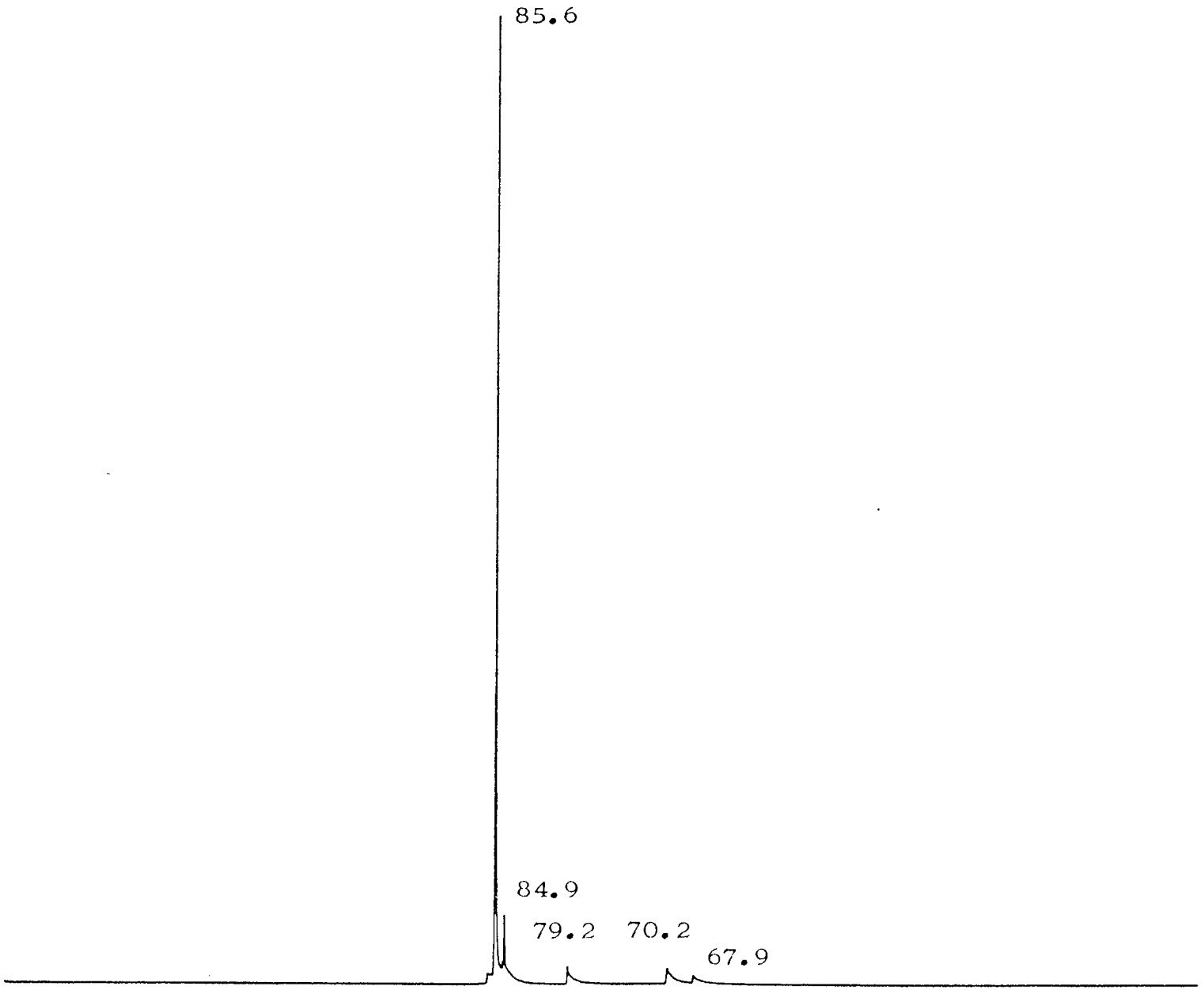

Figure A.9. ^{31}P NMR Spectrum of DiBDS.

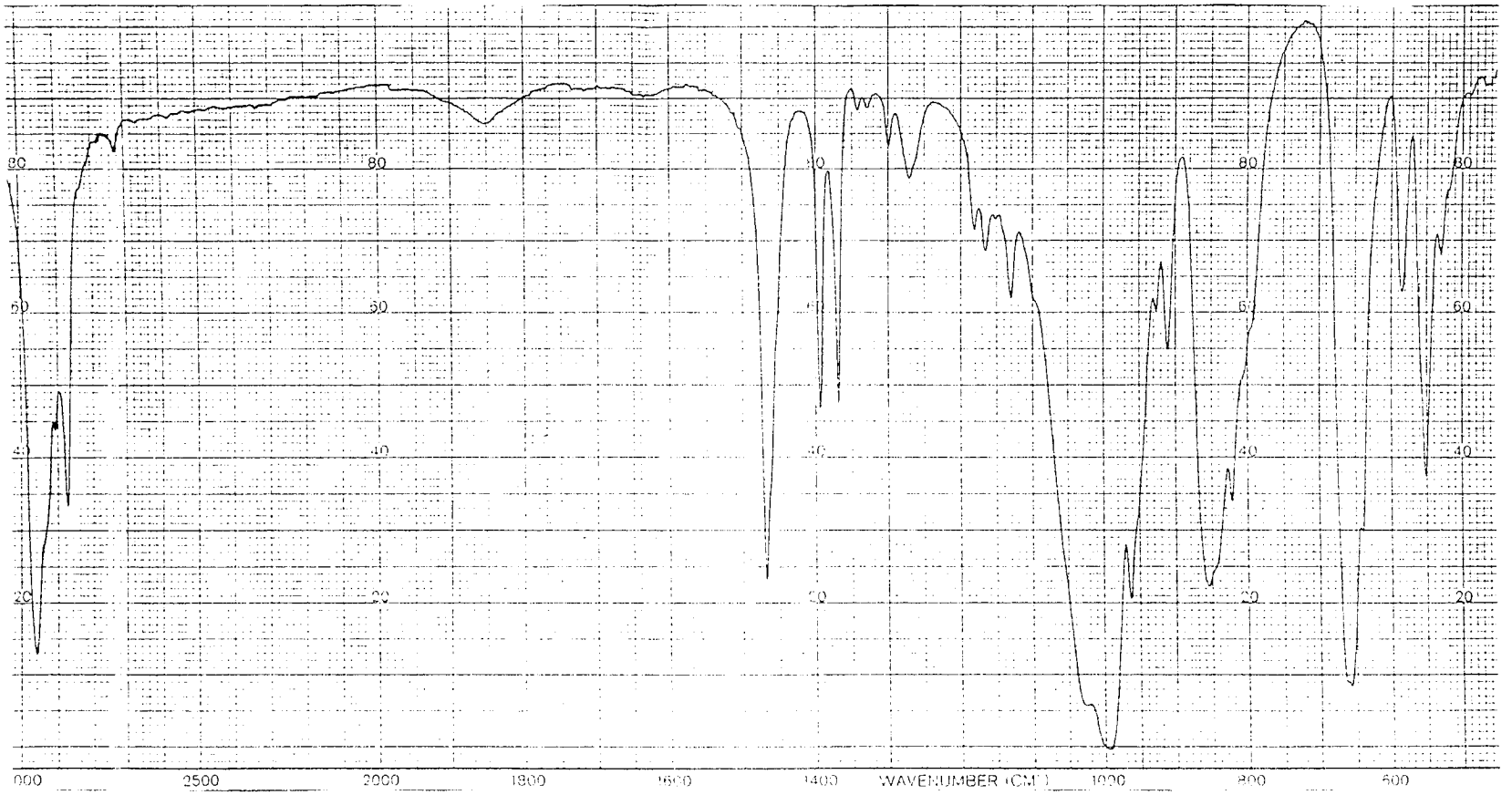

Figure A.10. IR Spectrum of ZnDiBP (KBr disc).

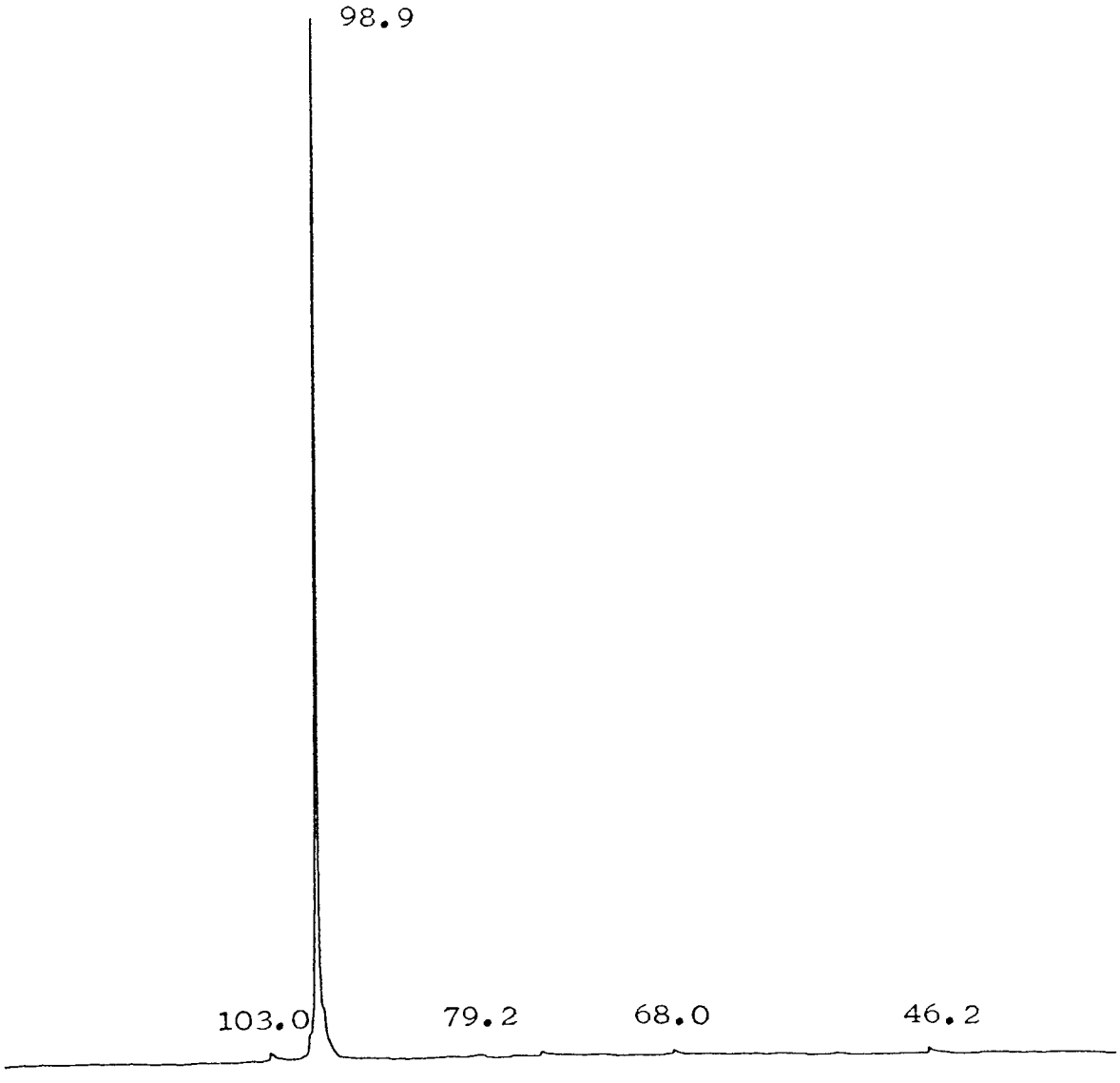

Figure A.11. ^{31}P NMR Spectrum of ZnDiBP.

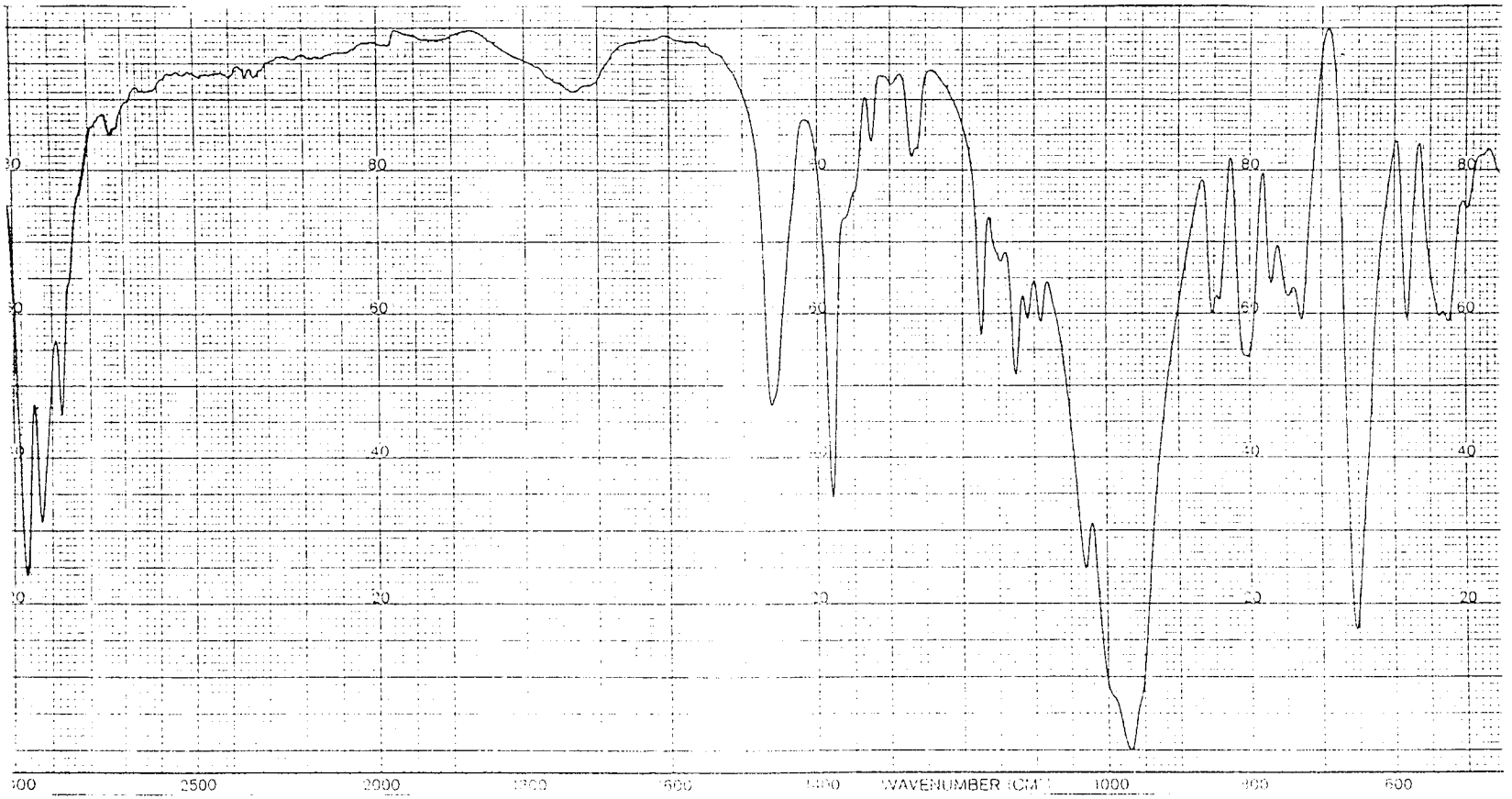

Figure A.12. IR Spectrum of ZnDsBP (KBr disc).

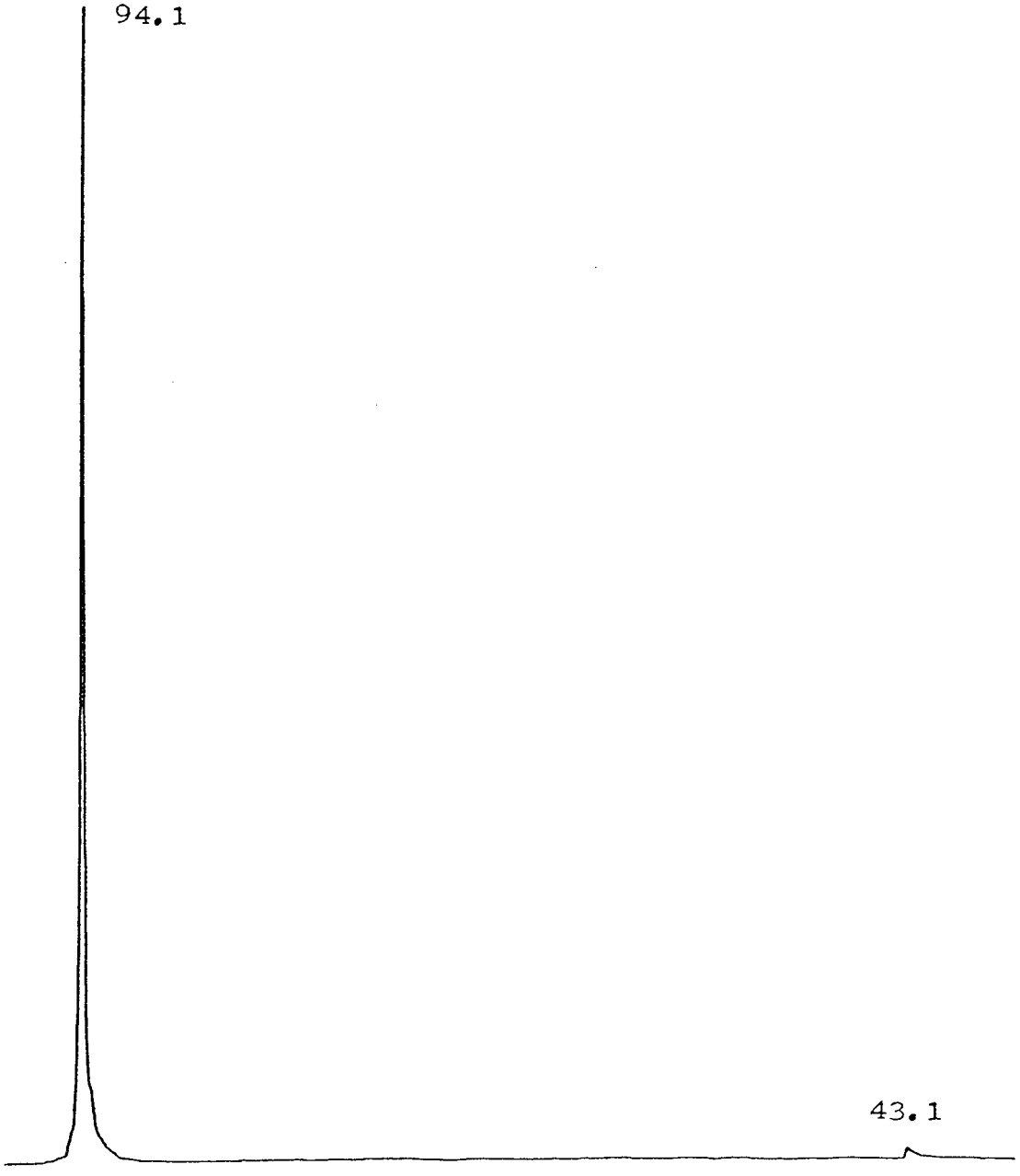

Figure A.13. ^{31}P NMR Spectrum of ZnDsBP.

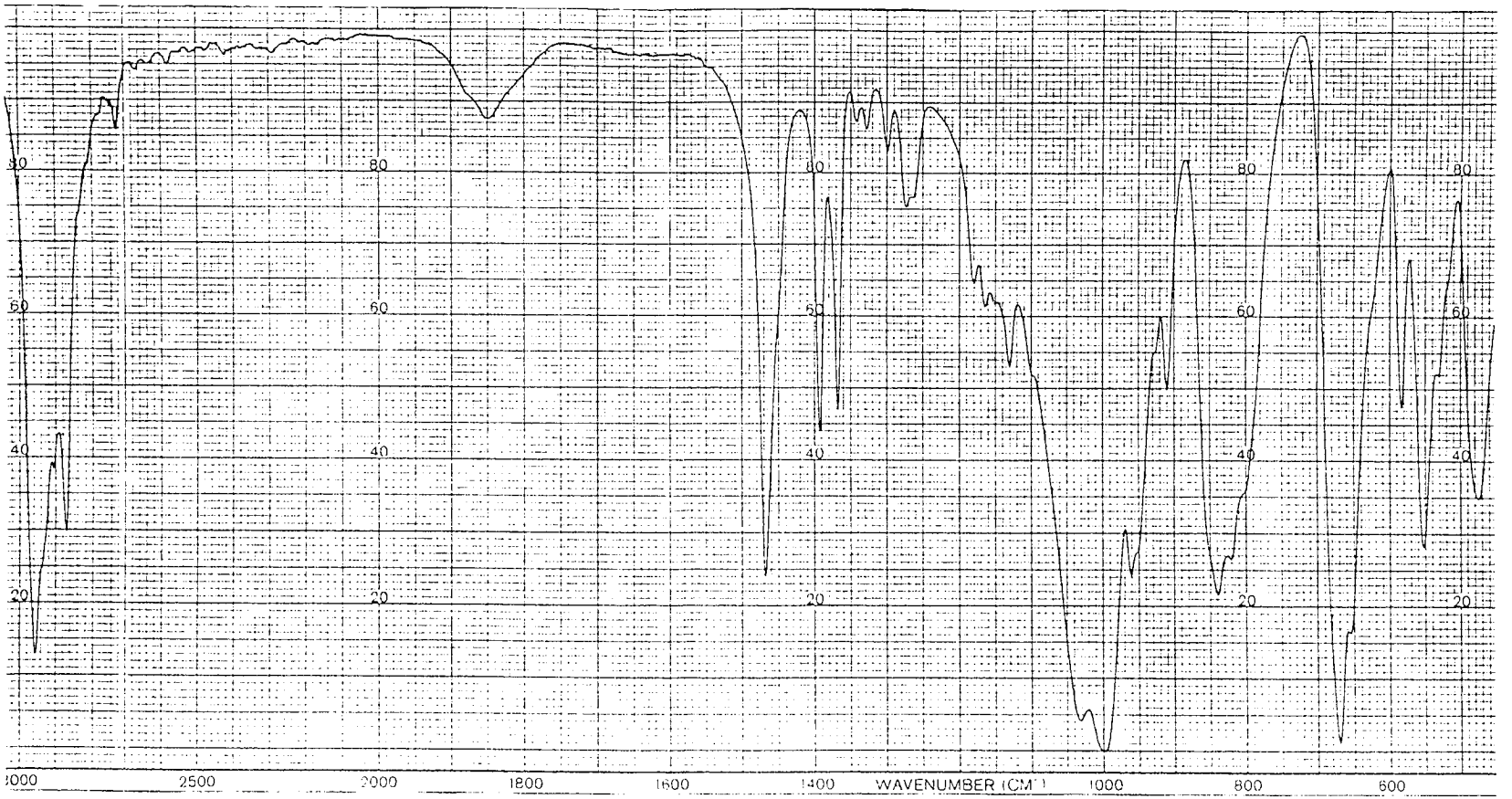

Figure A.14. IR Spectrum of b-ZnDiBP (KBr disc).

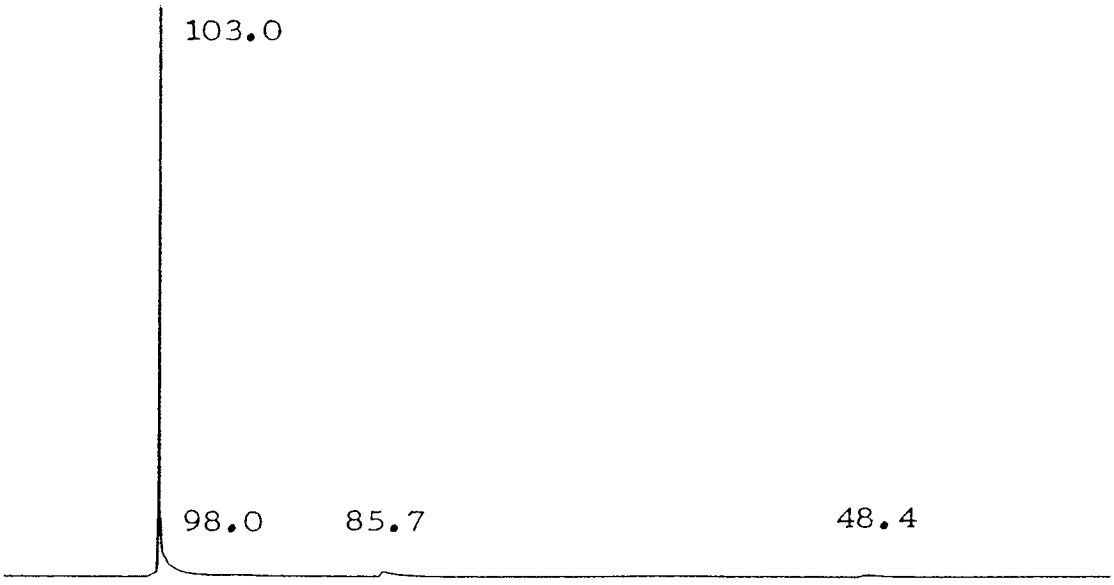

Figure A.15. ^{31}P NMR Spectrum of b-ZnDiBP (One Recrystallisation).

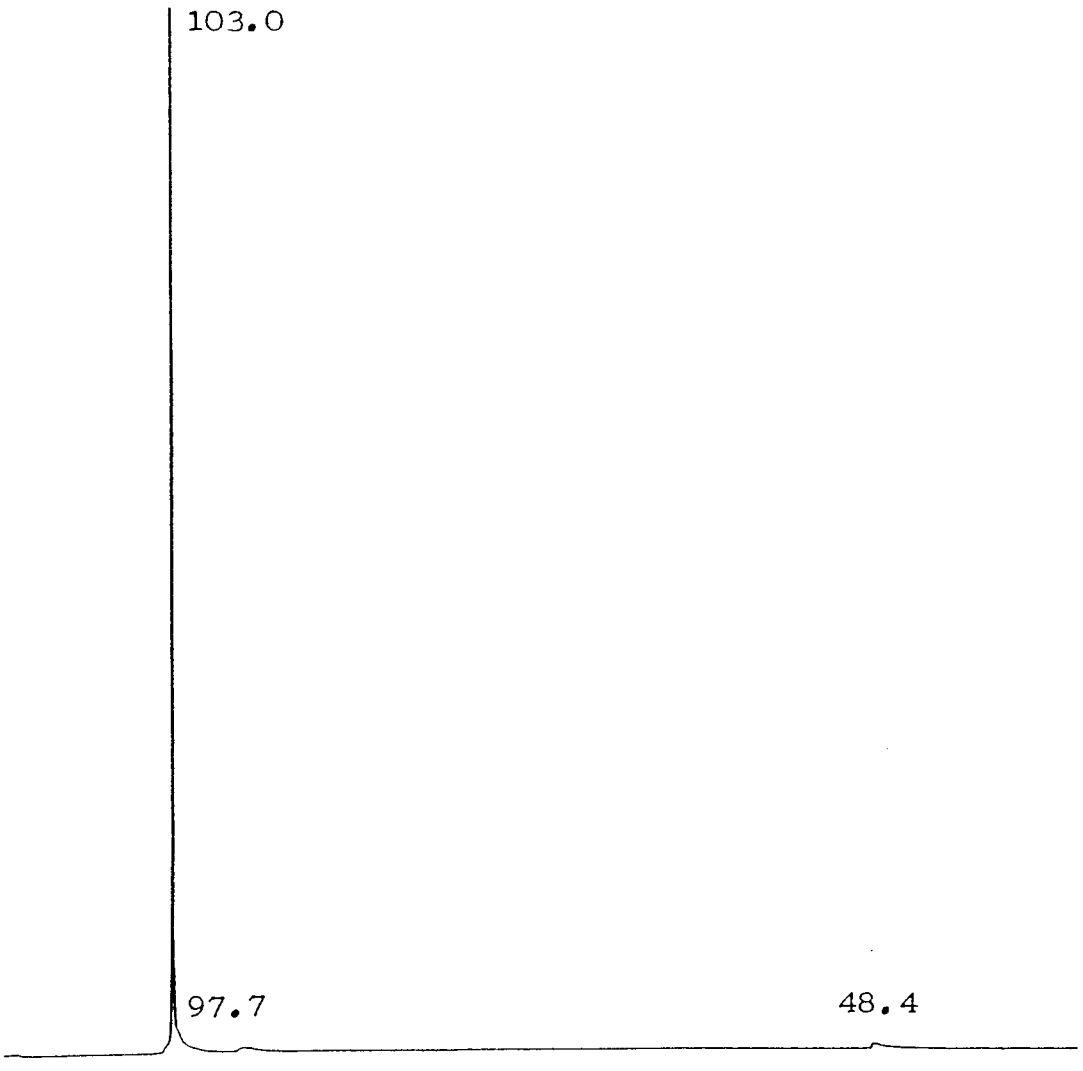

Figure A.16. ^{31}P NMR Spectrum of b-ZnDiBP (Two Recrystallisations).

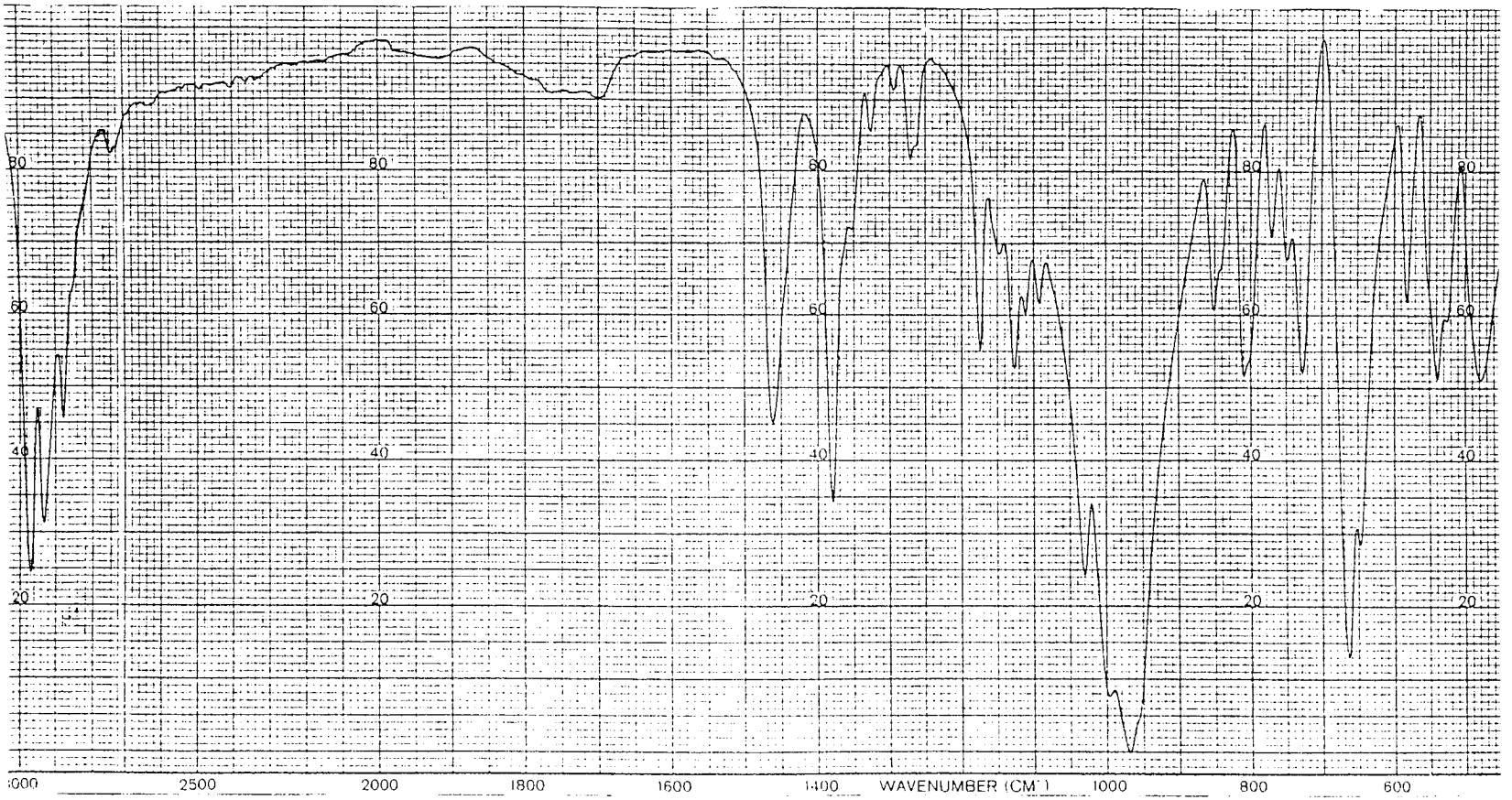

Figure A.17. IR Spectrum of b-ZnDsBP (KBr disc).

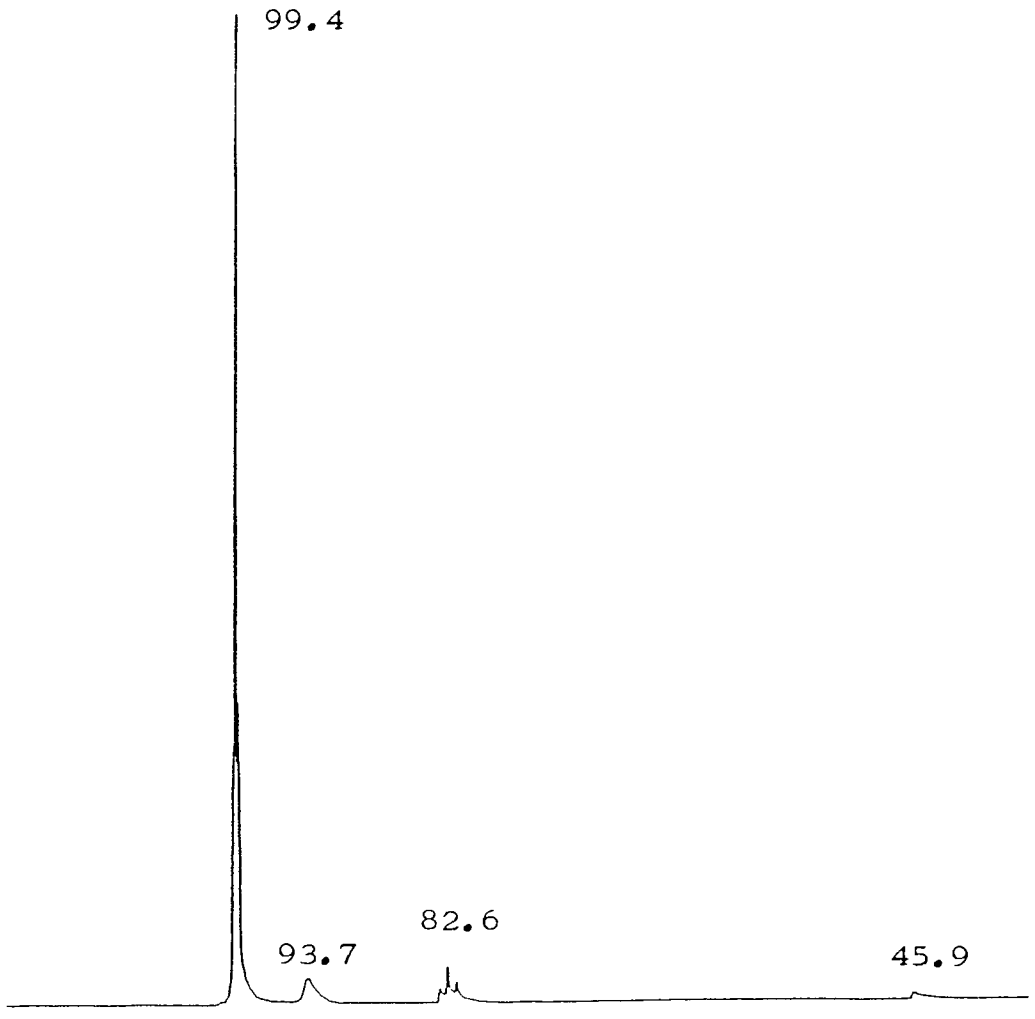

Figure A.18. ^{31}P NMR Spectrum of b-ZnDsBP (One recrystallisation).

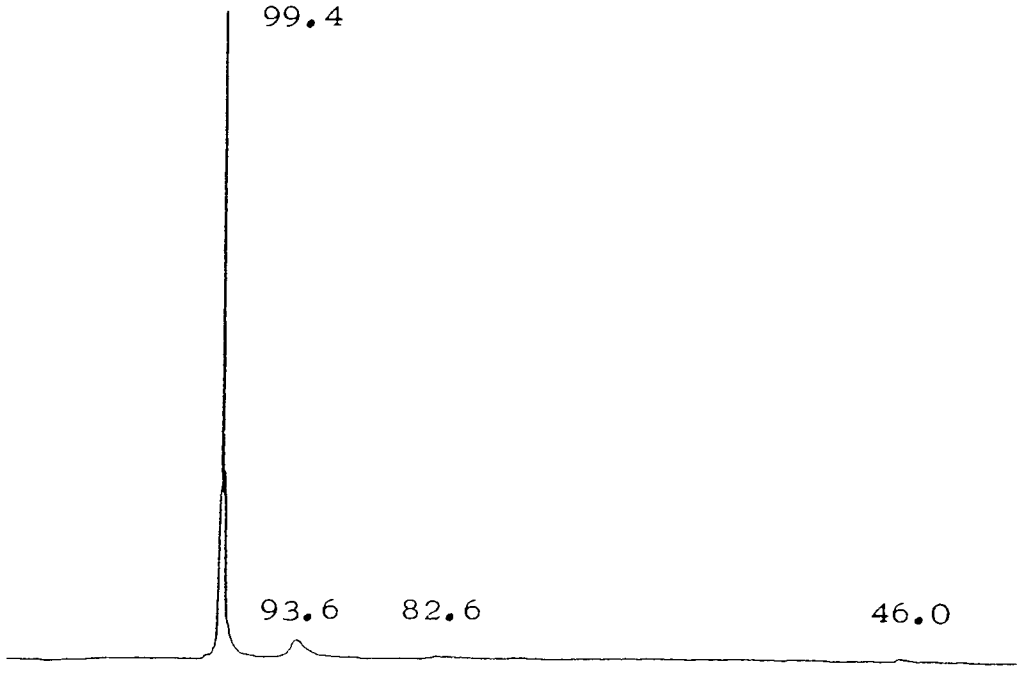

Figure A.19. ^{31}P NMR Spectrum of b-ZnDsBP (Two Recrystallisations).

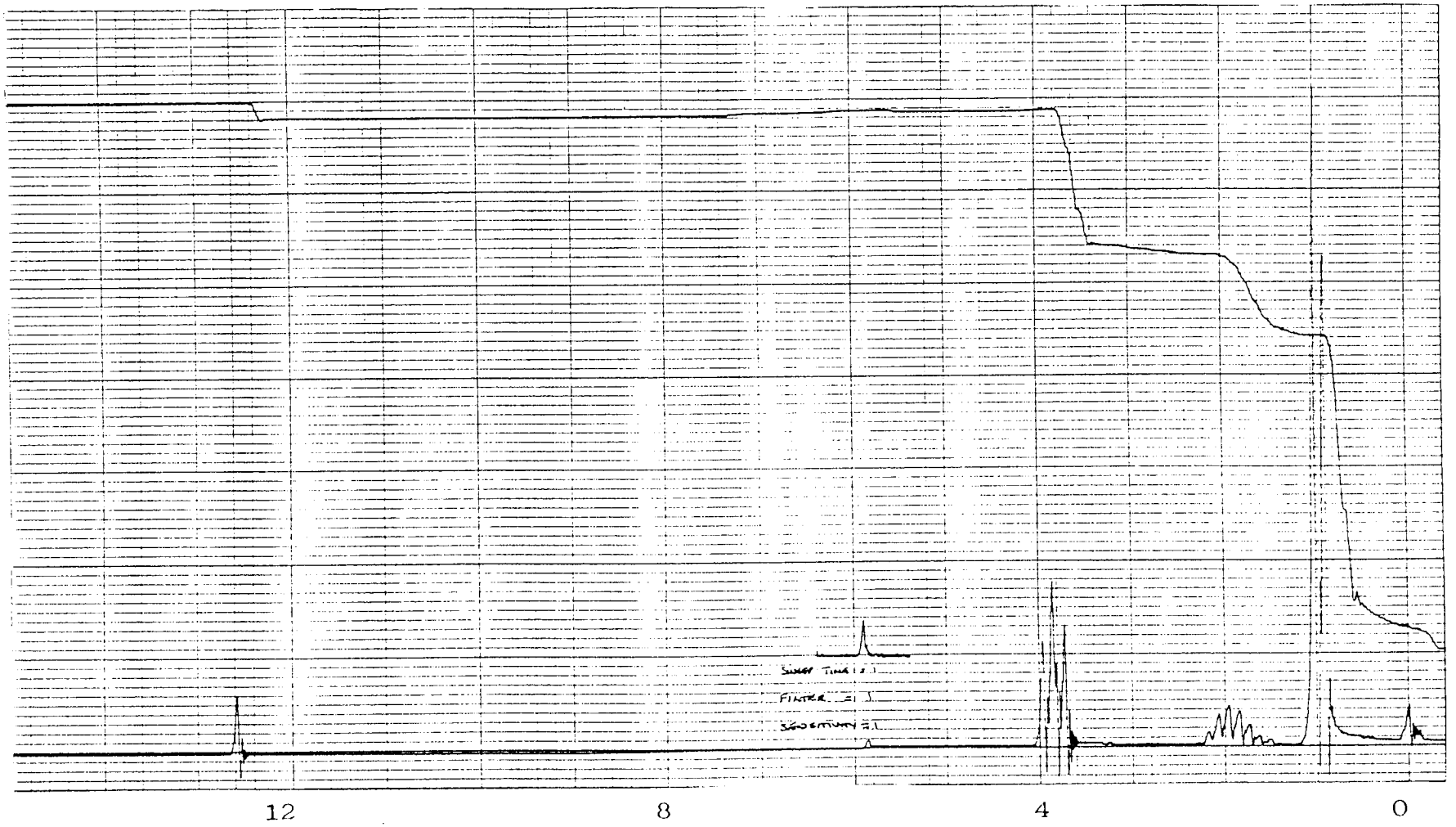

Figure A.20. ^{1}H NMR Spectrum of Di-isobutyl Hydrogen Phosphite.

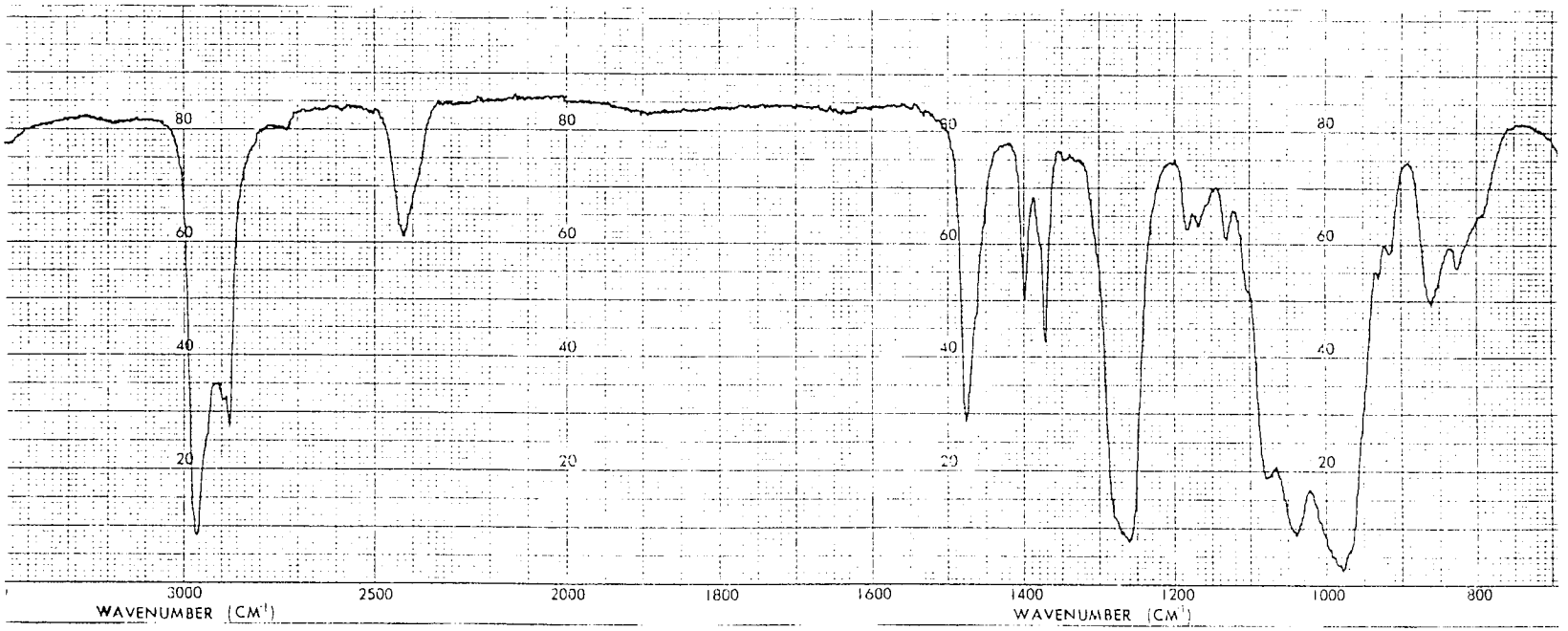

Figure A.21. IR Spectrum of Di-isobutyl Hydrogen Phosphite (Liquid film).

Figure A.22. IR Spectrum of DiBTPA (Liquid film).

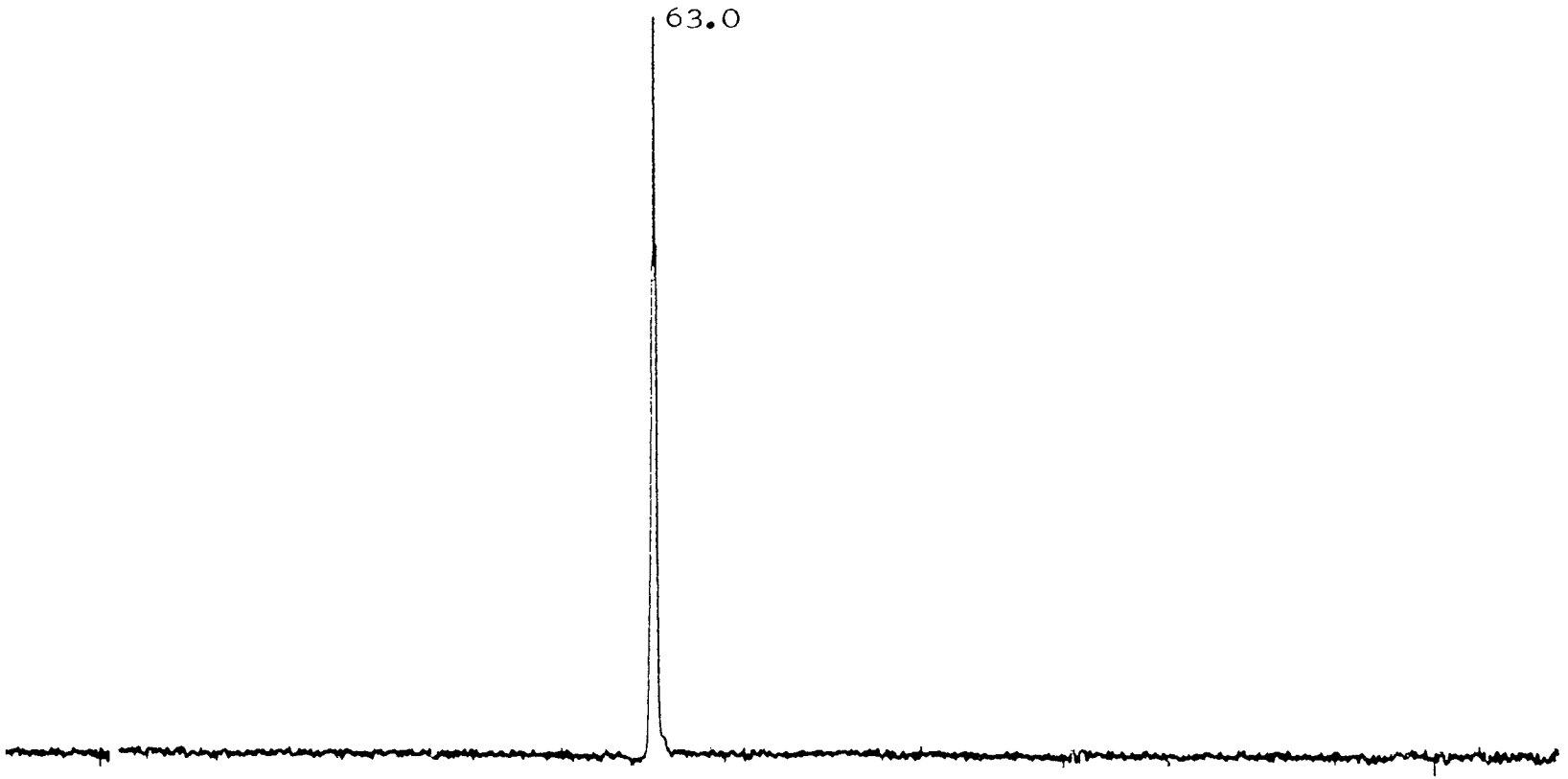

Figure A.23. ^{31}P NMR Spectrum of DiBTPA.

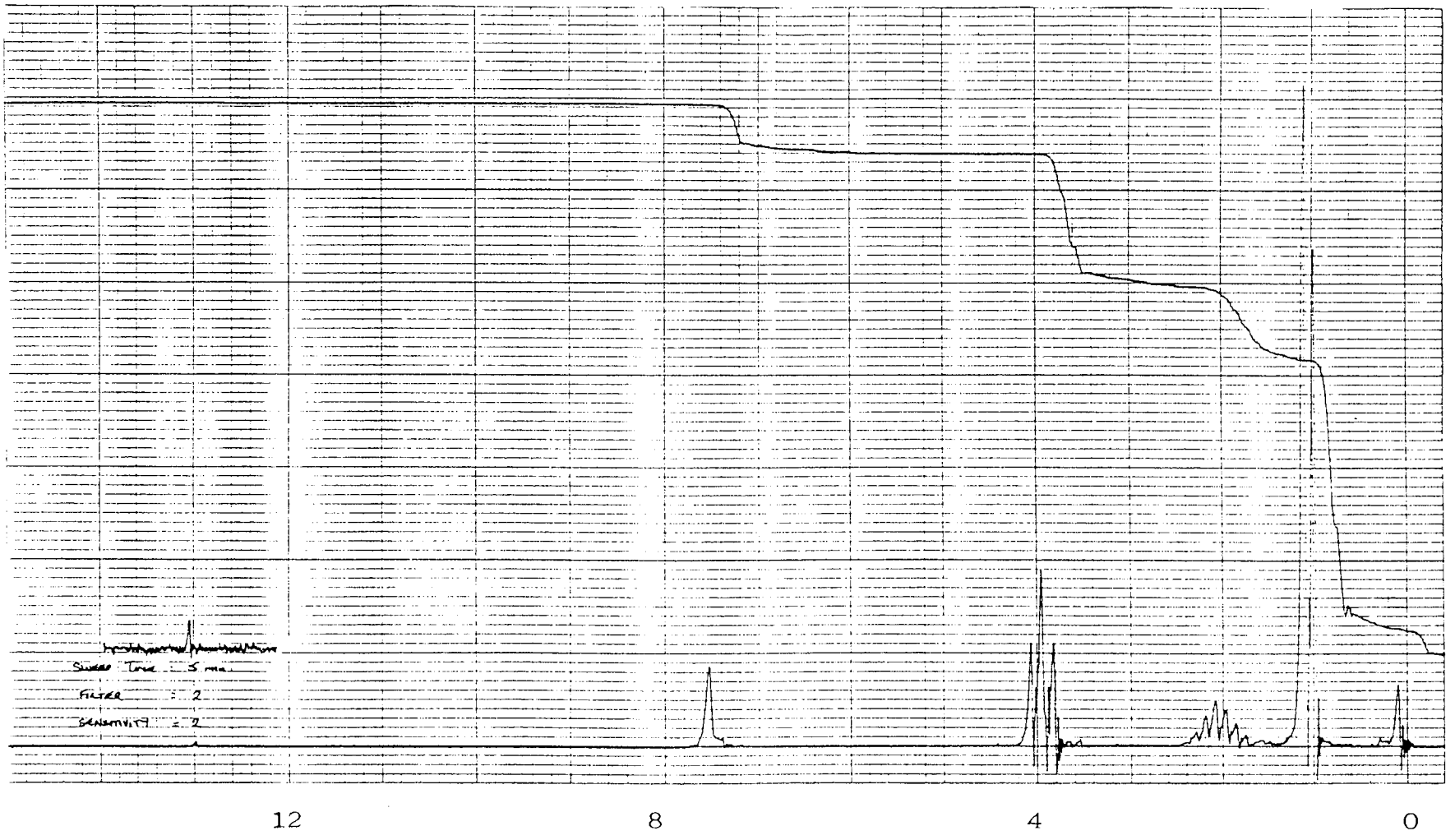

Figure A.24. ^{1}H NMR Spectrum of DiBTPA.

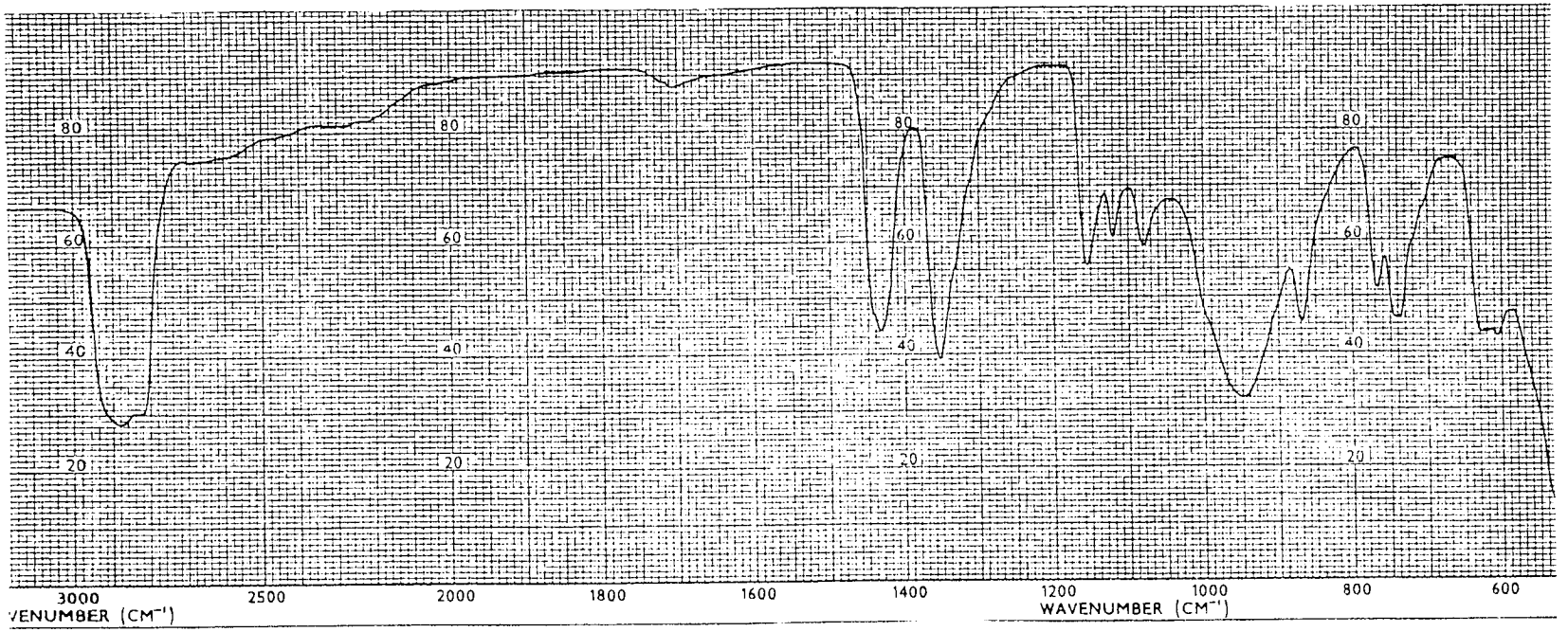

Figure A.25. IR Spectrum of FeDiPP (Nujol mull).

Figure A.26. IR Spectrum of FeST (Nujol mull).

REFERENCES

1. G. Scott. Atmospheric Oxidation and Antioxidants, Chapter 3, p66. (Elsevier, London, 1967)
2. Reference 1; Chapter 2, p41.
3. T. Colclough and F. Gibson. Paramins Report PMA 1AH 81.
4. S. Hsu and E. Klaus. A.S.L.E. Transactions 22, (1977), 135.
5. Reference 1; Chapter 7.
6. G. Scott. Developments in Polymer Stabilisation-4, Chapter 1. (Applied Science Publishers Ltd, 1980)
7. G. Kennerly and W. Patterson. Industrial and Engineering Chemistry 48, (1956), 1917.
8. H. Hock and S. Lang Berichte 77B, (1944), 257.
9. D. Shopov, S. Ivanov and V. Ivanova. Revue de l'Institute Francais du Petrole 22, (1967), 1520.
10. E. Rossi and L. Imperato. Chimica e Industria 53, (1971), 838.
11. J. Howard, Y. Ohkatsu, J. Chenier and K. Ingold. Canadian Journal of Chemistry 51, (1973), 1543.
12. J. Holdsworth, G. Scott and D. Williams. Journal of the Chemical Society (1964), 4692.
13. A. Burn, R. Cecil and V. Young. Journal of the Institute of Petroleum.57, (1971), 319.
14. M. Sexton. Journal of the Chemical Society, Perkin Transactions II (1984), 1771.

REFERENCES (continued)

15. M. Husbands and G. Scott. European Polymer Journal 15, (1979),249.

16. S. Ivanov. Developments in Polymer Stabilisation -3, Chapter 3. (Applied Science Publishers Ltd,1980)

17. V. Rabl and J. Mostecky. Ropa Uhlie 14, (1972), 496. (Chemical Abstracts 78:32330j.)

18. I. Shkhiyants, N. Voevoda, N. Komissarova, S. Chernyav, L. Kaya, V. Sher and P. Sanin. Neftekhimiya 14, (1974), 312. (Chemical Abstracts 81:13216x)

19. Y Ohkatsu, K. Kikkawa and T.Osa. Bulletin of the Chemical Society of Japan (1978), 3606.

20. P. Sanin, I. Blagovidov, A. Vipper, A. Kuliev, S. Krein, K. Ramaya, G. Shor, V. Sher and Y, Zaslavsky. Proceedings of the Eighth World Petroleum Congress 5, (1971), 91.

21. O. Grishina, M. Potekhina, V. Bashinova and E. Goldfarb. Neftekhimiya 22, (1982), 815.

22. S. Al-Malaika and G. Scott. Polymer Communications 23, (1983), 1711.

23. P. Kozak and V. Rabl. Scientific Papers of the Prague Institute of Chemical Technology D39, (1978), 141.

24. V. Sher, E. Markova, L. Khanakova, G. Kuzminav and P. Sanin. Neftekhimiya 13, (1973), 876. (Chemical Abstracts 80:95168z)

25. A. Bridgewater, J. Dever and M. Sexton. Journal of the Chemical Society, Perkin Transactions II (1980), 1006.

26. O. Grishina and V. Bashinova. Neftekhimiya 14, (1974), 142. (Chemical Abstracts 80:145654c)

27. M. Johnson, S. Korcek and M. Zinbo. Society of Automotive Engineers, Special Paper SP-558, (1983), 71.

28. O. Cherkasova, N. Mukmeneva, E. Chebotareva, V. Ovchinnikov, D. Pobedimskii and P. Kirpichnikov. Neftekhimiya 24, (1984), 76. (Chemical Abstracts 101:7303p)

29. J. Chenier, J. Howard and J. Tait. Canadian Journal of Chemistry 56, (1978), 157.

30. S. Al-Malaika and G. Scott. European Polymer Journal 16, (1980), 503.

31. J. Howard and J. Chenier. Canadian Journal of Chemistry 54, (1976), 390.

32. T. Colclough and J. Cuneen. Journal of the Chemical Society (1964), 4790.

33. A. Burn. Tetrahedron 22, (1966), 2153.

34. A. Burn. International Oxidation Symposium 1, (1967),323.

35. S. Korcek, L. Mahoney, M. Johnson and W. Siegl. Society of Automotive Engineers, Technical Paper 810014, (1981).

36. P. Willermet and S. Kandah. A.S.L.E. Transactions 27, (1983),67.

37. J. Howard and S. Tong. Canadian Journal of Chemistry 58, (1989), 92.

38. S. Cotton and J. Gibson. Journal of the Chemical Society (A) (1971), 803.

39. I. Kakovskii, E. Vershinin and A. Grebnev. Dokl. Akad. Nauk. SSSR 143, (1962), 649. (Chemical Abstracts 57;5552c)

40. C. Jorgensen. Journal of Inorganic and Nuclear Chemistry 24, (1962), 1571.

41. K. Homann, P. Saninaand K. Meyer. Trenie Iznos 3, (1982), 780. (Chemical Abstracts 98:56708c)

42. K. Meyer, K. Homann and H. Berndt. Vide, Couches Minces 201, (1980), 463.

43. J. Georges, J. Martin, T. Mathia, P. Kapsa, G. Meille and H. Montes. Wear 53, (1979), 9.

44. P. Willermet, S. Kandah, W. Siegl and R. Chase. A.S.L.E. Transactions 26, (1983), 523.

45. G. Marshall. Proceedings of Institute of Petroleum, London, 1982, (2 Petroanal), 409.

46. R. Barber and E. Yamaguchi. Discussion of Reference 48.

47. T. Colclough and H. Spedding. Paramins Report PMTA 1AGE 80.

48. R. Coy and R. Jones. A.S.L.E. Transactions 24, (1981), 77.

49. H. Spedding and R. Watkins. Tribology International 15, (1982), 9.

50. R. Coy and R. Jones Institute of Mechanical Engineers Conference Publications 1, (1982), 17.

51. J. Ford. Journal of the Institute of Petroleum 54, (1968), 198.

52. T. Colclough and H. Spedding. Paramins Report PMA 3AI 81.

53. K. Inoue and H. Watanabe. A.S.L.E. Transactions 26, (1983), 189.

54. L. Mikeska. U.S. Patent 2,471,115 (19/9/1946).

55. H. Luther, E. Baumgarten and D. Staeck. Erdoel und Kohle Erdgas Petrochemie 22, (1969), 530.

56. G. Kuzmina, V. Sher and P. Sanin. Neftekhimiya 10, (1970), 723.

57. W. Bacon and J. Bork. Journal of Organic Chemistry 27, (1962), 1484.

58. O. Foss. Acta Chemica Scandanavica 1, (1947), 8.

59. R. Vold and G. Hattiangdi. Industrial and Engineering Chemistry 41, (1949), 2311.

60. G. Hattiangdi, R. Vold and M. Vold. Industrial and Engineering Chemistry 41, (1949), 2320.

61. G. Macdougall and C. Ockrent. Proceedings of the Royal Society A180, (1942), 151.

62. M. Plant. Ph.D. Thesis, University of Aston (1972).

63. M. Kharasch, A. Fono and W. Nudenburg. Journal of Organic Chemistry 16, (1951), 113.

64. Private Esso Literature.

65. J. Dickert and C. Rowe. Journal of Organic Chemistry 32, (1967), 647.

66. C. Glidewell. Inorganica Chimica Acta 24, (1977), 255.

67. H. Laver. Developments in Polymer Stabilisation -1, Chapter 5. (Applied Science Publishers Ltd,1979)

68. M. Coker. Ph.D. Thesis (in preparation).

69. M. Crutchfield, C. Dungan, J. Letcher, V. Mark and J. Van Wazer. Topics in Phosphorus Chemistry, Volume 5,(Interscience, 1967).

70. J. Mostecky, V. Rabl, P. Kozak and R. Kubelka. Ropa Uhlie 16, (1974), 557. (Chemical Abstracts 82:50885f)

71. O. Grishina, V. Bashinova and V. Anoshina. Neftekhimiya 14, (1974), 648. (Chemical Abstracts 82:72500d)

72. R.Morrison and R. Boyd. Organic Chemistry, 3rd Edition, p167. (Allyn and Bacon, 1977)

73. Y. Ohkatsu. Yukagaka 26, (1977), 295. (Chemical Abstracts 87:47509j)

74. P. Sanin, V. Sher, I. Shkhiyants, G. Kuzmina,

N. Voevoda and A. Zhorba. Neftekhimiya 17, (1977), 290. (Chemical Abstracts 87:38616q)

75. S. Ivanov and I. Kateva. Neftekhimiya 18, (1978), 417. (Chemical Abstracts 89:146540k)

76. J. Lebedda and R. Palmer. Spectrochimica Acta (A) 29, (1973), 1371.

77. W. Hopkins and P. Mitchell. Unpublished work.

78. K. Hayashi, Y. Sasaki, S. Tagashira, S. Inomata, J. Rikitake, Y. Hisatomi and M. Suzuki. Bunseki Kagaku 33, (1984), 247.(Chemical Abstracts 101: 83102n)

79. C. Bovington and B. Dacre. A.S.L.E. Transactions 27, (1984), 252.